

Harpur Hill, Buxton  
Derbyshire, SK17 9JN  
T: +44 (0)1298 218000  
F: +44 (0)1298 218590  
W: [www.hsl.gov.uk](http://www.hsl.gov.uk)



**Mechanical, Control Systems and Ergonomics  
Integrity of the Safeco Crazy Frogs Type  
Amusement Device**

**ES/13/30**

Lead Author: **D. Riley**  
Contributing Authors: **C. Atkin, M. Birtles, J. Hobbs, D. Riley,  
J. Statham, T. Wynn**  
Technical Reviewer: **W. Geary**  
Editorial Reviewer: **E. Lower**  
Report Authorised for Issue By: **N. Corlett**  
Date Authorised: **25<sup>th</sup> November 2013**

## **ACKNOWLEDGEMENTS**

The authors would like to thank Mr Robert Wilkinson for his valued assistance during the collection of amusement device data.

## KEY MESSAGES

- The Safeco Crazy Frogs amusement device tested is capable of generating vertically acting accelerations that can be potentially harmful to passengers.
- The amusement device is also capable of being operated in a way that can potentially shorten the fatigue life of the structure of the device.
- The control system allows the amusement device to be operated beyond safe acceleration limits for passengers.
- The design of the foot pedal control appears to put the performance of the device and the safety of the passengers entirely under the control of the operator.
- Removal of the foot pedal control function would avoid the main source of risk.
- In order to address the potential for crack growth in the arms, a regime for regular (twice yearly) inspection of the device arms, including ultrasound techniques, is proposed.
- The passenger safety containment and restraint system on the device examined does not meet all of the requirements of BS EN 13814 (1).

## EXECUTIVE SUMMARY

The Safeco Crazy Frogs amusement device typically consists of a central hub that drives 12 radial arms through 360° in either direction. At the end of each arm is a passenger car which can typically carry up to three passengers. During the operation of the device each arm is driven vertically by a pneumatic ram, causing the passenger car to move up and down through an arc. The individual rams move independently and are used to create a range of synchronised patterns of motion that give the impression of a jumping or wave pattern.

There have been at least four incidents resulting in serious injury on these amusement devices in the past three years, and a number of minor incidents. The incidents on these machines are reported to come almost exclusively from:

1. Structural failure which results in collapse of a radial arm and passenger cars dropping to the platform/ground;
2. A control system which enables the operators to run the machine outside of safe operating parameters; in particular it enables arms to fall to a hard stop under gravity; or;
3. Passengers sustaining spinal injuries whilst riding the amusement devices, believed to be linked to high seat-to-head acceleration exposure and restraint/containment design characteristics..

### Objectives

1. To establish the main areas on the arm where structural fatigue is likely to occur and to develop a non-destructive testing and inspection (NDT) schedule for the machine;
2. To investigate ways in which a hard stop of the arm can be prevented or mitigated;
3. To establish the appropriate standard of passenger containment/restraint required for this machine.

### Method

The project team included ergonomists and engineers. The project plan was broadly defined by the following work packages:

1. Finite element analysis and fatigue assessment (followed by contract provision of a NDT schedule (Non-Destructive Testing)).
2. Assessment of radial arm actuation and prevention of uncontrolled descent;
3. Assessment of passenger safety and ergonomics.

An initial site visit to Nottingham Goose Fair was conducted as an information-gathering exercise.

### Main Findings

The findings are only applicable to devices similar to that which we tested. Devices differing in design, construction and size would need to be subject to a similar assessment.



## **Structural Fatigue Assessment**

Ideally, the cabling for the car should not run along a conduit tack welded to the top of the arm. The presence of the conduit masks part of the top of the arm in a high stress area, meaning that it is not possible to check for the presence of cracks in the area covered by the conduit. Also, the tack weld may act as stress raisers, encouraging crack initiation.

Although the fatigue analysis, replicating a typical fairground ride sequence showed that the fatigue life was acceptable with twice yearly inspections, the lack of regulation of the use of the foot pedal means that much quicker crack growth is possible if the foot pedal was used more extensively. It is proposed that the foot pedal operation is not used.

Due to the potential for increased crack growth rate through welds, it is strongly recommended that the side plates of the amusement device are not weld repaired.

An example NDT schedule is presented.

## **Failure Modes - Engineering and Control System Appraisal**

Assessment of the control system and examination of a number of SAFECO devices has identified a number of potential failure modes which may lead to the arm of the device falling in an uncontrolled manner, resulting in the passengers being subject to excessive vertical deceleration. The following components were identified:

- Position sensor movement or failure;
- Valve failure;
- Pneumatic flexible hose failure;
- Pneumatic actuator seal failure;
- PLC aberration;
- Mechanical failure of the arm;
- Operator error in actuating the foot pedal control.

## **Ride Motion and Passenger Safety**

The containment system, as designed, does not meet all of the requirements of BS EN 13814 (1).

The lap bar is not considered to be an effective restraint against the potential for passenger movement within the seat/car due to the lack of fit for a large proportion of the potential passenger population, it being located too far in front of the occupants, shared across multiple occupants, and not adjustable.

The automotive type inertia reel lap belt fitted does not currently meet the level of safety integrity required by BS EN 13814 (1) due to it being shared across multiple occupants, not interlocking with the control system, and being releasable by ride occupants during a ride sequence.

Existing guidance on acceptable acceleration levels for ride passengers focuses on the magnitude of the seat-to-head acceleration as a risk factor. There appears to be consensus on an upper limit of around 5 to 6 g for seat-to-head acceleration for passenger safety. The British Standard BS EN 13814 adopts a 6 g upper limit. The protective effects of this limit in terms of the proportion of the general population protected and, in particular, the implications of such a limit for younger and older passengers are uncertain.

The peak seat-to-head accelerations recorded during testing of the Wilkinson DJ Jump device were around 9 g. There appears to be nothing in the design of the device to prevent the acceleration experienced by passengers exceeding the 6 g maximum level indicated in the BS EN 13814 (1).

Although the measured levels of acceleration were achieved when operating the device under test conditions, since the highest levels occurred during operation of the foot pedal control, it is solely the operator that has control of the acceleration level, and therefore they could occur at any time that the operator were to make an error in timing the pedal operation.

## CONTENTS PAGE

<b>1.</b>	<b>INTRODUCTION .....</b>	<b>1</b>
1.1	Safeco Crazy Frogs amusement device	1
1.2	Rationale	2
1.3	Research aims	2
<b>2.</b>	<b>IMPLICATIONS .....</b>	<b>3</b>
2.1	Engineering and control system aspects	3
2.2	Finite element analysis and fatigue assessment	3
2.3	Ride motion and passenger safety	4
<b>3.</b>	<b>METHOD .....</b>	<b>5</b>
3.1	Summary of HSL's approach	5
3.2	Review of existing information	6
3.3	Examination of Safeco Crazy Frogs devices at Nottingham Goose Fair	6
3.4	Examination and testing of a Safeco Crazy Frogs device	6
<b>4.</b>	<b>RESULTS .....</b>	<b>12</b>
4.1	Review of existing HSL information	12
4.2	Description of the amusement device and the operator controls	17
4.3	Explanation of the information collected	22
4.4	Interaction of ride control elements and components	25
4.5	Potential failure modes of the amusement device	30
4.6	Means to mitigate uncontrolled arm descent	31
4.7	Amusement device motion analysis	32
4.8	Assessment of passenger restraint requirements	39
4.9	Existing containment and restraint system assessment	42
4.10	Finite element analysis and fatigue assessment	49
<b>5.</b>	<b>REFERENCES .....</b>	<b>62</b>
<b>6.</b>	<b>APPENDIX .....</b>	<b>65</b>
6.1	Review of previous information	65
6.2	Site visit – Measurement test run list	76
6.3	Acceleration measurement data set	78
6.4	Anthropometry	124
6.5	Non-destructive testing schedule	125

# 1. INTRODUCTION

As a result of a number of serious incidents HSL was commissioned to undertake a review of mechanical, control systems and ergonomics integrity of the Safeco Crazy Frogs amusement device by the HSE Entertainments and Leisure Sector.

## 1.1 SAFECO CRAZY FROGS AMUSEMENT DEVICE

The Safeco Crazy Frogs amusement device, as shown in Figure 1, typically consists of a central hub that drives 12 radial arms through 360° in either direction. At the end of each arm is a passenger car which can typically carry up to three passengers. During the operation of the device each arm is driven upwards by a pneumatic ram but falls under gravity, causing the passenger car to move up and down through an arc. The individual rams move independently, but by selecting a number of automated programs the operator is able to create a range of synchronised patterns of motion that give the impression of a jumping or wave pattern. There is also a manual control (foot pedal) mode of operation on some devices that initiates and controls the duration over which the arms are allowed to drop. Developing an understanding of the engineering of the device is part of our work, and therefore reported in our findings. The reader is referred to Section 4.2 for a detailed description the device.

A number of different Safeco Crazy Frogs- type amusement devices are manufactured across Europe. For example:

- La Sauterelle (Safeco: Spain);
- Techno jump (Sartori: Italy);
- Smashing Jump (Fabbri Group: Italy);
- Wild Spark (Technical Park: Italy);
- Twist and Bounce (Zamperla: Italy).

These amusement devices are known by a number of alternative names, such as City Hopper, Frog Hopper, Grasshopper, Jump & Smile, Jumpin'; Mexican Wave, DJ Jump, and Jumping Frog. An alternative design, with rotating cars at the end of each arm, known as the MAXI Jump is also available, but is outside the scope of this report. However, all the amusement devices examined during the course of this project were manufactured by Safeco. Also, all previous investigations undertaken by HSL on this type of ride , have been on amusement devices manufactured by Safeco.



**Figure 1** La Sauterelle (The Grasshopper)

## **1.2 RATIONALE**

HSL was advised by HSE's Entertainment and Leisure Sector that approximately 27 Safeco Crazy Frogs machines have been imported into the UK from Spain in the last 20+ years, and most are still working. There have been at least four incidents resulting in serious injury on the devices in the past three years, and a number of minor incidents.

The incidents on these machines are reported to come almost exclusively from:

- Structural failure which results in collapses of radial arms and passenger cars dropping to the platform/ground;
- A control system which enables the operators to run the machine outside of safe operating parameters. In particular, it enables arms to fall to a 'hard stop' under gravity;
- The passenger containment/restraint system failing to prevent passenger ejections. There is reported to be inconsistency between machines in terms of the restraint systems.

## **1.3 RESEARCH AIMS**

The aims for this piece of work are:

- To establish the main areas on the machine where structural fatigue are likely to occur;
- To develop an non-destructive testing (NDT) schedule for the machine (by using an external specialist);
- To investigate ways in which a hard stop of the arm can be prevented;
- To establish the appropriate standard of passenger restraint required for this machine.

## **2. IMPLICATIONS**

The findings of this work are specific to Safeco Crazy Frogs amusement devices similar to that which we tested. Devices differing significantly in design, construction and size would need to be subject to a similar assessment.

### **2.1 ENGINEERING AND CONTROL SYSTEM ASPECTS**

An assessment of the amusement device was conducted in order to establish if there were any potential means by which an uncontrolled descent of the arm and passenger car could be mitigated. However, assessment of the design and examination of the devices suggests this is not possible without substantial modification, other than by modification of the control system.

Good practice suggests that in the event of component failure the control system would terminate the ride sequence in a controlled and safe manner. This system should operate independently of the Programmable Logic Controller (PLC), so that in the event of an aberration of the system the actuator would not descend in an uncontrolled manner.

The foot pedal actuation and free fall mode both require further investigation to establish if the foot pedal does override other control functions, i.e. potentially allowing the passenger car to descend too far before deceleration, and establish why the Programme 2 / free fall mode results in higher passenger forces. Alternatively the foot pedal functions could be removed.

While it cannot be shown exactly how the pneumatic pressure affects the dynamics of the passenger, it is clear that the change in pressure can result in a change in performance of the amusement device and the acceleration forces to which the passengers are subjected. Passenger loads need to be evenly distributed between cars. Failure to do this may result in the operator increasing the operating air pressure in order to compensate for a heavily loaded car. This may then have an adverse effect on a lightly loaded car, in that it could be subject to higher than acceptable accelerations.

### **2.2 FINITE ELEMENT ANALYSIS AND FATIGUE ASSESSMENT**

Cablings for the car should not run along a conduit tack welded to the top of the arm.

The presence of the conduit masks part of the top of the arm in a high stress area, meaning that it is not possible to check for the presence of cracks in the area covered by the conduit. Also, the tack welds may act as stress raisers, encouraging crack initiation.

Although the fatigue analysis of a run replicating a typical fair ride sequence showed that the fatigue life was acceptable with twice yearly inspection, the lack of regulation of the use of the foot pedal means that much quicker crack growth is possible if the pedal was used more extensively. It is recommended that the foot pedal operation is not used.

Due to the potential for faster crack growth rate through welds, it is recommended that the side plates of the amusement device are not weld repaired.

An NDT schedule for inspection of the device arms has been provided. This includes inspection of the top of the arm between the central pivot and the apex and internal areas at the apex and along the internal stiffening plate. These areas were not included in some previous schedules reviewed. The internal areas would require ultrasonic inspection methods. The

proposed inspection interval, based on the findings of this investigation, has been reduced to twice yearly from yearly.

### **2.3 RIDE MOTION AND PASSENGER SAFETY**

The containment system on the device studied, as designed, does not appear to meet all the requirements of BS EN 13814 (1) and this is likely to be the case for the majority of the amusement devices of this design type, unless they have been modified.

While an appropriately designed and fitted automotive type lap belt has the potential to be effective in terms of passenger restraint and containment, it does not currently meet the level of safety integrity required by BS EN 13814 (1).

In terms of reducing the risks of spinal injury, any passenger restraint systems that prevent/restrict forward trunk flexion will increase tolerance to vertebral injury from high seat-to-head accelerations (2). One such system has been observed on a Safeco Crazy Frogs type amusement device.

The peak accelerations recorded during testing of the Wilkinson DJ Jump device are considered likely to be achievable by other amusement devices of this design type. Although the measured levels of acceleration were achieved when operating the device under test conditions, since the highest levels occurred during operation of the foot pedal control, it is solely the operator that has control of the acceleration level, and therefore they could occur at any time that the operator were to make an error in timing the pedal operation. Operator reliability in ensuring safe operation of the ride during use of the foot pedal will not be 100%. This has implications for passenger safety in terms of both the potential for structural failure and for spinal injury risk.

The frequency of repetitive acceleration events is considered to be important and is something that needs to be included in the standards for safety of amusement devices. This factor requires further exploration in order to understand the nature of its effects on the bodies of amusement device passengers. It is considered likely that the whole body vibration field may yield useful information.

To provide guidelines that better protect amusement device passengers, we need better data connecting exposure to seat-to-head acceleration exposure with risk of injury. This needs to include information relevant to young and old amusement device passengers.

## 3. METHOD

### 3.1 SUMMARY OF HSL'S APPROACH

In order to meet the aims of the research, it was necessary for HSL to provide a number of disciplines in the project team including ergonomists and engineers. The project plan was broadly defined by three HSL work packages and a contract stage:

1. Finite element analysis and fatigue assessment;
2. Assessment of radial arm actuation and prevention of uncontrolled descent;
3. Assessment of passenger safety and ergonomics;
4. Contract provision of NDT schedule (Non-Destructive Testing).

These work packages were achieved through the following activities.

An initial site visit to Nottingham Goose Fair was conducted as an information-gathering exercise. This visit allowed examination of several Safeco Crazy Frogs-type devices. This was conducted alongside a review of the existing information held by HSL.

The finite element analysis and fatigue assessment work package involved a series of tests and examinations to establish where on the arms the main areas and levels of structural fatigue are likely to occur. Initially, a finite element model was created to determine the location and magnitude of the highest stresses. The model was then validated with the results obtained during practical tests. A fatigue assessment was then performed to estimate the likely life of a cracked arm under normal operating conditions. This informed the creation of a Non-Destructive Testing (NDT) schedule for all rides of this type.

The assessment of the radial arm actuation and prevention of uncontrolled descent work package aimed to identify means of reducing the risk of serious injury to passengers from failure of the actuation system, resulting in radial arm descending in an uncontrolled manner. A design assessment of the existing pneumatic arrangements was conducted to establish whether the various rides employ a typical configuration, or if significant differences exist in the way the systems operate. This includes the pneumatic conditions (i.e. flow rates, volume etc., during both normal operation, and during failure conditions). An assessment of the potential failure modes was also conducted. Subsequently, a market survey was conducted to determine if there are any commercially available solutions or technology, either mechanical, pneumatic, or hydraulic that may be applicable to the existing designs.

The passenger safety and ergonomics work package used acceleration measurement data and video recordings to build up an understanding of the movement of the passenger seat on the ride, in order to establish what restraint/containment systems are appropriate, and whether the ride can present a risk of spinal injury. The ride motion information provided HSL with the data necessary to assess the ride against the requirements of BS EN 13814 (1) for passenger safety.

A key requirement of all three of the work packages was that data would be needed to carry out each work package to provide the necessary evaluations. There were three types of data required by the individual work packages. Work package 1 required strain gauge data and acceleration data in order to validate computer modelling of the device. Work package 2 required dynamic performance data and details of control inputs to allow an evaluation of the



behaviour of the ride and understanding of its performance. Work package 3 also required similar dynamic performance data in order to allow the ergonomic and passenger safety assessment. For this element of the work, dynamic performance data was required in the form of passenger seat acceleration data. These data sets could only be obtained during operation of a Safeco Crazy Frogs-type device. A number of options were explored as to how and where this could be done. Subsequently, it was decided that a series of tests would be conducted on a device provided under contract to HSL by a Mr R Wilkinson. This testing also allowed more detailed examination of the Safeco Crazy Frogs device, providing more information for the 3 work packages and enabling detailed understanding of the operation of the device.

A further stage of the project, following on from the structural assessment, was to provide a suitable NDT (Non-Destructive Testing) schedule for the Safeco Crazy Frogs-type ride. The aim of an NDT schedule is to ensure that the correct areas of an amusement device are inspected, that the inspections occur with the correct frequency, and that the correct procedures are followed. This was to be provided by a third party specialist, contracted to HSL.

Further detail of these activities follows.

### **3.2 REVIEW OF EXISTING INFORMATION**

Previous HSL reports and information were obtained; video footage and acceleration data were collated and reviewed for relevant information. This allowed HSL to determine the extent of variation in Safeco Crazy Frog amusement device characteristics, i.e. passenger containment. This work is summarised in Section 4.1 with further details provided in Appendix 6.1.

### **3.3 EXAMINATION OF SAFECO CRAZY FROGS DEVICES AT NOTTINGHAM GOOSE FAIR**

Two HSL researchers visited the Nottingham Goose Fair on 5th October 2012, in order to collect information on the Safeco Crazy Frogs-type amusement devices present. Also present was Mr Melvin Sandell (HSE Operational Policy, Entertainment & Leisure sector). During this visit, relevant measurements of four Safeco Crazy Frogs amusement devices were taken, including overall dimensions of the arms of the device, physical dimensions of the seating and passenger restraint system. The visit was made to establish if there were significant differences between different manufacturers' amusement devices as well as, if possible, a typical overall design and control system arrangement to inform the basis of the remaining stages of this project. Video footage was recorded of the devices in operation.

### **3.4 EXAMINATION AND TESTING OF A SAFECO CRAZY FROGS DEVICE**

Tests were conducted on an example amusement device to determine the structural, control system and operating characteristics (motion pattern, accelerations, cycles, etc). The DJ Jump amusement device (Manufacturer: Safeco; Model: Saltamontes 2000-P; Series: 900429) was made available by Mr Robert Wilkinson at his base site, with an operator to control the amusement device at all times (Figure 2). A total of five HSL researchers were involved in the site visits on 19<sup>th</sup> to 22<sup>nd</sup> November 2012.



**Figure 2** Mr Wilkinson's DJ Jump amusement device in operation

The testing program undertaken was devised in order to develop HSL's understanding of the device characteristics and capabilities. This was in order to establish what aspects of its operation warranted further consideration, and starting from a 'typical' device set-up. Although each measurement period typically lasted 11 minutes, there was a considerable amount of time involved in set-up for a measurement period, and in preparing the instrumentation for extraction of the collected data, particularly for those with the passenger car loaded. On the first day five measurement test runs were completed, seven on the second day, and 10 on the final day.

Testing comprised of instrumentation and video recording of the device during 22 test runs. All runs comprised the complete amusement device program function list (described in detail in Section 4.7 in Table 5) performed in the same order for each test run, unless otherwise stated (see Appendix 6.1). During each test run the operating pressure and timing of the manual foot pedal operation were varied. Also, different load configurations were tested, e.g. with an instrumented arm unloaded for initial trials and then loaded with 160 kg to replicate a passenger load (two diametrically opposite cars/arms were loaded to balance the ride). Where the amusement device was operated with a representative load (Figure 3), the weight of all load sacks was checked before use with a calibrated suspension scale. All sacks were found to be within 1 kg of 25 kg. To reach the desired total weight, two 10 kg sacks were added, checked using a calibrated Mecmesin 1000N force gauge.



**Figure 3** Representative load of 160 kg

### 3.4.1 Video footage

Each test run was video recorded. Figure 2 is an external overall view of the amusement device operation, captured via handheld digital camcorder; Figure 4 shows the additional perspectives captured: Figure 4a is an additional view of the amusement device, captured using a tripod mounted digital camcorder; Figure 4b is a view of the operator's control panel, captured using a handheld digital camcorder.

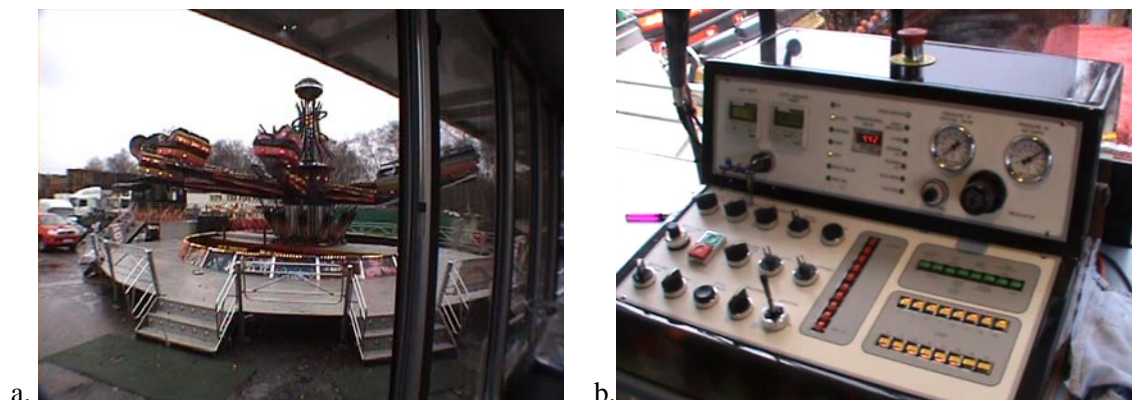


**Figure 4** Additional camera views

### 3.4.2 Instrumentation of the passenger carrying arm

Instrumentation of an arm was essential to provide quantitative data to inform the assessment of the amusement device ride motion characteristics both in terms of passenger safety and fatigue analysis.

Two accelerometers and two strain gauges were fixed to arm 12 of the DJ Jump amusement device and connected to a data logger (Figure 5). One strain gauge was positioned on the top of the arm, between the apex and the seats, approximately 600 mm from the apex. The axis of the strain gauge was orientated along the length of the arm to measure longitudinal strains. The second strain gauge was positioned on the underside of the U section support beam, as shown in Figure 5. The two accelerometers were fixed on the side of the arm: one just above the ram position and the other near the end of the arm below the seat. An additional stand-alone accelerometer was fixed above the ram on the other side of the arm for some of the test runs. A

single accelerometer was fixed onto the seat pan of car 12 to collect data specifically for the passenger safety element of the work. Details of the instrumentation used are listed in Table 2.

For the purposes of the finite element modelling and fatigue analysis, the instrumentation had three main aims:

1. **To establish the linear relationship between acceleration and strain.** Under sudden acceleration it may be possible for the arm to stop at the ram location but continue moving at the end while the arm flexes. This would cause the strain and acceleration measurements to be non-linear and out of phase, and require a dynamic finite element model to capture the full arm behaviour. A linear strain/acceleration relationship would allow a much more efficient quasi-static model to be used.
2. **Validation of the finite element model.** Validation of computer models is important to establish confidence in the results. Having data for strain gauge and acceleration enables the relationship between strain (and therefore stress) and acceleration to be obtained. Good agreement between the strain/acceleration relationships obtained experimentally and using finite element analysis would validate the approach used.
3. **To obtain load cycle data for the fatigue analysis.** The fatigue analysis requires the number and magnitude of the load cycles to be known. Therefore, acceleration data must be recorded from representative test runs to enable the fatigue calculation.

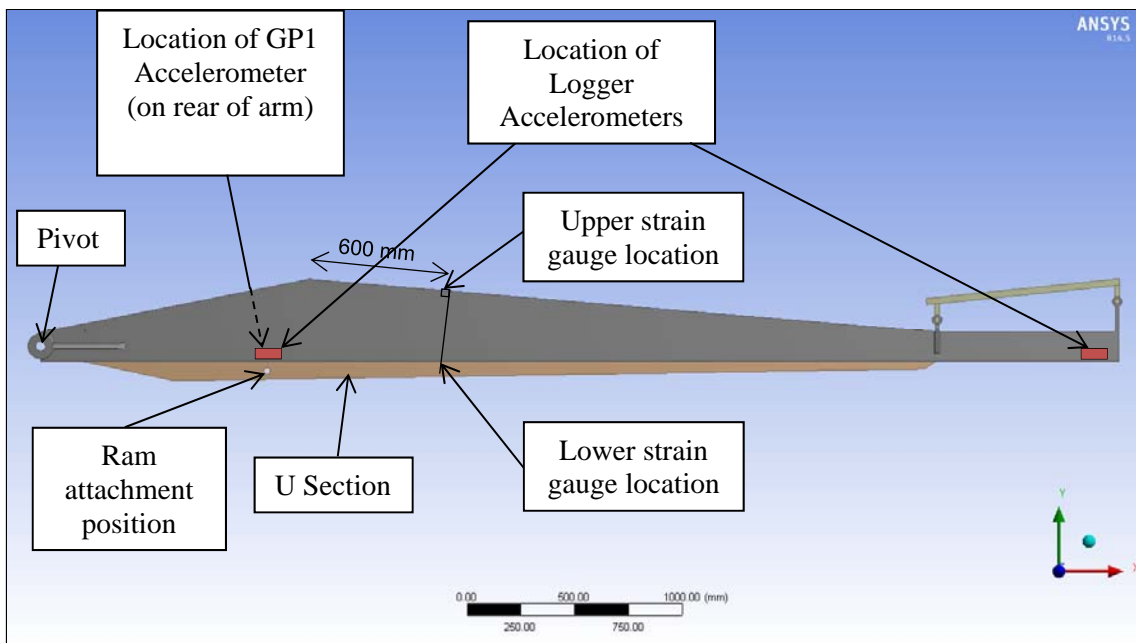


**Figure 5** Schematic diagram of arm with locations of instrumentation

### 3.4.3 Arm fall to hard stop (ram exhaust valve adjustment) and foot pedal operation investigation method

Due to the nature of the control system, the fall to hard stop event could not be replicated without risking damage to the amusement device (see section 4.2.1). The aim was to drop the arm through a very small distance initially, and incrementally increase the drop distance whilst recording strain and acceleration data. This could not be achieved, because the only manual control to drop the arm was the foot pedal/free-fall function, which we discovered would not

operate when the arm was raised by a small amount. The only way to set the arm into a low starting position for a drop was to set the operating air pressure low (< 3.5 - 4 bars). However, the pedal would not trigger the free-fall function at such low pressures. As a result the stresses and accelerations arising from this event could not be measured in the way anticipated. It was possible to investigate the performance of the 'air cushion' at the bottom of the pneumatic ram stroke under different conditions. This required the careful manual operation of the foot pedal at operating pressure at the minimum for the pedal/free-fall function to work (approximately 4.5 bar), and with the operator controlling the arm bouncing movement to achieve as low a travel as possible without risking damage to the amusement device. The screw adjuster position for the exhaust valve was incrementally adjusted between tests.

#### **3.4.4 Amusement device motion assessment method**

In order to take measurements of the amusement device motion, a tri-axial accelerometer (SENSR GP1, SN: SR002366) was attached to the seat of passenger car No. 2 (Figure 3d). This accelerometer was orientated such that its coordinate system was as indicated in Table 1. The output from the accelerometer was logged in accordance with BS EN 13814:2004 (1).

The coordinate axis system for the passenger seat accelerometer had its reference plane X and Y aligned with the seat pan. This is in accordance with the methods described in BS EN 13814:2004 (1). In the case of the Wilkinson's DJ Jump device, the seat pan is inclined at an angle of 14°-15° rearwards from horizontal. The acceleration due to the vertical movement about the pivot point, without the contributions from the rotating motion and gravity, were calculated, allowing for the seat inclination. More details of the adjustments can be found in section 4.10.6.1 and Table .

To assist in the understanding of acceleration exposure that is referred to in this report and its effects on a passenger, the following guidance is provided. The BS EN 13814:2004 (1) uses the unit of g-force for acceleration, expressing acceleration relative to free-fall. This unit is commonly used in the area of human tolerance to acceleration and will be used within this report. 1g is equivalent to 9.81 ms<sup>-2</sup> which is the magnitude of acceleration produced by gravity. All g-forces (accelerations) are described relative to the seat position (i.e. relative to the position of a seated person). For example, a positive g-force in the X-axis represents forwards acceleration, giving a passenger the sensation of being pushed back against the seat back, regardless of the orientation of the amusement device relative to the ground at that point in time.

**Table 1** Descriptions of accelerations

<b>Axis</b>	<b>Direction of acceleration (g)</b>	<b>Description of g-force accelerations on the amusement device</b>
<b>X</b>	Fore / aft	Positive (+gX) Device accelerating in a <u>forward</u> direction, in relation to the seat orientation
		Negative (-gX) Device accelerating in a <u>backward</u> direction, in relation to the seat orientation
<b>Y</b>	Side to side	Positive (+gY) Device accelerating to the <u>left</u> hand side in relation to the seat orientation
		Negative (-gY) Device accelerating to the <u>right</u> hand side in relation to the seat orientation
<b>Z</b>	Up / down	Positive (+gZ) Device accelerating <u>upward</u> in relation to the seat orientation
		Negative (-gZ) Device accelerating <u>downward</u> in relation to the seat orientation

**Table 2** Summary and specifications of measurement equipment

<b>Location</b>	<b>Equipment</b>	<b>Range</b>	<b>Sampling rate</b>
Side of arm above ram attachment point*	Sensr GP1 triaxial accelerometer (SN: SR002199)	±10 g	100Hz, internally filtered at 45Hz
On seat	Sensr GP1 triaxial accelerometer (SN: SR002366)	±10 g	100Hz, internally filtered at 45Hz
On side of the arm near end (under seat)	Entran EGCS3-A triaxial accelerometer (SN: Z00400)	±25 g	
Side of arm over ram attachment point	Spectrum 34200B triaxial accelerometer (SN: 1653A00505)	±25 g	
Strain gauges on top of arm and underside of U section	Gauges: Vishay L2A-06-062LW-120 Amplifiers: RDP DR7DC	-	
	Logger: (SN 43FF7205) DATAQ DI710-ULS running at 200Hz per channel	-	200Hz per channel (8 Channels)

## 4. RESULTS

The outputs of this study are presented in the following 10 sections.

### 4.1 REVIEW OF EXISTING HSL INFORMATION

Seven previous reports were identified as relevant:

- Boocock MG. A biomechanical appraisal of anterior wedge fractures of spinal vertebrae following an incident at a fairground ride. Sheffield, United Kingdom: Health & Safety Executive Research and Laboratory Services Division; 1992. EBS/92/7,(2);
- Jackson JA. Ergonomics assessment of selected amusement rides at Tilburg Fair, Holland. Sheffield, United Kingdom: Health and Safety Laboratory; 1995. Report No.: EWP/95/20, (3);
- Monnington S, Jackson JA, Milnes E. Passenger containment on a Jump and Smile fairground ride. Sheffield, United Kingdom: Health and Safety Laboratory; 2000. Report No.: ERG/00/12, (4);
- Jackson JA, Monnington SC, Boorman C and Milnes E. (2002) Establishing criteria for safe g-force levels for passenger carrying amusement rides HSL/2002/07, (5)
- Milnes E. Assessment of g-forces on Jumping Frogs ride. Sheffield, United Kingdom: Health and Safety Laboratory; 2004. Report No.: ERG/04/02, (6);
- Milnes E. Assessment of g-forces in the Crazy Frog amusement ride. Sheffield, United Kingdom: Health and Safety Laboratory; 2004. Report No.: ERG/04/20, (7); and
- Milnes E, Marlow P, Bunn J, Ferreira J, Jones A, Birtles M, et al. Passenger Behaviour on Amusement Rides: Field Study Report. Sheffield, United Kingdom: Health and Safety Laboratory; 2004. Report No.: ERG/04/24, (8).
- Joel S. Examination of items from the Crazy Frog fairground ride, Central Pier, Blackpool. Buxton: Health and Safety Laboratory; 2010. Report No.: ES/MM/LET/10/22, (9).

In addition, data was available from a reactive support project where HSL measured the acceleration characteristics as part of an HSE incident investigation, but did not provide a written report.

- PH05060 [No report] (Crazy Frog: Cambridge, 2009)

#### 4.1.1 Previous acceleration measurements

Acceleration data was not collected during the visit to Tilburg Fair (3), or the Monnington, et al. (4) examination of the Jump and Smile amusement device. Table 3 shows the minimum and maximum Z axis accelerations recorded during the course of HSL's previous work. As can be



seen, the maximum acceleration observed in HSL’s previous work was 4.6 g. A more detailed summary of previous data, is in Appendix 6.1.

**Table 3 Peak Z axis accelerations reported in previous work (g)**

	Minimum	Maximum
ERG/04/02 - Jumpin’ Ride: Glasgow (6)	-1.7	4.1
ERG/04/20 - Jumpin’ Ride: St Andrews (7)	-0.4	4.6
PH05060 – Safeco Crazy Frog: Cambridge	-0.02	4.5

#### **4.1.2 Previous passenger restraint system design**

Previous data regarding passenger containment and restraint systems is presented later in this report in Table 11; additional information is summarised in Appendix 6.1.

#### **4.1.3 Previous considerations of spinal injury risks from seat-to-head acceleration**

Scientific knowledge in this area is based on cadaver and military volunteer studies conducted from the 1940s to 1970s. For a description of the information reviewed, see Appendix 6.1 and Pinder (10).

The previous HSL reports relating to amusement device safety and spinal injury by Boocock (2) and Milnes (6;7) reviewed some of the scientific evidence on the response of the human spine to vertical (seat-to-head) acceleration. These HSL studies concerned two incidents where individuals were alleged to have sustained different vertebral injuries, Anterior Wedge Fracture (AWF) and Burst Fracture (BF) respectively. In particular, the work of Milnes (7) and the HSL measurements were in relation to reported injuries on Safeco Crazy Frogs devices (Table 3). Measurements of the devices in question, which did not have a free-fall/pedal function, indicated peak seat-to-head accelerations of 4.1 g to 4.6 g. The peak values were measured during a program producing small amplitude, high frequency motions, similar to those seen on the Wilkinson DJ Jump (see Table 5, Program 1 / D).

Kazarian (11), cited in (2), reports that vertebral fractures are associated with axial (compressive) loading, and occur mostly in the thoracic-lumbar region. More specifically, they are reported to be associated with high impact events, such as landing from a jump from height, high loading on the shoulder girdle, and vehicle accidents (Willen, Anderson, Toomoka, and Singer (12), cited in (7)).

In the historical literature, Glaister (13) states that human injury tolerance to short duration (less than 1 second) vertical acceleration while seated is determined by the mechanical strength of body tissues, but the nature of the internal forces leading to injury will depend on characteristics of the applied acceleration pulse, and the dynamic response characteristics of the human body.

From the information reviewed, the critical variables for fractures from seat-to-head acceleration appear to be:

- Characteristics of the applied acceleration
  - Rate of onset of acceleration (jerk/jolt)



- Magnitude
- Repetitive exposures and their frequency (cycles)
- Dynamic characteristics of the seat material
- Characteristics of the human body influencing dynamic response and the magnitude of transmitted force
  - Body mass (influencing the force transmitted through the spine)
  - Body posture (influenced by seat and restraint design)
  - Muscle tone and reaction time in response to acceleration exposure
- Relative strengths of the spinal structures involved and any predisposing factors
  - Body posture, predominantly the extent of forward trunk flexion influencing the nature of the loading within the spine
  - Individual factors (bone mineral content, cross sectional area, age, gender, degeneration, acquired defects, etc)

#### **4.1.3.1 Existing sources of guidance on limiting seat-to-head acceleration**

In relation to the effect of posture on the natural frequency of the human body, Glaister (16) noted that a seated man has a natural frequency in the region of 5.5 Hz and presents a graph in his paper (13) showing human tolerance to vertical impact. For an unrestrained seated occupant, the tolerance line is level at 5 g between durations of 0.1 and 1.0 s. For durations shorter than 0.1 seconds, the line slopes upwards to accelerations exceeding 100 g for very short duration impacts of 0.001 s. The plateau at 5 g between 0.1 s to 1.0 s is considered to be most applicable to the Safeco Crazy Frogs.

Tolerance in this context relates to survivability of military personnel, and of having reversible injuries. Tolerance in these circumstances is largely determined by the compressive strength of the spine which is transmitting the force necessary to accelerate the upper body (i.e. when the seated body is being accelerated upwards). Clearly a level of acceptability for amusement ride occupants will be at a level somewhat below those indicated by these studies.

The NASA Bioastronautics Data Book Chapter 6 (14) presents a graph for ‘survivable abrupt vertical impact’ collating data from several sources, including experimentation on animals and humans, based on data from Eiband (15). However, one data source is for voluntary human exposures (uninjured, undebilitated). The upper limit of acceleration tolerance for this data is at around 15 g for durations less than 0.05 s, dropping to 10 g at 0.1 s and 5 g at 0.15 -0.2 s. This therefore overlaps and is broadly consistent with the information from Glaister (13;16).

Sources of guidance for amusement devices identified by Jackson (5) and Milnes (7) in previous work are:

- RWTUV (17), Fairground Rides Attractions with Calculated Safety (no longer available);
- AS 3533.1 (18), Amusement Rides and Devices Part 1: Design and Construction. Appendix D: Basic Facts on the Effects of Acceleration on the Human Body.

Table 4 presents the acceleration level criteria from these sources along with those from the current ASTM and BS EN Standards.

**Table 4** Ride acceleration (g) criteria as extracted from the RWTUV, AS 3533.1 2009, ASTM F2291 11, and BS EN 13814 2004

Source	Z axis	
	Max	Min
TUV lower	4	-1.5
TUV upper	6	-2
AS 3533.1 (18)	None stated	None stated
ASTM F2291 11 (19)	6	N/A
BS EN 13814 (1)	6	-2
Glaister (13, 14) and Snyder (14)	5	N/A

BS EN 13814 (1) Annex G present guidance on tolerable acceleration levels for amusement ride passengers. In relation to vertical acceleration (z axis) it presents the following graph (Figure 6). The Standard states that the general limits presented are intended to prevent neck vertebrae injuries in rollercoasters with guided vehicles or similar . The accelerations stated are for a reference point 60 cm above the seat surface (this will not influence their applicability in the context of the Safeco Crazy Frogs device). The standard states that when impact forces are involved (these are not defined in the Annex), it is recommended to reduce the permissible values by a minimum of 10%. It may therefore be reasonable to consider a limit of 5.4 g for short duration vertical accelerations in relation to the Safeco Crazy Frogs device.

The ASTM F2291 11 (19) also presents acceleration limits which apply to accelerations of duration greater than 200 ms and less than 90 s (it defines impacts as accelerations of less than 200 ms). It also states that the limits apply to passengers larger than approximately 1220 mm in stature (48 inches).

The limits are presented in the form of a graph identical in profile to that presented in Figure 6 from BS EN 13814 (1) above. In relation to transitions from negative to positive z axis acceleration, the standard specifies that if the transition is from zero g or less to 2 g or more, the rate of change of acceleration should not exceed 15 g/s (a prerequisite for this statement is that the 1 g of gravity is aligned with vertical seat-to-head z axis of the passenger (i.e. an accelerometer reads 1 g in the z axis at rest). Apart from the BS EN, the other guidance sources do not state an intention to be protective for vertebral fractures.

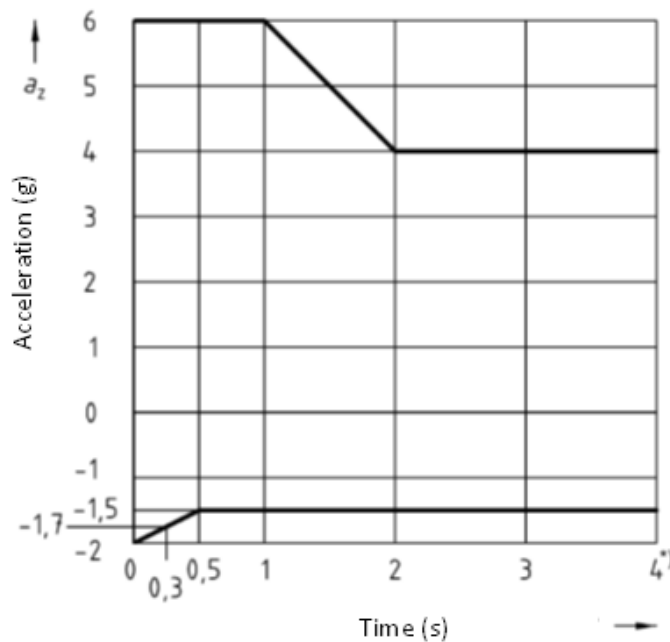


**Figure 6** Permissible vertical acceleration related to duration (s).  
Reproduced from BS EN 13814 Figure G.3.

Key \*) The area >4 s is not proven and requires further examination

#### 4.1.3.2 Summary on protective levels for seat-to-head acceleration

Boocock (2) suggests that it is difficult to specify acceptable (protective) levels of acceleration for amusement devices because of the variability in individual factors. The causality of spinal injury is complex and multifactorial, and there are difficulties associated with applying the results of scientific studies to predict outcomes in situations involving amusement device passengers.

The same acceleration exposure will mean different risks for different people, in different postures; there is therefore difficulty in generalising. The primary causal factor for spinal injury related to seat-to-head acceleration exposure is the force generated within the spine. The magnitude of the force resulting from a particular level of acceleration is not the same for everyone. It is influenced by posture and individual body mass. Whether or not the force generated within the spine will cause an injury is influenced by individual factors such as age, gender and bone mineral density.

Because of the range of uncertainty in these factors, producing estimates for protective acceleration levels is difficult as the range of vertebral strength appears to be very wide. The guidance contained in the sources referred to above represents the best information currently available. An upper limit of around 5 to 6 g appears to be the consensus for seat-to-head acceleration for events of longer than 0.15-0.2 s duration. However, it is not clear whether these sources are protective of young and older passengers, as the levels appear to be consistent with a basis in adult and military data. Peak positive z axis accelerations measured on amusement devices associated with injuries have been in the region of 4.1 to 4.6 g.

The key weakness in the data reviewed in this project, in relation to being able to recommend safe levels (and characteristics) for amusement device passenger accelerations, are the limitations of the source evidence in terms of how it applies to living people of a wide age range and physical condition. In particular, we do not currently have spinal injury information relating to children. Therefore any levels suggested as protective for adults may not be protective of children. Also existing data does not include consideration of people in the population over 60 years old.

Boocock (2) makes a valid observation that if vertebral fractures are the first kind of injury to be reported, i.e. before any pattern of ligamentous/muscle injuries or complaints of pain and discomfort, presumably amongst many thousands riders, then there is potential that the individuals concerned may in some way be predisposed to injury, or have otherwise been exposed to the effects of the accelerations in an untypical way.

## **4.2 DESCRIPTION OF THE AMUSEMENT DEVICE AND THE OPERATOR CONTROLS**

### **4.2.1 Description of arm mechanism**

Each of the 12 ride arm mechanism consists of three main components: the main arm; pneumatic ram; and passenger car, which are attached to the central hub of the device. These are shown in Figure 7. The inner end of the device arm and both ends of the pneumatic ram are connected to the central hub with pinned joints; this allows the arm to pivot about the inner end as the pneumatic ram extends and retracts. This action results in the passenger car, which is connected to the outer end of the arm, raising and lowering as the pneumatic ram extends and retracts. It can be seen from the position of the components in Figure 7 that, as the arm raises and lowers, the passenger car and passengers will travel along an arc in the vertical plane, while also rotating clockwise (forwards) or anticlockwise (backwards) around the central hub.

The central hub provides for the rotation of the ride, the arms being pinned to the hub in such a way that while the arm can pivot vertically, the arms have no freedom to rotate about the hub and will therefore accelerate and decelerate in conjunction with the central hub. The pneumatic actuator also has an air-cushion damper built into the bottom of the cylinder. This feature has two functions - partially acting as an air spring while also acting as a damper. The spring function results from some air being trapped within the cylinder while the damping is the result of some air being expelled and hence absorbing some energy. This spring damper works independently of any other controls and is an integrated part of the cylinder design. The damping of the cylinder occurs when the piston reaches a position near the base of the cylinder. The position of this spring damper cannot be adjusted as it is set by a machined feature in the cylinder. However, the effectiveness of the damper can be adjusted by means of an external bleed screw at the base of the cylinder. This adjustment varies the rate at which air can exit the cylinder when the piston has reached this position near the base of the cylinder and acts independently of the normal cylinder vent.

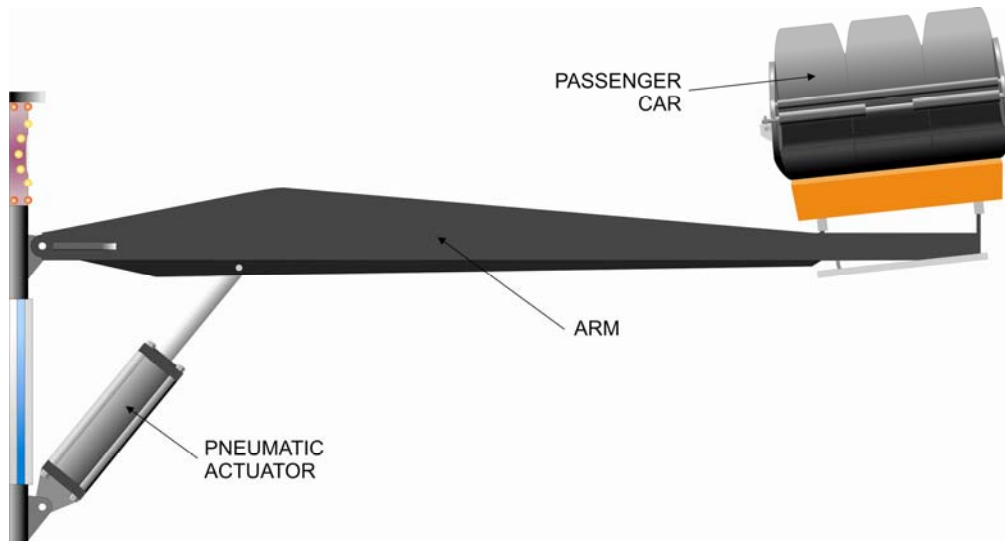


**Figure 7** Safeco arm mechanism

#### **4.2.2 Description of amusement device, operator controls**

The amusement device is controlled by the operator via a control panel as shown in Figure 8, as well as an adjacent foot pedal. The control panel has a number of controls and indicators, which the operator can select in order to control the function status of the device. The control panel has a number of control functions including a key switch to enable and disable the ride operation, a start/stop button which controls the rotation, an emergency stop button, passenger car lap-bar interlock controls, as well as adjustment of the operating air pressure supplied to the ride actuators and indication of the stored air pressure. The panel also allows the operator to individually select which arms and passenger cars are activated.

The operator can select a number of pre-programmed ride cycles or a combination of pre-programmed cycles, combined with user input via the foot pedal control. The programme control switch selects one of two sets of programs. The joystick is then used to select and activate one of eight sub-programs by either a single touch of one of the four joystick positions or a double touch, making a total of 16 possible pre-programmed cycles. These pre-programmed cycles control the vertical movement of the arms and passenger car. Each of the above pre-programmed cycles provides the device with different timing and sequence of operation of the 12 passenger cars. This control results in a range of patterns of movement of the 12 arms and passenger cars, including an alternating pattern, a synchronised pattern and a wave pattern. The pre-programmed cycles also control the range of vertical movement of the passenger cars.

There is a further pre-programmed cycle, the 'free fall' program. This is activated by an individual push button switch. This program raises all the passenger cars simultaneously to their highest position. Once at this height the passenger cars can 'free fall' simultaneously, on activation of the foot pedal control. It is understood that not all Safeco Crazy Frogs devices are fitted with the free fall and foot pedal control. The foot pedal operates in two positions, on and off, with no proportional control. Thus as the pedal is pressed, the arms and passenger cars are allowed to descend, and when the pedal is released the cars' descent will be retarded. The duration of the descent is controlled by the timing of the operator's foot control. This foot pedal operation can be repeated successively, the number of activations of the foot pedal also being

determined by the operator. This form of control would appear to be commonly conducted in combination with the free fall programme. However, the foot pedal control can be activated independently of the free fall, as long as sufficient air pressure is available.

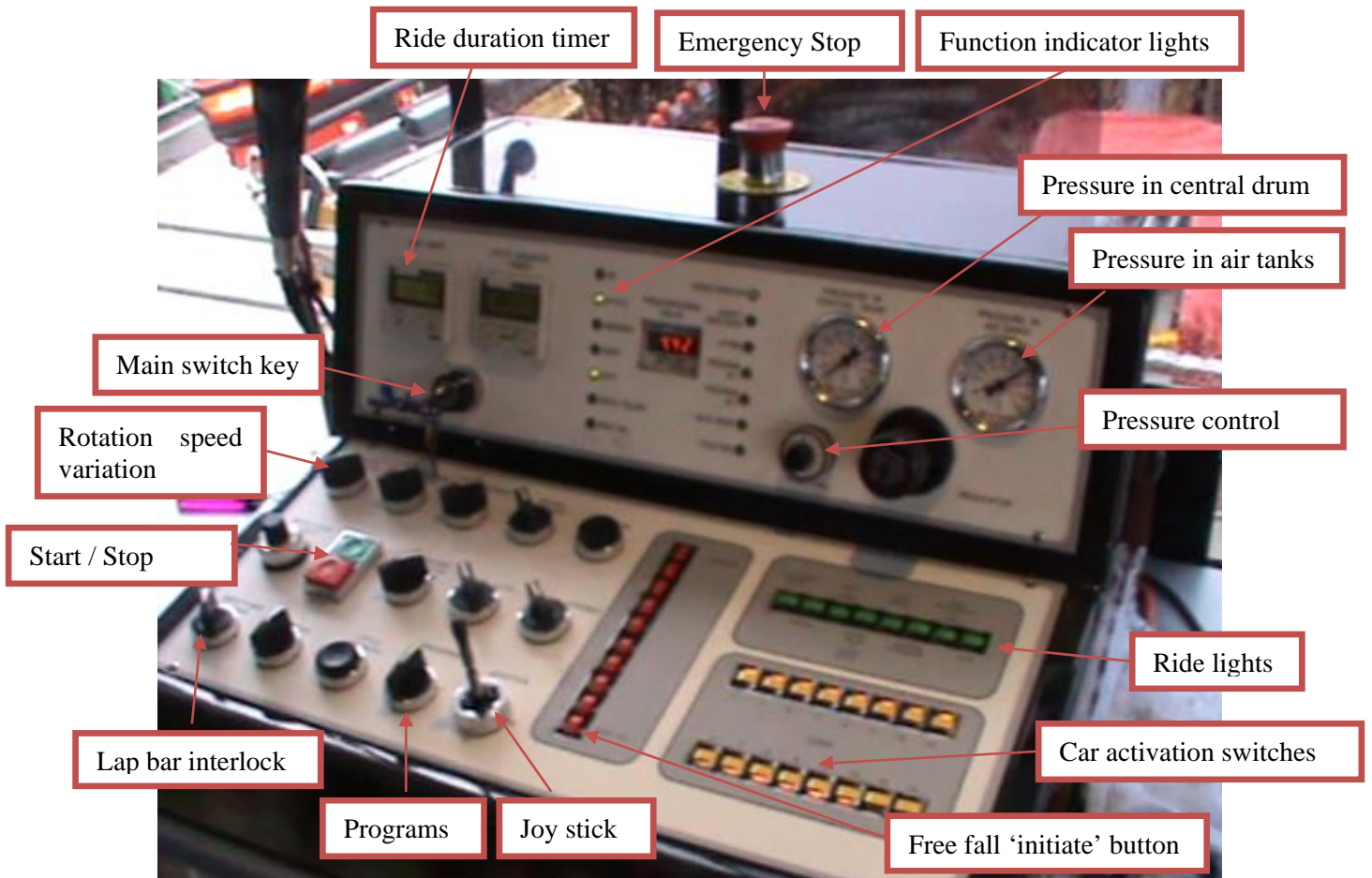


**Figure 8** DJ Jump operator control panel

The order in which these pre-programmed cycles is selected, and for how long, is at the discretion of the operator, as is the timing and duration of the pedal control. Typically it would appear that this type of device would provide a passenger ride of approximately five minutes, comprising a number of the pre-programmed cycles and free fall combined with foot pedal actuation. It should be noted that the ride controls of rotation and vertical motion are controlled independently, and require separate activation by the operator. Thus, each motion can be operated independently, i.e. the arms and passenger seats can bounce without any rotation of the central hub, and vice versa.

### 4.2.3 Description of amusement device control system

The amusement device is controlled and actuated by the five main components below:

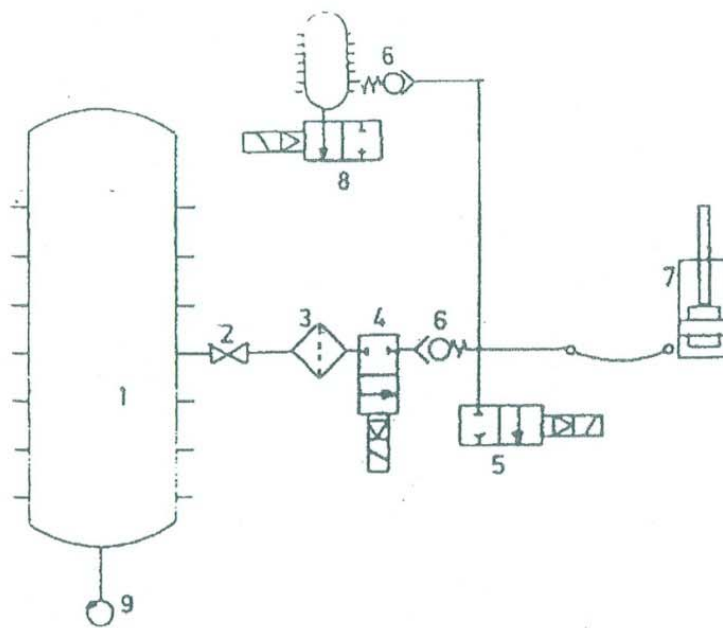
- Control panel and foot pedal;
- PLC – (programmable logic controller);
- Pneumatic control valves and associated circuits;
- Pneumatic actuators; and
- Proximity sensors.

The control panel and foot pedal, as described above in Section 4.2.2, allow the operator to select a pre-programmed cycle and interact with the control system including the PLC. Once the operator has selected a particular cycle, the PLC follows an internal logic-based program which performs the control sequence required to operate the other control devices, i.e. the pneumatic valves, which in turn activate the required sequence of movements via the pneumatic actuators. The main control of the arm is activated by the pneumatic circuit shown in Figure 9. The PLC provides the timed sequence of control signals individually to the 12 sets of pneumatic control valves, such that the desired pattern of movement of the 12 arms is achieved.

The pneumatic circuit, shown in Figure 9, comprises of two main valves connected directly to the cylinder of the actuator in order to control the extension and retraction of the ram. One valve is activated in order to extend the actuator under pressure, and a second valve allows retraction under gravity as the pressurised side of the actuator is vented. This ability to extend and retract the actuator from the normal operating position allows the control system to create the various patterns of passenger car movement, with simple alterations to the timing and direction of the actuator sequences. These sequences comprising jumps and dips as the actuators are extended and retracted. Similarly, as each actuator is controlled independently, the sequence of movement is controlled such that the overall pattern of the 12 cars can be timed to create different patterns. These variations in sequence and timing, when combined with the natural damping of the pneumatics and dynamics of the passenger car, form the motions created by the 16 pre-programmed cycles.

The control system is also provided with inputs from a pair of proximity sensors mounted adjacent to the pneumatic actuator, which indicates to the control system when the actuator is in one of two positions. These are shown in Figure 10. It is not understood whether these are linked via the PLC or hardwired into the control system.

The control system also has a foot pedal which is often used in conjunction with the freefall program, but can also be used when the device is operating in the normal mode. The foot pedal, when used, appears to override the timing and positional control of the control system. Application of the foot pedal results in the actuator exhaust valve opening when the pedal is pressed and closing on release of the pedal. It is not clear in this case if the actuator travel is limited by the proximity sensors or only by release of the pedal. The duration of actuating this foot pedal control appears completely at the discretion of the operator. This subject and the effect of the pedal control are discussed further in Section 4.4.1.4. It was noted during testing that the foot pedal would not activate if the air pressure control was not set sufficiently high enough.



## SECONDARY CIRCUIT

### LEGEND

Position	Denomination
1	Central collector
2	Stopcock
3	Filter
4	2/2 NC electrovalve (admission)
5	2/2 NC electrovalve (escape)
6	Poppet
7	Pneumatic cylinder
8	2/2 NC electrovalve (slow descend)
9	Revolving connector

**Figure 9** Safeco secondary pneumatic circuit diagram (20)



A control sequence is also used to perform the freefall program. This differs from the other pre-programmed cycles in that, when activated, this cycle controls a proportional valve which raises the set air pressure above that set by the operator on the control panel. This in turn raises the passenger cars above their normal operating position to the full extension of the actuators. When this position is reached, an indicator is illuminated and the operator can activate the simultaneous descent of the passenger cars with the foot pedal. When this cycle is complete the air pressure reverts back to that set by the dial on the control panel, and the cars return to the normal operating height.



**Figure 10** Proximity sensors

### **4.3 EXPLANATION OF THE INFORMATION COLLECTED**

The following results are based upon consideration of the information collected during the testing of Mr Wilkinson's DJ Jump amusement device. The results are described in detail in the following sections (4.4 to 4.9). However, a brief explanation of the information collected will assist understanding.

#### **4.3.1 Video observations**

Video recordings of the ride motion and the operator actions during the tests were an important record of the actual motion characteristics of the ride during the tests, as well as the operator inputs. The video recordings were not used alone, but in parallel with the instrumentation data for ride motion, using the [Observer® XT 10](#) (Noldus Information Technology) software program, to understand and assess the ride motion characteristics from the passenger perspective.

## 4.3.2 Measurements

### 4.3.2.1 Strain

Strain gauge data was logged from the two strain gauges attached to the arms for all the tests. The main purpose for collecting the data was to verify the finite element model. By comparing strain values obtained from the model to those obtained from strain gauges during testing, the accuracy of the model can be verified.

### 4.3.2.2 Acceleration

Acceleration data collected at the passenger seat was used to inform general understanding of the ride functionality, and to understand and assess ride motion characteristics from the perspective of passenger safety. Acceleration data collected at the arm locations was used alongside the strain gauge data to verify the finite element model (see section 4.10.4 for more details).

The raw passenger seat acceleration data was processed in accordance with BS EN 13814 and analysed using both Microsoft Excel 2010 and SigmaPlot® Version 12 (Systat Software Incorporated).

An example of the acceleration data collected at the passenger seat is presented in Figure 11 (see Appendix 6.3 for the full acceleration data set), along with an indication of the physical position or state of motion of the passenger seat in relation to the acceleration data. The acceleration trace of concern is that in the Z axis (seat-to-head direction, see Section 4.7) shown in green. The data for this axis includes the effect of gravity at all times, and this is manifest as (approximately) 1 g acceleration when at rest (instead of registering zero). The 1 g baseline when stationary is approximate because the seat pan is inclined backwards at all times, and is also subject to changing lateral inclination, during arm movement. As a consequence of the instrument recording the effect of gravity, the acceleration measurement made during movement of the ride effectively has a zero level at the 1 g line. Since the passenger experiences the effect of gravity, we want to include it, and do not correct for it for passenger safety purposes.

Our analysis indicates that the peak positive acceleration occurs when the passenger car vertical motion changes direction from down to up at the bottom of the arm movement stroke (car location 1), and the peak negative acceleration occurs when the vertical car motion changes direction from up to down at the top of the arm movement stroke (car location 3). The direction of the acceleration changes from positive to negative and vice versa approximately on the 1 g line (car location 2, with directions of movement indicated by the arrows on Figure 11).

Data for the X and Y axes is included for information. The X axis (forward-rearward) acceleration varies in phase with the Z axis acceleration and arises because the seat is tilted backwards, and so a component of vertical acceleration is included in the X axis. The Y axis (lateral) acceleration also varies in phase with arm movement and arises as the inclination of the car changes with each arc swept by the arm.

Consideration of the vertical acceleration (data from the passenger seat) was used to assist HSL's understanding of the functioning of the device and the effect of variables such as operating pressure; passenger loading, etc., (see section 4.4)**Error! Reference source not found.**

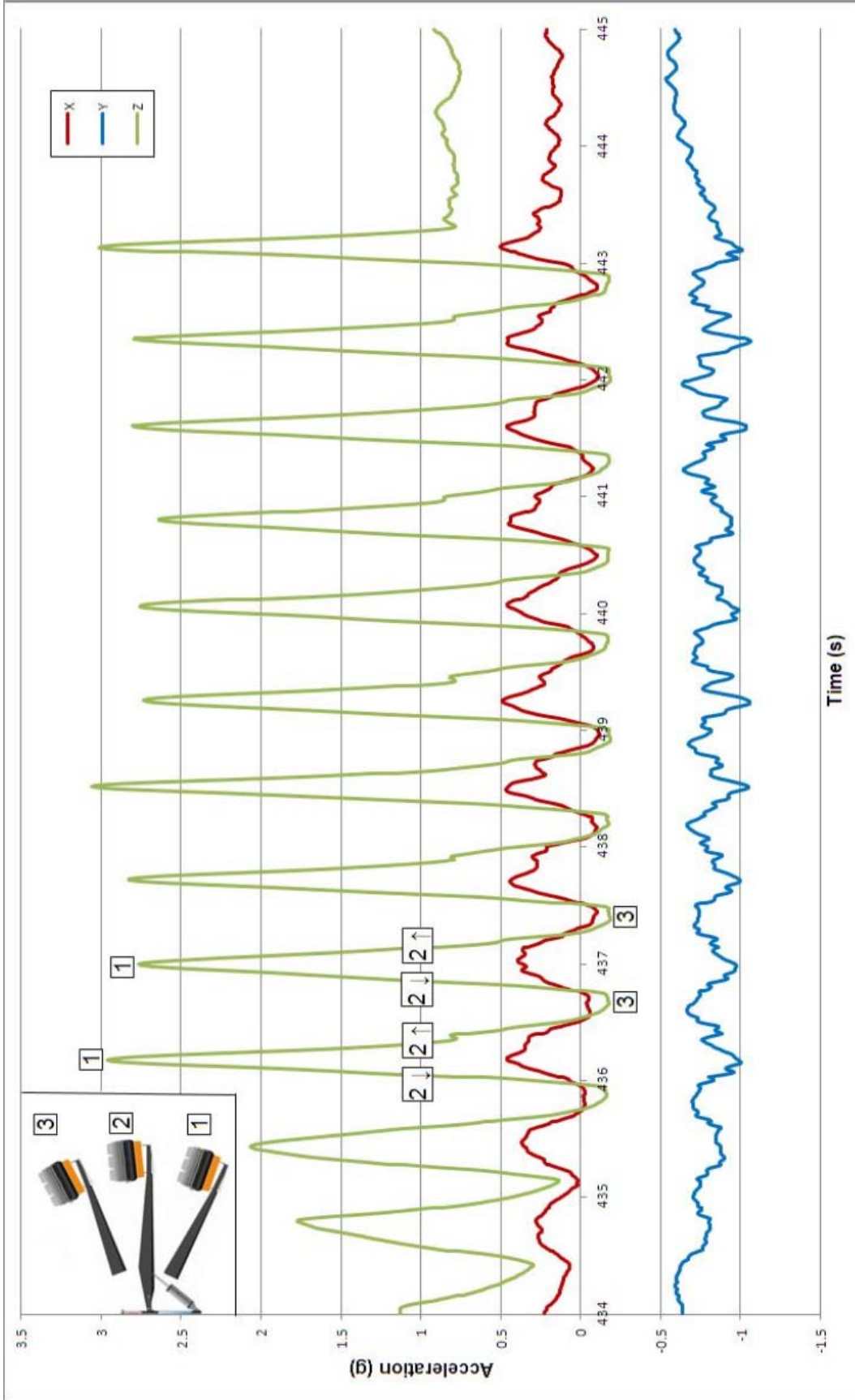


**Figure 11** A sample of acceleration data (Test Run 11, Program 1 A) indicating the pattern of seat-to-head acceleration (z axis) corresponding to ride motion. X and Y axis acceleration traces are included for information

#### **4.3.2.3 Frequency and rate of change of acceleration (onset rate)**

Frequency of vertical arm movement for the ride programs was calculated by dividing the time period of the program by the number of movement cycles recorded. Rate of change of acceleration (onset rate) for ride programs was calculated by taking an average of three graph slope figures for each program element. There were essentially only two programmed motion types. Both of these occur in Program 1 setting, and one occurs in Program 2 setting..

#### **4.4 INTERACTION OF RIDE CONTROL ELEMENTS AND COMPONENTS**

Assessment of the control system showed that there were a number of factors which could potentially influence the dynamic behaviour of the device. These are:

- Air pressure low and high;
- Passenger load;
- Passenger load and low air pressure;
- Damper exhaust valve adjustment;
- Number of cars in use;
- Central hub stationary, only one passenger car active;
- Use of foot pedal control; and
- Freefall operation.

A series of dynamic tests were conducted to investigate how these parameters affected the behaviour of the passenger car. These tests are described further in Section 3.4. The results are summarised below.

##### **4.4.1 Air pressure**

A number of tests were conducted to establish how the air pressure in the cylinders would affect the dynamic loads imposed on the passengers. The operator adjusts the air pressure control such that the cars are raised to a position where they can perform the programmed sequences without being too close to either the bottom or top of the actuator travel during the cycle. It was clear that this adjustment was dependent on passenger load. The operator did not refer to any factory recommended setting or instructions, but relied on personal judgement.

Tests were conducted with a lower operating pressure; this resulted in the car nominally operating in a lower position closer to the bottom of the actuator travel. It was anticipated that the car may reach the end of the actuator travel, resulting in impact and higher upward (seat-to-head) acceleration of the passenger car. However, the results showed that the peak accelerations were actually lower than those when operated at the 'normal pressure'. Test runs 4 and 5 show lower peak acceleration during the pre-programmed cycles than earlier test runs at a typical air pressure selected by the operator. These results are shown in Table 6. It can be deduced from this that the actuator was being retarded due to approaching the end of travel but, as the descent was from a lower starting point, the inertia is less, resulting in a more progressive deceleration.

Tests were also conducted at a higher pressure; this showed that, with the car nominally operating at a higher position, a higher upward acceleration could be achieved during the programmed cycle. Test runs 12 and 20 show higher peak acceleration during the pre-programmed cycles than earlier test runs at a typical air pressure selected by the operator. These results are shown in Table 6. This, it is deduced, is due to the greater retardation resulting from the higher pressure in the actuator acting on the passenger car with the same inertial properties.

While it cannot be shown exactly how the pressure affects the dynamic motion of the passenger, it is clear that the change in pressure can result in a change in performance of the amusement device, specifically the accelerations and therefore forces, to which the passengers are subjected.

#### **4.4.2 Passenger load**

The tests conducted show that the operator is required to adjust the air pressure depending on the passenger load in the cars. Clearly, heavily loaded cars will require higher air pressure than lightly loaded ones to achieve the same operating position. If a lightly loaded car is operated at a higher pressure, this is likely to result in greater accelerations than a fully loaded car at the same pressure, due to its lower inertia.

The difficulty presented by this variable from an operational point of view is that where differing passenger loads occur, it may not be possible to achieve a suitable compromise if, for example, one car was heavily loaded and one only lightly loaded. Ideally the loads would be distributed evenly, but this may be impracticable. If the air pressure is adjusted to suit an unevenly loaded set of cars and the pressure is set such that the lighter cars have an acceptable ride performance, the heavily loaded cars may not achieve a position where the ride performance is acceptable from an entertainment perspective, but would potentially be safer. However, if as is possibly more tempting for the operator, the pressure is raised to provide a more acceptable dynamic performance for heavily loaded cars, the lighter cars may be subject to unacceptable accelerations. While unloaded tests may be unrepresentative of working conditions, they do show that passenger load affects the ride dynamics and can increase the accelerations and forces.

#### **4.4.3 Interaction between passenger load and pressure**

If the passenger load is low or the air pressure high, there is potential for the actuator to become fully extended; this is discernible when operating the ride as a sound is made by the actuator reaching full extension. This motion could potentially affect passenger containment and is discussed further in Sections 4.7 and 4.8.

If the passenger load is high when combined with a relatively low air pressure, then it was anticipated that the actuator may reach the fully retracted position. However, when operated in the pre-programmed mode the control system would appear to prevent the actuator reaching the fully retracted position. The magnitude of the accelerations generated during the pre-programmed cycles is discussed in Section 4.7.

#### **4.4.4 Use of 'free fall' mode and foot pedal control**

Tests conducted with the device controlled using the foot pedal showed that it was possible to extend the range of free fall of the passenger car beyond the range achieved when used in the pre-programmed cycles. Tests were conducted with the passenger cars circulating in the normal operating position combined with the foot pedal operation, as well as tests with the free fall mode combined with the foot pedal operation. During the latter tests the foot pedal was activated for as long a duration as was acceptable to the ride operator. This resulted in a more vigorous operation of the ride and passenger cars than during the pre-programmed cycles. It was not possible to determine what would happen if the foot pedal was activated for sufficiently long to potentially allow the ram to reach the end of its travel, as it was considered potentially damaging to the ride. It was considered that the actuator could potentially retract fully, in an uncontrolled manner, resulting in rapid deceleration of the ride arms and potential overload.

However, it was possible to show that the device can generate higher upward accelerations when used with the foot pedal control than when used in the pre-programmed cycles. The results also show that, when used in freefall mode (2 Foot Pedal in Figures below), activation of the foot pedal can result in higher peak positive accelerations than when used in the normal mode; see Figure 12 and Figure 13. In particular, the rate of change (onset rate) of positive acceleration appears greatest following the freefall function (Figure 14). Onset rate is discussed in Section 4.1.3.

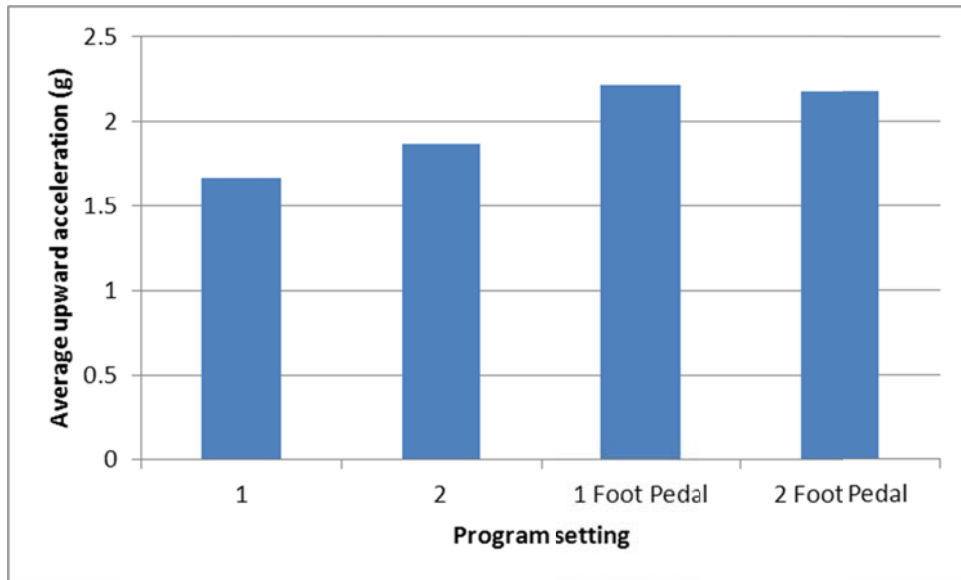


**Figure 12** Average positive acceleration for each program setting

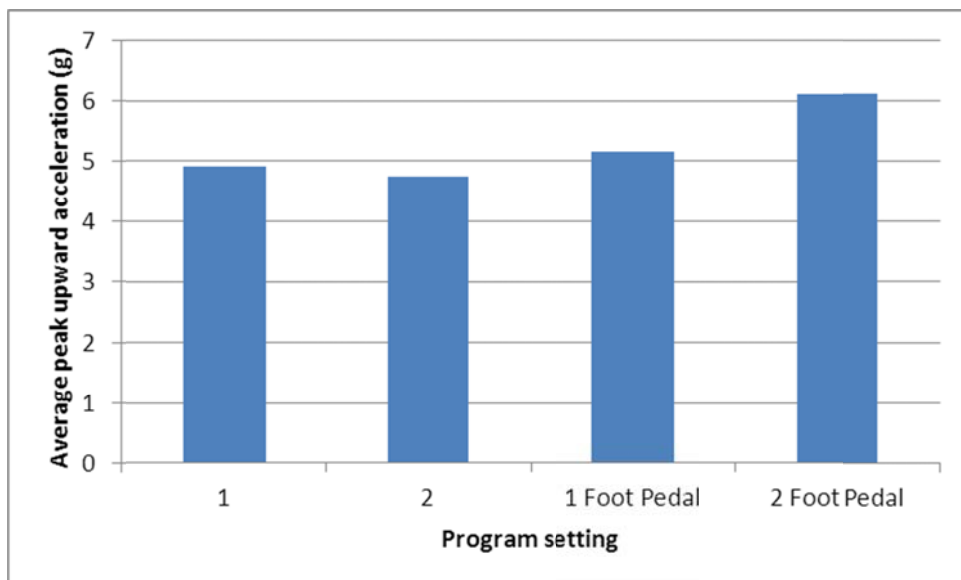


**Figure 13** Average peak positive acceleration for each program setting

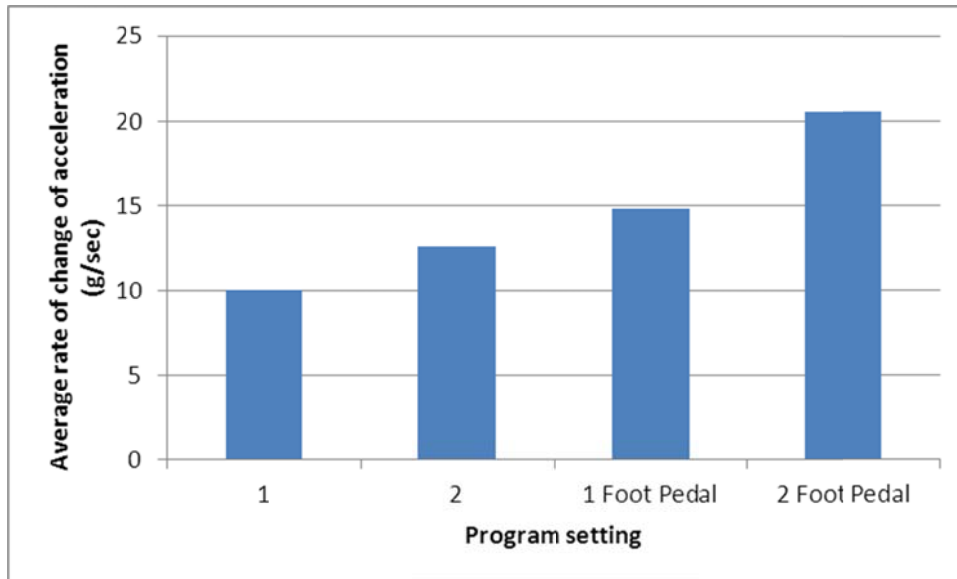


**Figure 14** Average rate of change (onset rate) of positive acceleration for each of the program settings

Use of the foot pedal control also required the operator to synchronise the activation of the foot pedal with the action of the passenger cars. If the timing of the pedal activation is irregular or out of synchronisation, the passenger cars will tend to rise and fall out of synchronisation with each other. While this loss of synchronisation may not be significant dynamically to individual car occupants, it does not allow the operator to observe and track the motion of all 12 passenger cars simultaneously. Therefore, it is possible that one car may be descending further than the others without being observed, indirectly resulting in the car and passengers being subject to increased dynamic forces. The distribution of passenger loads between cars may also have a significant effect on how easily the cars remain in synchronisation, although this was not tested.

The dynamics of the freefall and foot pedal control do not appear to have been considered by other assessments of this type of device.

#### **4.4.5 Central hub stationary, only one passenger car active**

Tests were also conducted to establish if the number of cars in use, or whether the central hub being stationary had any influence on the dynamics of the ride. It was not possible to determine any significant change in dynamics of the passenger car from these results.

#### **4.4.6 Pneumatic actuator bleed valve adjustment**

As explained previously (Section 3.4.2), the 'fall to hard stop' event could not be replicated without risking damage to the amusement device. A test was conducted in order to explore the effect of adjusting the lower actuator bleed valve (described in 4.2.1). This was done by making a number of adjustments to the valve ranging from fully closed to 1.25 turns out from closed. During the tests the ride was operated with the foot pedal control in order to attempt to use the full travel of the actuator. The results indicate a possible relationship between damper adjustment and peak upward acceleration and that there may be an optimum valve setting (Figure 15 and Figure 16). However, although the results might suggest a dip in peak acceleration at the 6 g level at the ½ turn position, this is not to be considered indicative of the

damper providing an adequate means to control passenger car acceleration because it proved difficult to consistently control the travel of the arm using the foot pedal and only a single set of tests were performed in a controlled manner so as not to risk damage to the device,.

It was observed that when the valve was approaching being closed the actuator did take longer to settle to the retracted (passenger boarding and alighting) position, which is likely to be unacceptable operationally.

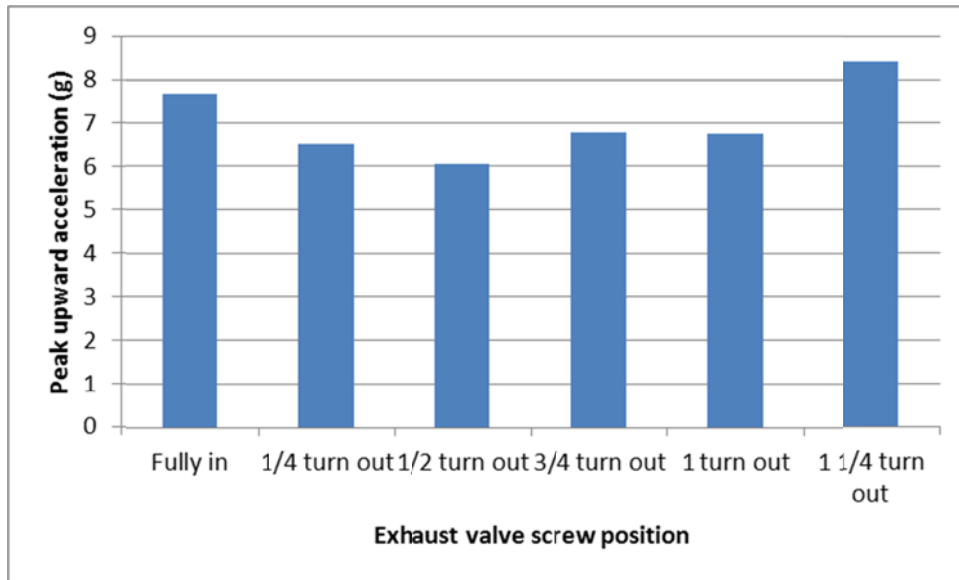


**Figure 15** Peak acceleration with exhaust valve screw position

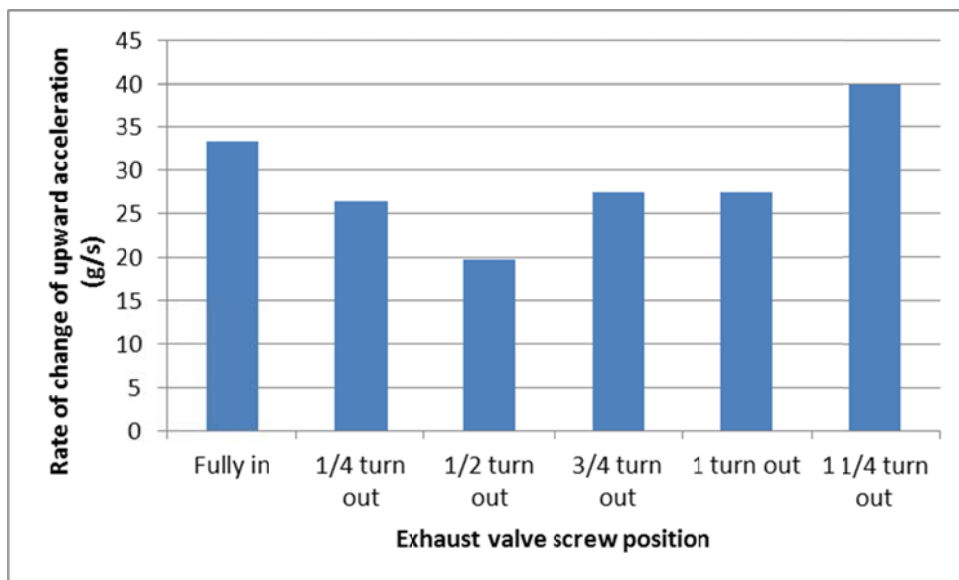


**Figure 16** Rate of change of acceleration with exhaust valve screw position



## 4.5 POTENTIAL FAILURE MODES OF THE AMUSEMENT DEVICE

Assessment of the control system and examination of a number of SAFECO devices has identified a number of potential failure modes which may lead to the arm of the device falling in an uncontrolled manner, resulting in the passengers being subject to excessive upward acceleration. The following components were identified:

- Position sensor movement or failure;
- Valve failure;
- Pneumatic flexible hose failure;
- Pneumatic actuator seal failure;
- PLC aberration;
- Structural failure of the arm.

The failures fall into three main categories - control system failure, mechanical component failures and structural failures. These are discussed below.

The PLC may perform an aberrant function, i.e. it may not follow the correct logical sequence as intended. This could result in the uncontrolled descent of an arm should the PLC fail in this way. The type of PLC used on the Safeco Crazy Frogs would not normally be incorporated in a safety-critical system. However, this type of PLC is not uncommon in this type of amusement device.

Examination of the device tested showed that the position sensors were not securely located on the tube to which they were mounted. The sensors could be moved relatively easily requiring little force and could foreseeably be moved inadvertently during assembly or disassembly of the device. Examination also showed that the sensors were not positioned consistently from one arm of the device to another. This may result in different dynamic performance between one passenger car and another. Should a sensor become displaced significantly, this may result in a loss of control. Also, failure of the component may also lead to a lack of control. A detailed assessment of how these sensors interact with the control system was not undertaken as this information was not available, and was also beyond the scope of this project. Therefore, it is not possible to comment on the full implications of this type of failure. However, good practice would suggest that they would be incorporated in a fail-safe manner, i.e. that in the event of component failure the control system would cease to function in a controlled and safe manner. It is also recommended by the authors that such systems would also operate independently of the PLC control, so that in the event of an aberration of the system the actuator would not descend in an uncontrolled manner.

As the main power source which lifts the arms is pneumatic, failure of the ram seal itself, a sticking vent valve or a ruptured flexible hose may lead to an uncontrolled descent of the arm. While the pneumatic circuit diagram, shown in Figure 9, would suggest that the valves would default to a closed, de-energised position should the control system power fail, this arrangement does not prevent a vent valve which sticks remaining open permanently or for too long. Means to prevent this type of failure are discussed in section 4.6 below.

Clearly a structural failure of the arm or its connections could lead to a collapse of the arm, which cannot be mitigated. The structural integrity of these components is explored in Section 4.10.

#### **4.6 MEANS TO MITIGATE UNCONTROLLED ARM DESCENT**

An assessment of the amusement device was conducted to establish if there was any potential means by which an uncontrolled descent of the arm and passenger car could be mitigated. However, assessment of the design and examination of the device would suggest this is not possible without substantial modification, other than by modification of the control system as discussed earlier.

The main reason for the limited scope for modification is that the device currently uses all the available pneumatic ram travel i.e. from full extension when the free fall programme is used, to fully closed when parked and loading passengers. This use of the actuator does not allow any portion of the travel to be used to decelerate the arm in the event of a control failure. Also, much of the routine controlled motion of the arm takes place within a relatively short distance from the fully closed position of the ram. This, in the event of a control failure, would present a very short distance in which to potentially retard the collapse, as well as a very short time period. Therefore any active system, such as a system which could respond to excessive airflow, would require extremely fast response and any passive system, such as a shock absorber or damper, would need to be incorporated within the existing ram travel.

Given that in order to prevent spinal injury of passengers, the retardation would need to restrict decelerations to less than 6 g, the travel required may be considerable in relation to the existing actuator travel. This retardation distance would potentially need to be added to the existing length of the actuator or would require the lower end of the operating range to be raised. Clearly, raising the lower end of the range of ram travel during operation could be achieved relatively easily, but this would reduce the overall travel of the arm and potentially reduce the attraction of the device to passengers.

The air-cushion damper currently incorporated in the base of the actuator is not capable of safely decelerating the arm in the event of a control failure. The damper is active over only a relatively short portion of the ram travel. This device is considered only as a means to protect the actuator itself from damage. As tests have shown, if the exhaust valve is adjusted so the damper is more effective, then the ability of the ride to settle to a parked position where the passengers can alight is unacceptably slow.

A number of pneumatic companies were contacted in order to establish if this type of flow control was currently possible. The consensus was that, with the required flow and response, there was nothing currently available that would provide a solution. A number of devices are available which protect equipment in the event of hose failure but the sensitivity of these may not be appropriate for this type of equipment and the flow capacity available may not be sufficient. This type of device would only be likely to protect one failure mode i.e. the burst hose.

All the rides examined as part of this project had pneumatically actuated arms, were all manufactured by SAFECO, and were of similar design. It is understood that some of this generic design of systems may be hydraulically actuated, in which case there may be more scope for incorporating systems such as burst hose protection to prevent a collapse in that event.

## 4.7 AMUSEMENT DEVICE MOTION ANALYSIS

A breakdown of each of the individual programs, describing the pattern of motion (Table 5), was derived from Z-axis accelerometer data and video footage captured during the visit [Test runs 1 to 21]. Data was combined in the Observer® XT 10 software program for analysis.

**Table 5** Individual program motion descriptions

<b>Program</b>	<b>Description</b>
<b>1</b>	
<b>A</b>	Low amplitude high frequency bounces around bottom of arc, each arm offset to create a wave motion
<b>B</b>	Large amplitude low frequency bounce motion through full range of arc, each arm offset by a small amount to create a wave motion
<b>C</b>	Low amplitude high frequency bounces around bottom of arc, each arm offset to create a wave motion
<b>D</b>	Large amplitude low frequency bounce motion through full range of arc, alternate arm to create an extreme wave pattern
<b>AA</b>	Low amplitude high frequency bounces around bottom of arc, each arm offset to create a wave motion
<b>BB</b>	Low amplitude high frequency bounces around bottom of arc, each arm offset to create a wave motion
<b>CC</b>	Low amplitude high frequency bounces around bottom of arc, each arm offset to create a wave motion
<b>DD</b>	Large amplitude low frequency bounce motion through full range of arc, each arm offset by a small amount to create a wave motion
<b>2</b>	
<b>A</b>	Large amplitude low frequency bounce motion through full range of arc, each arm offset by a small amount to create a wave motion
<b>B</b>	Large amplitude low frequency bounce motion through full range of arc, groups of three arms alternate to create an extreme wave pattern
<b>C</b>	Large amplitude low frequency bounce motion through full range of arc, groups of two / three arms alternate to create an extreme wave pattern
<b>D</b>	Large amplitude low frequency bounce motion through full range of arc, alternate arm to create an extreme wave pattern
<b>AA</b>	Large amplitude low frequency bounce motion through full range of arc, each arm offset by a small amount to create a wave motion
<b>BB</b>	Large amplitude low frequency bounce motion through full range of arc, groups of two arms alternate to create a wave pattern
<b>CC</b>	Large amplitude low frequency bounce motion through full range of arc, 2-1-2-1 pattern of offset to create wave motion
<b>DD</b>	Large amplitude low frequency bounce motion through full range of arc, groups of three arms, offset slightly, alternate to create an extreme wave pattern

The motion oscillation frequency and the acceleration profile produced by the amusement device ride programs are shown in Figure 17 and Figure 18. Overall, two key types of the ride motion were identified that are used to create the different patterns of motion:

1. A low-frequency (0.6-0.7 Hz), large-amplitude motion; and
2. A high-frequency (1.3 Hz), low-amplitude motion.

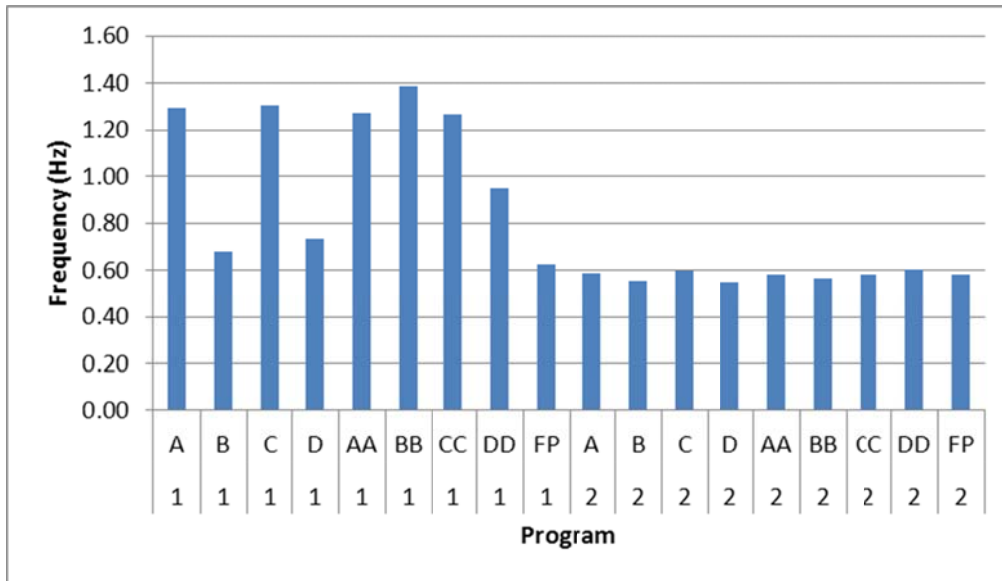


**Figure 17** Chart showing how the frequency of arm vertical oscillation varied with ride program elements (Test Run 11)

#### 4.7.1 Acceleration levels

The focus in terms of human tolerance to acceleration in relation to this amusement device is the peak vertical (positive z axis) acceleration that causes compression of the spine. This would be experienced by passengers when the device arm (car and seat) direction of motion is changing from downwards to upwards motion at the bottom of its movement cycle. As described in Section 4.1.3.2, there appears to be the consensus on an upper limit of around 5 to 6 g for seat-to-head acceleration (for events of longer than 0.15-0.2 s duration). This is supported by the British Standard (1). The results in Table 6 indicate that peak levels exceeding 9 g were recorded, associated with the use of the foot pedal control. However, the period for which accelerations exceed the 6 g level can be very short. These levels were recorded with a simulated load, and when operating beyond what the operator reports to be normal conditions. Nonetheless, because the highest levels of acceleration appear to be associated with the foot pedal operation, we believe that the levels of acceleration to which passengers are exposed are entirely under the control of the operator and are not governed by the control system. Section 4.8 deals with the consideration of the direction and magnitude of accelerations which may act to eject a passenger from the ride. For this amusement device, because the passenger is seated conventionally in relation to the ground, the motion of the passenger car and seat most likely to result in passenger ejection is a rapid change of direction from upwards to downwards. This motion occurs when the device arm, car and seat, changes direction from upward to downward motion at the top of the arm movement cycle. Peak downward acceleration of the seat can exceed that of gravity, and therefore there is potential for the passenger to separate from the seat unless they are contained/restrained within the car.

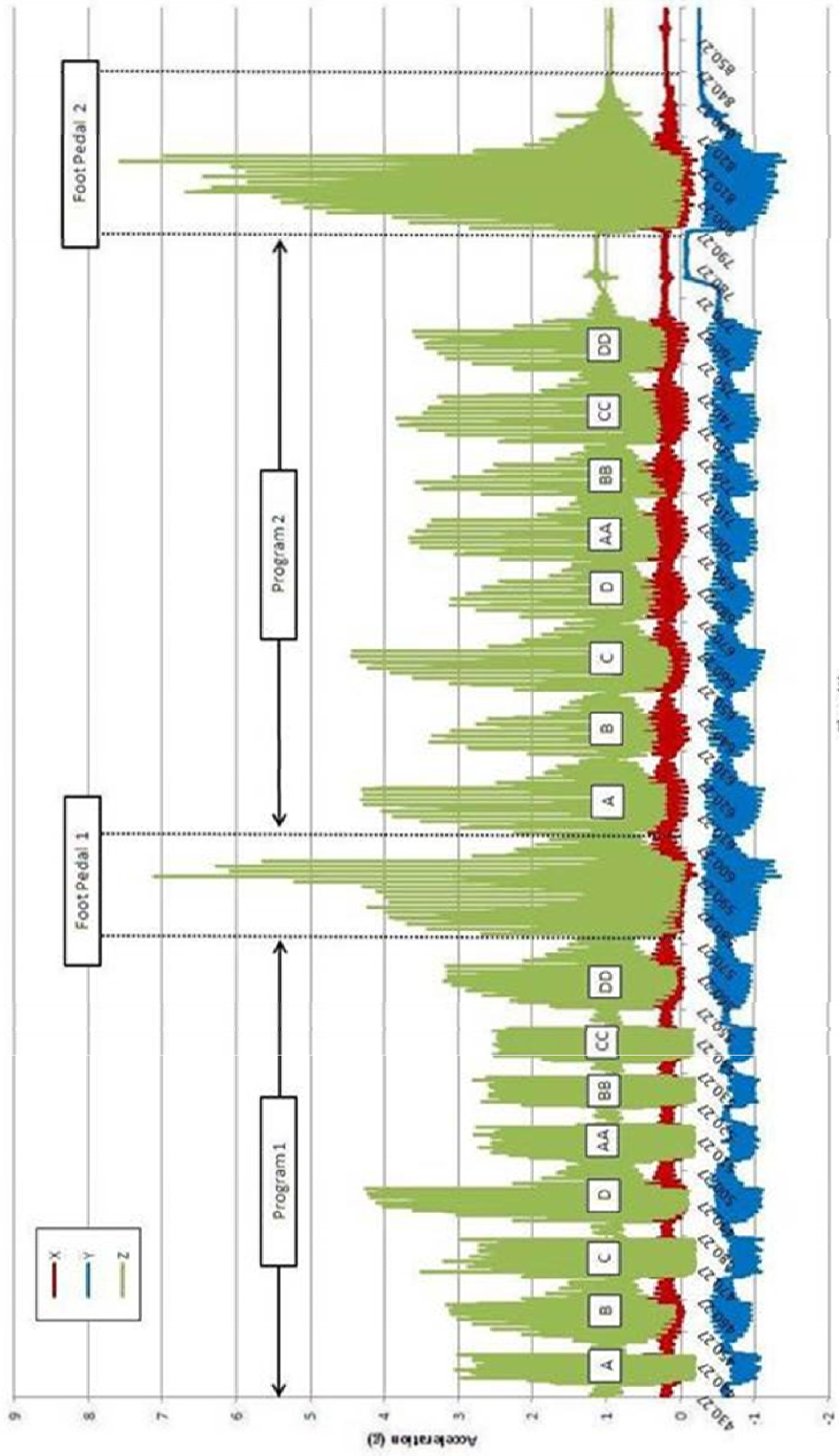


Figure 18 Program sequence breakdown (Test Run 11)

**Table 6 Acceleration data**

Car loaded/unloaded	Run No.	Prog No.	Arms active	Pressure setting (kPa)	Average frequency of bounces		Mean (>+g)	Max (g)	Average rate of change (g/sec)		No of excursions beyond 'n' (g)						Mean excursion time beyond 'n' (s)								
					Lo	Hi			-ve	+ve	LoHz	HiHz	<0	1	2	3	4	5	6	3	4	5	6		
	1	1	All	-	0.74	1.34	1.51	0.3	5.18	18	4	81	231	68	15	5	3	-	0.16	0.41	0.17	0.16	0.12	0.03	-
	1	1FP	*	-	0.63	-	1.98	0.12	4.36	12.8	-	13	22	16	12	9	0	-	0.24	0.62	0.31	0.2	0.06	-	-
	1	2	*	-	0.6	-	1.73	0.04	4.65	11.6	-	3	102	66	39	18	0	-	0.11	0.68	0.28	0.17	0.08	-	-
	1	2FP	*	-	0.64	-	2.03	0.18	4.98	11.2	-	15	26	18	15	12	0	-	0.34	0.59	0.31	0.2	0.11	-	-
	2	1	All	-	-	-	1.68	0.3	5.28	-	-	80	142	87	22	10	8	-	0.2	0.49	0.18	0.16	0.12	0.04	-
	2	1FP	*	-	-	-	2.01	0.12	4.81	-	-	10	21	15	12	10	0	-	0.3	0.62	0.31	0.19	0.1	-	-
	2	2	*	-	-	-	1.84	0.12	4.81	-	-	10	112	80	50	26	0	-	0.3	0.63	0.27	0.17	0.08	-	-
	2	2FP	*	-	-	-	2.03	0.3	7.87	-	-	34	87	64	49	30	13	8	0.31	0.58	0.29	0.18	0.12	0.01	0.06
	3	1	2* and 12	-	-	-	1.69	0.28	5.02	-	-	75	140	67	20	6	1	-	0.17	-0.12	0.2	0.16	0.12	0.01	-
	3	1FP	*	-	-	-	2.01	0.11	4.37	-	-	8	16	12	9	7	-	-	0.27	0.64	0.31	0.19	0.09	-	-
	3	2	*	-	-	-	1.8	0.03	4.68	-	-	0	103	67	40	20	-	-	-	0.62	0.28	0.17	0.08	-	-
	3	2FP	*	-	-	-	2.31	0.27	7.71	-	-	21	36	26	22	18	11	7	0.41	0.5	0.3	0.2	0.13	0.11	0.07
	4	1	All	4.5	0.73	1.31	1.75	0.3	4.97	8.2	4.9	96	179	122	27	11	-	-	0.26	0.42	0.19	0.15	0.11	-	-
	4	1FP	*	-	0.69	-	2.54	0.17	5.26	11.4	-	14	21	19	18	16	4	-	0.3	0.44	0.28	0.17	0.09	0.05	-
	4	2	*	-	-	-	1.66	0.12	3.69	-	-	0	40	23	8	-	-	-	-	0.55	0.23	0.11	-	-	-
	4	2FP	*	-	0.69	-	2.32	0.18	7.01	15.6	-	16	27	20	18	15	8	4	0.31	0.47	0.28	0.18	0.11	0.09	0.06
	5	1	All	6	0.74	1.32	1.65	0.32	5.14	10.6	4.2	87	188	100	33	12	10	-	0.23	0.49	0.2	0.17	0.13	0.06	-
	5	1FP	*	-	0.63	-	2.61	0.29	7.62	23	-	12	17	16	12	11	9	6	0.48	0.51	0.29	0.22	0.15	0.11	0.08
	5	2	*	-	0.68	0.69	1.91	0.19	5.09	11.7	-	29	124	93	65	46	2	-	0.15	0.67	0.31	0.2	0.11	0.04	-
	5	2FP	*	-	0.64	-	2.41	0.33	8.54	20.5	-	17	26	19	16	14	12	7	0.42	0.52	0.29	0.2	0.16	0.11	0.08
	6	1	All*	6	-	-	1.55	0.3	4.66	-	-	55	202	60	16	5	-	-	0.18	0.36	0.19	0.14	0.11	-	-
	6	1FP	*	-	-	-	2.17	0.18	5.1	-	-	12	21	17	14	9	1	-	0.35	0.59	0.31	0.2	0.11	0.04	-
	6	2	*	-	-	-	1.9	0.05	4.48	-	-	17	107	79	56	29	-	-	0.04	0.04	0.67	0.31	0.16	0.07	-
	6	2FP	*	-	-	-	2.17	0.18	5.28	-	-	14	21	17	14	10	2	-	0.35	0.58	0.32	0.2	0.11	0.06	-

Unloaded





Run No.	Prog No.	Arms active	Pressure setting (kPa)	Average frequency of bounces		Mean (>+1g)	Max (g)	Average rate of change (g/sec)		No of excursions beyond 'n' (g)											Mean excursion time beyond 'n' (s)					
				Lo	Hi			-ve	+ve	Lo Hz	Hi Hz	<0	1	2	3	4	5	6	<0	1	2	3	4	5	6	
12	2FP			0.58	-	2.11	0.12	9.43	30.4	-	34	65	26	24	22	20	11	0.18	0.35	0.28	0.19	0.14	0.10	0.06		
13	Total	12	6.5	-	-	1.63	0.07	8.25	-	-	34	509	147	130	102	26	12	0.14	0.3	0.23	0.14	0.08	0.04	0.03		
14	Total	1 and 12	6.5	-	-	1.83	1.25	9.49	77.9	-	136	710	261	228	188	90	47	0.44	0.35	0.26	0.17	0.1	0.08	0.07		
15	Total	12	6.5	-	-	1.77	0.3	9.1	-	-	39	112	61	50	43	16	13	0.33	0.53	0.25	0.16	0.09	0.09	0.07		
16	1	6 and 12	7	0.74	1.33	1.7	0.17	4.97	16.4	6.8	73	146	103	23	7	-	-	0.2	0.47	0.16	0.14	0.1	-	-		
16	1FP	*	*	0.59	-	2.16	0.05	5.3	11.6	-	8	15	13	9	7	5	-	0.07	0.54	0.28	0.19	0.12	0.04	-		
16	2	*	*	0.59	-	1.93	0.04	5.28	15	-	11	118	84	60	45	11	-	0.07	0.61	0.28	0.18	0.1	0.04	-		
16	2FP	*	*	0.59	-	2.21	0.05	5.6	17.9	-	22	31	22	19	17	6	-	0.06	0.51	0.3	0.2	0.12	0.06	-		
17		6		-	-	-	-	-	-	-	-	-	-	-	-	-	-	-	-	-	-	-	-	-		
18		7.5		-	-	-	-	-	-	-	-	-	-	-	-	-	-	-	-	-	-	-	-	-		
19	1	6 and 12	6	-	-	1.8	0.2	4.99	-	-	69	120	92	47	5	-	-	0.23	0.38	0.17	0.07	0.06	-	-		
19	1FP	*	*	-	-	2.14	0.05	4.29	-	-	0	15	3	11	7	-	-	-	0.54	0.28	0.16	0.05	-	-		
19	2	*	*	-	-	1.75	0.2	4.33	-	-	0	84	57	31	7	-	-	-	0.56	0.25	0.13	0.05	-	-		
19	2FP	*	*	-	-	1.98	0.01	4.57	-	-	0	26	16	13	12	-	-	-	0.49	0.29	0.18	0.08	-	-		
20	1	6 and 12	7.5	-	-	1.7	0.17	5.31	-	-	83	161	93	31	13	8	-	0.18	0.46	0.17	0.16	0.1	0.03	-		
20	1FP	*	*	-	-	2.44	0.1	5.66	-	-	19	17	17	13	11	4	0	0.07	0.58	0.3	0.21	0.13	0.07	-		
20	2	*	*	-	-	2.08	0.07	5.76	-	-	29	117	92	69	55	24	0	0.05	0.62	0.3	0.19	0.12	0.06	-		
20	2FP	*	*	-	-	2.19	0.07	5.95	-	-	16	28	16	16	13	1	0	0.04	0.46	0.32	0.21	0.13	0.1	-		
21	Part 1	6 and 12	-	-	-	2.19	0.11	6.05	19.8	-	26	46	33	27	23	7	1	0.08	0.49	0.29	0.19	0.11	0.07	0.02		
21	Part 2	*	*	-	-	2.52	0.12	6.79	27.5	-	37	50	36	35	33	13	8	0.11	0.44	0.3	0.2	0.12	0.09	0.05		
21	Part 3	*	*	-	-	2.61	0.13	6.75	27.5	-	69	62	47	44	41	38	9	0.14	0.42	0.29	0.2	0.14	0.07	0.05		
21	Part 4	*	*	-	-	2.6	0.17	8.41	39.9	-	60	91	49	46	43	30	19	0.17	0.31	0.29	0.2	0.13	0.1	0.06		

Loaded





**Table 7** Summary of acceleration data for individual program elements (typical conditions, Test Run 11, Z axis only)

	Total mean (g)	Mean (>+1g)	Max (g)		Total time above 6g	No of excursions	Mean time per excursion above 6
			-ve <sup>1</sup>	+ve			
<b>Programme 1</b>							
A	0.841	1.880	-0.184	3.056	-	-	-
B	0.970	1.618	-	3.159	-	-	-
C	0.845	1.887	-0.194	3.505	-	-	-
D	0.965	1.792	-0.103	4.262	-	-	-
AA	0.853	1.708	-0.182	2.789	-	-	-
BB	0.873	1.604	-0.186	2.806	-	-	-
CC	0.881	1.575	-0.177	2.528	-	-	-
DD	0.960	1.624	-	3.207	-	-	-
Foot pedal	0.963	2.317	-0.054	7.102	0.11	3	0.036
<b>Programme 2</b>							
A	0.970	2.018	-	4.309	-	-	-
B	0.967	1.588	-	3.395	-	-	-
C	0.972	1.979	-	4.446	-	-	-
D	0.961	1.720	-	3.115	-	-	-
AA	0.953	1.891	-	3.660	-	-	-
BB	0.972	1.648	-	3.573	-	-	-
CC	0.963	1.867	-	3.838	-	-	-
DD	0.977	1.680	-	3.610	-	-	-
Foot pedal	1.003	1.513	-0.051	7.564	0.29	6	0.048

<sup>1</sup> Missing values indicate that no negative g was measured

#### 4.8 ASSESSMENT OF PASSENGER RESTRAINT REQUIREMENTS

The amusement device characteristics measured on the Wilkinson's DJ Jump amusement device were assessed against the requirements of the British and European Standard for Fairground and amusement park machinery and structures safety, BS EN 13814:2004 (1). This Standard presents guidance on the levels of acceleration to which it is acceptable to subject passengers, as well as characteristics of the restraint systems to limiting passenger movement appropriate to the accelerations.

Specifically relating to passenger restraint, the Standard contains some general requirements (Clause 6.1.6.2) for design before indicating the type of restraint appropriate to the dynamic performance and inclination of the amusement device (Clause 6.1.6.2.4). HSL's interpretation of the information provided in this section of the Standard is that:

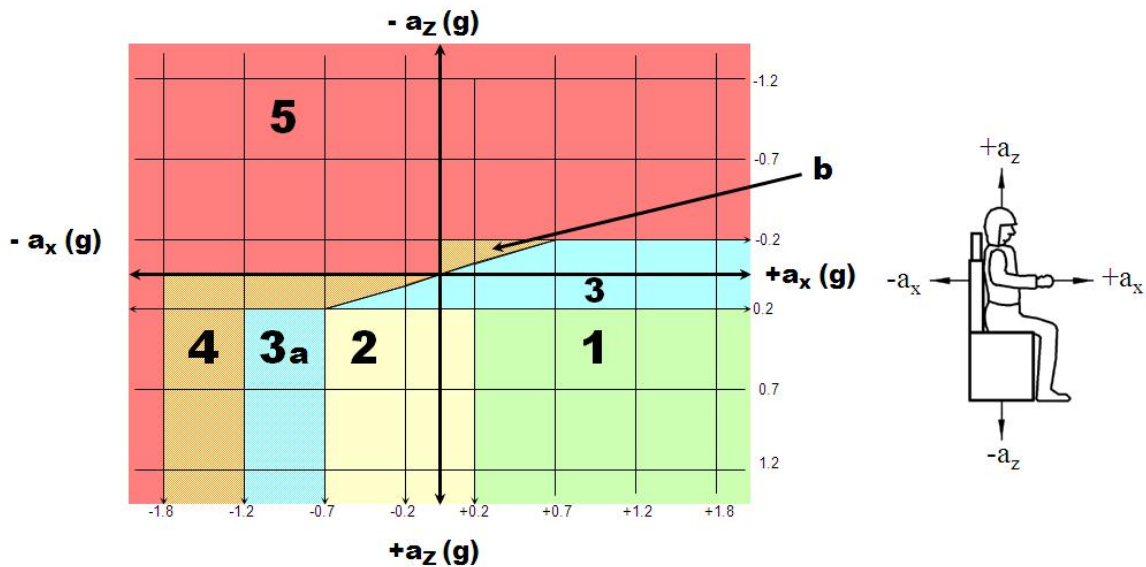
- It applies predominantly to seated occupants;
- It applies only for accelerations in the Z and X axes;
- If the amusement device seat is accelerating downwards and/or backwards relative to the seat, the occupant can be at risk of separating from the seat, and needs to be restrained in order to maintain contact with it;

- The magnitudes of the accelerations in these axes in combination dictate the extent to which the passenger needs to be restrained.

This approach mirrors that presented in the American Standard, Standard of Practice for Design of Amusement Rides and Devices ASTM F2291-11 (19).

BS EN 13814:2004 (1) does not stipulate any minimum duration for an acceleration event. ASTM F2291-11 (19) does, and excludes events of less than 200 ms duration. For this duration threshold and longer, the ASTM vertical upward acceleration (+Z) limit is 6 g, reducing after 1s duration. If there are combinations of acceleration events on different axes, the ASTM Standard (19) presents diagrams from which to derive a combined limit values for 2 axes.

BS EN 13814:2004 (1) provides requirements for amusement device passenger restraint systems based up on the accelerations developed by the amusement device. For combinations of acceleration in the X and Z axes, this is expressed as a diagram, known commonly as the 'restraint rose'. The restraint rose gives five zones, overlaid on the x-axis and z-axis accelerations recorded on (or calculated to be generated by) an amusement device at the passenger location. The five zones indicate where a set of requirements for the passenger restraint systems needs to apply to ensure passenger safety. HSL's interpretation of BS EN 13814:2004 (1) in relation to passenger restraint during exposure to X and Z axis acceleration is made whilst awaiting clarification from Technical Committee MCE/3/4 (Correspondence dated 17/11/2010). Our interpretation is based upon using the adapted diagram shown in Figure 19.



<sup>a</sup> Footrests and handrails are required.

<sup>b</sup> Area in category 4 if no lateral design forces and duration of  $a_z$ -acceleration less than 0.2 sec at boundary cases the lower category may be chosen.

**Figure 19** BS EN 13814 (2004) Restraint diagram, adapted by HSL<sup>1</sup>

Our interpretation of the acceleration data measured during the site visit is that during each of the normal operating programs, where none of the  $+X$  accelerations exceed  $1g$  and the  $-Z$  accelerations are less than  $-0.2$ , the amusement device falls into Area 3 of the restraint rose. The requirements of an Area 3 restraint system are shown in Table 8. The current restraint system on the DJ Jump amusement device does not fully meet this standard of protection, because it is reliant on a shared lap belt that is not interlocked (see section 4.9 for a discussion of whether the existing restraint will contain amusement device passengers). However, during operation of the foot pedal, combined accelerations of greater than  $+1g$  in the  $X$  axis and  $-0.2g$  in the  $Z$  axis were recorded. This shifts the amusement device into Area 5 of the restraint rose, where the current system does not meet the standard of protection specified (Table 9).

**Table 8** BS EN 13814 Area 3 restraint systems

Area 3: Restraint of at least the following type required:	
A1	Collective device for two or more passengers
B2	Individually adjustable locking position

<sup>1</sup> Permission to reproduce extracts from BS EN 13814 2004 is granted by BSI. British Standards can be obtained in PDF or hard copy formats from the BSI online shop: [www.bsigroup.com/Shop](http://www.bsigroup.com/Shop) or by contacting BSI Customer Services for hardcopies only: Tel: +44 (0)20 8996 9001, Email: [cservices@bsigroup.com](mailto:cservices@bsigroup.com).

C3	Manually locked by the operator or attendant
D1	Manually unlocked by the passenger
E1	No warning at all
F1	Manual
G2	Redundant only concerning locking device (functional)
H2	One restraint for each passenger

---

**Table 9** BS EN 13814 Area 5 restraint systems

---

<b>Area 5: Restraint of at least the following type required:</b>	
A2	Individual device for each passenger
B3	Minimum closed position automatically controlled
C5	Automatically locked in the operating positions and locked position controlled
D3	Unlocked by operator or attendants by means of a centralised system.
E3	Light and / or acoustic warning and start inhibition
F1	Manual
G3	Redundant (functional and construction)
H3 / H4	Two redundant restraints or one intrinsically redundant restraint

---

#### **4.9 EXISTING CONTAINMENT AND RESTRAINT SYSTEM ASSESSMENT**

Dimensions of the passenger containment and restraint system components (Figure 20) were recorded using a standard tape measure. Table 11 (column 9) provides a summary of the measurements taken from Mr Wilkinson's amusement device. The key amusement device dimensions were then compared to relevant child and adult population anthropometric data (PeopleSize Pro 2008, v2.01, Open Ergonomics Ltd unless otherwise stated). The key passenger containment and restraint dimensions are considered to be:

- Seat back height;
- Seat width;
- Seat depth;
- Popliteal height (seat pan height above footrest);
- Footrest depth;
- Grab rail;
- Lap bar.



**Figure 20** DJ Jump seating and restraint system

#### **4.9.1 Height restrictions**

The manufacturer user guide (20) states that:

*“Guests who are shorter than one metre may not ride the device;*

*Guests who are between 1 and 1.4 metre may ride accompanied; and*

*Guests who are taller than 1.4 metre can ride unaccompanied”.*

The British Standard (1), presents approximate boundaries of child stature (height restriction criteria) for different ages of children. It indicates that a height restriction of 1.05 m will restrict access to children of approximately age 4 and above, and a height restriction of 1.4 m will restrict access to children of approximately age 10 and above. In reality, the situation is not quite so clear cut.

Table 10 shows the proportion of children in the UK population of different age groups who meet these height restrictions. Based on this information, the youngest age groups that can realistically meet (exceed) the height restriction for riding accompanied are 3 year-olds (The 1 m height restriction would allow approximately 47% and 37% of 3 year old boys and girls respectively). At age 5, around 98% of children could exceed the 1 m height restriction.

The youngest passenger that the 1.4 m height restriction would permit to ride unaccompanied would be 8 year old British children (around 10% and 7% of 8 year old boys and girls respectively). Over half of all 10 year old boys and girls would be permitted to ride unaccompanied.

While, around 34% of 9 year old boys and 63% of 10 year old boys would be able to ride alone (approximately 66<sup>th</sup> and 37<sup>th</sup> percentile respectively). Similarly, around 28% of 9 year old girls

and 55% of 10 year old boys would be able to ride alone (approximately 72<sup>th</sup> and 46<sup>th</sup> percentile respectively).

On this basis, key body dimensions for 3 and 8 year old children are presented in Appendix 6.4.

**Table 10** Proportion of children in the UK at different ages compared with the minimum height restrictions (1000 mm accompanied, 1400 mm unaccompanied)

Age	Percentile stature		Per cent in age group who could ride	
	1000	1400	1000	1400
<b>Boy</b>				
2	98.6	>99.9	1.4	<0.01
3	53.7	>99.9	46.3	<0.01
4	15.7	99.99	84.3	0.01
5	1.5	99.99	98.5	0.01
6	0.06	99.95	99.94	0.05
7	<0.01	99.5	>99.9	0.50
8	<0.01	90	>99.9	10
9	<0.01	66.4	>99.9	33.6
10	<0.01	36.8	>99.9	63.2
11	<0.01	13.9	>99.9	86.1
<b>Girl</b>				
2	98	>99.9	2	<0.01
3	64.1	>99.9	35.9	<0.01
4	15.5	>99.9	84.5	<0.01
5	2.6	99.9	97.4	0.01
6	0.07	99.96	99.93	0.04
7	0.01	98.8	99.99	1.2
8	<0.01	93.4	>99.9	6.6
9	<0.01	72.4	>99.9	27.6
10	<0.01	45.5	>99.9	54.5
11	<0.01	13.7	>99.9	86.3

As well as influencing body size, child age is also likely to influence behaviours. It is not clear if this is a consideration in either the Safeco recommended height restriction criteria, or those in the British Standard.

#### 4.9.2 Seat width

There are three seats provided per car, with a total width of 1120 mm. However, it would be awkward to accommodate three average sized adults. This is acknowledged in the Safeco Health and Safety Guide, which claims that the seat is designed to accommodate two 95<sup>th</sup> percentile male adults and in some cases there may be enough room for two adults and a child. The shoulder breadth (bideltoid) measurement of 95<sup>th</sup> percentile British male adults (18-64) is 516 mm. The hip breadth of 95<sup>th</sup> percentile British male adults (18-64) is 432 mm, meaning that the seat could comfortably accommodate two large passengers, particularly as they could adjust their seating positions to make room for each other's upper body.

### 4.9.3 Lap bar and seat depth

The DJ Jump amusement device has mechanical restraint bars that swing down from overhead and come to rest in front of the occupant, above their thighs. These are referred to as a lap bar and grab rail. Depending upon the size of the occupant and where they sit in the seat, they may actually be some distance in front of the occupant's torso. The amusement device operator (or assistant) controls the operation of the bars. When lowered, there is no adjustment of the bar and it comes to rest and locks in a fixed location at the front of the seat side panel/armrest.

The distances from the seat back to the lap bar and the seat pan depth were both measured at 390 mm. The corresponding anthropometric measurement is buttock to popliteal length. The buttock to popliteal length of a 95<sup>th</sup> percentile 3 year old is 330 mm for a boy and 305 mm for a 95<sup>th</sup> percentile girl. While the buttock – popliteal length of a 95<sup>th</sup> percentile 8 year old is 375 mm for a boy and 400 mm for a 95<sup>th</sup> percentile girl. This indicates that only the tallest of 8 year olds will be able to sit with their back against the seat back and still be able to bend their knee at the front of the seat pan.

The simultaneous accelerations in the X and Z directions will tend to make occupants with smaller thigh depth, torso depth, and hip widths more vulnerable to movement in the seat and could allow occupants to become displaced from their seats.

The vertical gap between the seat pan (front edge) and the lap bar is 120 mm (uncompressed padding). This is a relatively small dimension compared to the thigh depth of British adults, requiring some leg tissue/bar padding compression to fit most adults. The 120 mm gap approximates to the thigh depth of the largest 8 year old children (Belgian boys and girls, Appendix 6.4).

The lap bar may act as a restraint to upward vertical movement for most adults and some children over the age of 8 years; although for many it will be too far in front of the body to be reliably effective.

It is difficult to predict the smallest likely thigh depth from the passenger height restriction, as thigh depth cannot be predicted from stature. Pheasant (21) reported that girth and depth measurements have a stronger correlation with weight than stature.

To investigate whether the lap bar could act as a restraint to forward movement, including downward movement, i.e. slumping or 'submarining', under the lap bar, the 120 mm gap was compared with relevant body dimensions. Chest depth is the critical anthropometric dimension, because although abdominal depth is generally greater, there is more scope for compression of the abdomen. The chest depth for an 8 year old boy is approximately 119 to 203 mm (5<sup>th</sup> to 95<sup>th</sup> percentile). It would technically possible for an 8 year old child (likely youngest unaccompanied) of around 5<sup>th</sup> percentile or smaller in chest depth to slide down in the seat and fit through the gap. Around 50% of 3 year olds could fit through the same gap (5<sup>th</sup> to 95<sup>th</sup> percentile range equates to 105 to 145 mm).

Therefore, the lap bar acts as a restraint device mainly for forward horizontal movement, which is not a significant risk on this amusement device. The lap bar is unlikely to be a reliable restraint to protect against upward or downward movement from the seat for children under the age of approximately 13 (5<sup>th</sup> percentile 13 year thigh depth approaches the 120 mm dimension). This is especially so given that the lap bar is so far in front of the occupant.



#### 4.9.4 Grab rail

The distance between the grab rail and seat back is 502 mm; this corresponds to the anthropometric measurement 'Forward Reach to Grip (seated) (22). The maximum 'Forward Reach to Grip (seated)' length of a 3<sup>rd</sup> percentile 8 year old is 489 mm for a boy and 484 mm for a 3<sup>rd</sup> percentile girl (50<sup>th</sup> percentile Boy = 547, 97<sup>th</sup> = 609; 50<sup>th</sup> percentile Girl = 540, 97<sup>th</sup> percentile = 601). Therefore, the majority of unaccompanied occupants are able to use a combination of the back rest and the grab rail to brace against the forces and prevent forward displacement in their seat. However, the maximum 'Forward Reach to Grip (seated)' of a 3<sup>rd</sup> percentile 3 year old is 368 mm for a boy and 362 mm for a 3<sup>rd</sup> percentile girl (50<sup>th</sup> percentile Boy = 432, 97<sup>th</sup> = 499; 50<sup>th</sup> percentile Girl = 420, 97<sup>th</sup> percentile = 484), which suggests that the 3 year old child population would find it extremely difficult to reach the handrail without leaning forwards significantly. Around 50% of 6 year olds would be likely to be able to reach and brace. This is offset, to some extent, by the seat belt and presence of an accompanying adult. Although an inertia reel seat belt across the lap is considered to be a potentially suitable restraint for this type of amusement device, the type fitted is shared across passengers, is not interlocked and can be easily operated by the occupant, assuming it is used in the first instance. Similarly, adults should not be relied upon to provide child restraint, as they will be subject to the same accelerations and amusement device motions and may need to brace themselves.

#### 4.9.5 Side supports - Seat back height

In terms of lateral protection, the side of the seat is open with a curved bar attached to the seat back to prevent lateral movement of the upper torso (Figure 20b). To prevent sideways ejection the side containment should come to above the sitting centre of mass (COM) of large (95th percentile) males. In the absence of British data regarding seated COM, data from the United States Air Force (USAF) has been used as a comparison. Schultz, et al. (23) calculated the whole body centre of mass location of 69 seated subjects, anthropometrically representative of the USAF fighter pilot population<sup>2</sup>. The average centre of mass in the Z axis (head to seat pan) was 262 mm ( $\pm 14$  mm) for male participants and 234 mm ( $\pm 10$  mm) for female participants. The current side restraint measures 400 mm at the front edge of the seat pan 380 mm at the midpoint and 520 mm at seat back. In this instance, COM is within the containment provided by the seat and side bar making it unlikely that an occupant would be ejected sideways from the device.

#### 4.9.6 Foot rest seat pan distance

The distance from the seat pan front edge to the footrest ranged between 480 and 550 mm. This corresponds to the anthropometric measurement 'popliteal height' (i.e. the distance from the bottom of the foot to the back of the knee). The minimum distance (480 mm) equates to 81<sup>st</sup> percentile male and 99<sup>th</sup> percentile female, meaning that less than 20% of the population would be able to reach the footrest at the minimum distance when seated. As such, the foot rest cannot be used as a bracing point. The tread depth of the footrest provided measures 250 mm. This

---

<sup>2</sup> This sample is not representative of the wider population. The measurements in relation to the British population (24) were as follows: Average weight Male = 78.5 kg = 42<sup>nd</sup> PCTL British Male (18-64); average weight Female = 58.5 kg = 25<sup>th</sup> PCTL British Female; average height Male = 176.8 cm = 60<sup>th</sup> PCTL British Male; and average height Female = 162.5 cm = 50.8<sup>th</sup> percentile British Male.

exceeds the 220 mm minimum tread size stated in Building Regulations (25) for a private staircase and as such is considered adequate as a step.

#### **4.9.7 Alternative seat and restraint system design**

An alternative seat design (shown in Figure 21) was observed during the visit to Goose Fair (a Safeco 'Jump and Smile' device). This design includes an over the shoulder restraint that closes downwards over the shoulders of the passenger. The over shoulder restraint is lowered manually by the ride operator (or assistant). It is not known whether the closure of the restraint is interlocked with the control system to prevent the ride being operated until locked. There is an additional fastening mechanism in the form of a seat-belt type buckle. The closure of the shoulder restraint with the seat pommel will prevent passengers sliding downwards/forwards in the seat, but will limit the devices ability to fit to the passenger's body size. It is not known if this seat belt buckle is interlocked with the control system, and it is considered likely to be within reach of the passengers, so could potentially be released during ride operation. However, in principle, this type of restraint is considered likely to provide the level of protection appropriate to this type of amusement device.



**Figure 21** Alternate passenger restraint design

#### **4.9.8 Passenger containment and restraint summary**

The combination of the containment provided by the car/seat structure and the restraint systems in the form of the shared interlocked lap bar and shared inertia reel seat belt is not considered to meet the standard set out in BS EN 13814 (1) (see Table 8 and Table 9) in relation to the accelerations recorded during ride sequence motions. Although the lap bar will be likely to prevent a passenger moving forward off the seat pan, it does not appear to be able to reliably protect passengers and children in particular against lateral and fore-aft movement within the car, upward movement in/from the seat, or downward slumping or movement under the lap bar.

The automotive type inertia reel seat belt fitted, while in principle being an effective restraint type for this type of amusement device, cannot be considered adequate due to the fact that it is shared across multiple passengers, i.e. will not fit the smaller passenger, is not interlocked with the control system, and can be released by passengers during the ride sequence.

**Table 11** Relevant amusement device dimensions

	Previous HSL Reports			Nottingham Goose Fair					
	Safeco	Jump and Smile (2000)	Jumpin' (2004)	Jumping Frog (2009)	Jump and Smile (Mr Burrows)	Jump and Smile (Mr Mulhearn)	City Hoper	Froggit	Mr Wilkinson's DJ Jump
<b>Measurement description</b>									
Seat back rest height	500	500	500	455	500	520	-	-	515
Seat pan width (complete)	1050	1100	1020	-	1080	-	-	-	1120
Seat pan depth	430	410	410	410	-	430	-	-	390
Seat pan height	-	-	-	-	-	-	-	-	515-640
Side support height above seat pan	100-450	410	200	-	-	-	-	-	380 – 520
Side support depth	-	370	-	-	-	-	-	-	582
Seat back rest angle (from vertical, approx.)	23°	-	-	-	-	-	-	-	-
Seat surface angle (from horizontal, approx.)	15°	-	-	-	-	-	-	-	15.3°
Leg rest angle (from vertical, approx.)	32°	-	-	-	-	-	-	-	-
Distance between grab-rail and seat back	520	472	450	-	-	-	-	-	502
Distance between lap-bar and seat back	420	420	400	400	390	-	-	-	390
Distance between grab-rail and seat pan	300	-	340	340	-	-	-	-	325
Distance between lap-bar and seat pan	100	160	120	130	116	-	-	-	120
Diameter of grab-rail (incl. padding)	50	25	60	-	-	-	-	-	50
Diameter of lap-bar (incl. padding)	80	-	90	-	85	-	-	-	80

## 4.10 FINITE ELEMENT ANALYSIS AND FATIGUE ASSESSMENT

### 4.10.1 Previous Fatigue Assessments

Following an incident at Blackpool Central Pier (9) in which an arm on a Safeco Crazy Frogs type amusement device failed, HSL was asked to comment on two previous fatigue assessments done on this type of amusement device. The first assessment was performed by Instituto Tecnologica de Aragon (ITA) (26) on behalf of the manufacturer, SAFECO, and the second by Dr M Lacey at Advanced Computational Analysis (27). Both analyses used a similar approach, i.e. measuring accelerations on a Safeco Crazy Frogs, performing finite element analysis to obtain stresses and then using the stresses in a fatigue assessment. The two analyses used different Standards to perform the fatigue assessments, but they both used the same S-N curve approach. In this approach, the relationship between stress (S) and number of cycles to failure (N) is given for given types of welds. Therefore, if the number of stress cycles of any given magnitude is known, the proportion of the fatigue life that those cycles use up can be calculated.

Lacey (27) calculated that for the most highly stressed area on the arm for the range of stress cycles assumed that each year of usage would consume 0.19 of the fatigue life of the arm. Therefore, the arm was calculated to have a life of approximately 5 years.

Lacey (27) used the following assumptions in his analysis:

- seat mass of 85 kg;
- passenger mass of 3 x 75 kg, i.e. total of 225 kg;
- models run with varying loads of full (60% of rides), 2/3 load (16%), 1/3 load (12%) and empty (12%);
- maximum acceleration of 3.9 g (excluding gravity);
- highest stress of 198.3 MPa;
- Usage assumed to be 30 rides/day for 200 days per year. i.e. 6000 rides/year.

Some of the assumptions used by Lacey (27) are conservative compared to those used in this study. The maximum passenger mass of 225 kg was based on three 75 kg passengers, but due to the width of the seat, it would be difficult to accommodate three people of this mass. However, the assumption that the seat would not be fully loaded for every ride counteracts the higher maximum load. Also, the total number of rides per year was higher, at 6,000 compared to 4,250 rides/year assumed in this study. The maximum acceleration used by Lacey was somewhat lower than that used in the HSL analysis.

The fatigue life obtained by Lacey (27) of 5.19 years was comparable to the life of 6 years obtained in the ITA report. The fatigue life was based on stress ranges from the maximum recorded principal stress to the minimum recorded. Typically, the minimum stress was in the order of 17% of the maximum. It was not clear that the minimum stresses recorded were in the same locations and directions as the highest stresses, and therefore, it would be more conservative to assume a minimum stress of zero in a fatigue analysis. If a zero minimum stress had been assumed, the fatigue life calculated would have been approximately half that obtained, i.e. 2.5 years.

The ITA report (26) considered the highest acceleration (not including gravity) as 3.0 g, which was significantly lower than the values obtained in HSL's testing. The highest stress in the ITA report (26) was 130 MPa. Unusually, the highest stress was compressive, and occurred in the U section stiffener beam attached under the main arm. No results were shown of maximum principal stress. In contrast to the Lacey (27) work, the minimum stress was assumed to be zero

in the ITA analysis. While compressive stresses do need to be considered in fatigue analysis, especially in the region of welds, fatigue cracks are more likely to grow in areas of tensile stress.

#### 4.10.2 Checking linearity of strain/acceleration relationship

The relationship between the strains and accelerations measured on the arm were assessed. A section of data containing a number of relatively high accelerations was used to determine the relationship between acceleration at the end of the arm (measured by the accelerometer under the seat) and the strains recorded.

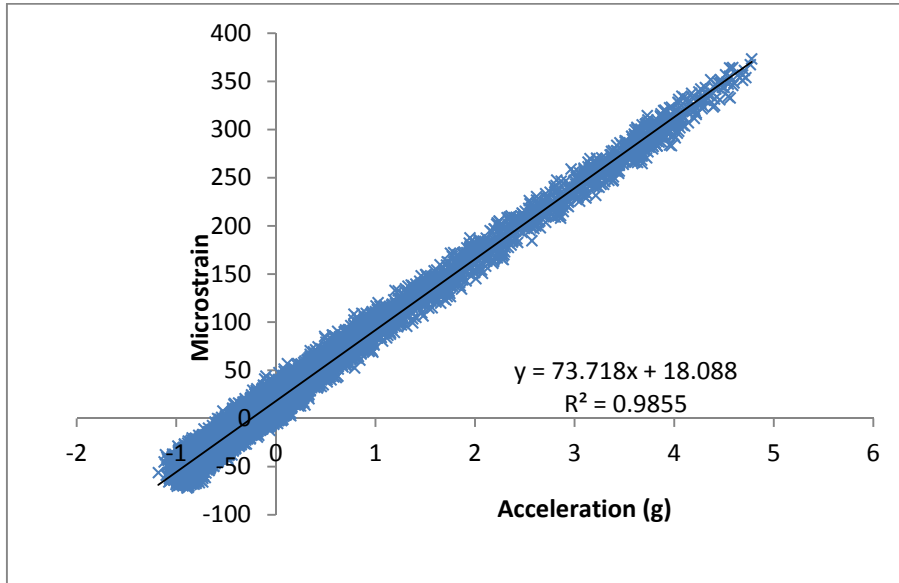


Figure 22 Relationship between strain on the top of the arm and acceleration

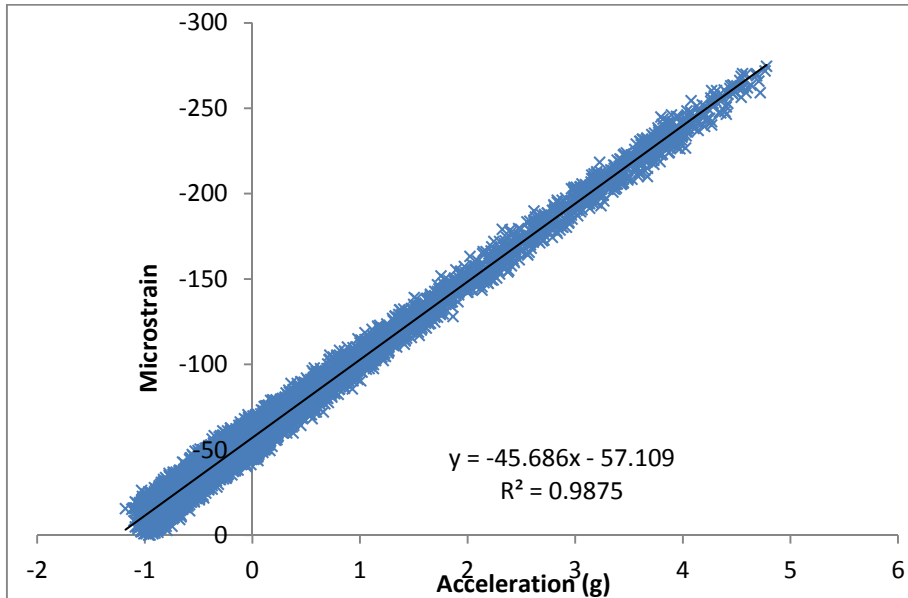


Figure 23 Relationship between strain on the underside of the U Section and acceleration

As can be seen from the results shown in Figure 22 and Figure 23, there is a good linear relationship between the strains measured at both locations and the accelerations. If there were dynamic effects due to sudden changes in acceleration, the strain results at the highest accelerations, which must be a peak where the acceleration changes rapidly, would not follow the same linear relationship. These results indicate that a quasi-static approach to the modelling is valid, which significantly reduces the computation time.

#### **4.10.3 Details of the FE Models**

The finite element models were created using Ansys 14.5 and consisted of three components - the main arm, the U section beam attached under the main arm and the seat, as shown in Figure 24. The arm consisted of a U section channel of varying height with a plate welded across the top to make a box section. An internal stiffening plate was assumed to run from a position just above the ram attachment position up to the apex. Although internal inspection of amusement device was not possible, it was included in other assessments made of the amusement device (e.g. Lacey (27)) and could be seen on a failed amusement device arm investigated by HSL (9). Examination of this arm showed that the plate was welded to each side of the arm, but not to the bottom of the arm, or the apex.

On the failed arm (9), there were also hollow square section rods connecting the two sides near the top of the section at regular intervals. These were included in one model but as they were not found to affect the results, they were omitted from subsequent models. These rods were probably used to maintain the separation of the side plates during manufacture of the arm, rather than to add any structural strength.

The U section beam under the arm was reinforced around the ram attachment point with four plates welded to make a box. Two plates were welded to the side of the U section to increase the effective thickness with the other plates welded across to join the two sides.

The seat was represented by a simple plate with a mass of 45 kg. The mass of the seat was assumed to be 85 kg (assumed by Lacey (27)). During the experimental work with the amusement device, a load of 160 kg was added to the seat to represent two passengers, making a total of 245 kg. Therefore, a point mass of 200 kg was added to the seat plate to represent the correct total seat mass.

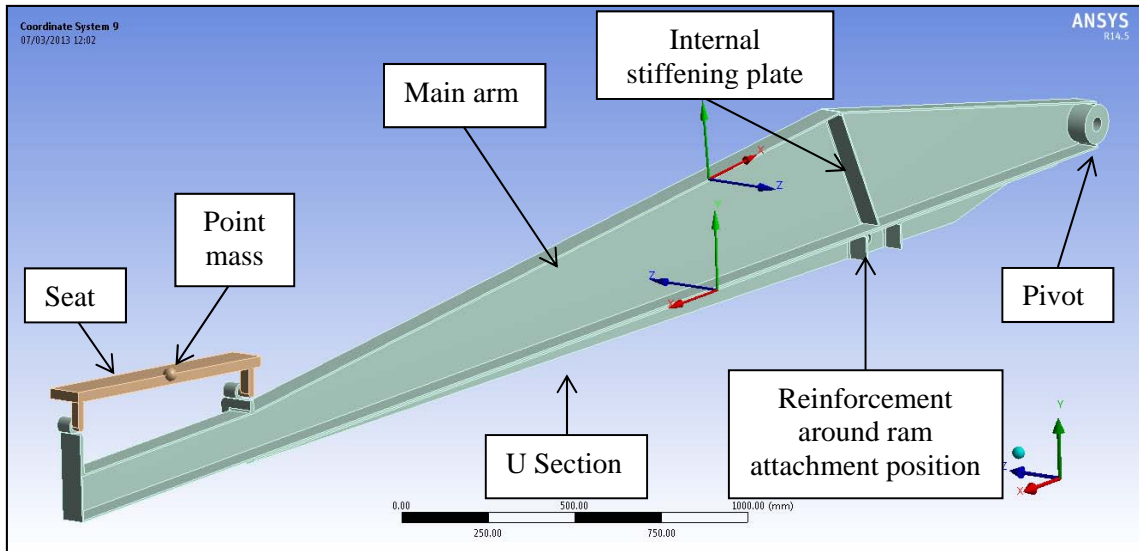


**Figure 24** Overview of finite element model

The following material properties were used:

- Young's modulus,  $E = 200 \text{ GPa}$
- Poisson's ratio,  $\nu = 0.3$
- Density,  $\rho = 7850 \text{ kg/m}^3$

As the model was assumed to be linear elastic, the yield stress and tensile strength of the material were not needed for the model.

The following constraints and loads were applied to the models.

- A vertical symmetry plane was assumed along the length of the arm (symmetry in the  $x$ - $y$  plane in the figures).
- The internal surface of the hole through the central pivot boss was constrained using cylindrical constraints. This would allow rotation about the axis of the pivot, but no translation.
- The surfaces of the pin holes through the U section when the ram is attached were given compression only constraints.
- The top edges of the U section were bonded to the lower face of the main arm.
- The pins of the seat were bonded to the inner surfaces of the pin holes of the arm.
- An acceleration due to gravity ( $9.81 \text{ m/s}^2$ ) was applied to all components. The arm was assumed to be in the horizontal position.
- An angular acceleration was applied to all components with the centre of rotation set as the centre of the central pivot boss.

Solid, mainly hexahedral brick, elements were used throughout the model.

A model with a relatively coarse mesh was used for validation, as the stress was not expected to vary significantly in the areas of interest. This model contained approximately 40,000 elements. For the main model used for the stress analysis, the mesh was greatly refined in the area around the apex and around the seat connections. In these areas, the element size was chosen so that there would be at least 3 elements through the wall thickness. This model contained approximately 80,000 elements.

Solution times for the more detailed models were in the order of 20 minutes.

#### 4.10.4 Validation of FE models

The results shown at 4.10.2 also give a relationship between acceleration and strain that can be used to validate the finite element model. On the charts in Figure 22 and Figure 23 are the equations of the linear relationships between acceleration and strain. In these relationships, the gradient is more important than the intercept, as the intercept may not be accurate due to the strain gauges being applied while the arm was loaded by gravity and a true zero strain reading therefore being difficult to ascertain.

The results from the validation model are shown in Table . The results are in terms of microstrain per unit of acceleration (in g). There was excellent agreement between the results obtained using the finite element model and the experimental results obtained from the instrumented arm.

**Table 12** Comparison of results from experimental tests and model, expressed in terms of microstrain per g of acceleration

Location	Experimental	Finite Element Model	Difference
Top of arm	73.72	73.65	0.1%
U Section	-45.69	-43.93	3.8%

#### 4.10.5 Main finite element results

The main high stress areas are shown on the outside of the arm and inside the arm in Figure 25 and Figure 26 respectively. The highest stresses were found to occur on the underside of the weld across the top of the arm, as shown in Figure 26. At this location, the top plate weld was under bending, with the maximum principal stress being 217 MPa, which was in the longitudinal direction. The top of the weld was in compression, with the stress in the longitudinal direction being -130 MPa. This stress configuration could lead to extensive internal crack propagation before any part of the crack reached the accessible external side of the plate.

High stresses also extended along the top of the arm from the highest point towards the central pivot. Although the stresses in this area were not as high as those under the top of the weld, the stresses across this area were fully tensile through the thickness of the plate.

The weld connecting the inner plate to the sides of the arm were also found to be highly stressed, as shown in Figure 26. For this location, as the peak stress was occurring at a sharp corner at the weld toe, the hot spot stress was calculated. To calculate the hot spot stress, which is the geometric stress without the influence of the weld stress concentration, the stress at the toe is extrapolated from the stress values obtained at  $0.4t$  and  $1.0t$ , where  $t$  is the plate thickness. This method of evaluating stresses at welds is commonly used when evaluating fatigue using the S – N curve method (see section 4.10.6.2 for more details).



To ascertain the stresses occurring in the side plates of the arm, assuming a full width through thickness crack removed the loadbearing capacity of the top plate, an additional model was run with the top plate removed over the areas of interest. This model showed lower stresses around the apex, with the highest stresses occurring in the top plate between the apex and the pivot. The main results are shown in Table .

**Table 13** Results from the finite element analysis

Location	Stress (MPa)
Inside apex, longitudinal stress	217
Outside apex, longitudinal stress	-145
Top of arm between pivot and apex	151
At weld of internal plate (hot spot stress)	223

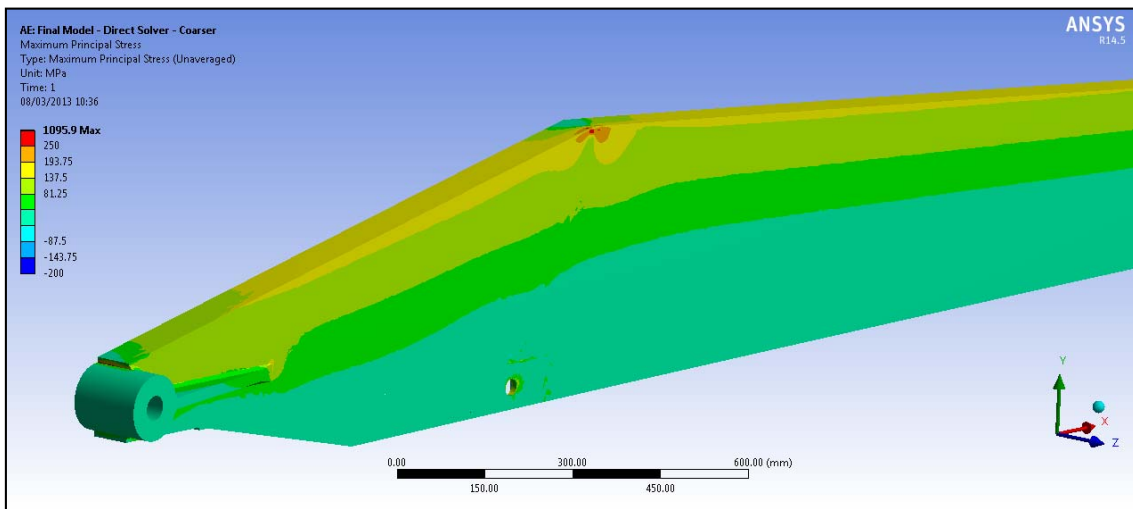


**Figure 25** Plot of maximum principal stress

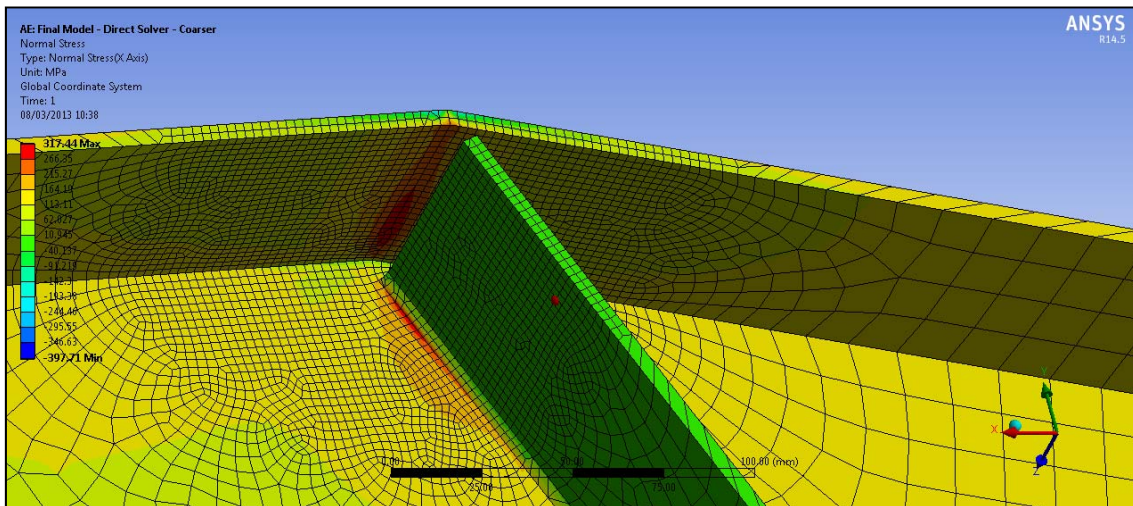


**Figure 26** Normal stress (longitudinal direction) on inside of the arm

#### 4.10.6 Fatigue Analysis

There are two main methods for evaluating the fatigue life of structures, the S-N curve approach, and the fracture mechanics approach. The S-N curve approach is widely used in design and is the basis of the methods in standards such as BS7608:1993 Fatigue design and assessment of steel structures and BS1993-1-9:2005 Eurocode 3: Design of steel structures – Part 1-9: Fatigue. Using this approach, strength (S) - fatigue life (N) curves are used to assess the proportion of the fatigue life that each stress range in the expected stress history uses. Summing the proportions for each stress range gives a proportion of life used per year of operation, which could be inverted to give an expected life.

For the fracture mechanics approach, an existing defect is assumed to be present in the structure and the growth rate of the defect is estimated. The size of the existing defect would normally be set to a size that could reasonably be missed at a routine inspection. Using this approach, it is possible to estimate a number of load cycles between an inspection, and the crack growing to a critical size that would cause failure of the component.

The Crackwise programme was used for this analysis. This software implements BS7910:2005 Guide to methods for assessing the acceptability of flaws in metallic structures (28).

BS7910:2005 (28) contains a number of different solutions for different geometries, such as cracks in flat plates, cylinders and spheres. However, it does not contain a solution for a thin-walled box section beam. The analysis was therefore split into two parts, using plate solutions for the top plate and the side plate separately. It was assumed that the top plate had a central through thickness crack, and an edge through thickness crack at the top of the side plate.

One factor in the fatigue assessment that has a large influence on the fatigue life is the assumed size of the initial crack. As crack growth is slowest when the cracks are short, a small change in the initial crack size can have a much larger effect on life than a change in critical crack size, when the crack is growing rapidly.

In the absence of actual data on the sizes of cracks found during an inspection, an initial crack size must be assumed. This should be based on the maximum size of crack that could be missed during an inspection. This is highly dependent on the detection technique used, the geometry and condition of the component, the conditions under which the inspection takes place and the skill and diligence of the operator. In the case of the Safeco Crazy Frogs type amusement device, access to the highly stressed top surface of the arm may be restricted by the presence of a conduit carrying cabling to the car at the end of the arm. Therefore, as it cannot be shown that there is no crack under the conduit, it would be appropriate and conservative to assume that a 10 mm through thickness crack is present under the conduit.

For cracks propagating down the side of the arm it would be likely that they would start at the top where the stresses are highest and where welds may act as initiators. All of the side plate, including the radius into the top plate, should be accessible, therefore in this region it was assumed that a crack of 5 mm in length would be detectable, which would equate to the thickness of the top plate.

The weld connecting the internal stiffening plates to the side plates is not accessible so a visual method of inspection would not be possible. Therefore, a method such as ultrasonic inspection would be required. An initial defect with a depth of 2.5 mm (half plate thickness) and 10 mm long was assumed for the fatigue analysis.

#### 4.10.6.1 Assessment using data collected from the Wilkinson's DJ Jump amusement device

Data from two test runs from the site visit to Mr Wilkinson's DJ Jump device were used for the fatigue assessments. The first assessed was test run 22, which was requested by HSL to be representative of a standard ride sequence that would be given to customers at a fair. This included the use of the foot pedal, although the accelerations achieved during this test were somewhat lower than those obtained during other tests.

The second dataset assessed was test run 12, which cycled through the full range of programmes with an operating pressure of 7.5 bar. The accelerations obtained in this test run were considerably higher. The numbers of load cycles<sup>3</sup> occurring for each load range for the two datasets used as listed in Table . Although this was not intended to represent a standard ride sequence, it illustrates the magnitude of accelerations possible with the use of the foot pedal. One difficulty with assessing the operation of the amusement device is the fact that the severity of the ride sequence is very dependent on how the foot pedal is used. Aggressive or mis-timed use of the foot pedal may even increase stresses further. The fatigue assessment performed using this ride sequence data therefore illustrates the possible implications of foot pedal use.

Due to technical problems with the data logger on some test runs, the full runs were not recorded on the logger. Therefore, the data from the GP1 accelerometer placed on the seat was used for the analysis.

This accelerometer was not perfectly aligned to the ride arm due to the inclination of the seat, both in terms of the seat base tilting back and the seat being higher at the outer end of the seat. The inclinations were corrected for and the accelerations due to gravity and the rotation of the ride were removed to give the actual acceleration (due to motion) of the arm at the seat location. When the arm was level and rotating, the accelerometer on the seat would be recording accelerations due to gravity and centrifugal forces as listed in Table 6. Subtracting the values in Table from the accelerometer readings for the three components and then finding the resultant from the corrected components gave the actual radial acceleration of the arm. This was found to be approximately 0.9 g less than the recorded Z component, therefore, 0.9 g was subtracted from the Z component when calculating the stresses for the fatigue assessments. It should be noted that the Z component, as recorded, would be what the passengers would experience, including the effect of gravity.

**Table 14** Components to be subtracted from accelerometer reading to obtain accelerations due to change in velocity

Accelerometer axis	Gravity component (g)	Centrifugal component (g)
X	0.24	-0.01
Y	0.08	-0.53
Z	0.97	0.04

<sup>3</sup> A load cycle refers to one raise and lower cycle of the arm.

**Table 15** Loading spectrums assumed for the fatigue analysis. The acceleration values do not include the effect of gravity

Range (g)	Test Run 12		Test Run 22	
	Count	Average (g)	Count	Average (g)
0-1	196	-	155	0.24
1-2	76	1.34	66	1.68
2-3	31	2.61	44	2.49
3-4	46	3.67	52	3.63
4-5	41	4.52	3	4.14
5-6	13	5.59	-	
6-7	1	7.03	-	
7-8	2	8.41	-	

#### 4.10.6.2 Fatigue analysis

The welds connecting the inner stiffener plate to the side plates of the main arm were found to have the highest hot spot stress, so this area was assessed using the design life approach, to provide a comparison to previous assessments. The assessment was performed for both test run 12 and test run 22. The full table of results for test run 12 is shown in Table .

The calculated life for the standard fair test run 22 was 3 years. This is comparable to the life that Lacey would have calculated if he had assumed a zero minimum stress, but is significantly lower than the 5.19 years calculated by Lacey or the 6 years obtained by the ITA report.

If the weld is assessed using the more severe test run 12 stress history, this results in a reduction in life to 1.5 years. The assessments were based on the class D design curve, which is the mean curve minus two standard deviations, giving a 95% probability of survival. Therefore, these results are not predicting that the actual life would be 1.5 years under these loadings, but are conservative and appropriate for a safety-critical structure.

**Table 16** Fatigue Assessment of internal stiffener plate weld for Test Run 12

Load (g)	Stress (Hot-spot stress), MPa	Load Cycles per ride	Yearly load cycles n	N (Class D Design Curve)	n/N
1.34	55.7	76	323000	8786635	0.04
2.61	85.8	31	131750	2408207	0.05
3.67	110.9	46	195500	1115359	0.18
4.52	131.0	41	174250	676319	0.26
5.59	156.3	13	55250	397970	0.14
7.03	190.4	1	4250	220221	0.02
8.41	223.0	2	8500	136953	0.06
				<b>Sum (n/N)</b>	0.66
				<b>Life (years)</b>	1.51

Three different areas were assessed - the apex, an area between the apex and the central pivot (zone 2), and the weld of the inner stiffening plate. The top plate at the apex was in bending, with the underside in tension and the top in compression.

The first two areas were assessed for two sequences of crack propagation. The first sequence assessed the crack growth across the top plate and then down the side plates once the top plate had failed. The stresses used in the side plate analysis were those obtained from the models with the top plate removed. The second sequence assumed that a crack at the top edge of the arm grew down the side plate before the top plate had failed. For this analysis, the stresses in the side plate were taken from the model with the top plate intact.

For the assessment of a crack originating from the toe of the internal plate weld, the stresses were based on the model with the top plate intact.

For the top plate, the initial defect assumed was a through thickness crack of 10 mm total length. This was chosen as a crack of this size may not be detectable under the conduit welded to the top of the arm. If possible, it would be preferable not to tack weld the conduit along the top of the arm but to find another route for the cables, such as under the removable lighting panels. The solution for a through thickness crack takes into account the width of the plate, assuming an increase in global stress as the proportion of the plate carrying load reduces as the crack grows. For the arm, the load would be transferred to the side plates. Therefore, the assumed width of the plate was increased from the actual 140 mm so that the global stress with a 140 mm crack would be the same as the stress at the top of the side plates with no top plate modelled.

For the top plate at the apex, it was assumed that the crack grew through the weld, and that no post-weld heat treatment had been applied. Therefore, residual stresses equivalent to the yield strength of the parent material were assumed. As recommended by BS7910, the crack growth laws assumed for the weld were the upper bound (mean plus two standard deviations). For non-welded areas (the side plates) the mean crack growth law was used. However, for all areas, the growth law for load ratios,  $R^4 > 0.5$  were used for conservatism.

For the side plates, the long surface crack solution was used. Although this solution is intended primarily for long cracks running along the surface of plates, it is possible to use this solution for edge cracks under bending. For analysis of the side plates, it was assumed that the initial crack was 5 mm in length, equivalent to the thickness of the top plate.

At the internal plate weld, a surface crack was assumed to be growing from the toe of the weld into the parent metal of the arm side plate. The residual stress distribution for this analysis was that recommended in BS7910, i.e. equal to the residual stress at the toe of the weld and reducing through the thickness of the plate. The crack growth laws assumed were the mean plus two standard deviations growth law for a stress ratio  $R > 0.5$  to allow for the weld residual stresses.

The material properties were taken from documents obtained from Safeco [Certificates, technical reports and tests of materials report concerning the Safeco Crazy Frogs fair ride mentioned below (Series no. 900421)", SERCO, 2003]. These were:

- Yield stress - 440 MPa

---

<sup>4</sup> The  $R$  ratio is the ratio of minimum stress occurring in the fatigue cycle to the maximum stress. Therefore, if a minimum stress of zero is assumed, the  $R$  ratio would be zero. A  $R$  ratio of 0.5 implies a minimum stress of half the maximum.

- UTS - 540 MPa
- Fracture toughness was based on the minimum Charpy impact energy of 77 J, converted to 97 MPa√m using the conversion tool in Crackwise (upper limit for Kmat).

As the fatigue analysis predicted brittle failures, the exact values of yield stress and UTS used would not be likely to significantly affect the results. Also, as crack propagation rates would be high immediately prior to failure, although using a higher fracture toughness would be likely to increase the critical crack size, the increase in life would be small.

Some of the assumptions used in the analysis were conservative.

- The car was loaded with 160 kg for every ride. With the car unloaded, stresses would be approximately half those with the car loaded. Crack growth rate is highly sensitive to stress range, so very little crack growth would occur if the car was empty.
- The analysis of cracking in the side plates ignores any possible load shedding onto the other side of the arm. In effect, it was assumed that both sides of the arm were cracking simultaneously.

The results of the fatigue analysis are listed in Table .

**Table 17** Results of the fatigue analysis in terms of ride cycles<sup>5</sup> to failure

Area	Crack location	Test Run 12	Test Run 22
<b>Zone 2</b>	Top plate	2370	>8500
	Side plate (top plate failed)	860	2070
	Side plate (top plate intact)	4240	>8500
<b>Apex</b>	Top plate	70	460
	Side plate (top plate failed)	7500	>8500
	Side plate (top plate intact)	>8500	>8500
<b>Internal Plate Weld</b>	Surface crack at weld toe	860	2380
<b>Zone 2</b>	Top plate weld repair		1550
	Side plate weld repair (top plate intact)	-	170

The analysis has extended to 8500 ride cycles, as this would correspond to two years of normal use.

According to the procedures in BS7910:2005 (28), unless post-weld heat treatment has been used to relieve residual stresses in the area of a weld, stresses equal to the yield stress of the parent material should be assumed. This can have a significant effect on the critical defect size. The procedure also recommends that the upper bound crack growth law is used (mean plus two standard deviations (SD)) and an R ratio of more than 0.5 unless evidence can be shown to support the use of less conservative growth laws. The R ratio is the ratio of the minimum stress in the load cycle to the maximum stress. A load cycle ranging from zero up to the maximum

<sup>5</sup> Ride cycles refer to a full ride sequence that a passenger would experience in normal operation

(which is assumed for this assessment) would have an R ratio of zero. However, tensile residual stresses due to welds would increase the minimum stress in the cycle, and therefore increase the R ratio.

The effect of using the mean plus 2 SD law increases the growth rate by approximately a factor of two and the higher R ratio growth law has an even larger effect, although the exact magnitude of the difference is dependent on the stress ranges. Therefore, these two factors act to significantly reduce the calculated fatigue life, although some of the reduction will be due to an increase in conservatism to take into account the greater uncertainty concerning the material properties and stress states in the weld vicinity.

Due to the high level of bending, and the assumptions for welds as discussed, the top plate at the apex is assumed to exhibit rapid crack growth. This would be from the inside, due to the direction of the stresses, and it may be possible that a crack would grow extensively on the inside before breaking the surface and being visible on the outside.

However, due to the stresses in the side of the arm at the apex being lower than in the area between the apex and the pivot when the top plate is assumed to have failed, the crack growth from the apex down through the side wall was much slower. Therefore, for both ride sequences, the worst case was for cracks between the apex and pivot, rather than at the apex. This is where the failure occurred in the 2009 failure at Blackpool (9). A weld repair in this location probably contributed to the failure, although the fact that this area needed repair may support the hypothesis that this is an area prone to fatigue.

From the above analysis, it would appear that shorter fatigue lives are obtained for the scenario where the crack grows through the top plate first, then down the side plates.

The analysis of cracks originating from the toe of the welds connecting the inner stiffening plate to the side plates resulted in the lowest number of cycles to failure. At 2,380 cycles for the standard ride cycles (test run 22), this represents just over half a normal yearly total. While it would be normal to schedule inspections at around half the expected number of cycles to failure, the assessment contains sufficient conservatism arising from conservative growth laws and assuming fully loaded car for every ride to allow less frequent inspections.

Heavy use of the foot pedal, with the associated higher accelerations and stresses on the arm, could reduce the fatigue life of the amusement device. Based on the assumptions used here, an assumed initial defect could grow to a critical length (leading to catastrophic arm failure) after approximately 900 ride sequence cycles. This analysis was based on large accelerations and the car being fully loaded at all times. It is therefore likely to be conservative, but it is clear that twice yearly inspections would not be sufficient under this loading regime.

If a weld repair has been used on a highly stressed area of the arm (and this would include much of the top half of the beam either side of the apex), the fatigue life could be severely compromised. Due to the assumed residual stresses present after welding, and the fact that BS7910 recommends the use of the upper bound crack growth law for welds as discussed earlier, the fatigue life was calculated to be 170 standard (test run 22) ride sequence cycles, even if the majority of the top plate was intact. This is for repair welds running down the side plates. Repair welds only across the top plate would last longer (1550 ride cycles from Table 17) and would benefit from the 2070 ride cycles to grow a crack through an unrepaired side plate. A 5 mm long crack in at the top of side plate would already be critical under the more severe loading ride sequence cycle. While repair welds on any part of the arm reduce the fatigue life, it is therefore strongly recommended that weld repairs are not performed on the side plates of the arms.

#### **4.10.7 NDT Schedule**

The aim of an NDT schedule is to ensure that the correct areas of an amusement device are inspected, that the inspections occur with the correct frequency, and that the correct procedures are followed. This should allow any defects to be detected before they jeopardise the structural integrity of the amusement device. Advice on NDT schedules can be found in the HSE guidance document HSG175 Fairgrounds and amusement parks – Guidance on safe practice (29) and in Safety of Amusement Devices: Non-destructive Testing (30) published by the Amusement Device Safety Council. The latter document lists the information of be included in an NDT schedule as:

- Component parts that require NDT inspection;
- The frequency of testing;
- NDT methods for each component part;
- Defect acceptance criteria;
- Name of the competent person issuing the NDT schedule;
- Date of issue.

A number of existing NDT schedules for Safeco Crazy Frogs devices were reviewed, all of which consisted of yearly magnetic particle inspections (MPI) of the arm (although ultrasonic techniques were required for other components). Argyll-Ruane Level 3 services department developed an NDT schedule for assessment of the arm, which is included as Appendix 6.5. This includes assessment of the top of the arm (not included in some early schedules) and requires the ultrasonic testing of some areas (under the apex and the side plates in the region of the internal stiffener plate) to detect internal cracks.

The recommended inspection interval has been reduced to six months rather than yearly as in previous schedules. As the usage of the amusement devices is seasonal rather than even throughout the year, the interval should be interpreted as halfway through the season, rather than six months, as it could be possible to have nearly a full year's worth of ride cycles occurring in six calendar months.



## 5. REFERENCES

- (1) British Standards Institution. Fairground and amusement park machinery and structures. Safety (Incorporating corrigendum 2011). BS EN 13814: 2004.
- (2) Boocock MG. A biomechanical appraisal of anterior wedge fractures of spinal vertebrae following an incident at a fairground ride. Sheffield, United Kingdom: Health & Safety Executive Research and Laboratory Services Division; 1992. Report No.: EBS/92/7.
- (3) Jackson JA. Ergonomics assessment of selected amusement rides at Tilburg Fair, Holland. Sheffield, United Kingdom: Health and Safety Laboratory; 1995. Report No.: EWP/95/20.
- (4) Monnington S, Jackson JA, Milnes E. Passenger containment on a Jump and Smile fairground ride. Sheffield, United Kingdom: Health and Safety Laboratory; 2000. Report No.: ERG/00/12.
- (5) Jackson JA, Monnington S, Boorman C, Milnes E. Establishing criteria for safe g-force levels for passenger carrying amusement rides . Sheffield, United Kingdom: Health and Safety Laboratory; 2002. Report No.: HSL/02/07.
- (6) Milnes E. Assessment of g-forces on Jumping Frogs ride. Sheffield, United Kingdom: Health and Safety Laboratory; 2004. Report No.: ERG/04/02.
- (7) Milnes E. Assessment of g-forces in the Crazy Frog amusement ride. Sheffield, United Kingdom: Health and Safety Laboratory; 2004. Report No.: ERG/04/20.
- (8) Milnes E, Marlow P, Bunn J, Ferreira J, Jones A, Birtles M, et al. Passenger Behaviour on Amusement Rides: Field Study Report. Sheffield, United Kingdom: Health and Safety Laboratory; 2004. Report No.: ERG/04/24.
- (9) Joel S. Examination of items from the Crazy Frog fairground ride, Central Pier, Blackpool. Buxton: Health and Safety Laboratory; 2010. Report No.: ES/MM/LET/10/22.
- (10) Pinder ADJ. Risks associated with increased speed ratings for energy accumulation lift buffers with nonlinear characteristics. Buxton: Health and Safety Laboratory; 2013. Report No.: HuSU/13/12.
- (11) Kazarian LE. Standardization and interpretation of spinal injury criteria. Wright-Patterson Air Force Base: Aerospace MEDical Research Laboratory; 1978. Report No.: AMRL-TR-75-85.
- (12) Willen J, Anderson J, Toomoka K, Singer K. The natural history of burst fractures at the thoracolumbar junction. *Journal of Spinal Disorders* 1990;3(1):39-46.
- (13) Glaister DH. Human tolerance to impact acceleration. *Injury* 1978;9(3):191-8.
- (14) Snyder RG. Impact. In: Parker JF, West VR, editors. *NASA Bioastronautics data book*. 2nd ed. Washington DC: National Aeronautics and Space Administration, Scientific and Technical Information Office; 1973.

- (15) Eiband AM. Human Tolerance to Rapidly Applied Acceleration. Washington, USA.: National Aeronautics and Space Administration; 1959. Report No.: NASA Memorandum 5-19-59E.
- (16) Glaister DH. Human response to +Gz ship-shock acceleration. Farnborough: Institute of Aviation Medicine; 1974. Report No.: Scientific Memorandum S109 .
- (17) RWTUV GmbH. Fairground Rides: Attractions with Calculated Safety. The Strain on Passengers, Limit Values for Roller Coaster (No longer available). TUV Newsletter 2004.
- (18) Standards Association of Australia. AS 3533.1 Amusement Rides and Devices part 1: Design and Construction. Appendix D: Basic Facts on the Effects of Acceleration on the Human Body. 1997.
- (19) ASTM International. F2291 - 11: Standard Practice for Design of Amusement Rides and Devices. West Conshohocken, PA : ASTM International; 2011.
- (20) Safeco. S-86 User Guide. Zaragoza: Spain: Safeco; 2005.
- (21) Pheasant ST. Bodyspace: Anthropometry, ergonomics and design. 2nd ed. London: Taylor & Francis; 1996.
- (22) Steenbekkers LPA. Child development, design implications & accident prevention. The Netherlands: Delft University of Technology; 1993. Report No.: No 1. in the Physical Ergonomics Series.
- (23) Schultz RB, Obergefell LA, Rizer A, Albery CB. Whole body center of gravity and moments of inertia study. Brooks AFB, Texas: Armstrong Laboratory; 1996. Report No.: 96MM6643.
- (24) *PeopleSize Professional 2008* [computer program]. Version 2.01. Melton Mowbray, United Kingdom: Open Ergonomics; 2009.
- (25) The Building Regulations, Part K: Protection from falling, collision and impact. 2010.
- (26) Varona Badorrey JL. Fatigue analysis of the metallic mobile beams belonging to "Jumping Frogs" machine. Zaragoza, Spain: Instituto Tecnológico de Aragón; 2005. Report No.: 250\_I050037.
- (27) Lacey D. Structural verification of SAFECO 'Jumping Frog' amusement ride. Nottingham, United Kingdom: Advanced Computational Analysis Consultants; 2006. Report No.: 061215-2.
- (28) British Standards Institution. Guide to methods for assessing the acceptability of flaws in metallic structures. BS 7910: 2005.
- (29) Health and Safety Executive. Fairgrounds and amusement parks: Guidance on safe practice. Sudbury: HSE Books; 2007. Report No.: HSG 175.
- (30) Amusement Device Safety Council. Safety of Amusement Devices: Non-destructive Testing. Sunderland, United Kingdom: ADIPS Ltd; 2012.

- (31) Ruff S. Brief Acceleration: Less than one second. In: United States Air Force (USAF), editor. German Aviation Medicine in World War II (Volume 1). Washington DC: Government Printing Office; 1950. p. 586-7.
- (32) Brinckman P, Biggemann M, Hilweg D. Fatigue fracture of human lumbar vertebrae. Clinical Biomechanics 1988;1(Suppliment No. 1):1-23.
- (33) NATO. Methodology for Protection of Vehicle Occupants against Anti-Vehicular Landmine Effects. Paris, France: Research and Technology Organisation (NATO).; 2007. Report No.: RTO-TR-HFM-090 AC/323(HFM-090)TP/72.

## **6. APPENDIX**

### **6.1 REVIEW OF PREVIOUS INFORMATION**

#### **6.1.1 Tilburg Fair Holland 1995 (EWP/95/20)**

This work was undertaken at the request of HSE. The aim of the study was to provide ergonomics advice regarding any problems with rides that were being considered for the Glasgow Christmas Fair. Four rides were selected for assessment; the Sky Tower, Spin Ball, Evolution and Crazy Jump. No acceleration data was recorded for the Crazy Jump. The report does include an assessment of the passenger restraint, which concluded that the current design makes it unsuitable for children. This was due to the large distance between the restraint bar and the seat pan that could potentially allow a passenger to slip under the restraint bar and be ejected from the ride. This may also be an issue for adults who cannot brace their feet against the foot rest. The report recommends a minimum height restriction of 1.4 meters (corresponding to a 5<sup>th</sup> PCTL 12 year old).

#### **6.1.2 Jump and Smile (La Sauterelle) – Nottingham 2000 (ERG/00/12)**

This report details a joint visit to Nottingham Market Square to undertake an ergonomics assessment of the La Sauterelle fairground ride (Figure 27) following concerns regarding the effectiveness of the passenger containment system. The ride was manufactured by Safeco. No acceleration data was collected. It does include a qualitative assessment of the passenger containment system. The dimensions of the relevant containment system components and their associated body dimensions are given in Table . Analysis of the ride dimensions and associated body parts suggest that the fit of the restraint may not sufficiently contain large proportions of the potential ride passengers.

The ride has no means for passengers to brace against the rides forces using their legs and feet. There is a foot plate (step) below the seat pan, but this is designed to enable passengers to step into the car. The gaps between seat pan and lap bar and seat back and lap bar suggest that smaller passengers gain little support from these structures. As a result bracing and containment relies mainly on the hand rail and seat back rather than containment of the lap bar to contain them. This, in conjunction with the dynamics of the ride, has the potential for passengers to move voluntarily and involuntarily into a position where they could be ejected by the ride forces. The main recommendation arising from this report was that the passenger containment system should be reviewed by a competent person and improvements made to increase the effectiveness of the lap bar system and to improve the potential for passenger bracing against the ride forces.



**Figure 27** La Sauterelle

**Table 18** Relevant containment system components and their associated body dimensions

Dimension	Measurement (mm)	Body dimension (mm)	Passenger range	Data (mm)	Mismatch (mm)
Backrest height	500	Seated shoulder height	Large	658	-158
Seat pan height	560 to 660	Popliteal height	Small	415	-145 to -245
Seat pan depth	410	Buttock to popliteal	Small	416	6
Backrest width	1100 (3 seats)	Bideltoid	Large	(486 x 3) = 1458	-358
Side support height	370	Seated shoulder height	Large	658	-288
Side support depth	410	Buttock to popliteal	Large	544	-134
Backrest to lap bar	420	Abdominal depth	Small to large	200 to 325	-220 to 95
Seat pan to lap bar	160	Thigh thickness	Small to large	127 to 176	-33 to -16
Seat back to hand rail	472	Forward reach	Small to large	628 to 834	156 to 362
Diameter handrail	25	Grip diameter	Small	44	19

### 6.1.3 Crazy Frog – 2004 – Scotland (Glasgow / St Andrews) ERG/04/02 and ERG/04/20

This work was undertaken in response to an incident in 2003, when a female member of the public (IP) sustained an injury whilst on a Jumping Frogs ride (Figure 28). The objectives of this study were:

1. To record g-forces exerted on passengers by the Jumping Frogs ride;
2. To determine the likelihood of spinal (or any other) injury due to the ride forces or ride environment;
3. To provide recommendations on ways to reduce the risk of injury from exposure to ride forces

Two visits were made in order to measure the ride g-forces. In order to take measurements of the ride motion an Entran® +/-25g, tri-axial accelerometer was attached to the seat. This accelerometer was orientated such that its coordinate system was as indicated in Table . The data was recorded onto a data logger (HSL proprietary equipment: 'e-fairlog') at 40Hz and downloaded onto a laptop computer using HSL proprietary software and the results were then passed through a Butterworth 10 Hz low pass filter in accordance with BS EN 13814:2004.

1. Performed a low-pass software filter (Butterworth 10Hz) to remove noise.
2. Imported data file into Excel and identified any z-axis data points that exceeded 2g and -0.1g
3. Identified peak values and match these with types of ride motion. From the initial tests at St Andrews, 2 key types of ride motion were identified. These types of motion, described below, can be alternated between cars to create different overall patterns of motion:
  - a. Low-frequency high-amplitude 'wave' motion;
  - b. High-frequency low-amplitude 'bouncing' motion.
4. Calculated the typical jerk (rate of onset / change of g) values for periods of the main motion types.

Two main types of ride motion were identified and examined; Low-frequency (1.2 Hz) wave type motions and higher-frequency (0.6Hz) bouncing motions. The g-forces found ranged between approximately 2.8 and 3.3g (peak) for the wave motions and approximately 2.6 and 4.1g (peak) for the bouncing motions. The g forces recorded during the visits are shown in (Figure 29 to Figure 34). The g-forces, as single case events, are not believed to present a significant risk of injury to the majority of the population. However, the repetitive nature of the accelerations may present a risk of injury to some people primarily because of individual differences (i.e. lower than normal bone density, previously cumulated bone fatigue, damaged intervertebral discs). There is also some suggestion that rapid onsets of g may give insufficient time for muscular damping systems to react fully effectively, and that consecutive accelerations may therefore result in greater than expected applied stress to the vertebrae.

**Table 19** Descriptions of g-force accelerations and their perceived effects on fairground ride occupants (E-Fairlog coordinate system)

<b>Axis</b>	<b>Direction of g-force</b>	<b>Description of g-force accelerations on the ride</b>	<b>Perceived effect of g-force on passenger (i.e. ride 'sensation')</b>	
<b>X</b>	Fore / aft	Positive (+gX)	Ride accelerating in a <u>backward</u> direction, in relation to the seat orientation	<b>Occupant feeling like they are being forced <u>forwards</u>, away from the seat back</b>
		Negative (-gX)	Ride accelerating in a <u>forward</u> direction, in relation to the seat orientation	<b>Occupant feeling like they are being forced <u>backwards</u>, into the seat back</b>
<b>Y</b>	Side to side	Positive (+gY)	Ride accelerating to the <u>right</u> hand side in relation to the seat orientation	<b>Occupant feeling like they are being forced to their <u>left</u> hand side, in relation to the seat</b>
		Negative (-gY)	Ride accelerating to the <u>left</u> hand side in relation to the seat orientation	<b>Occupant feeling like they are being forced to their <u>right</u> hand side, in relation to the seat</b>
<b>Z</b>	Up / down	Positive (+gZ)	Ride accelerating <u>upward</u> in relation to the seat orientation	<b>Occupant feeling like they are being forced <u>downwards</u>, into their seat</b>
		Negative (-gZ)	Ride accelerating <u>downward</u> in relation to the seat orientation	<b>Occupant feeling like they are being forced <u>upwards</u> (i.e. weightless), out of their seat</b>

*N.B. The coordinate system used in previous reports differs from that specified in BS EN 13814:2004 (in the direction of the Z axis). This is due to the historical development of the HSL g-force measuring system predating the Standard, and for consistency in HSL reports.*

Trunk posture is another important factor in determining the stress which vertebrae will experience under a particular g-force. Studies indicate that trunk flexion postures (i.e. head nodding forwards, bending the trunk forwards) will lead to localised increases in the compression forces acting on the vertebrae (particularly at the front/anterior edges). Rate of onset levels (rate of onset of g) were determined from the data. The maximum rate of onset levels were significantly lower than those referred to in the studies identified in the literature. It is therefore not possible to say whether the rate of onset levels could be a risk factor on this particular ride. However, in view of the lack of research on repeated rate of onset exposure at the levels measured, it may be useful to assume for the time being that they could be a contributing risk factor and take steps to reduce exposure to them.



**Figure 28** Safeco Crazy Frogs 11<sup>th</sup> August 2003 at St Andrews street fair

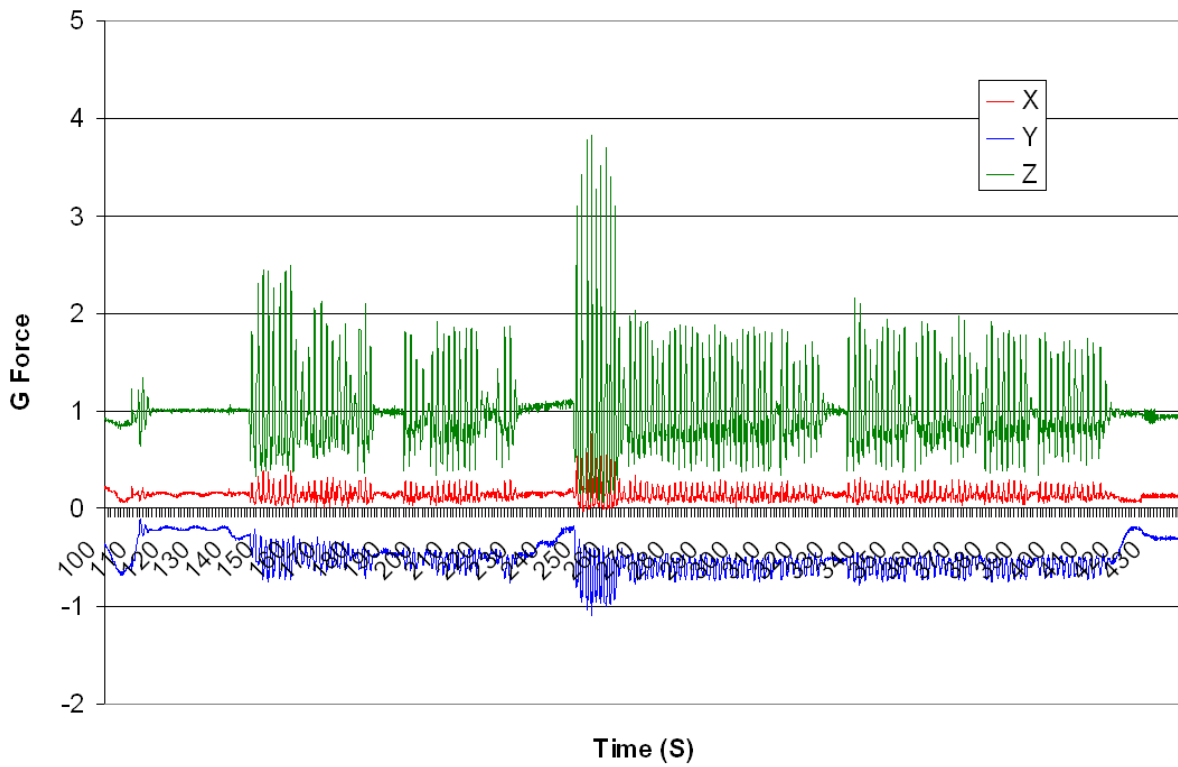


**Figure 29** St Andrews Test 1



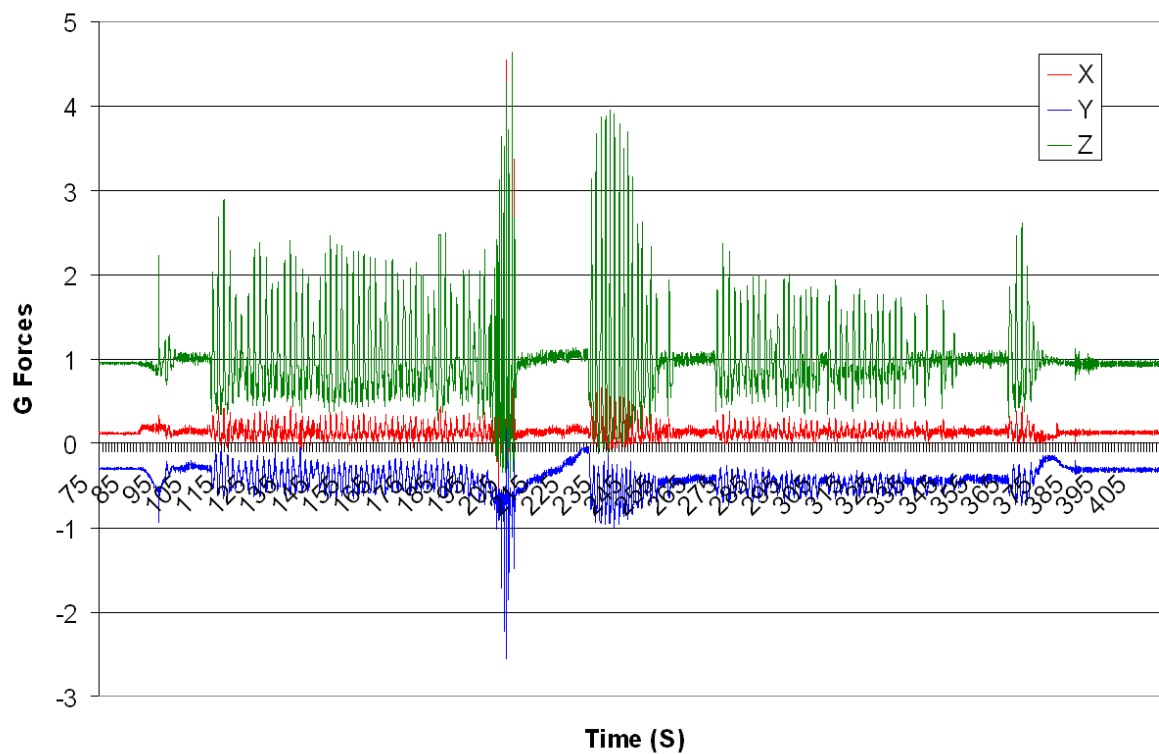


**Figure 30 St Andrews Test 2**

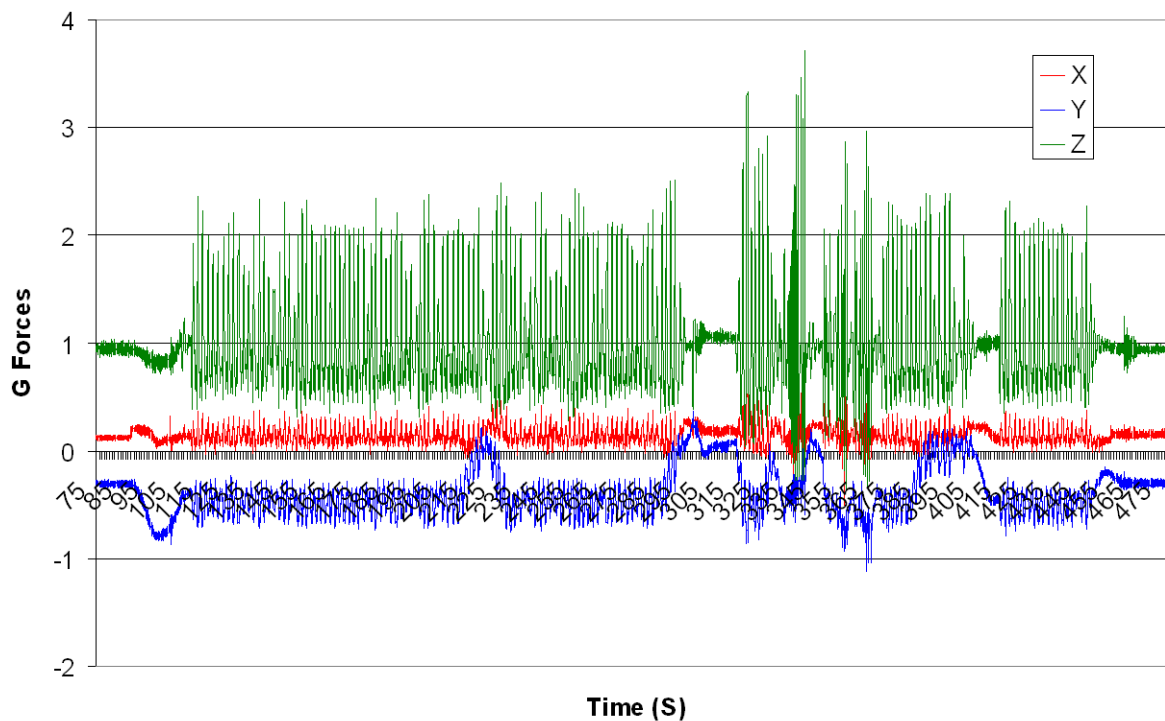


**Figure 31 St Andrews Test 3**



Figure 32 9<sup>th</sup> December 2003 at Horne's Yard in Glasgow

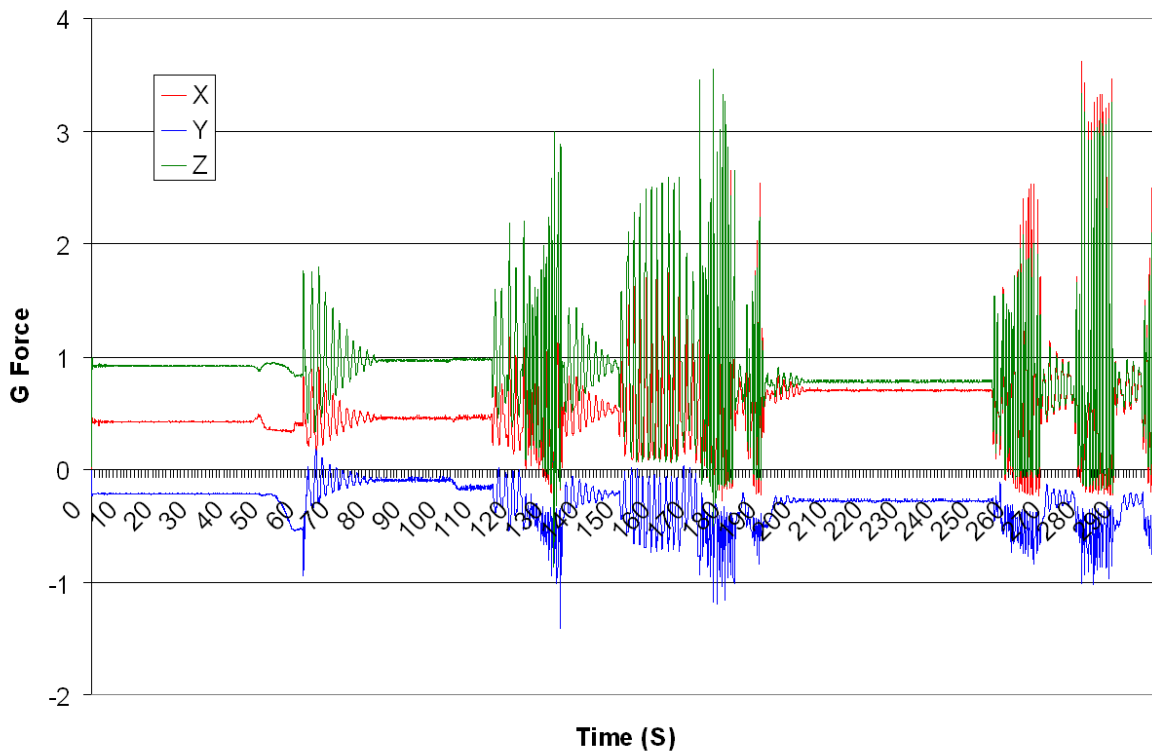
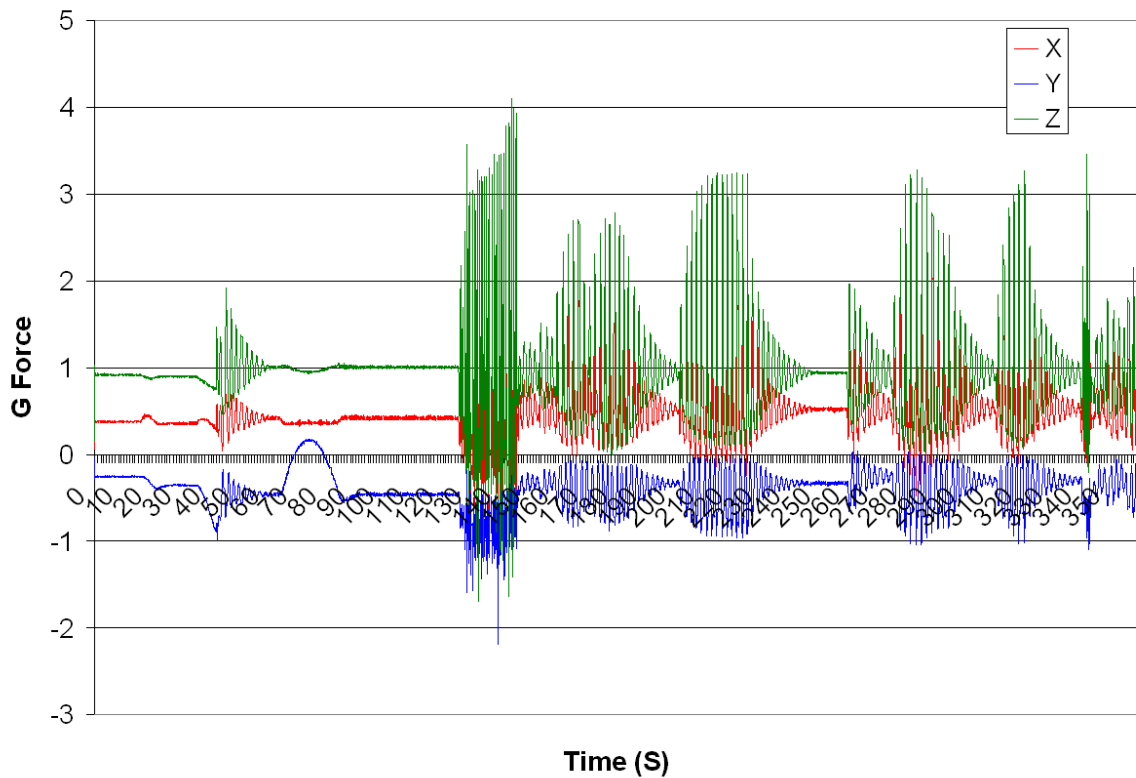


Figure 33 Glasgow Test 1



**Figure 34** Glasgow Test 2

The following conclusions were reached as a result of this study:

- Steps should be taken to warn or try to filter out potential passengers from ‘at risk’ groups. This could involve a combination of effective signage, verbal information and observation by the operator(s).
- The high-frequency bouncing motion should be used as sparingly as possible, and in particular should be avoided while the ride is running in reverse.
- Changes to the containment/restrain system could be made to lead passengers to adopt less risky postures (such as bending forwards) during upwards accelerations (e.g. over shoulder restraints or chest belts).

#### **6.1.4 Crazy Frog – Cambridge, 2009**

This work was undertaken in response to an incident in 2009, when a member of the public sustained an injury whilst on a Jumping Frogs ride. Measurements of the amusement device accelerations and passenger containment dimensions were taken during a site visit to the Cambridge Midsummer Fair (Figure 35). This work was undertaken on behalf of Mr Edmund Milnes (HSE Specialist Inspector), who produced an incident report based on the data provided in Figure 36. HSL carried out no further analysis and no HSL report was produced.



**Figure 35** Safeco Crazy Frogs – Cambridge, 2009

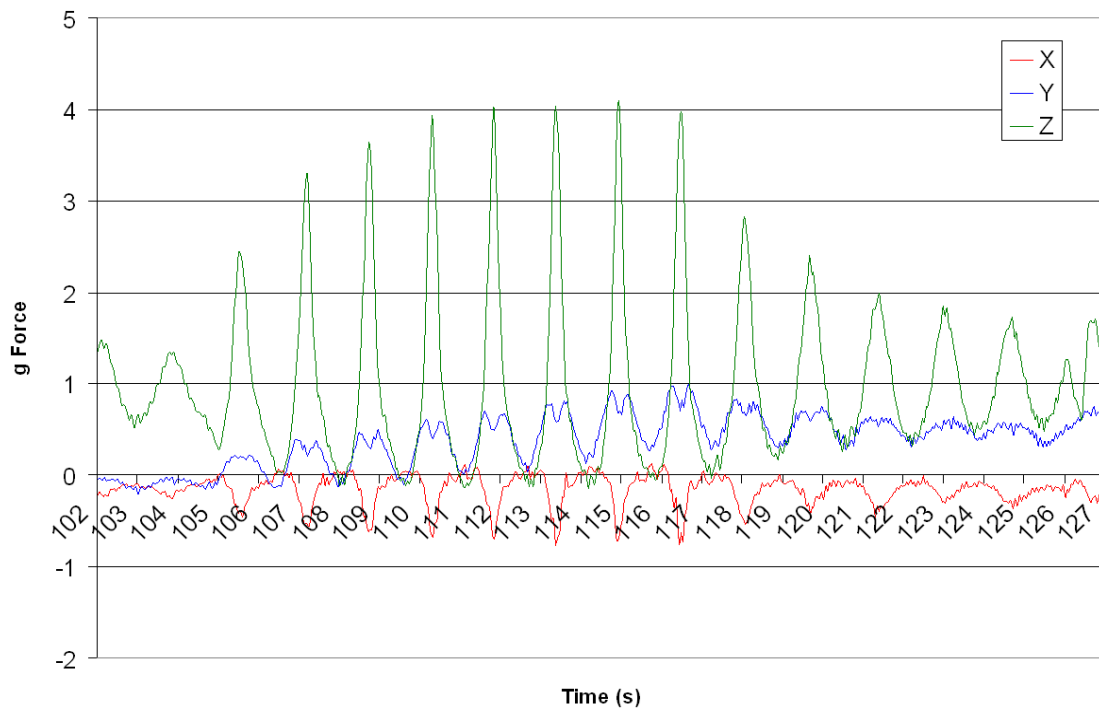


**Figure 36** Safeco Crazy Frogs – Cambridge, 2009 25 s ride cycle

### **6.1.5 Evidence of seat-to-head acceleration exposure causing injury on amusement devices**

Milnes's (6;7) measurements on a Safeco Crazy Frogs were made in a car in a partially loaded state (single average weight adult occupant dummy, approx. 70 kg) with a pneumatic pressure setting of 6.6 kgf/cm<sup>2</sup>, and with the accelerometer mounted within the test dummy abdomen. Milnes's measurements will therefore be influenced by the dynamic response of the test dummy which is unknown, but which it is understood is not intended to accurately replicate the dynamic response of the human body in this situation. The test dummy used was an Occupant Protection Assessment Test (OPAT) dummy. When designed in 1972, the mannequin was intended to be representative of a 50th percentile adult male in size (1680 mm stature) and weight (70.6 kg). It was designed to provide human-like behaviour when used to evaluate lap-shoulder belt systems. The mannequin features a human-like clavicle and floating scapula design, and its rib cage mimics the shape of the human. However, it is somewhat limited in its ability to simulate the behaviour of a person, as its neck and back are rigid structures and unable to rotate or bend forwards, backwards, or sideways.

The operating pressure was set to account for the response of the other (unloaded) arms operating during the measurement period. This is likely to have reduced the measured acceleration recorded in the car due to the pressure being somewhat lower than it could be for a loaded condition.

Milnes (7) sets out to link the levels of measured acceleration on the ride to an injured person's (IP) probability of injury through estimating the compression forces generated within the IP when riding, and comparing this with reported compressive strength data for vertebrae.

Milnes (7) cites a study by Ruff (31) who is reported to have calculated that the L1 vertebrae typically supports approximately 50% of the body weight. It is not known whether this relates to a seated subject or not. Milnes (7) uses this relationship to estimate the mass supported above the injured persons L1 vertebrae as approximately 37 kg.

Using the simple force = mass x acceleration model to estimate force within the IP's spine (ignoring any biodynamic response of the human body), with the mass of 37 kg and acceleration of 4.1 G, the peak forces within IP's spine were estimated to be around 1500 N.

Assuming that the ride caused the IP's injury, and that the IP's vertebral ultimate compressive strength (UCS) was reduced through repetitive exposure, Milnes (7) used the information from Brinkmann (32) regarding repetitive loading to revise the range of UCS strength of the IP's vertebra. Milnes (7) produced estimates for the 10 bounces which constituted the highest accelerations recorded, revising the UCS value for the IP's vertebra upwards to 2258 N. This was within the range reported in the scientific studies for any fracture type and being approximately 9th percentile (including data from individuals over 60 years of age).

It might then be argued that the 4.1 g acceleration presents a risk of injury to 10% of the population with a body mass similar to the IP. If their body mass were greater, then the compression forces would be greater, and the risk of injury would be greater for a similar UCS.

### **6.1.6 Ultimate compressive strength (UCS) of vertebrae**

Reported compressive strengths of isolated vertebrae show high variability, between 3 to 12 kN (Brinkmann et al. (32), cited in Boocock (2)). Milnes (7) reports a wider data set for compression forces measured to produce a variety of fractures, including that presented by Hansson et al. (33), cited in Milnes (7)) whose sample included subjects aged over 60 years.

Taking data across all studies, (n=90) the minimum, mean and maximum reported L1 UCS were 1520 N, 5299 N and 12535 N respectively.

#### **6.1.7 Compression forces generated by acceleration exposure**

Studies of instrumented cadavers subjected to seat to head accelerations (while seated) with varying forward trunk flexion have reported compression forces within the lower end of the range stated above (Hodgson et al (34), cited in Milnes (7)). For example, King and Vulcan (35), cited in Milnes (7) report an acceleration of 9 g at an onset rate of 1500 g/s as producing a vertebral compression force of 3.6 kN. Boocock (2) suggests this as a possible upper protective limit. This may be because the compression force value corresponds to an established biomechanical risk criterion for compression force within the spine during manual lifting.

#### **6.1.8 Compressive strength of vertebrae and body weight**

Milnes (7) reports that UCS is associated with body weight, and greater body weight will result in larger compressive forces within the spine when subjected to axial (seat to head) acceleration. Body weight is also reported to be a factor for spinal injury in NATO Publication TR-HFM-090-03 (33).

The strength and nature of the interaction is not reported. The connection is likely to be strongest where individuals have developed their bone structure with a high body weight, and remained physically active, whereas an individual who is sedentary, and or gained weight quickly is less likely to have developed a high bone strength. Weight/Body Mass Index (BMI) will be an influencing factor in the probability of vertebral fractures, but other (interacting) factors such as bone mineral density, age, and gender are likely to be of significant importance.

#### **6.1.9 The effect of load cycles on compressive strength of vertebrae**

The Safeco Crazy Frogs ride motion is repetitive, and will impose repetitive compressive loading on the spine of the rider. Brinkmann ((32), cited in Milnes (7)) found that following 20 load cycles, some vertebrae were found to fail at between 43% and 72% of their UCS. It was calculated that repetitive loading at approximately 60 to 70% of the UCS for 10 cycles presented a 9% probability of fracture.

#### **6.1.10 Reaction time and muscle tone**

It may be unlikely that reaction time will be sufficiently fast to enable an individual to respond to a single or initial acceleration event. However, it will be possible for riders to respond to successive events. The effect is not certain, but muscle contractions around the spine will generally have the effect of increasing the compressive forces acting within it. However, abdominal muscle contractions may also tend to increase intra-abdominal pressure (IAP), which can have a mitigating effect on spinal loading. Muscle activity is something that is not accounted for in the studies performed on cadaver specimens.

**6.2 SITE VISIT – WILKINSON DJ JUMP AMUSEMENT DEVICE (20<sup>TH</sup> – 22<sup>ND</sup> NOVEMBER 2012): MEASUREMENT TEST RUN LIST**

<b>Run</b>	<b>Description</b>
<b>1</b>	All arms operating. Pressure adjusted when cars lifted to compensate for no load. There is some video of a running check following Run1, because cars 2 and 4 appeared to be running much higher than car 12.
<b>2</b>	All arms operating. During the final free fall pedal operating section for Prog 2, Jonathan operates the pedal after the operator has done it for a short while. The difference in timing of the bounce results in cars becoming out of synchronisation. This is followed by some further attempts by the operator to allow the arms to drop low to the bottom of the travel.
<b>3</b>	Arms 2 and 12 operating. Car 2 GP1 fitted. During the final free fall pedal operation phase the operator attempted to achieve a harder drop to the bottom of the travel.
<b>4</b>	All arms operating. Car 12 only with GP1 fitted. The operator adjusted the pressure to a “lowered setting” based on how he felt the arms were running after lift, 3.5 – 4.5 bar on the setting dial. This was lower than normal operation.
<b>5</b>	All cars running. 6 bar displayed on the pressure dial
<b>6</b>	Repeat of Run 5. All cars running, 6 bar displayed on the pressure dial.
<b>7</b>	Only cars 12 and 6 running, both loaded with 160 kg of pea gravel. 7 bar displayed on the pressure dial.
<b>8</b>	Repeat of Run 7. Recorded consecutive to Run 7.
<b>9</b>	Only cars 12 and 6 running, both loaded with 160 kg of pea gravel. “Low pressure” setting, 6.5 bar was displayed on the pressure dial.
<b>10</b>	Repeat of Run 9. Cars 12 and 6 loaded with 160 kg of pea gravel. Operator attempted more ‘aggressive’ use of the foot pedal during program 2, by allowing the arms to drop further before the pedal is released.
<b>11</b>	Only cars 12 and 6 running, both loaded with 160 kg of pea gravel. “Low pressure” setting, 6 bar was displayed on the pressure dial.
<b>12</b>	Only cars 12 and 6 running, both loaded with 160 kg of pea gravel. “High pressure” setting, 7.5 bar was displayed on the pressure dial. Recorded consecutive to Run 11.
<b>13</b>	Only Car 12 running, unloaded, with central hub stationary. This run was an attempt to investigate the effects of the pneumatic cushion at the bottom of the ram. This was to be done by achieving an arm drop from the lowest possible height with the hub stationary. The starting position was programme 1, in the default “floating” position between programme inputs, i.e. in a low position. The drop was triggered by use of the foot pedal. The arm height was controlled by altering the pressure. The adjustment of the exhaust valve at the base of the ram was investigated. The screw head slot was horizontal at start, and was screwed in through 2.5 turns to reach a hard stop position. This resulted in the air cushion being apparent, but the arm would not lower to its stop position. The exhaust valve was then backed off ¼ turn. This appeared to achieve a cushion at the bottom of the ram travel which very slowly lowered the arm when switched to off/end position.
<b>14</b>	Only Car 12 running, unloaded, with central hub stationary. 5 bar was displayed on the pressure dial. Some programmes plus the foot pedal were used to try to bounce the

	arms to bottom of ram travel. Exhaust valve $\frac{1}{4}$ turn open from fully closed.
<b>15</b>	Repeat of Run 14. Only Car 12 running, unloaded, with central hub stationary. 4 bar was displayed on the pressure dial. Cushion exhaust valve $\frac{1}{4}$ turn out from fully in.
<b>16</b>	Repeat of Run 14, using a few programmes plus foot pedal use. The pressure was down to around 4 bar on the dial at the end of Run 15. Only cars 12 and 6 running, both loaded with 160 kg of pea gravel. "High pressure" setting, 7 bar was displayed on the pressure dial. Recorded consecutive to Run 15.
<b>17</b>	6 bar was displayed on the pressure dial. Void data on GP1
<b>18</b>	7.5 bar was displayed on the pressure dial. Recorded consecutive to Run 17. Void data on GP1
<b>19</b>	Arms 6 and 12 operating. 6 bar was displayed on the pressure dial. Cushion exhaust valve $\frac{1}{4}$ turn out from fully in.
<b>20</b>	Arms 6 and 12 operating. 7.5 bar on dial. Cushion exhaust valve $\frac{1}{4}$ turn out from fully in. Recorded consecutive to Run 19.
<b>21</b>	A succession of free-fall pedal actions to investigate changes in exhaust valve adjustment: Part 1. $\frac{1}{2}$ turn out from fully in; Part 2. $\frac{3}{4}$ turn out from fully in; Part 3. 1 turn out from fully in; Part 4. 1 $\frac{1}{4}$ turns out from fully in; Part 5. Fully in.
<b>22</b>	A 'typical routine' run through. Initially, all arms were lifted to the 'float' position and then only arms 6 and 12 operated. The operator reported that this it was typical practise to raise the unloaded arms, usually to the top position, for situations where the ride was operated partially loaded, as lifting the cars afford better visibility of the ride surrounds for safety reasons. Subsequently, all arms were activated (at around 6 minutes). At around 8:45 minutes the unloaded arms are deactivated once more, and held at the 'float' position while arms 6 and 12 operate. This was done largely as a work around for the different loading conditions. There was some adjustment of pressure during the ride session.



### 6.3 ACCELERATION MEASUREMENT DATA SET

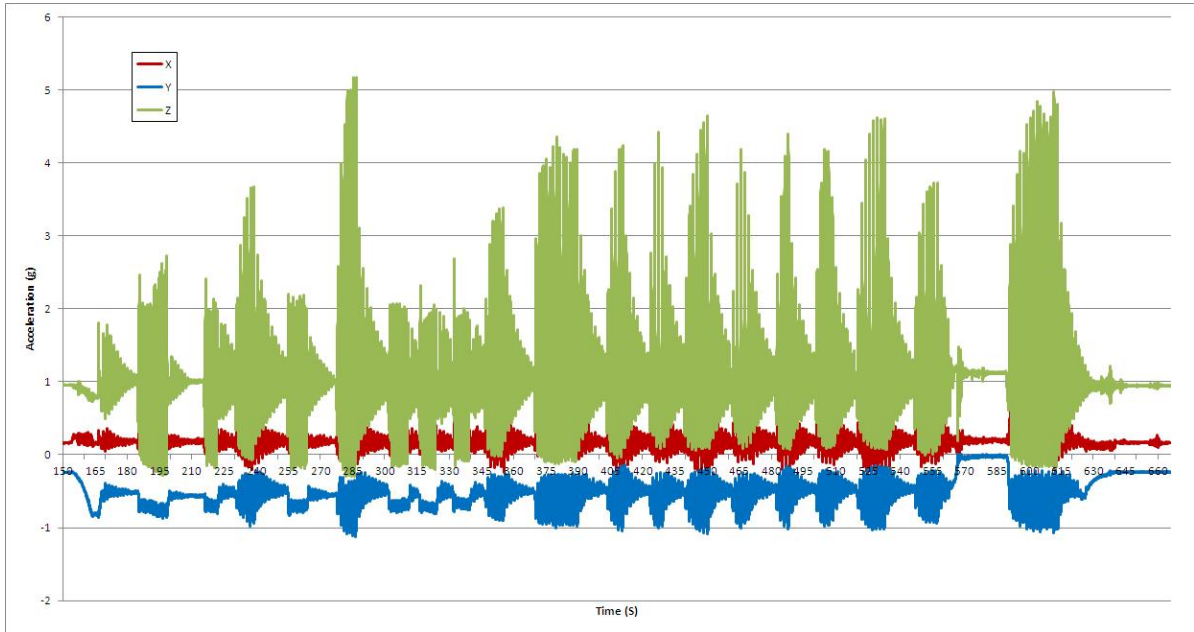


Figure 37 Test run 1 full

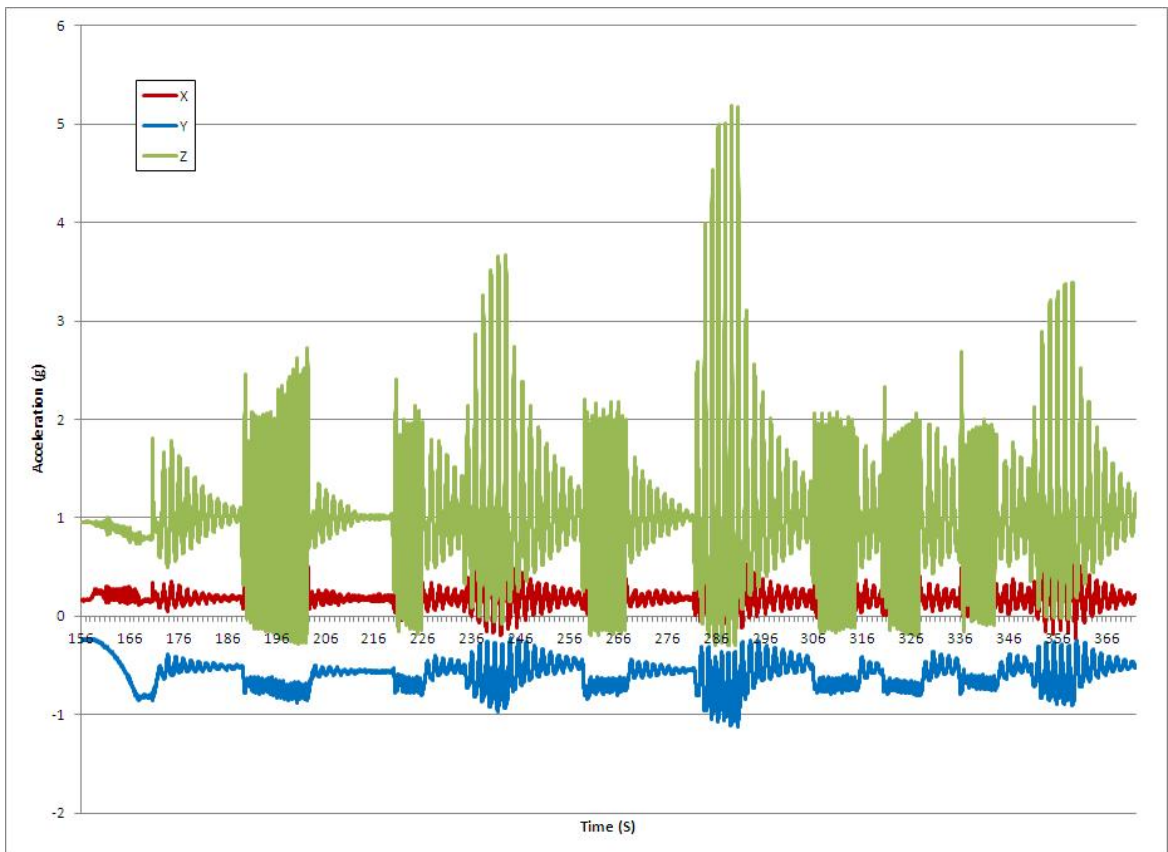
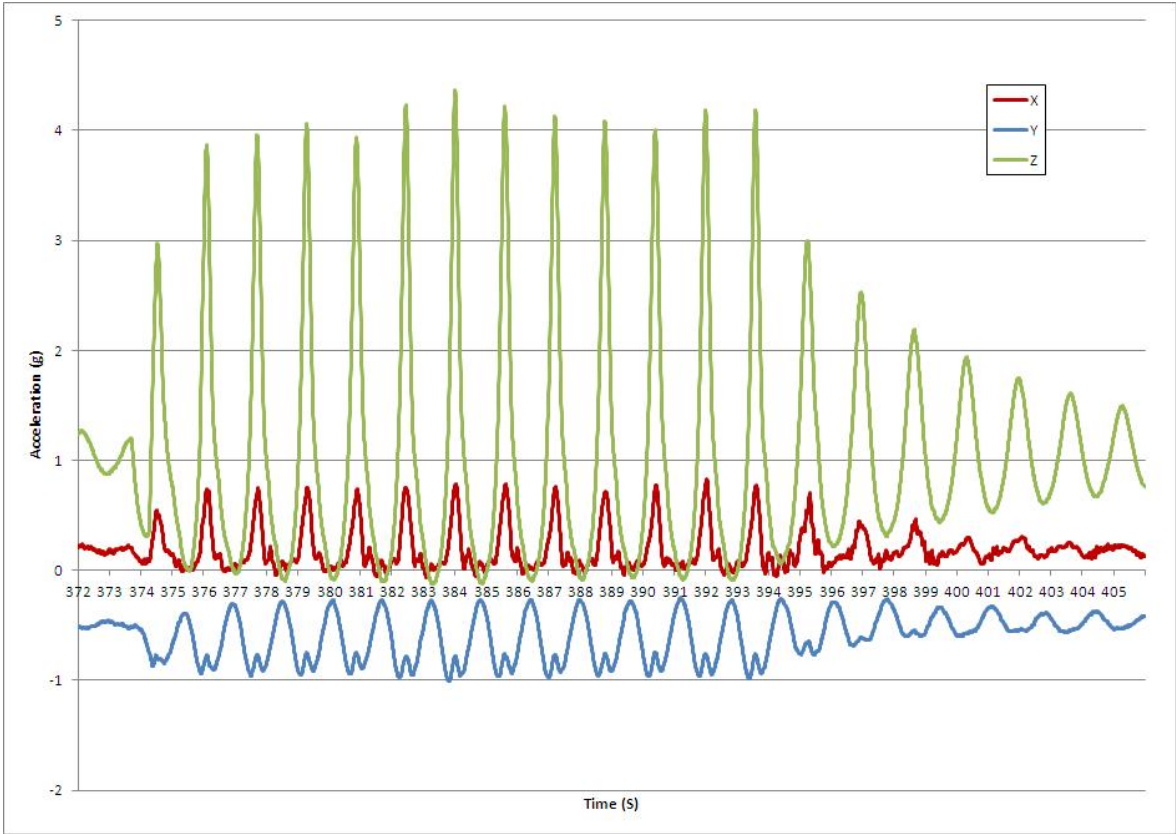
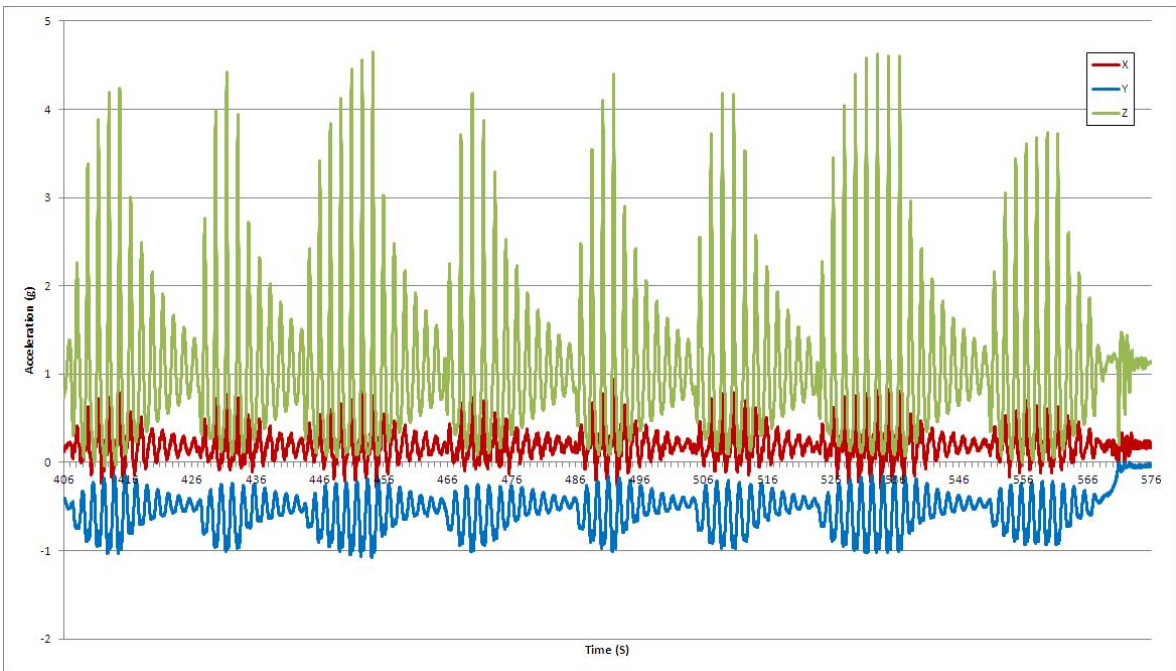


Figure 38 Test run 1, Program 1



**Figure 39** Test run 1, Program 1, Foot Pedal



**Figure 40** Test run 1, Program 2

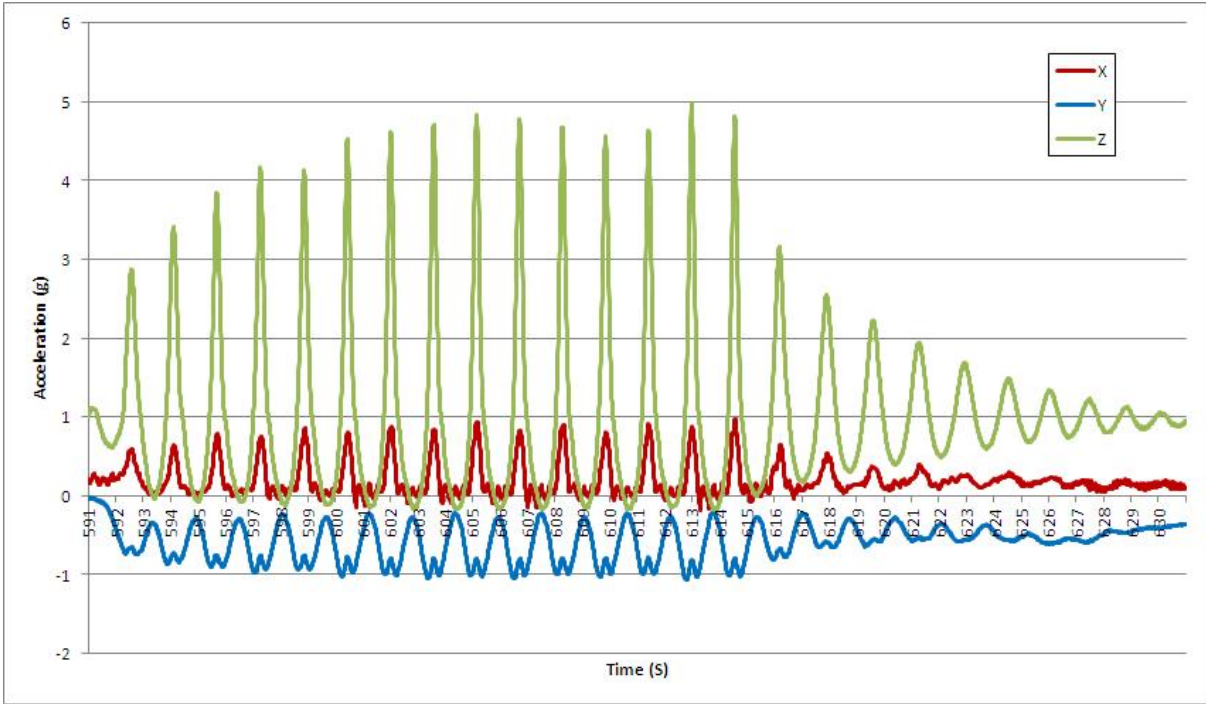


**Figure 41** Test run 1, Program 2, Foot pedal

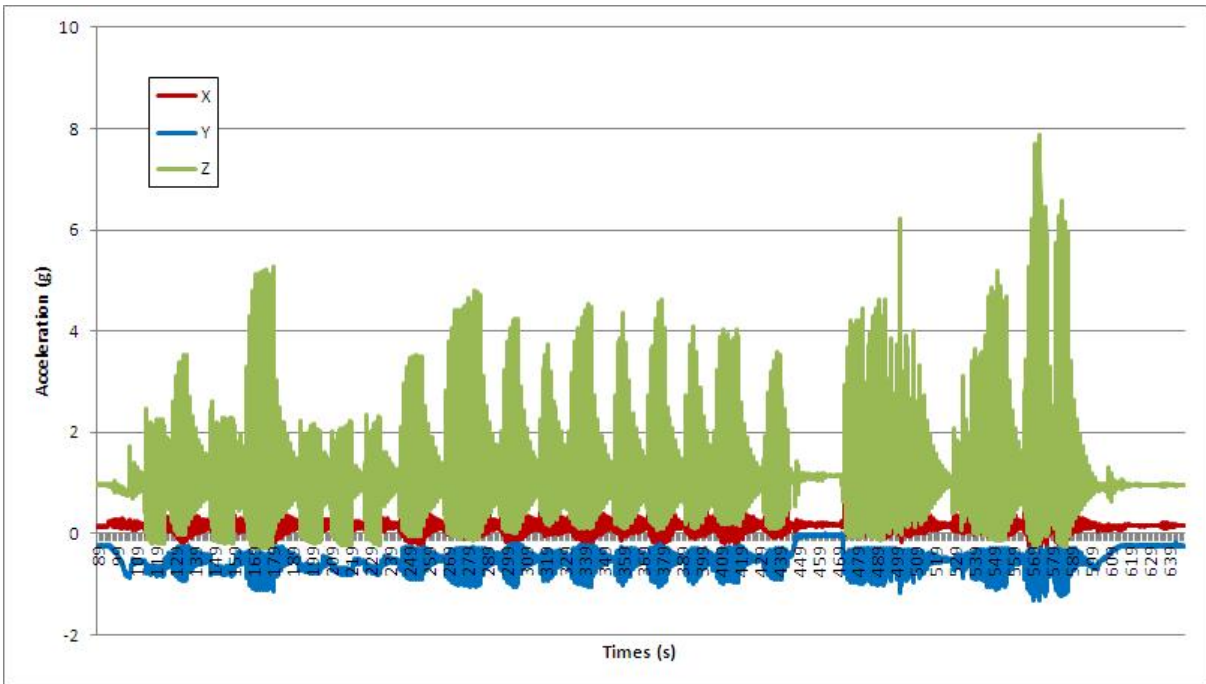


**Figure 42** Test run 2 Full

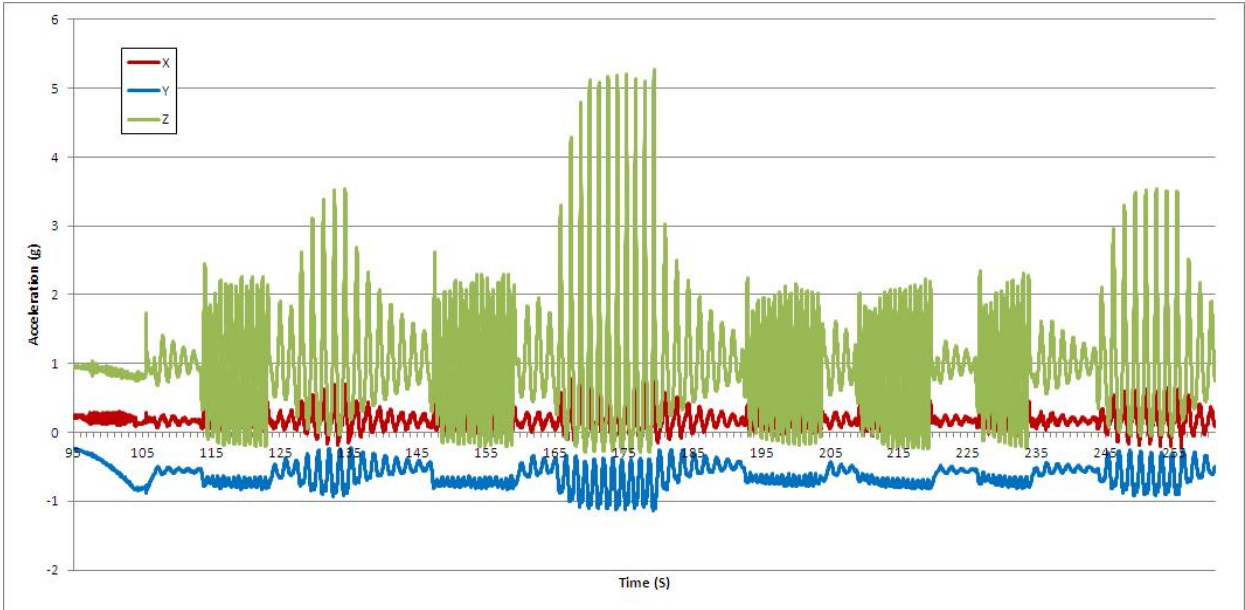


**Figure 43** Test run 2, Program 1

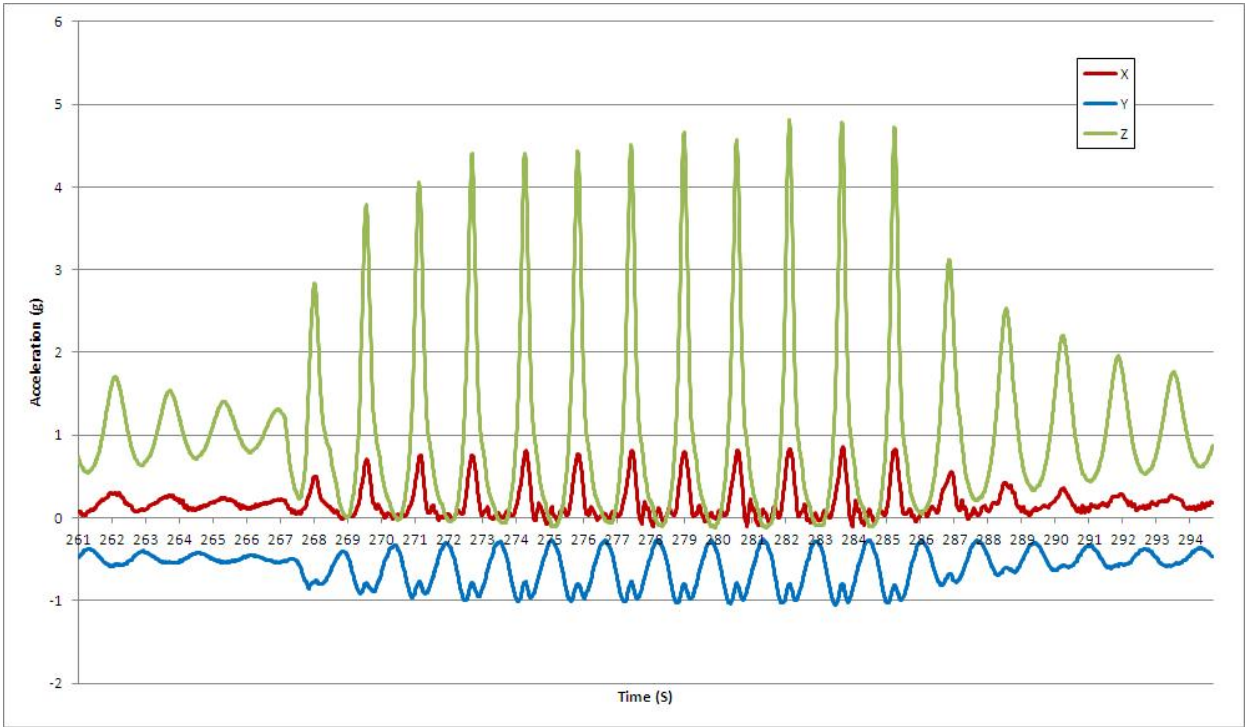


**Figure 44** Test run 2, Program 1, Foot pedal





**Figure 45** Test run 2, Program 2

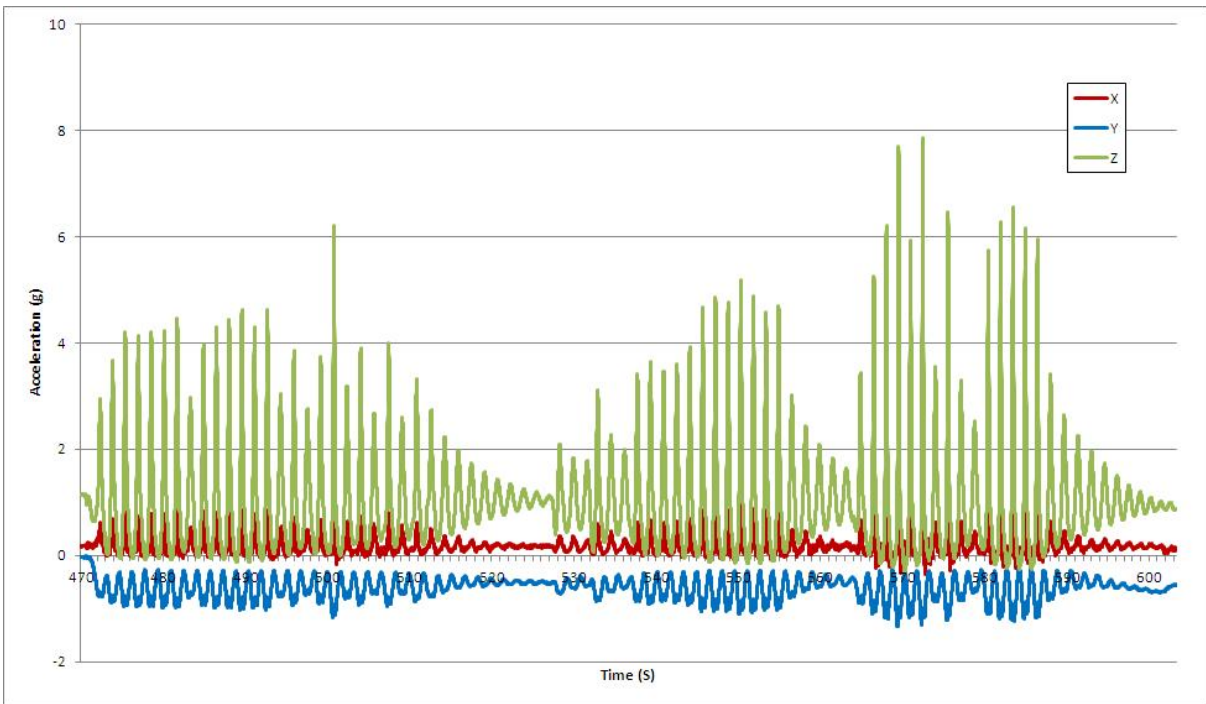


**Figure 46** Test run 2, Program 2, Foot pedal

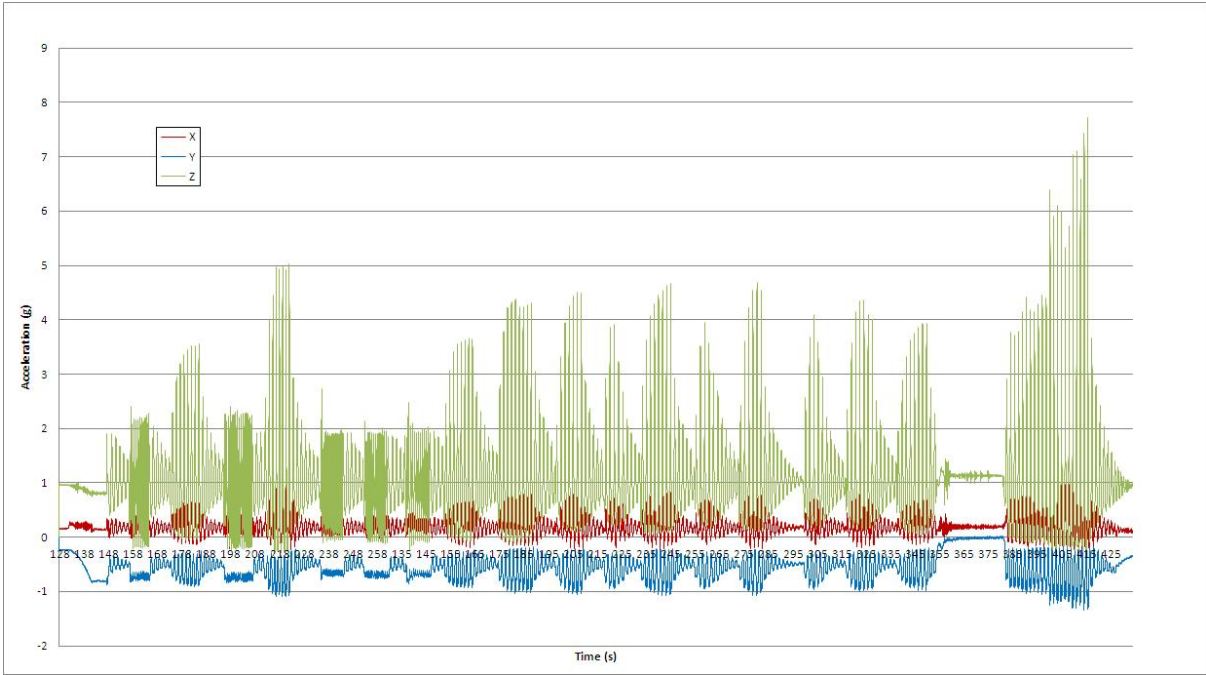


**Figure 47** Test run 3 Full

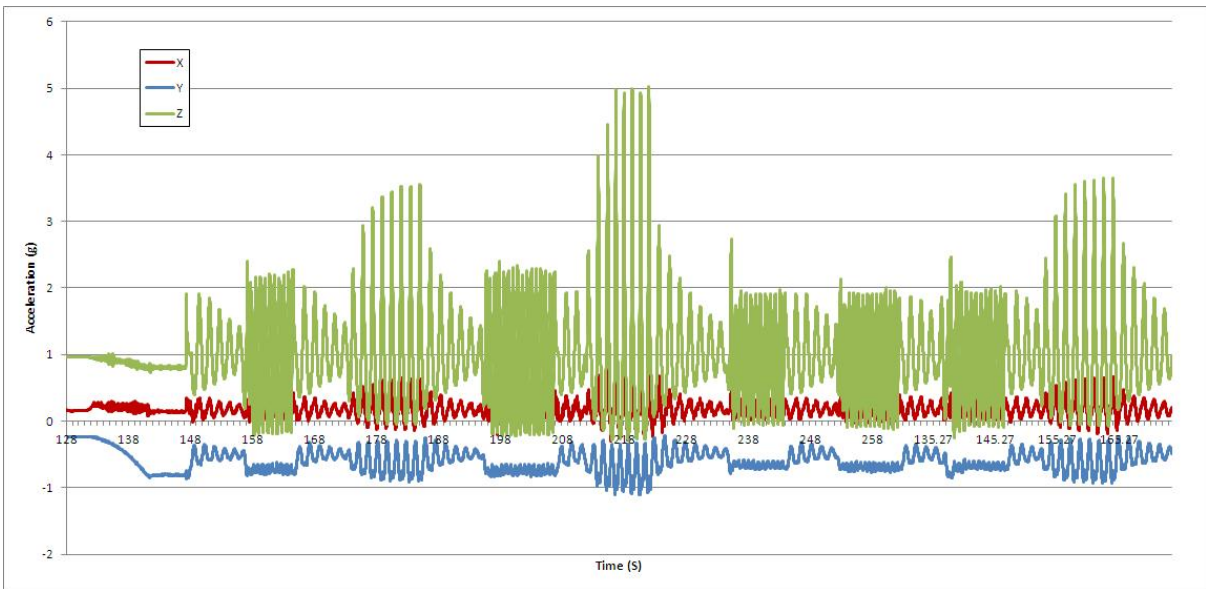


**Figure 48** Test run3, Program 1

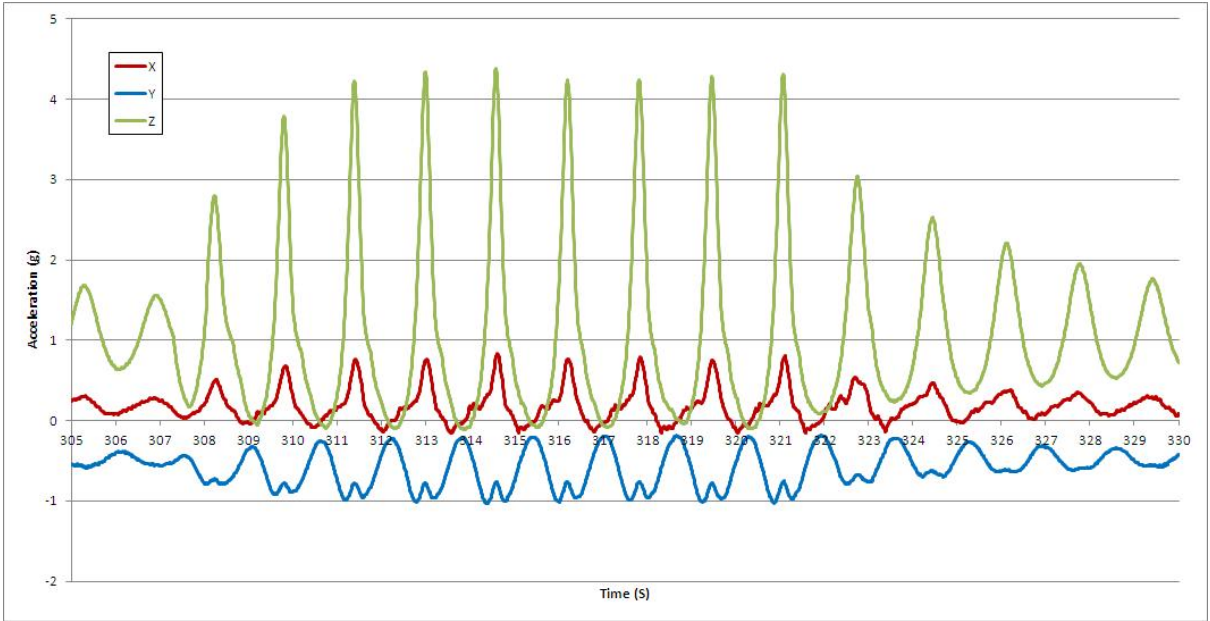


**Figure 49** Test run 3, Program 1, Foot pedal

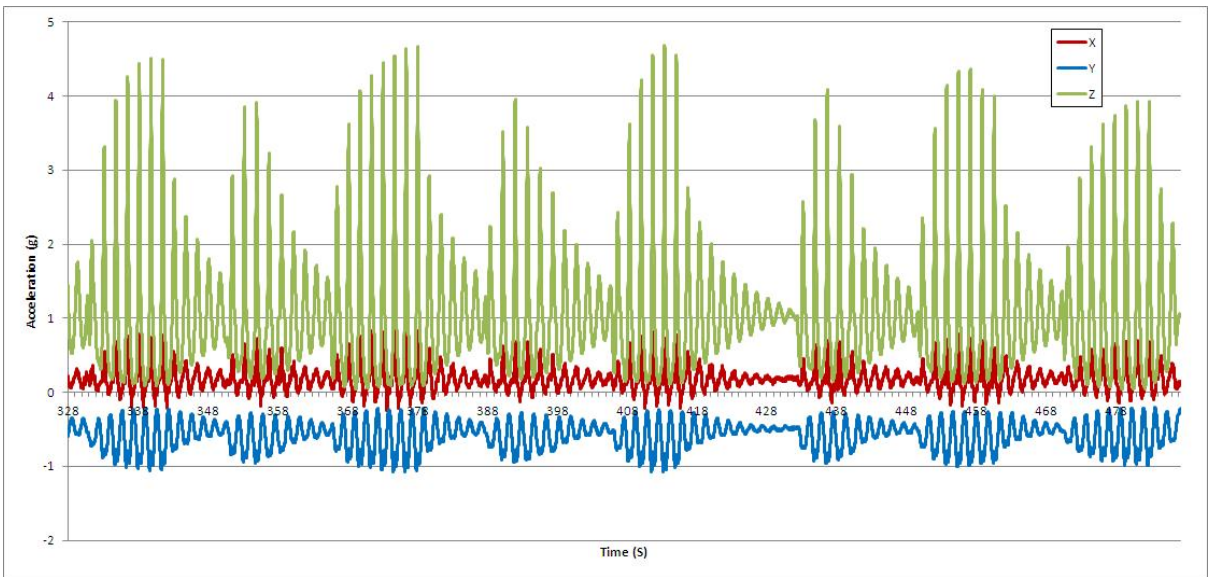


**Figure 50** Test run 3, Program 2

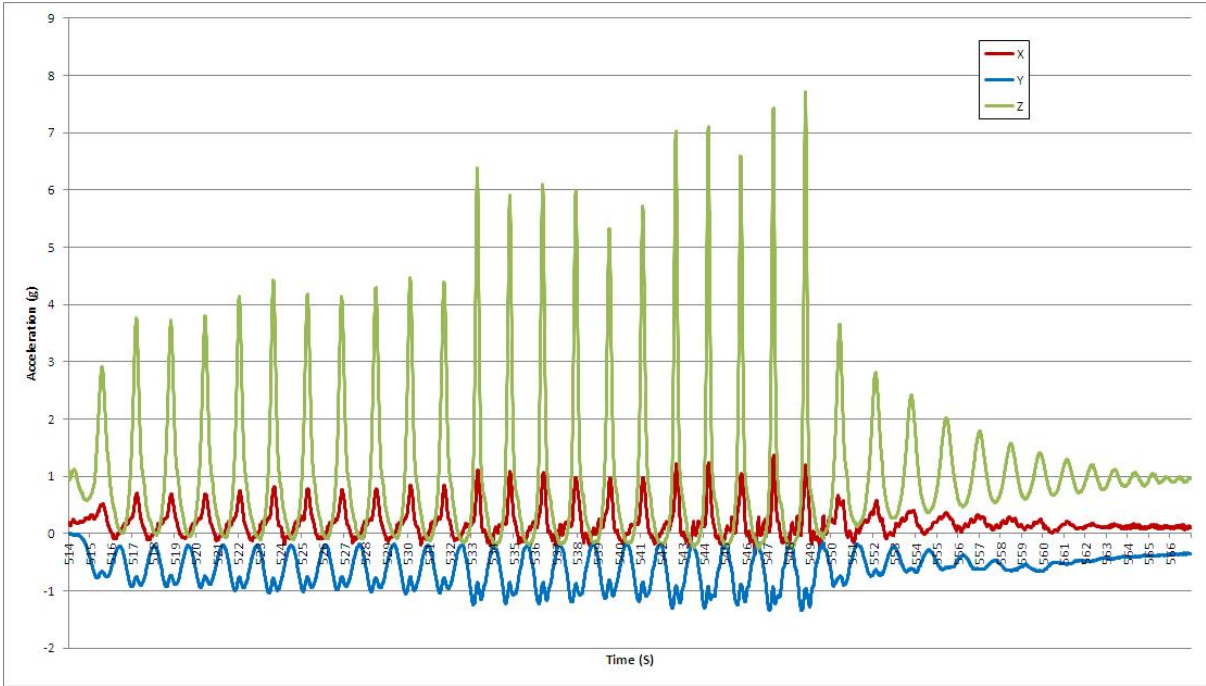


**Figure 51** Test run 3, Program 2, Foot pedal

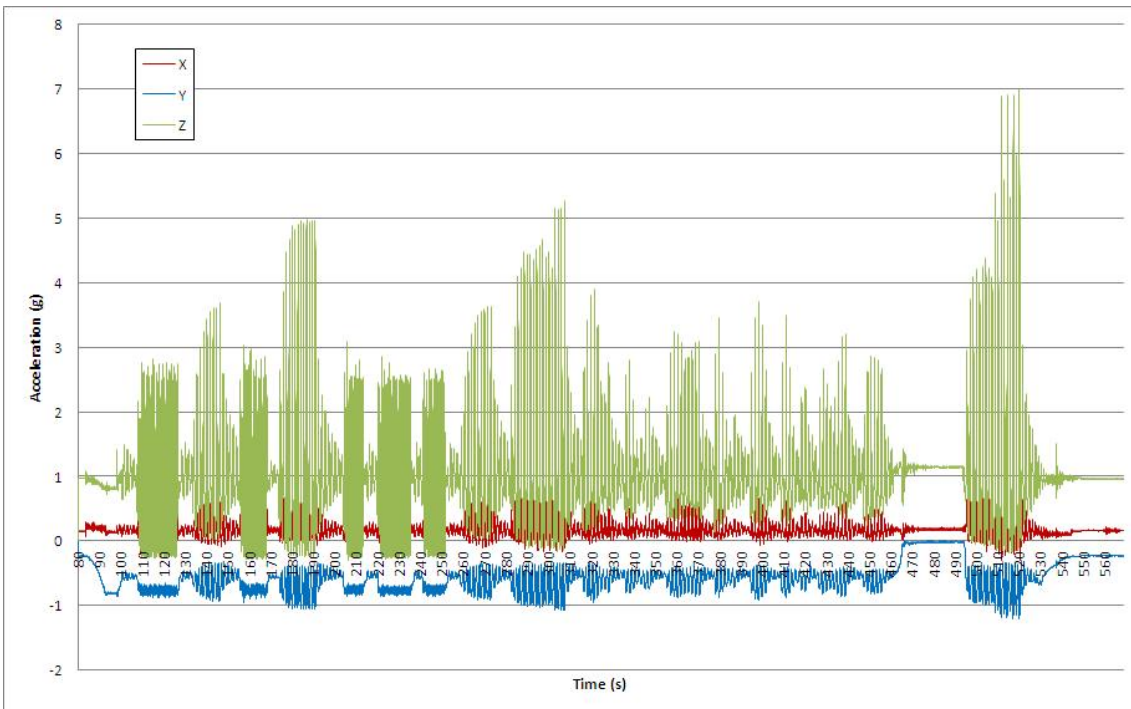


**Figure 52** Test run 4 Full



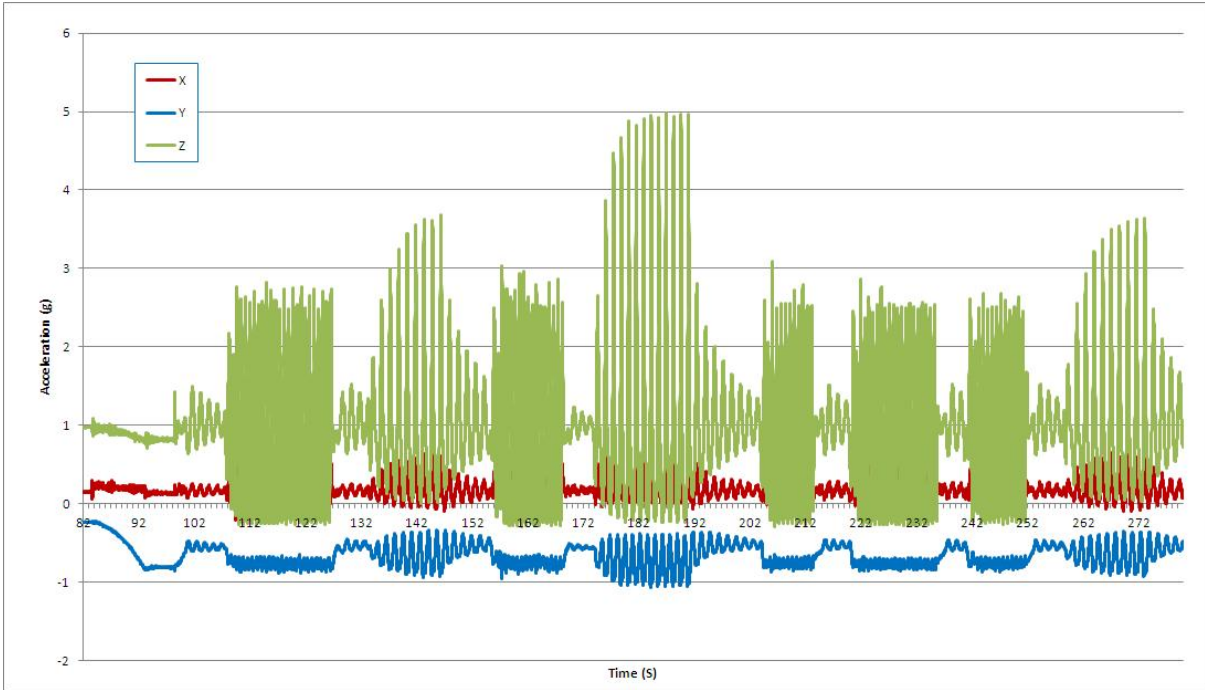


**Figure 53** Test run 4 Program 1

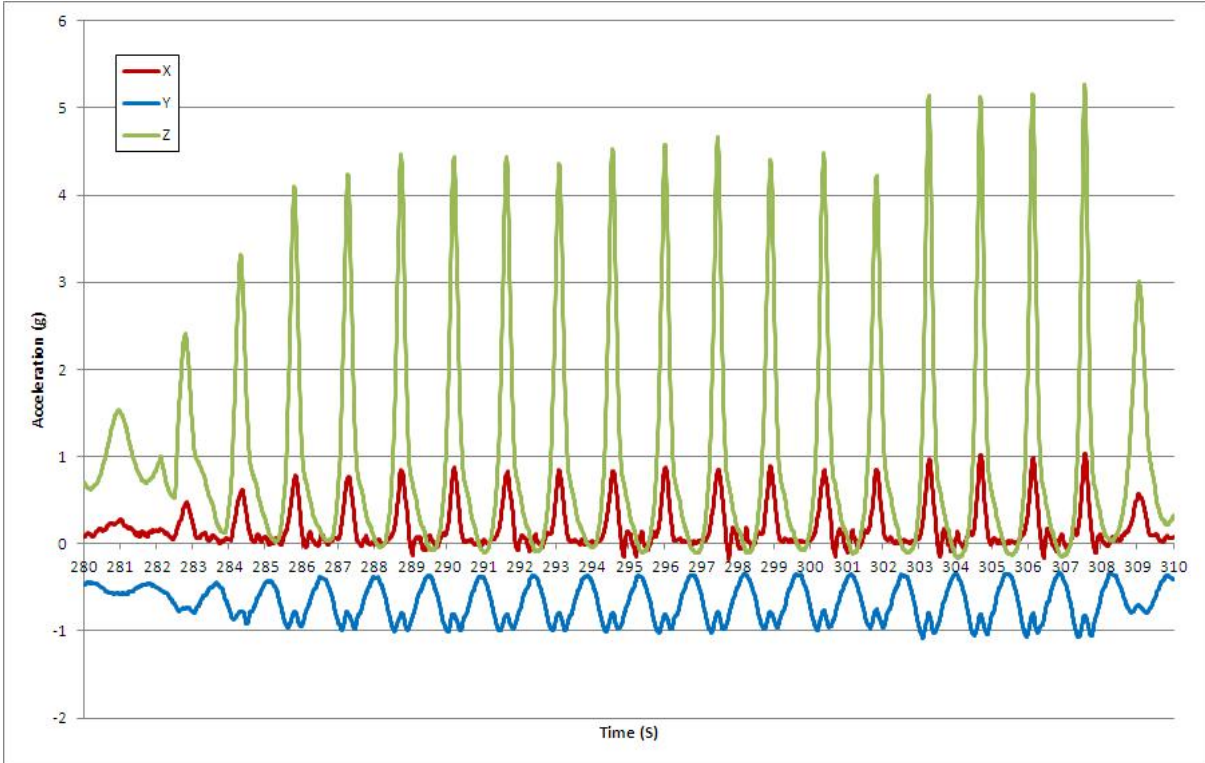


**Figure 54** Test run 4, Program 1, Foot pedal

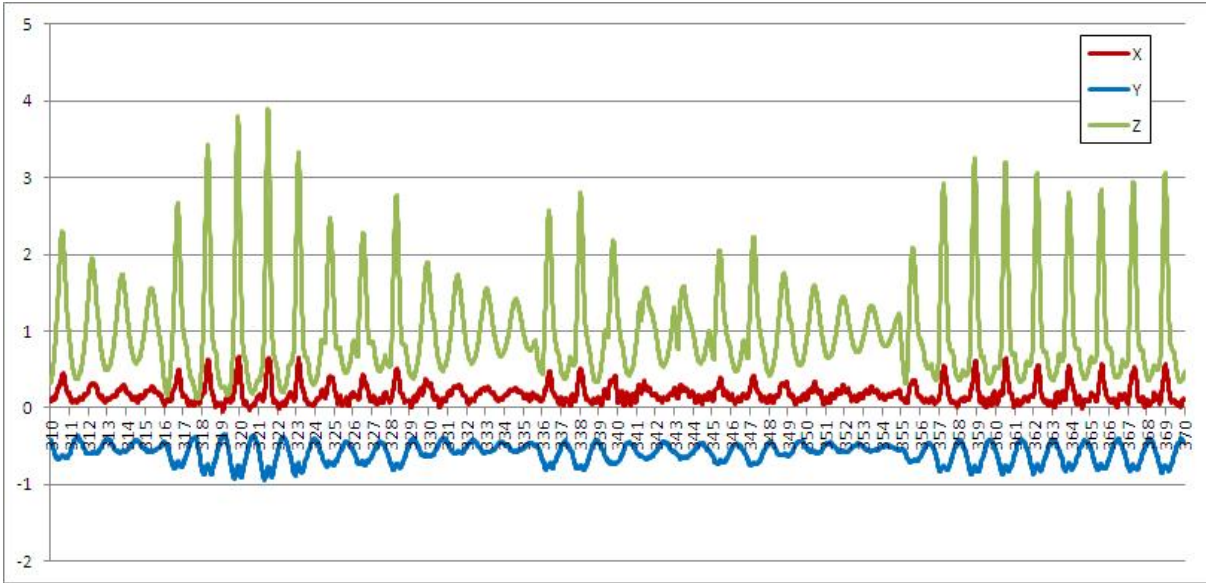


Figure 55 Test run 4, Program 2

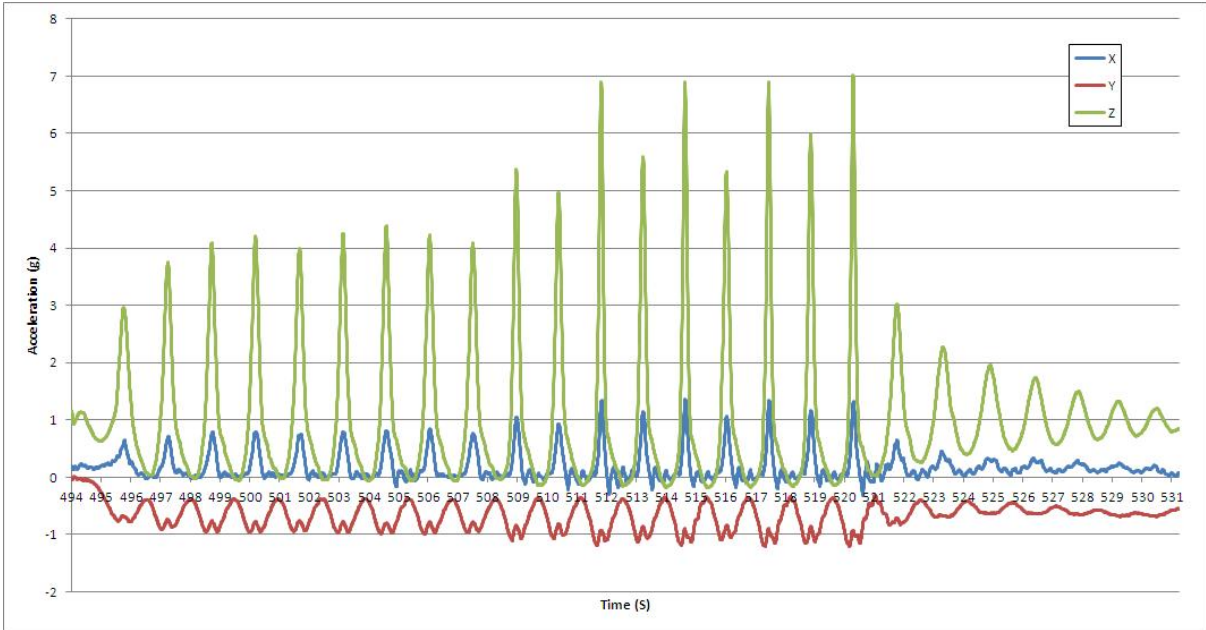
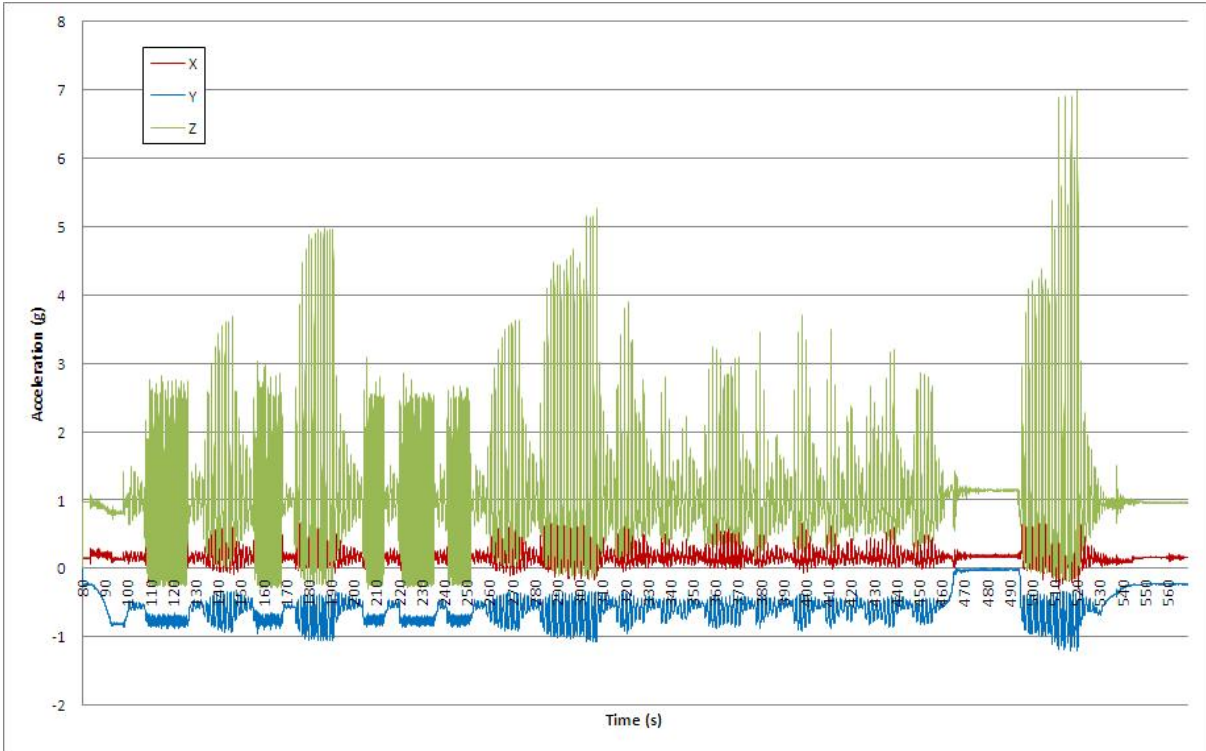
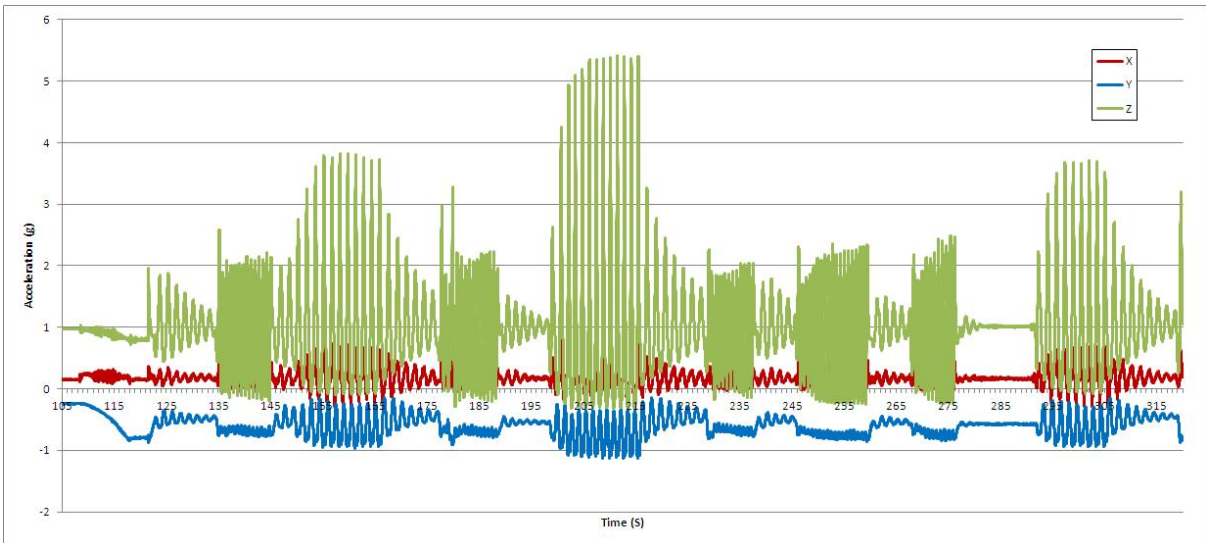


Figure 56 Test run 4, Program 2, Foot pedal



**Figure 57** Test run 5 Full



**Figure 58** Test run 5, Program 1

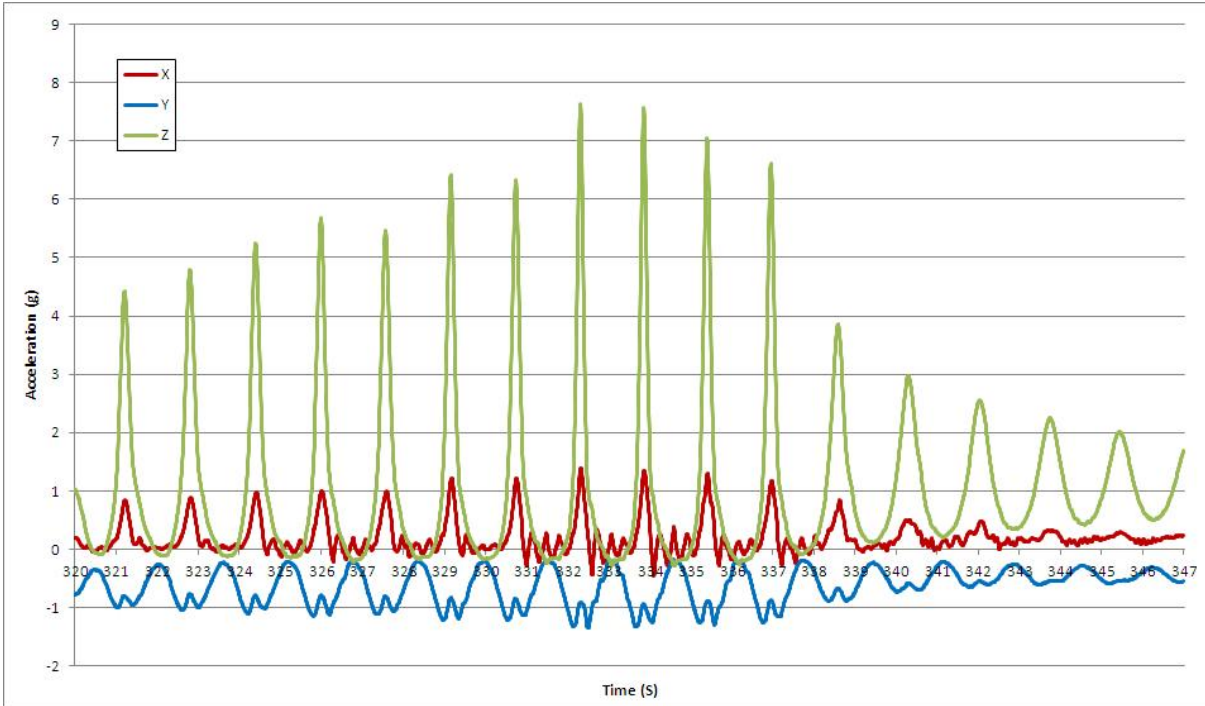


**Figure 59** Test run 5, Program 1, Foot pedal

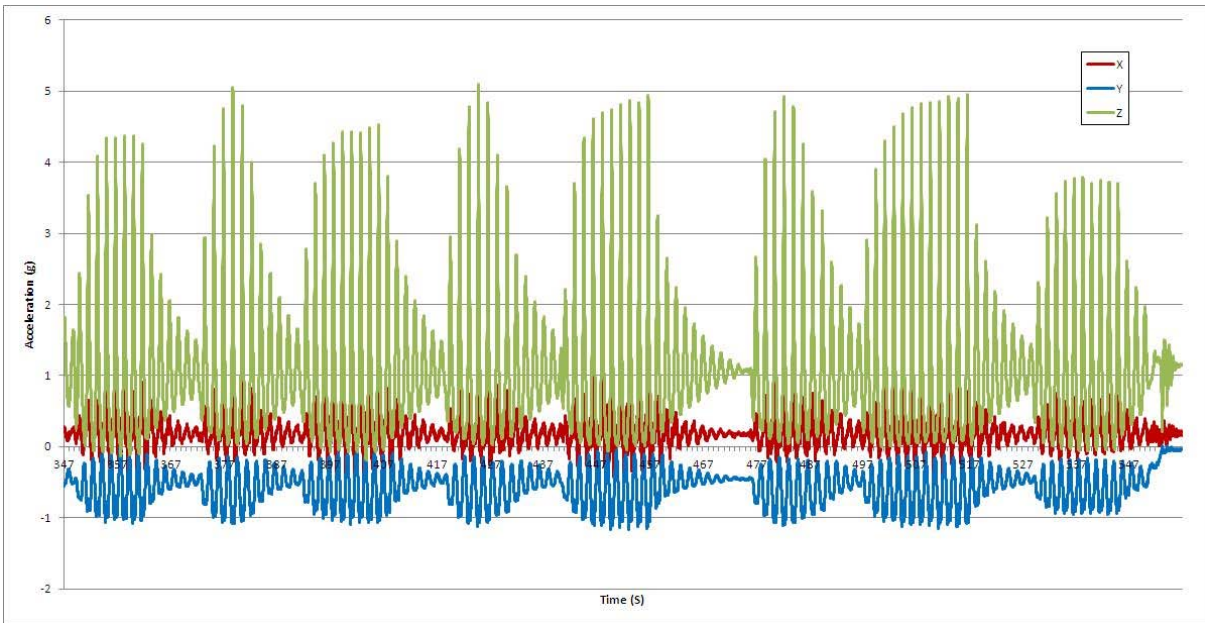


**Figure 60** Test run 5, Program 2



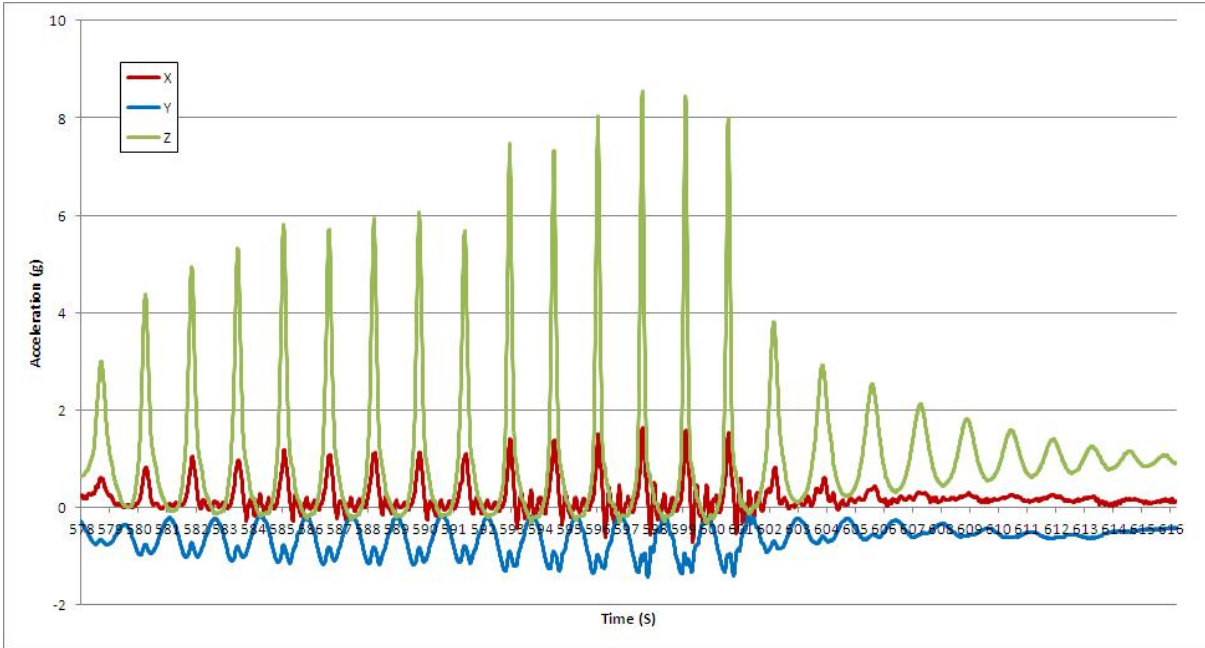


**Figure 61** Test run 5, Program 2, Foot pedal

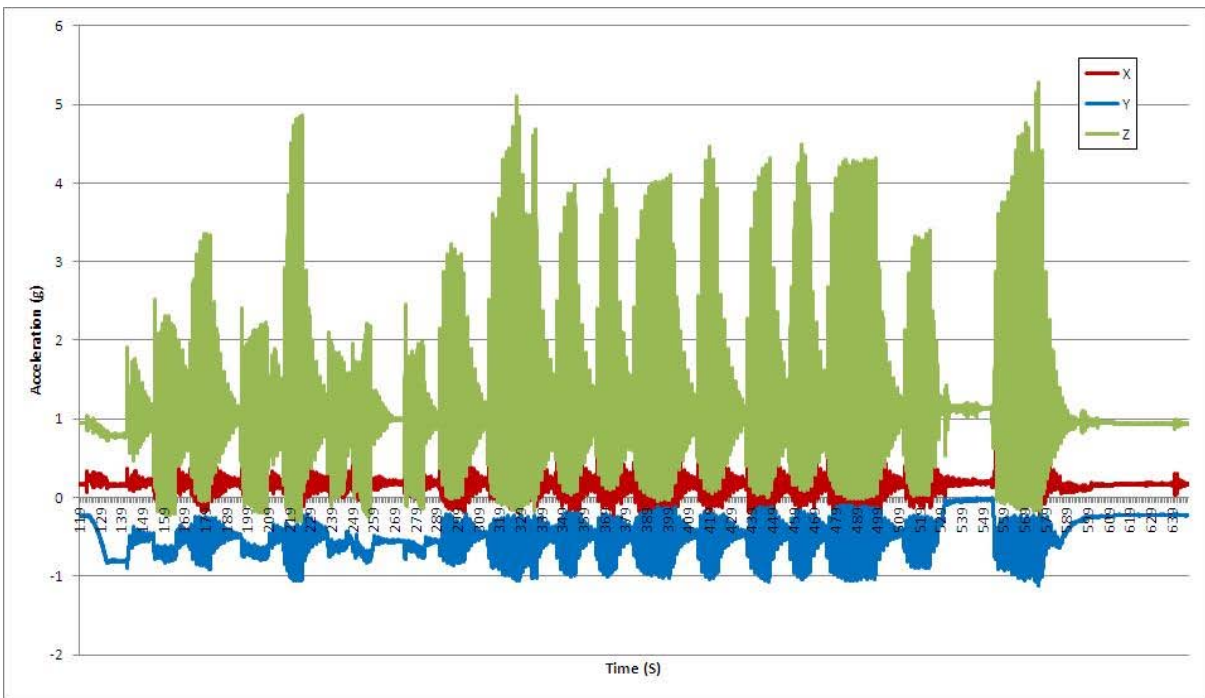


**Figure 62** Test run 6 Full

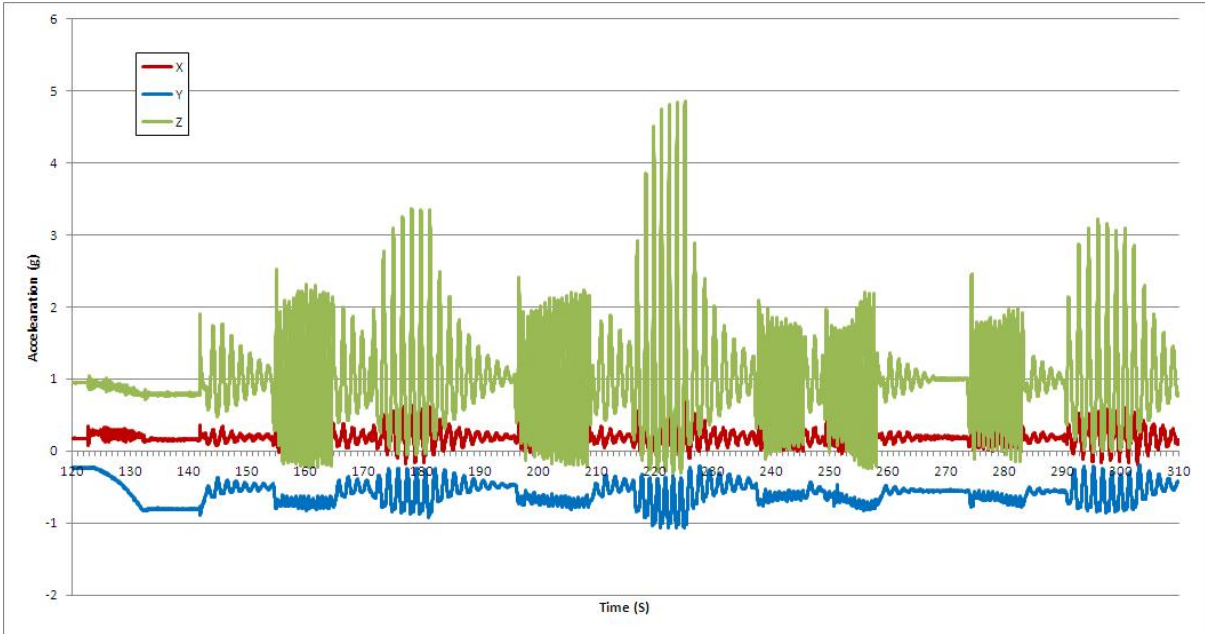


**Figure 63** Test run 6, Program 1

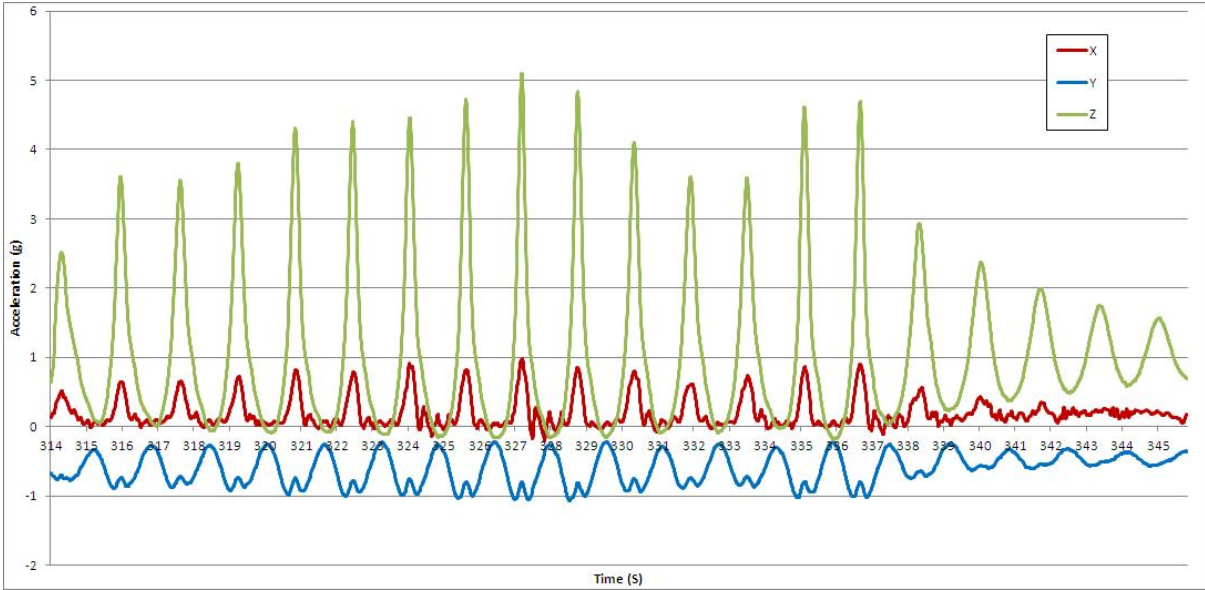


**Figure 64** Test run 6, Program 1, Foot pedal

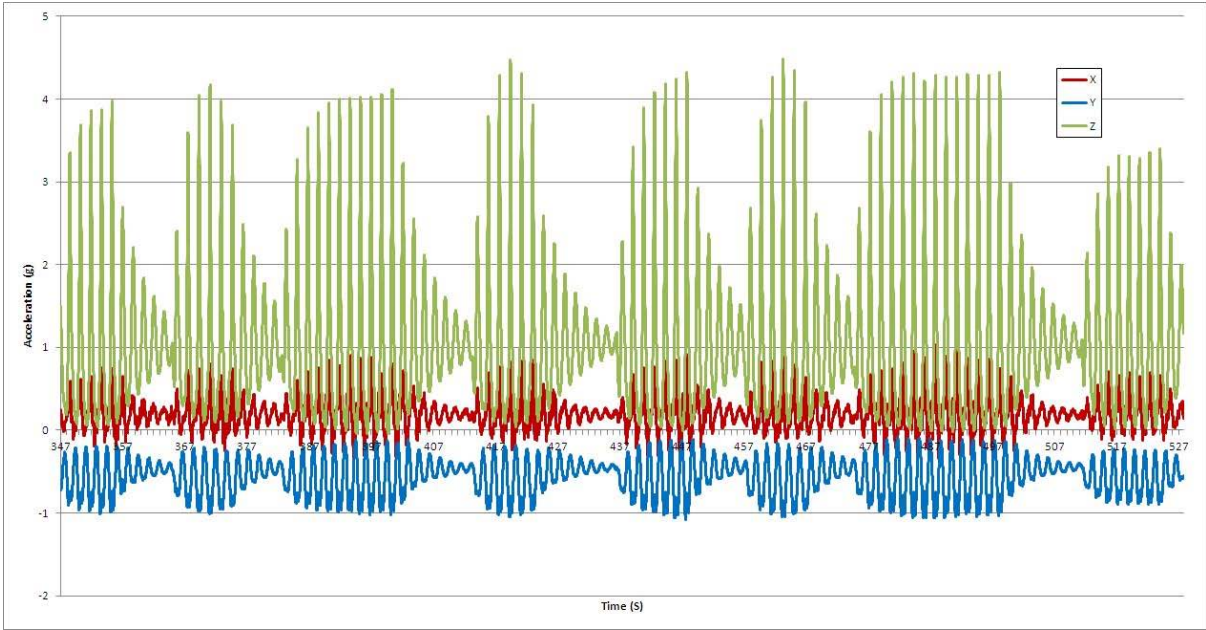


Figure 65 Test run 6, Program 2

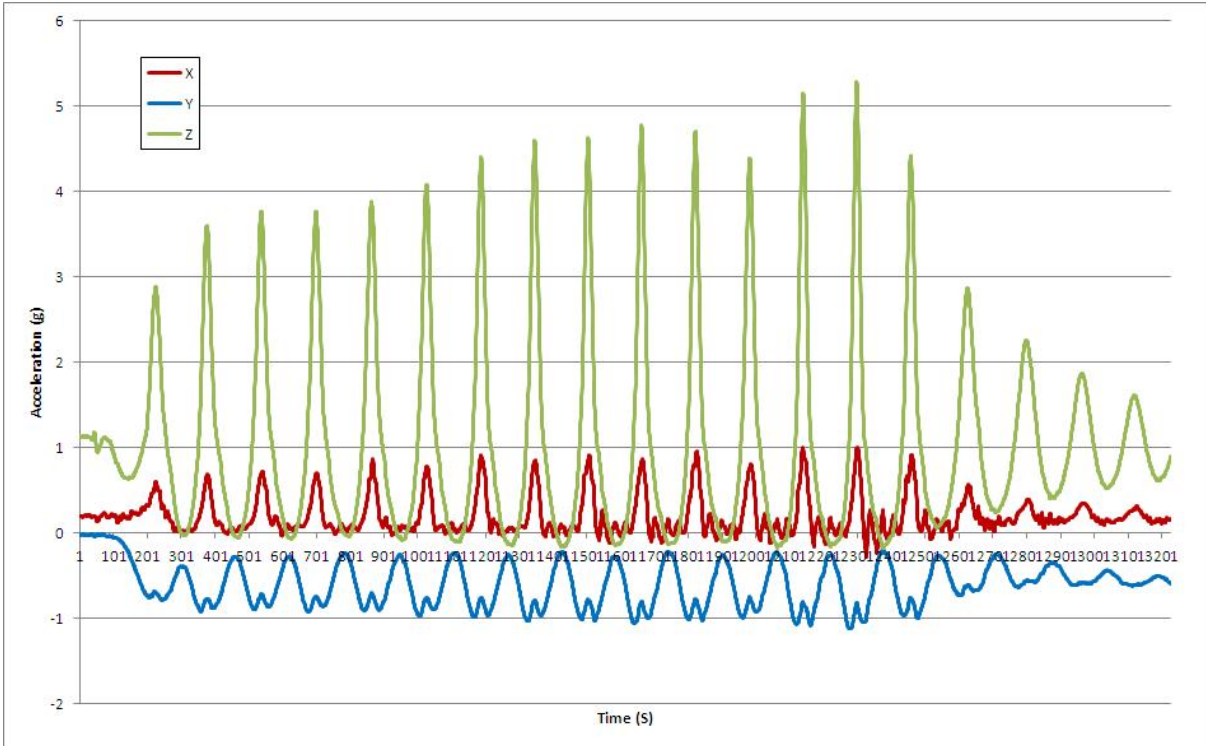
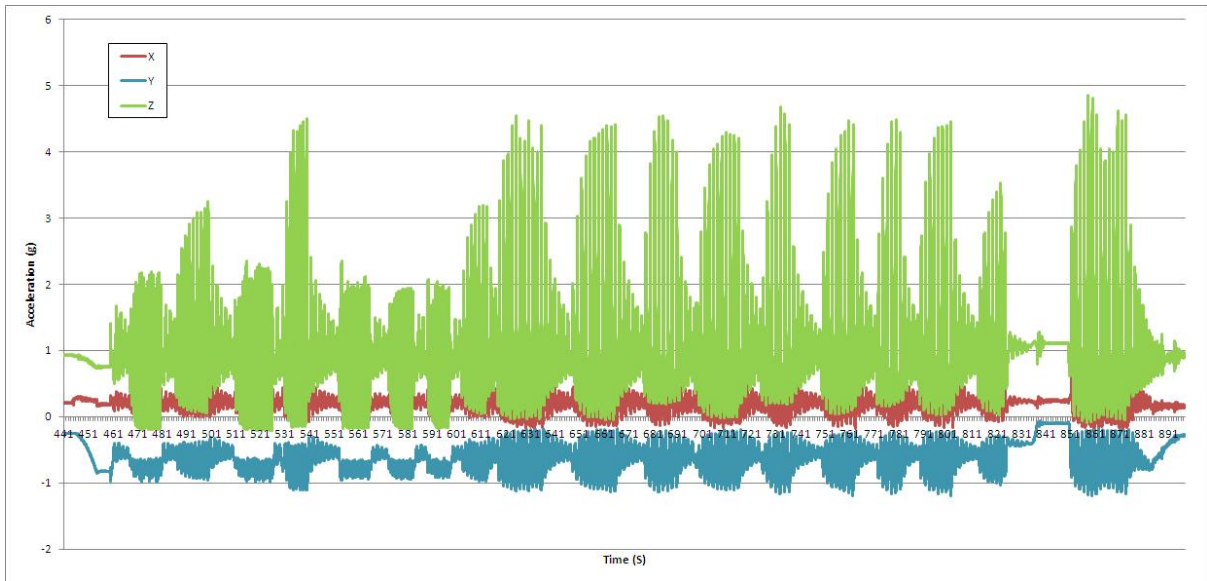
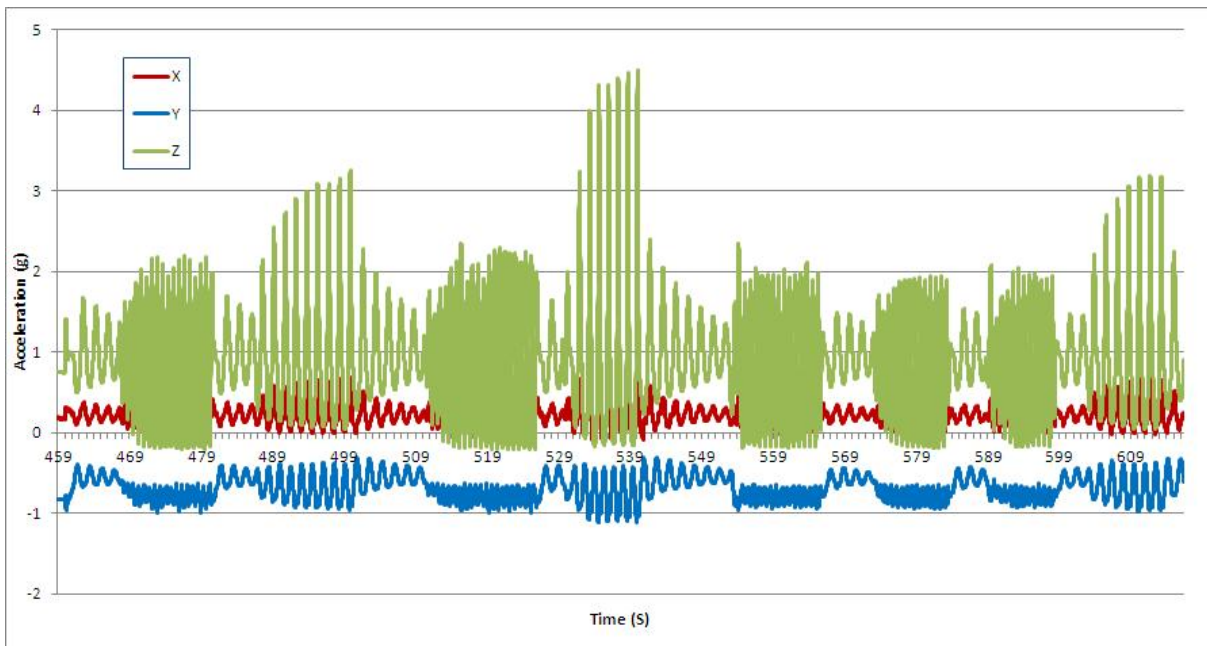


Figure 66 Test run 6, Program 2, Foot pedal



**Figure 67** Test run 7 Full



**Figure 68** Test run 7, Program 1



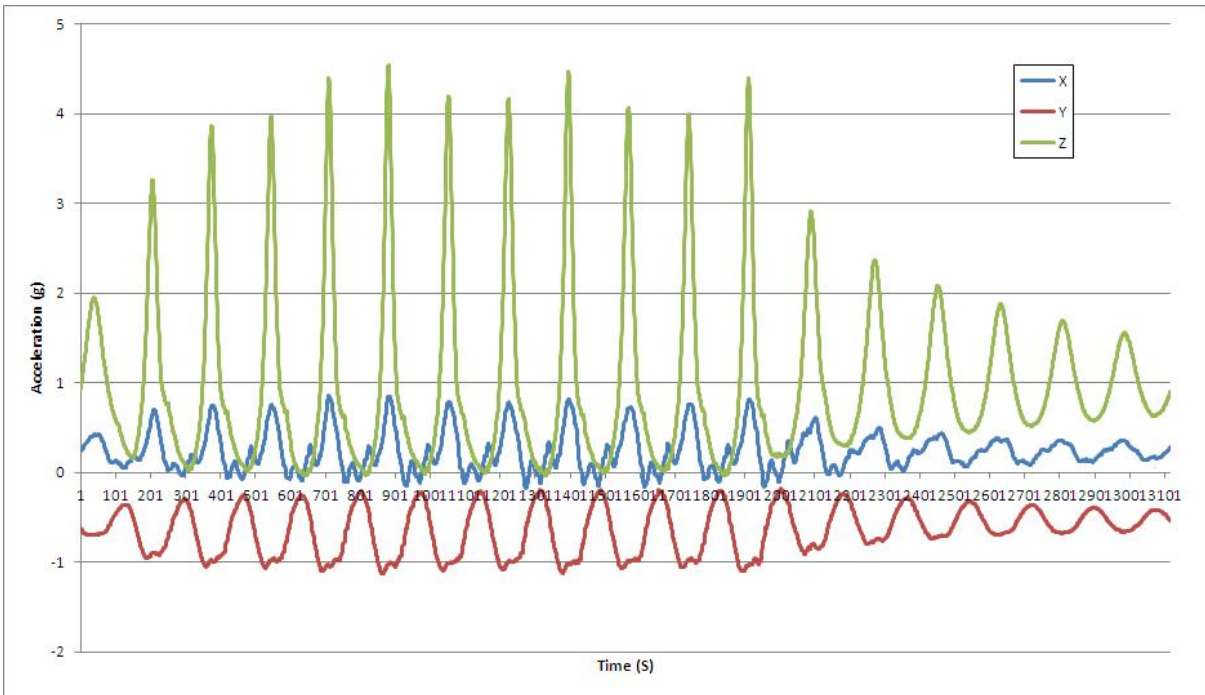


**Figure 69** Test run 7, Program 1, Foot pedal

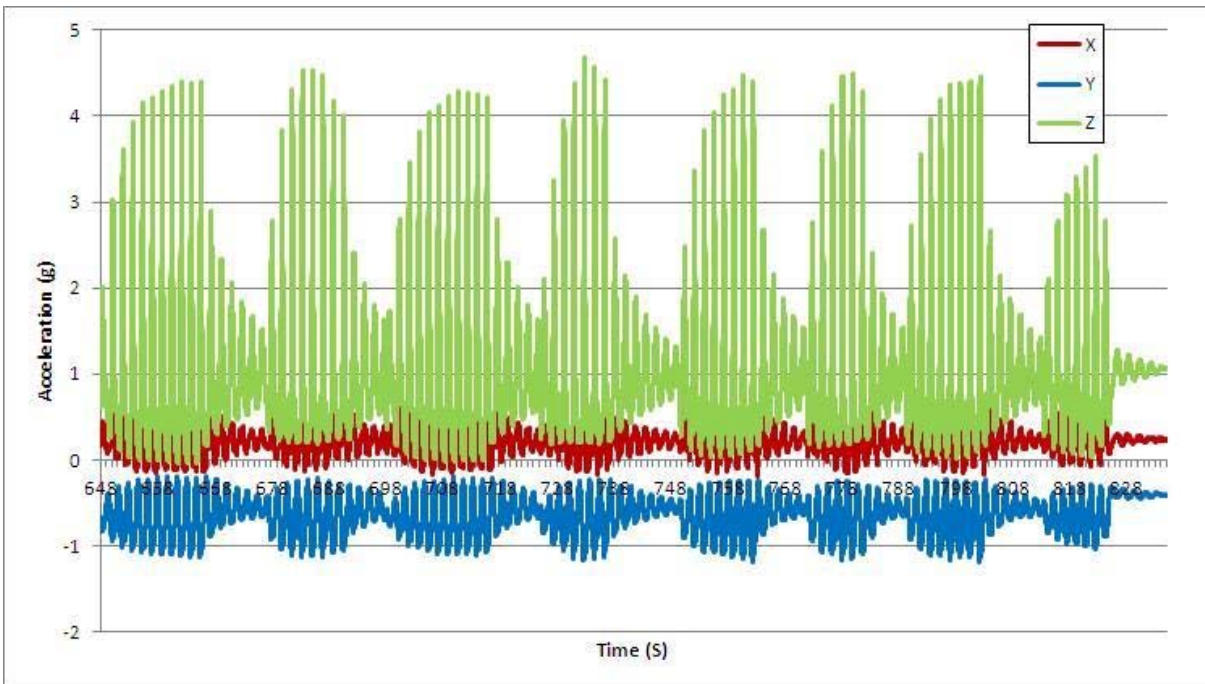


**Figure 70** Test run 7, Program 2

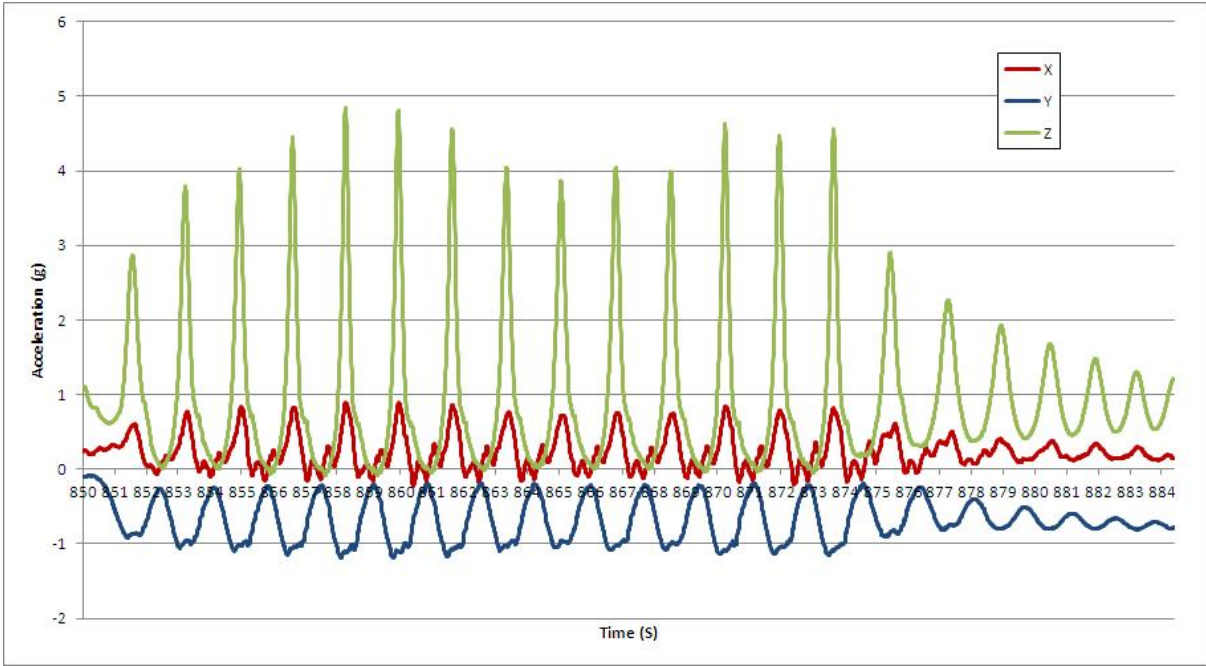


**Figure 71** Test run 7, Program 2, Foot pedal

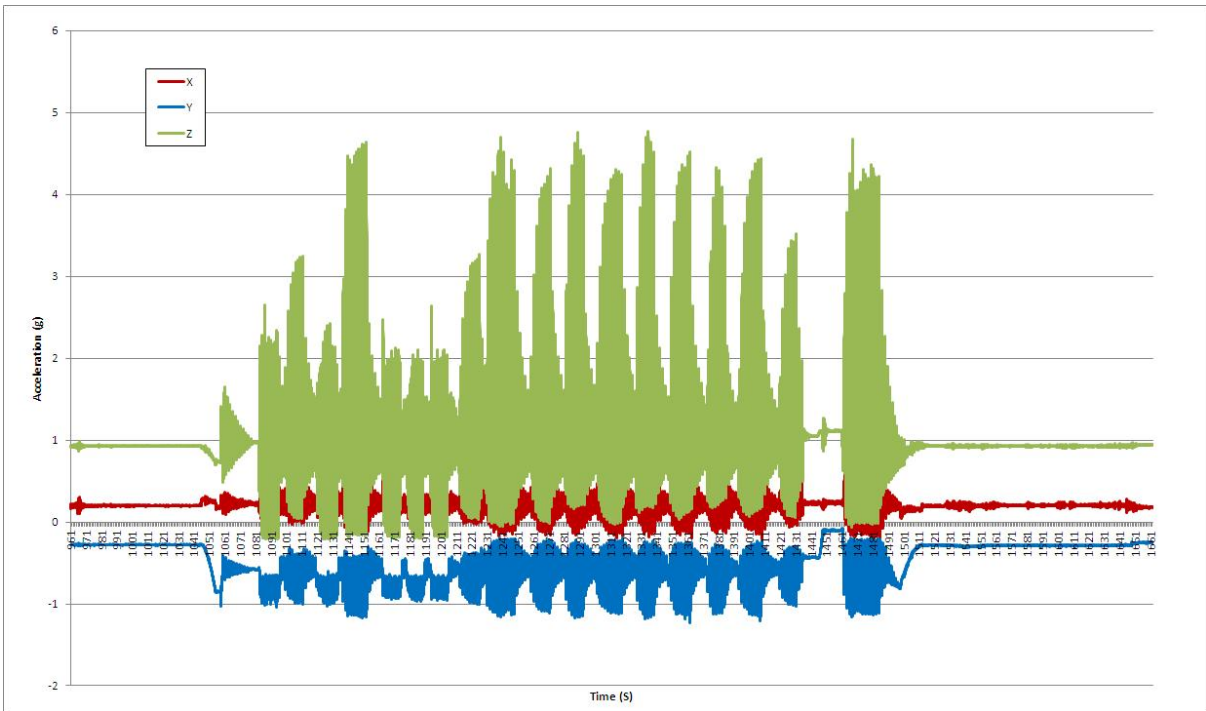


**Figure 72** Test run 8 Full

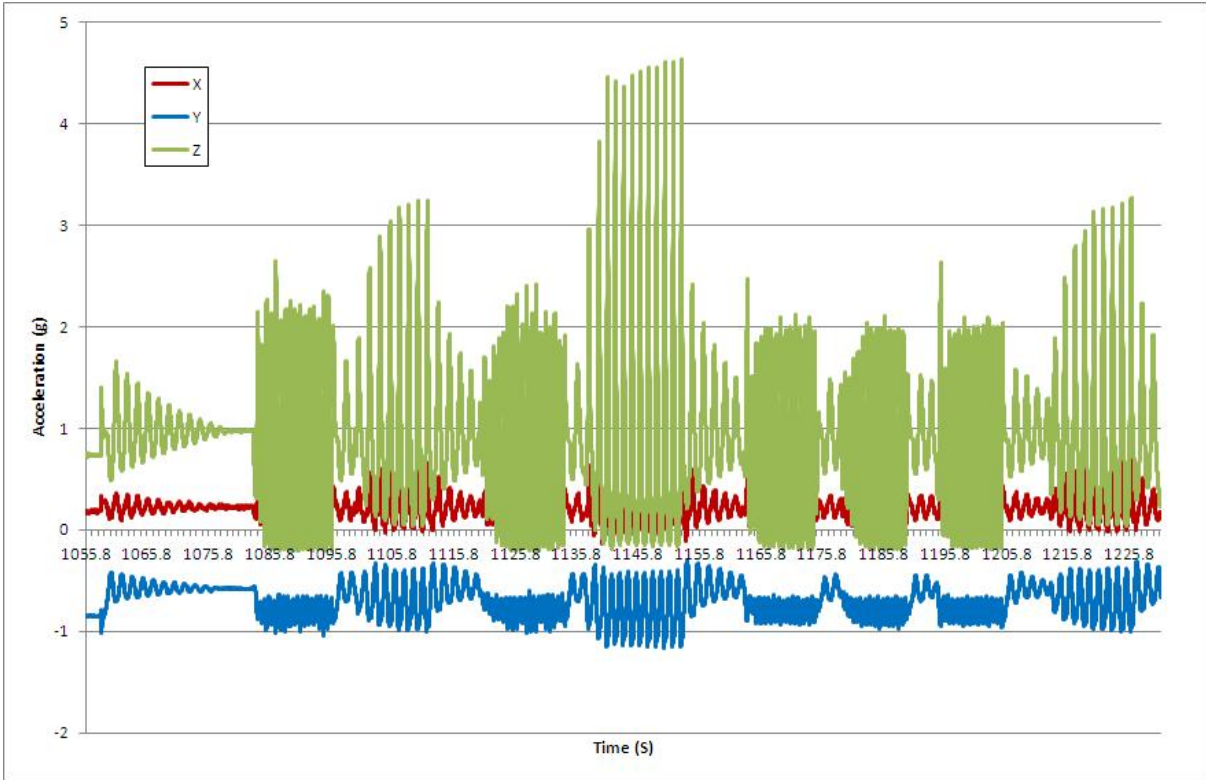


**Figure 73** Test run 8, Program 1

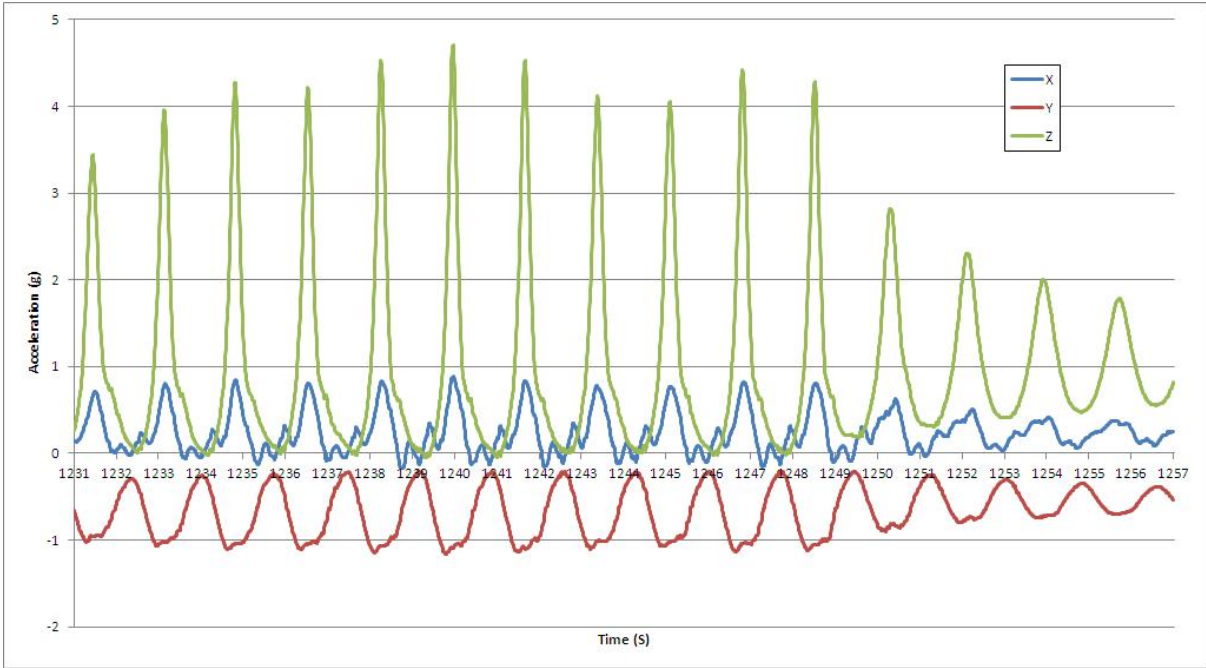


**Figure 74** Test run 8, Program 1, Foot pedal



**Figure 75** Test run 8, Program 2

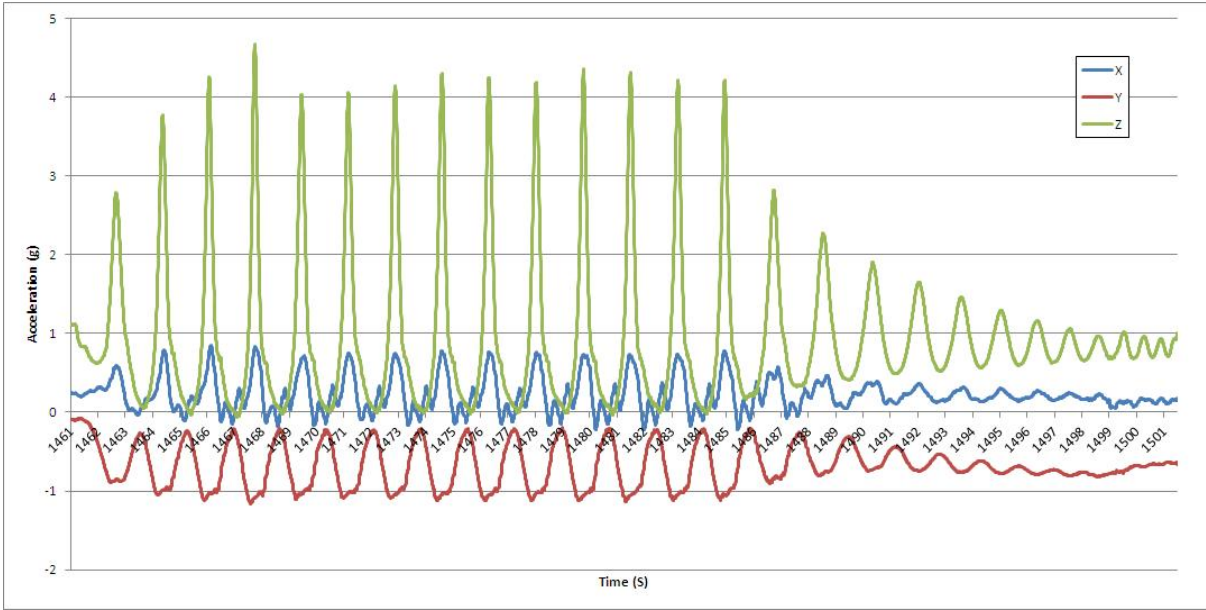


**Figure 76** Test run 8, Program 2, Foot pedal



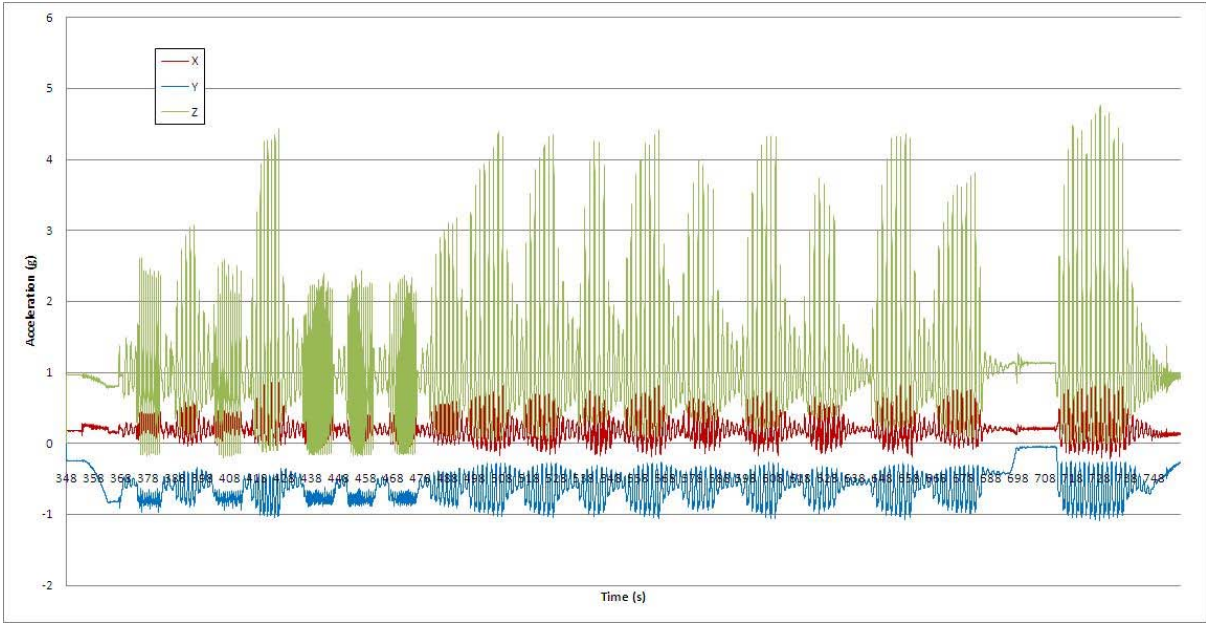


**Figure 77** Test run 9 Full

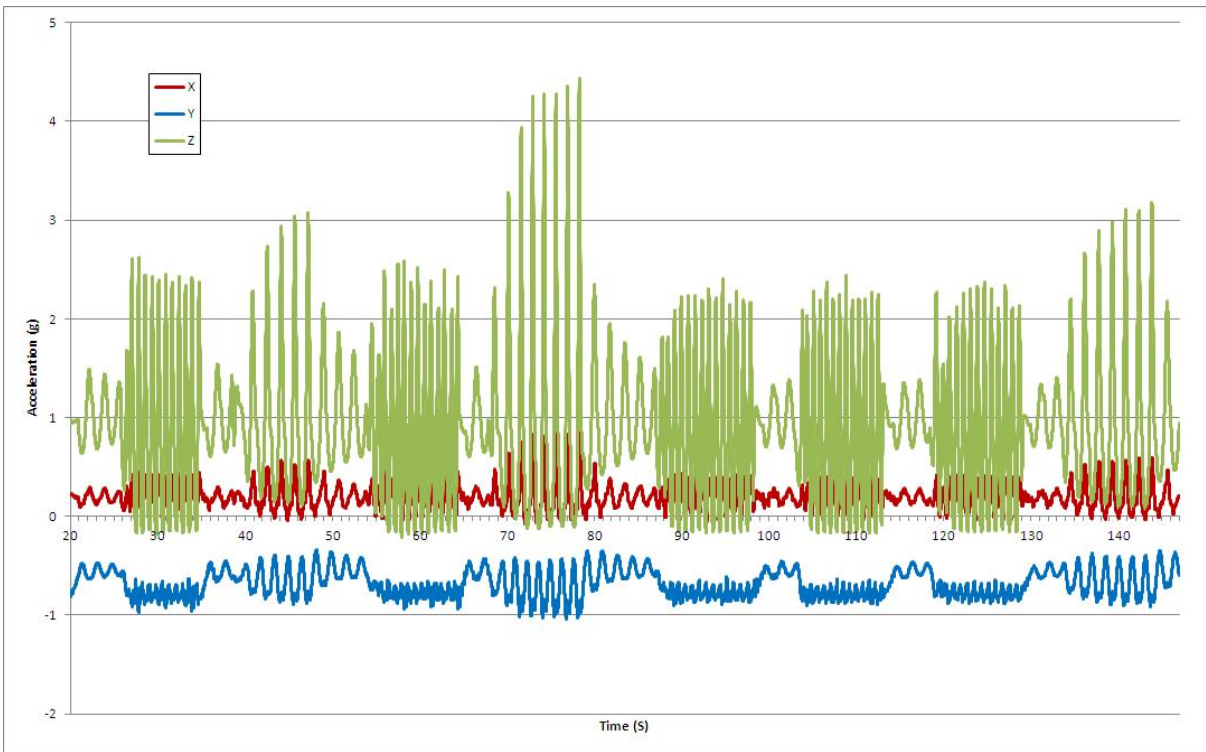


**Figure 78** Test run 9, Program 1

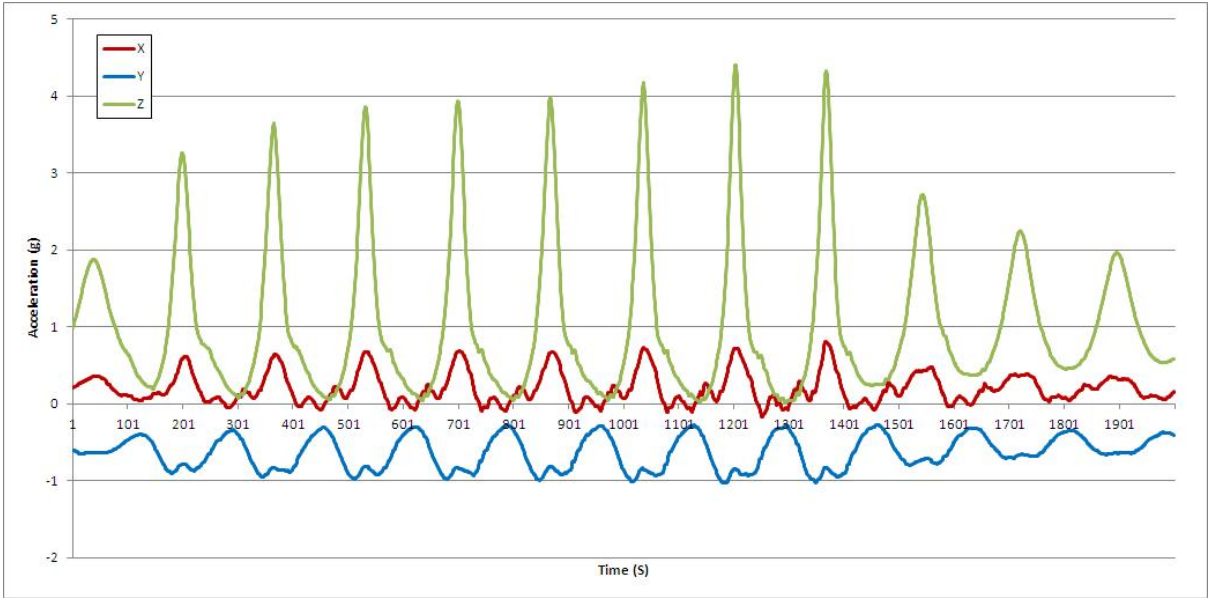


**Figure 79** Test run 9, Program 1, Foot pedal

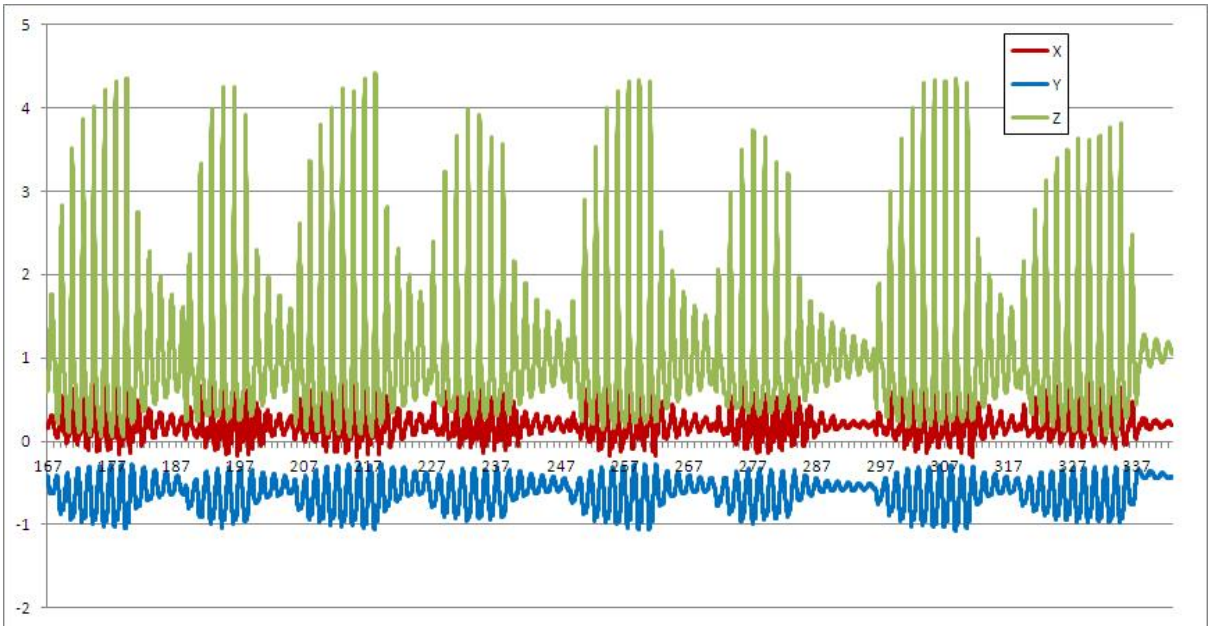


**Figure 80** Test run 9, Program 2

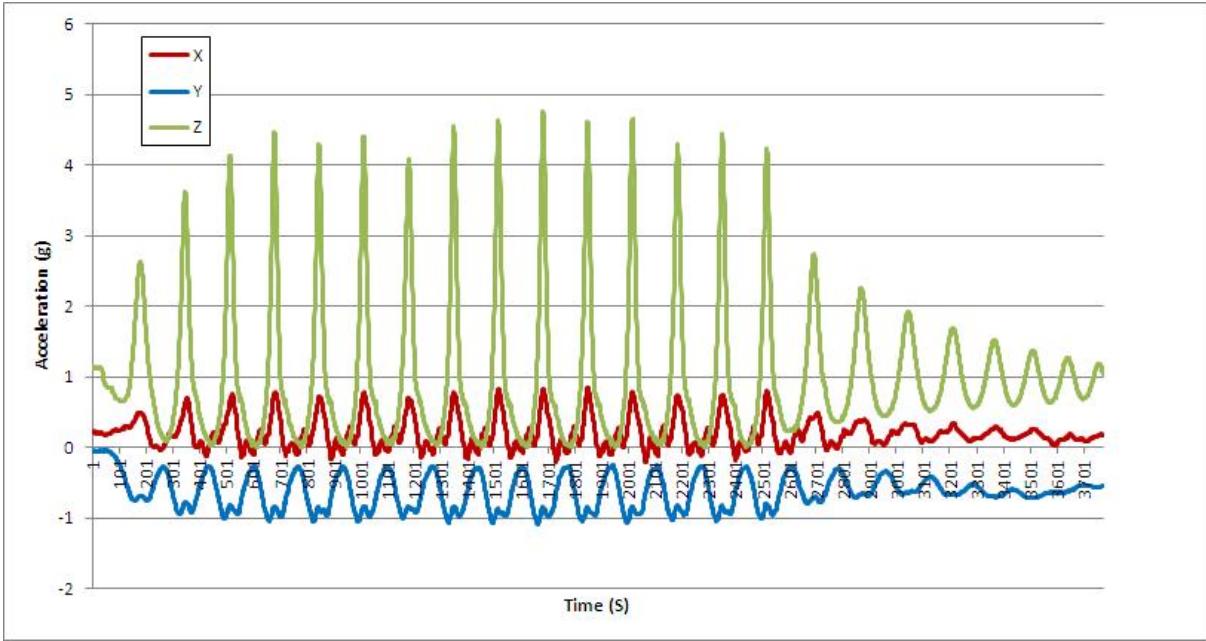


**Figure 81** Test run 9, Program 2, Foot pedal

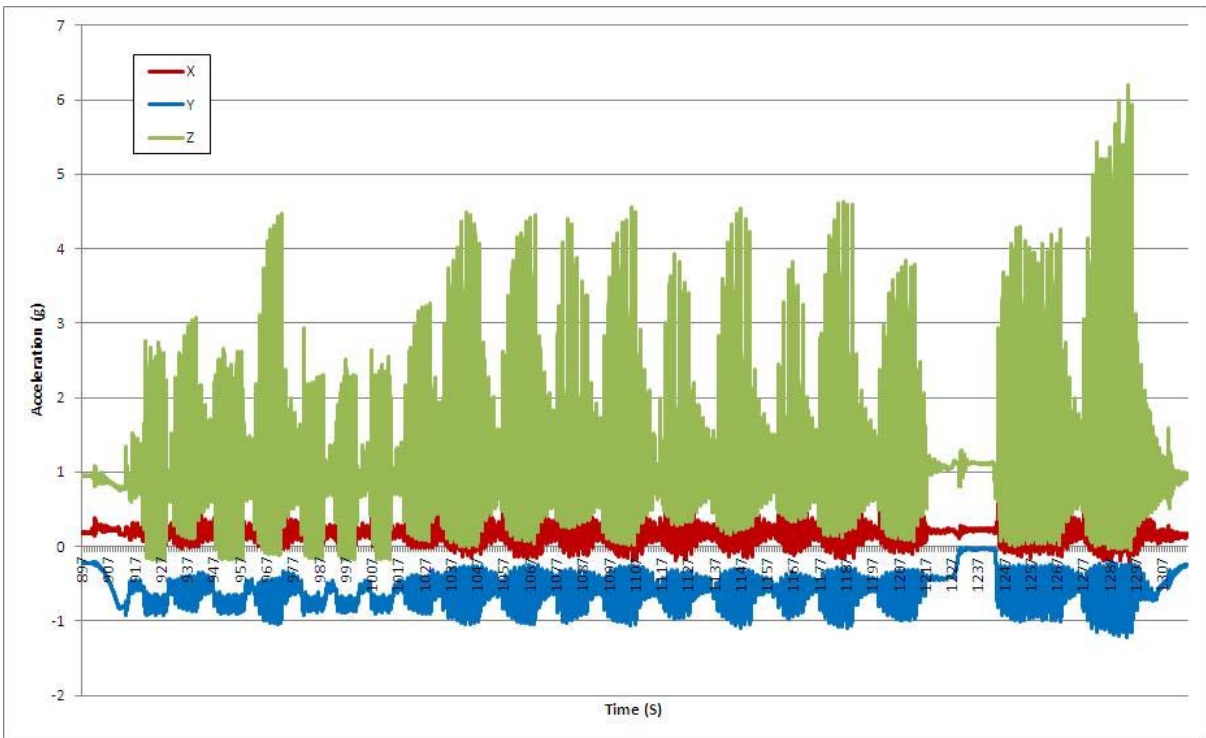


**Figure 82** Test run 10 Full

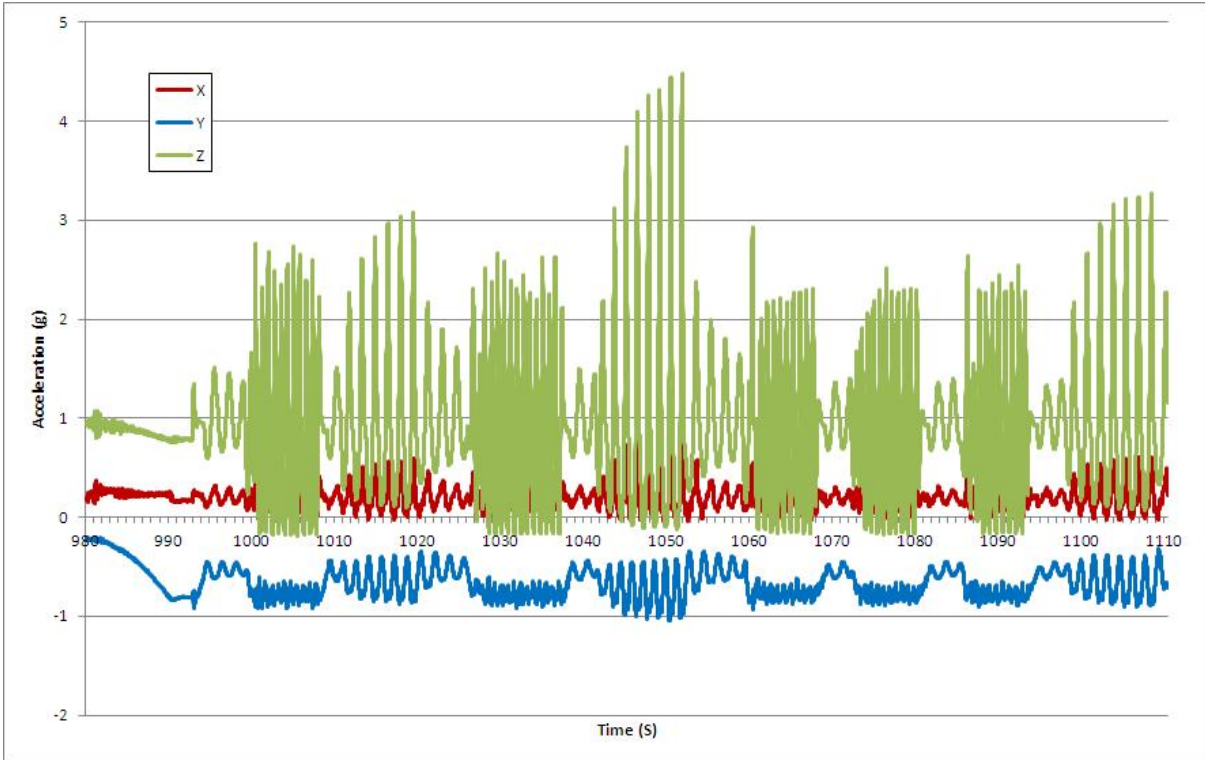


**Figure 83** Test run 10, Program 1

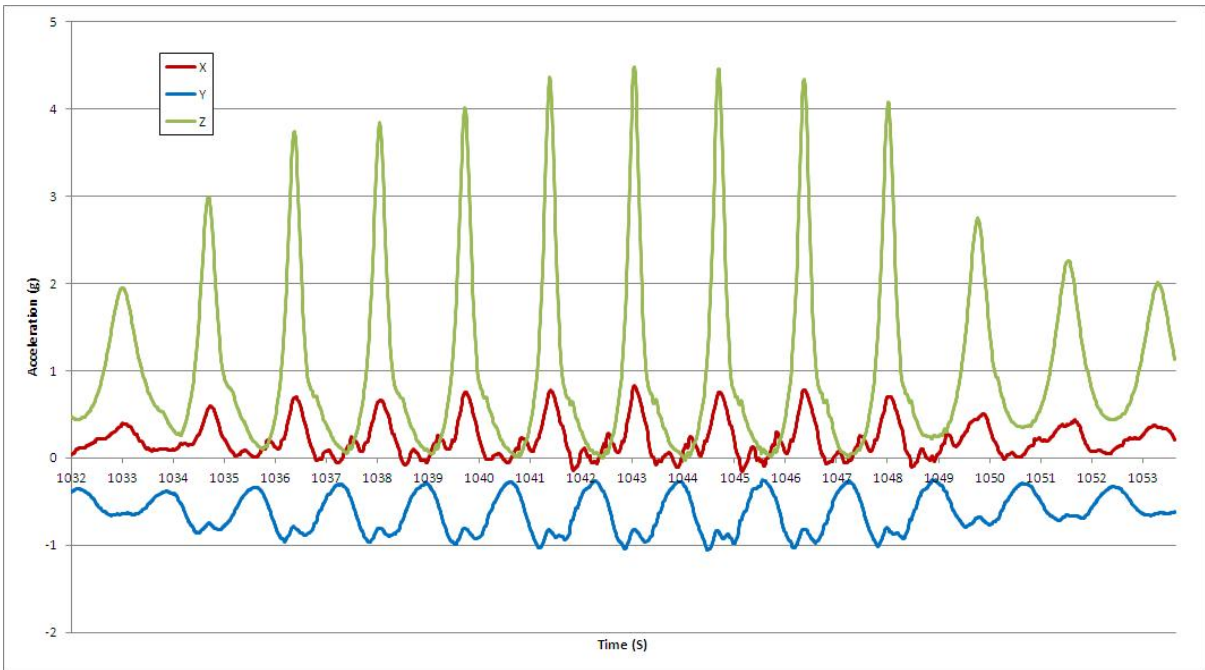


**Figure 84** Test run 10, Program 1, Foot pedal



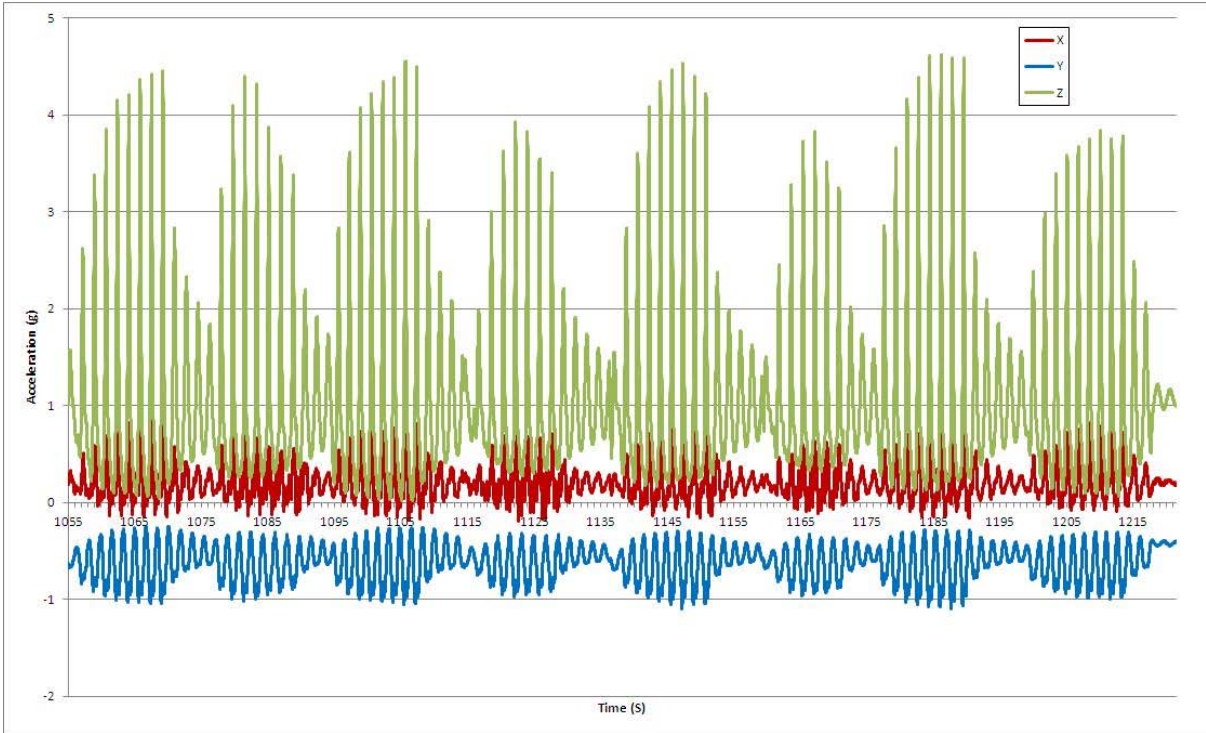


**Figure 85** Test run 10, Program 2

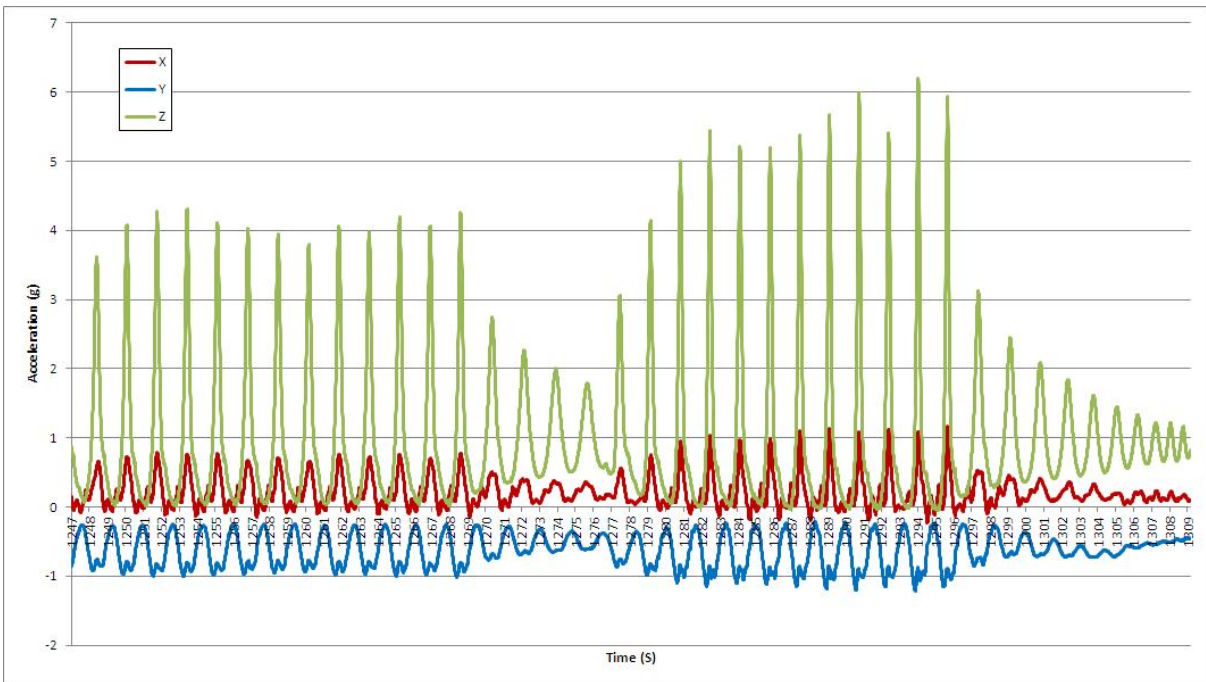


**Figure 86** Test run 10, Program 2, Foot pedal

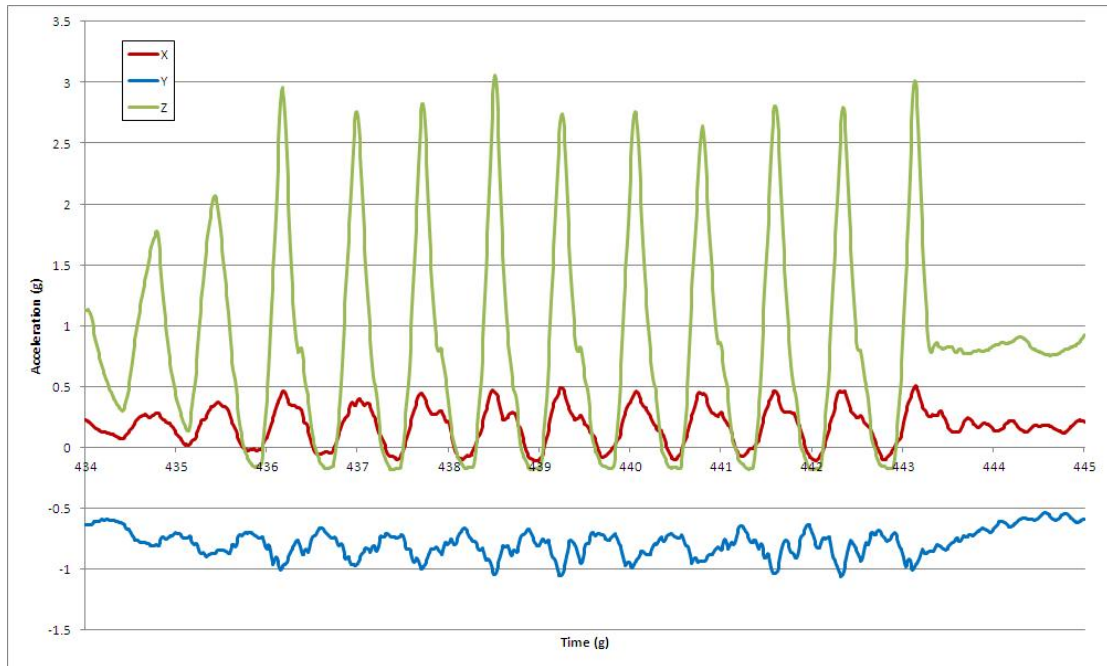


**Figure 87** Test run 11, Prog 1, A

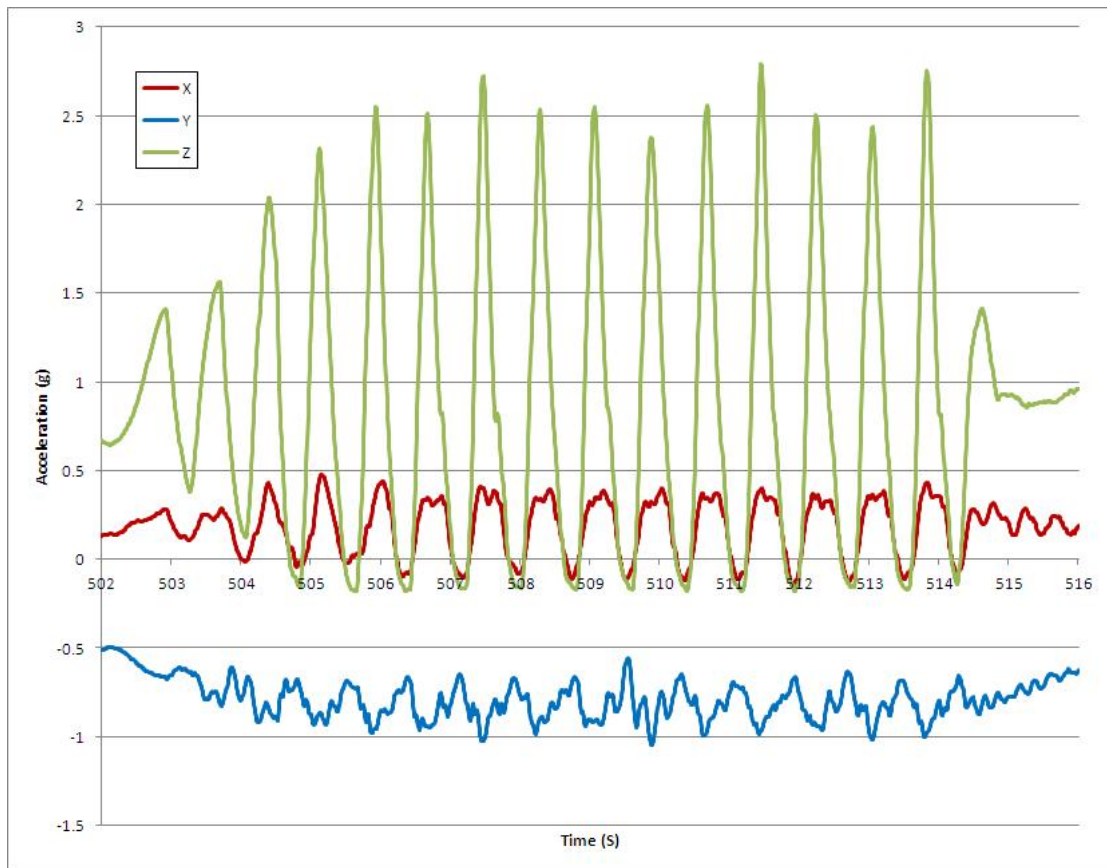


**Figure 88** Test run 11, Prog 1, AA

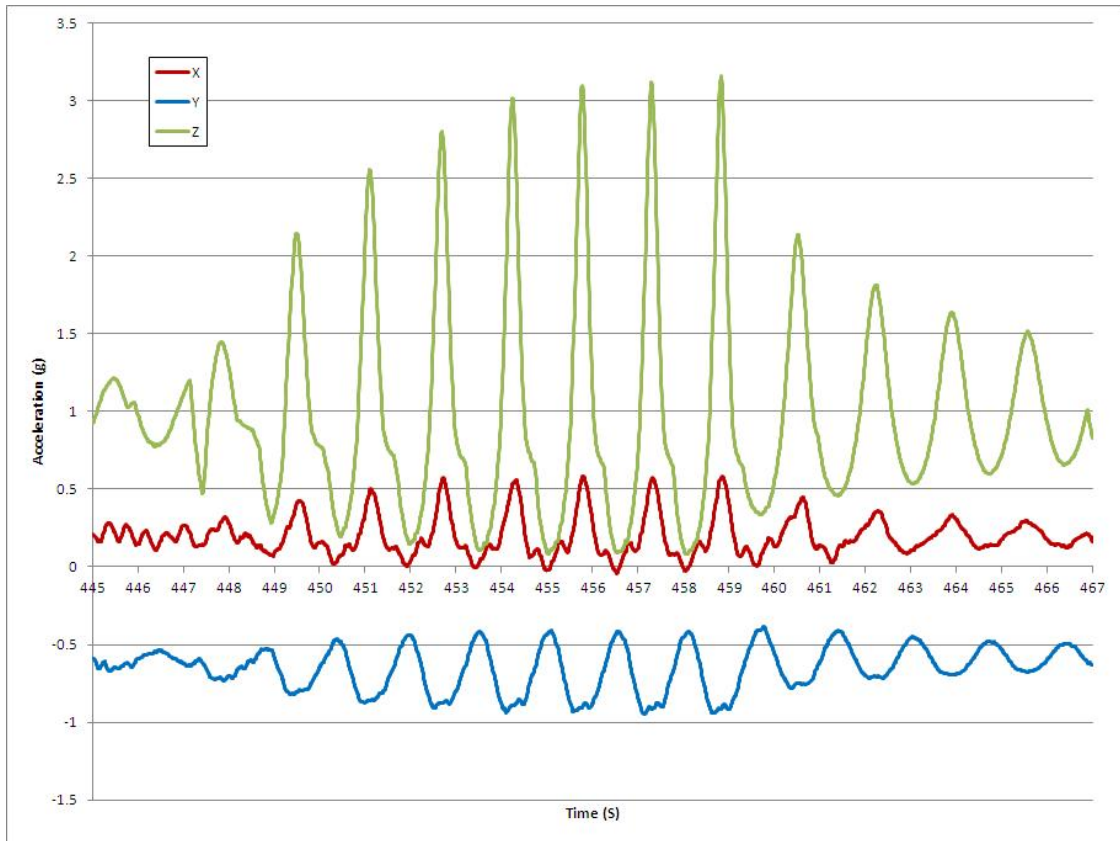


**Figure 89** Test run 11, Prog 1, B

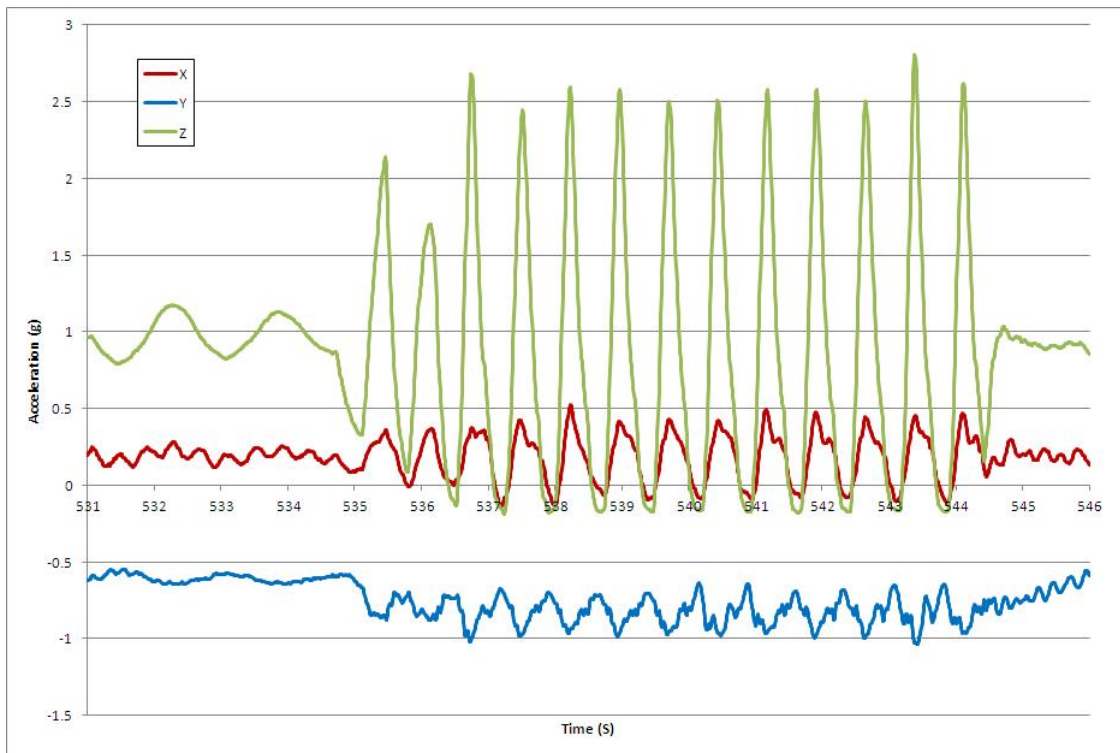


**Figure 90** Test run 11, Prog 1, BB

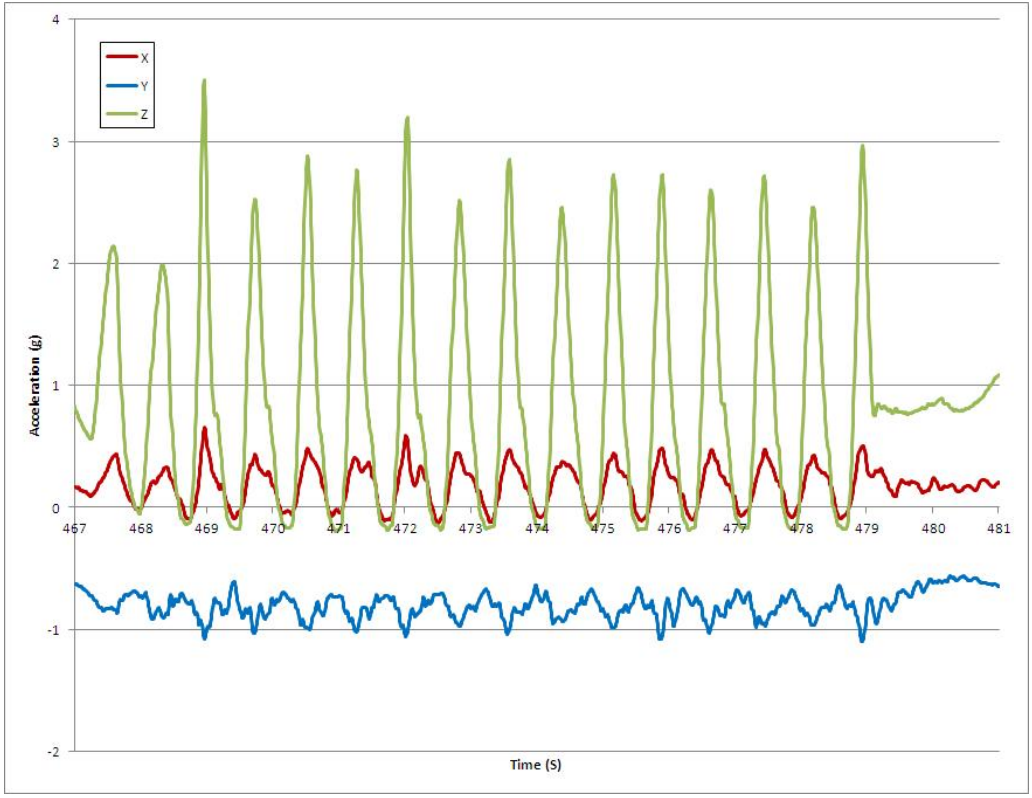


**Figure 91** Test run 11, Prog 1, C

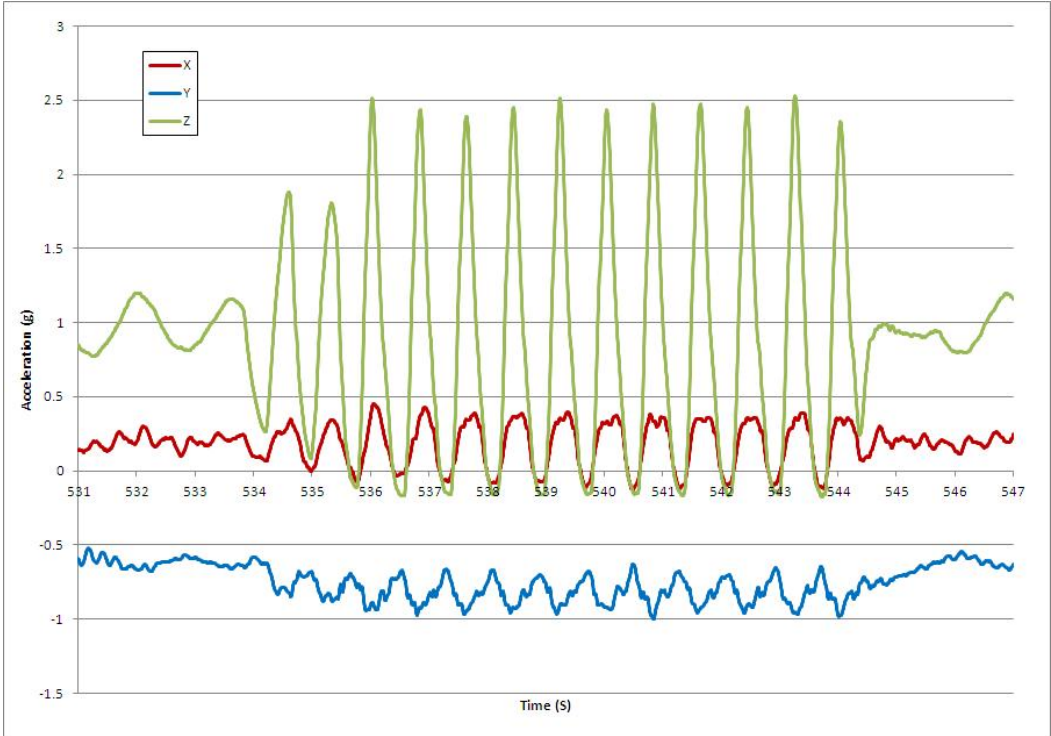


**Figure 92** Test run 11, Prog 1, CC



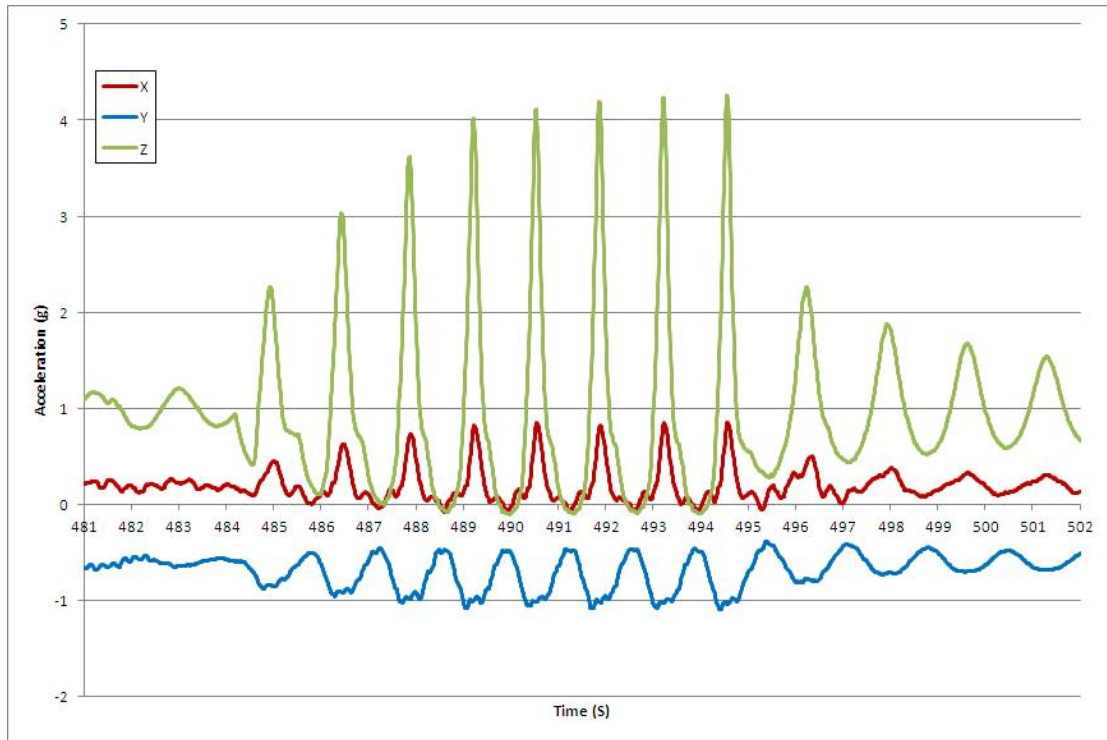


**Figure 93** Test run 11, Prog 1, D

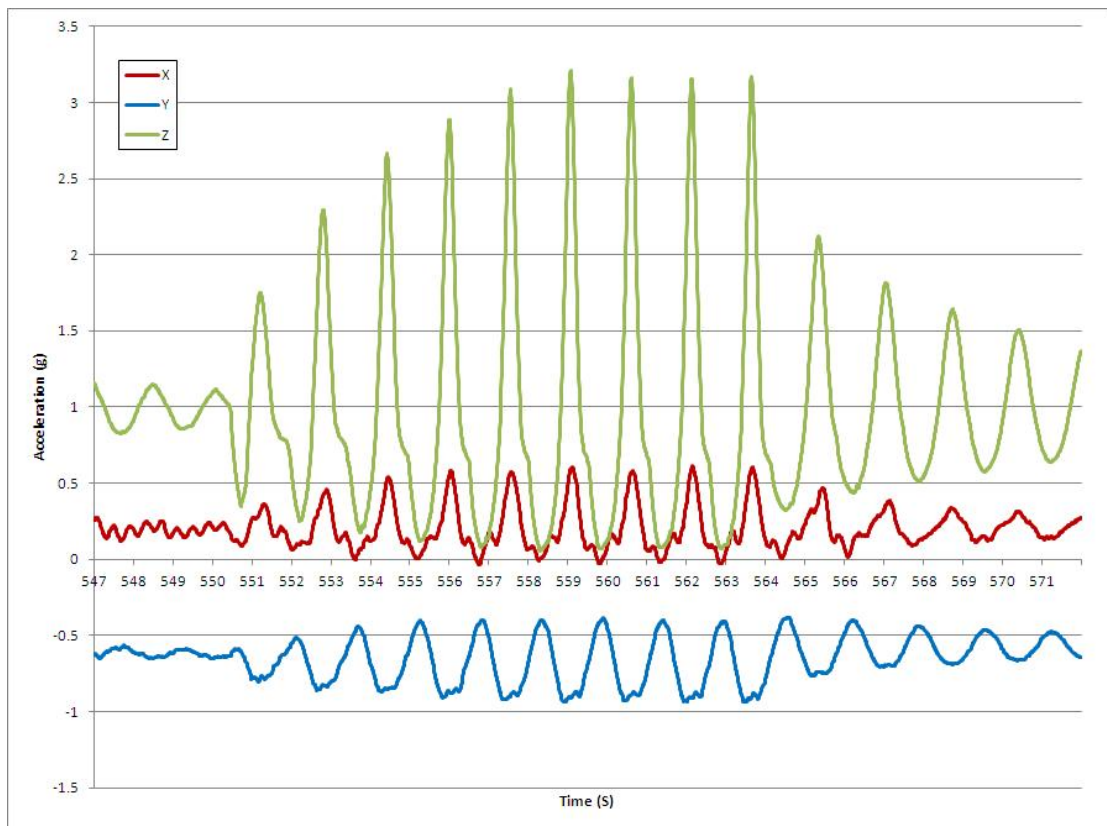


**Figure 94** Test run 11, Prog 1, DD

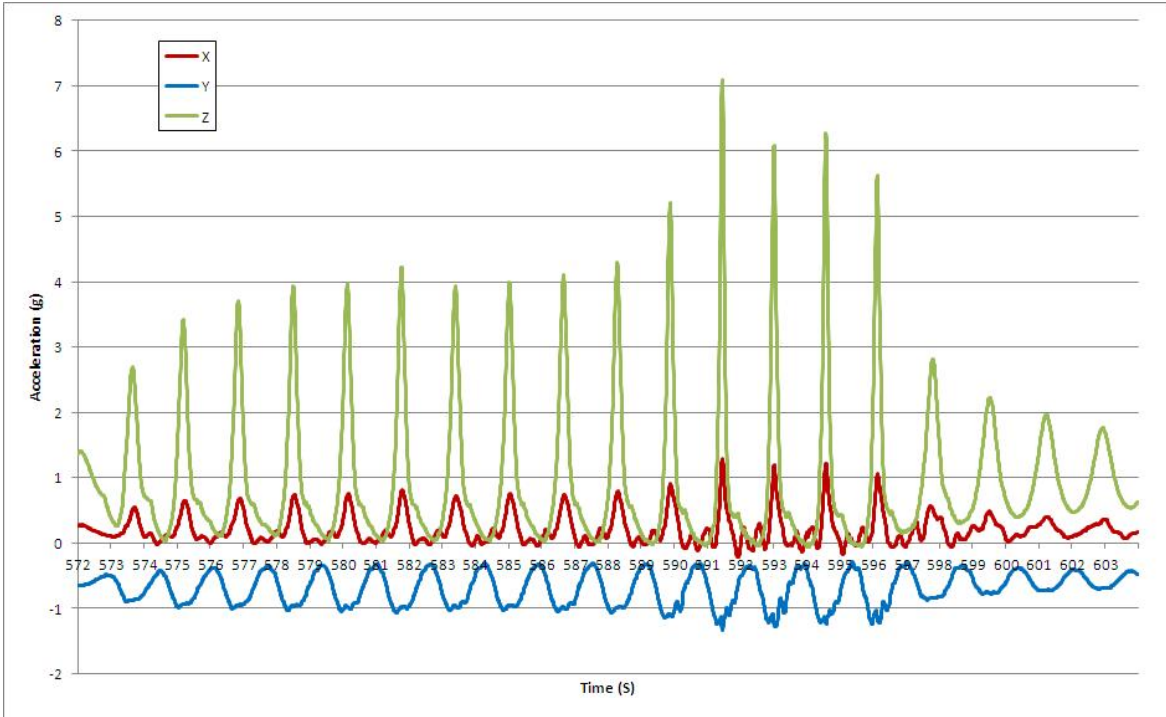


**Figure 95** Test run 11, Prog 1, Foot pedal

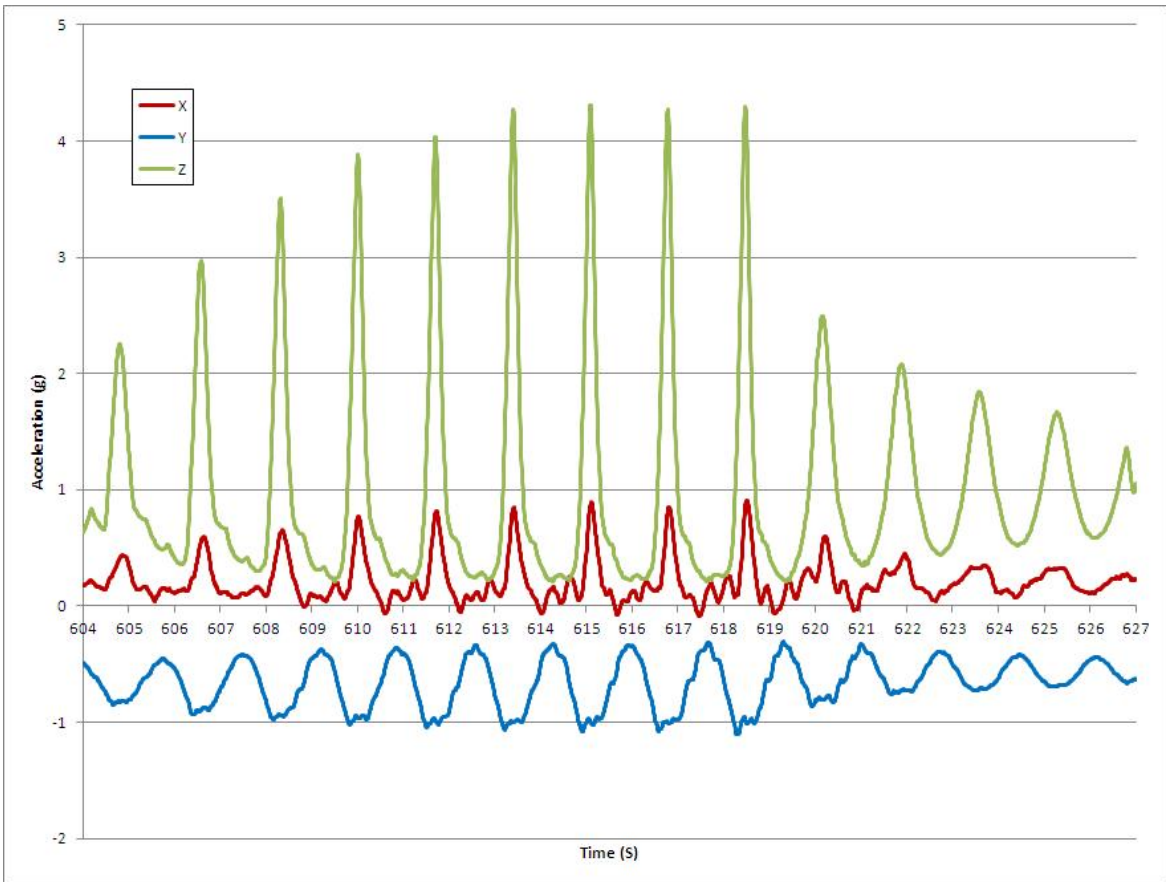


**Figure 96** Test run 11, Program 2, A

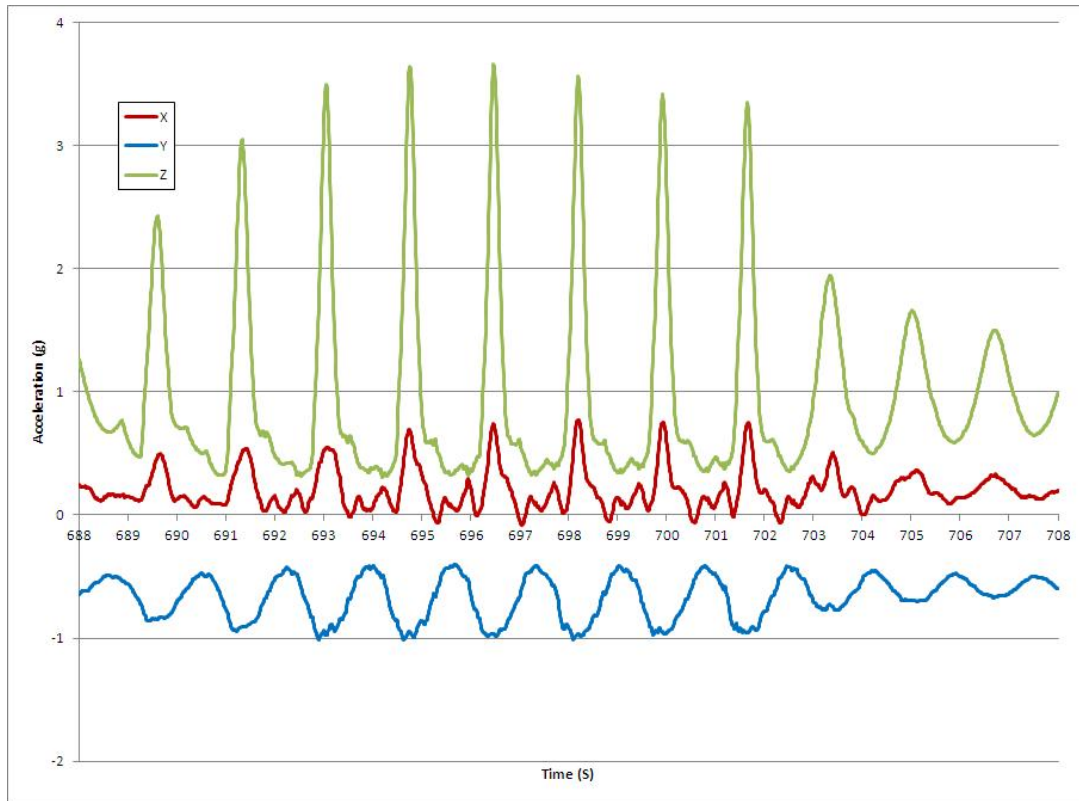


**Figure 97** Test run 11, Program 2, AA

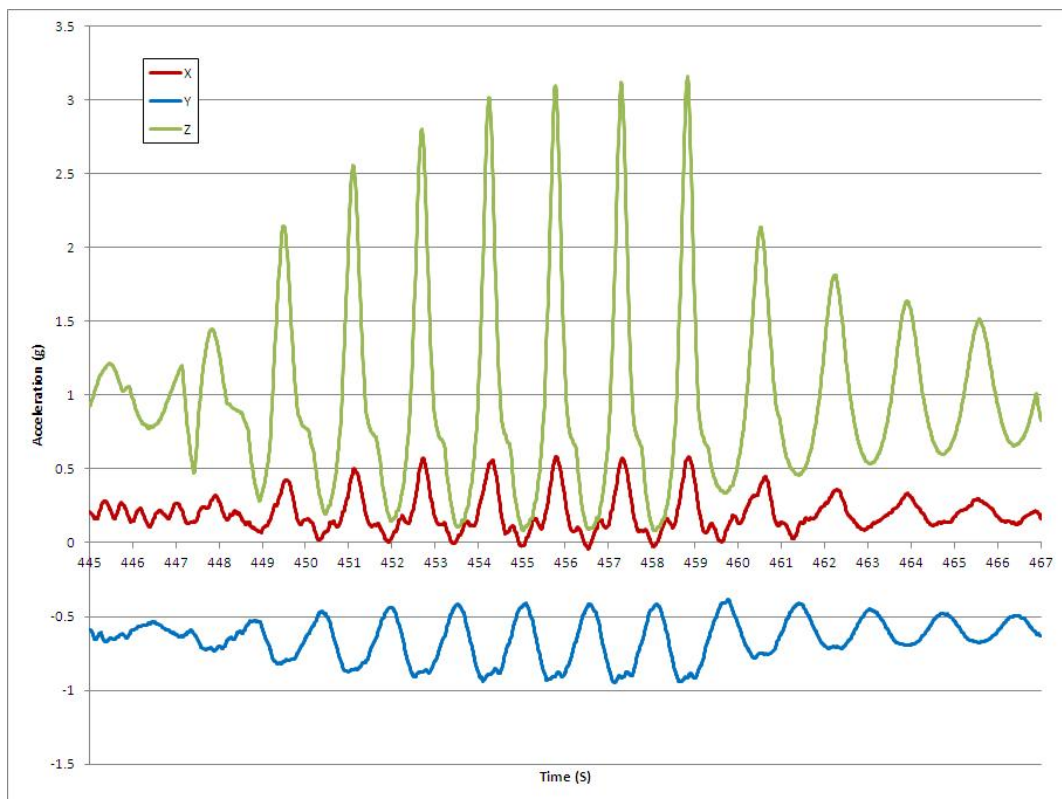


**Figure 98** Test run 11, Program 2, B

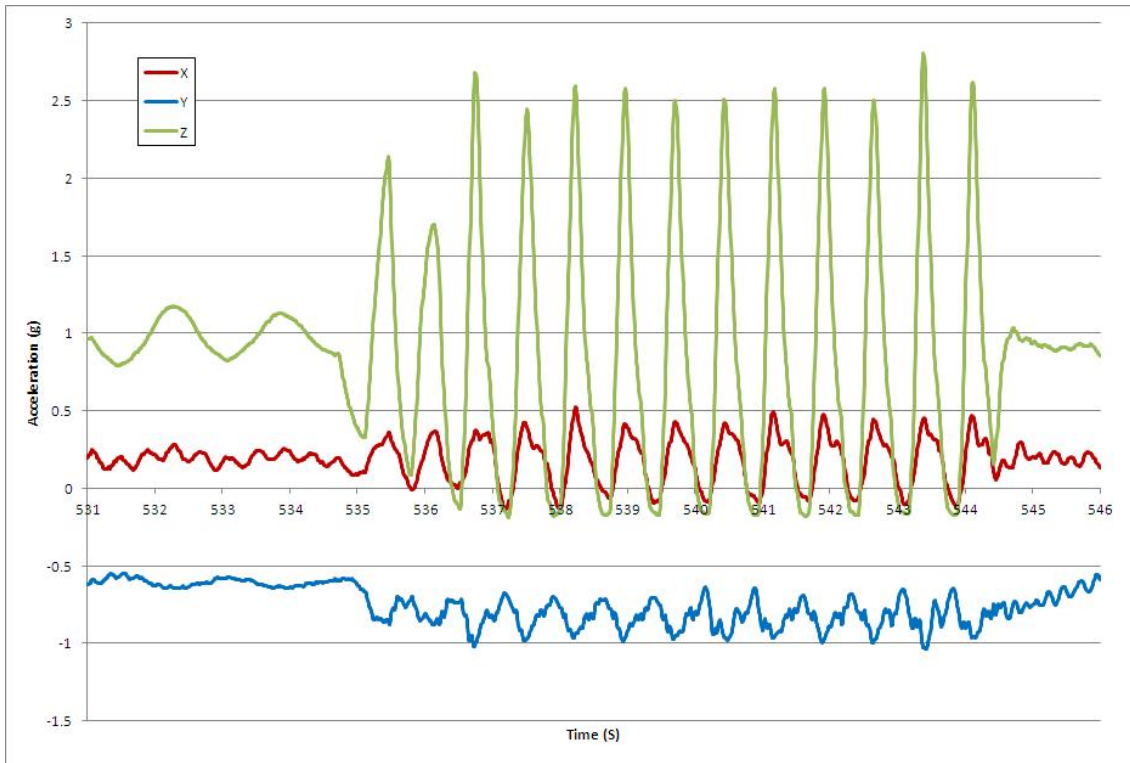


**Figure 99** Test run 11, Program 2, BB

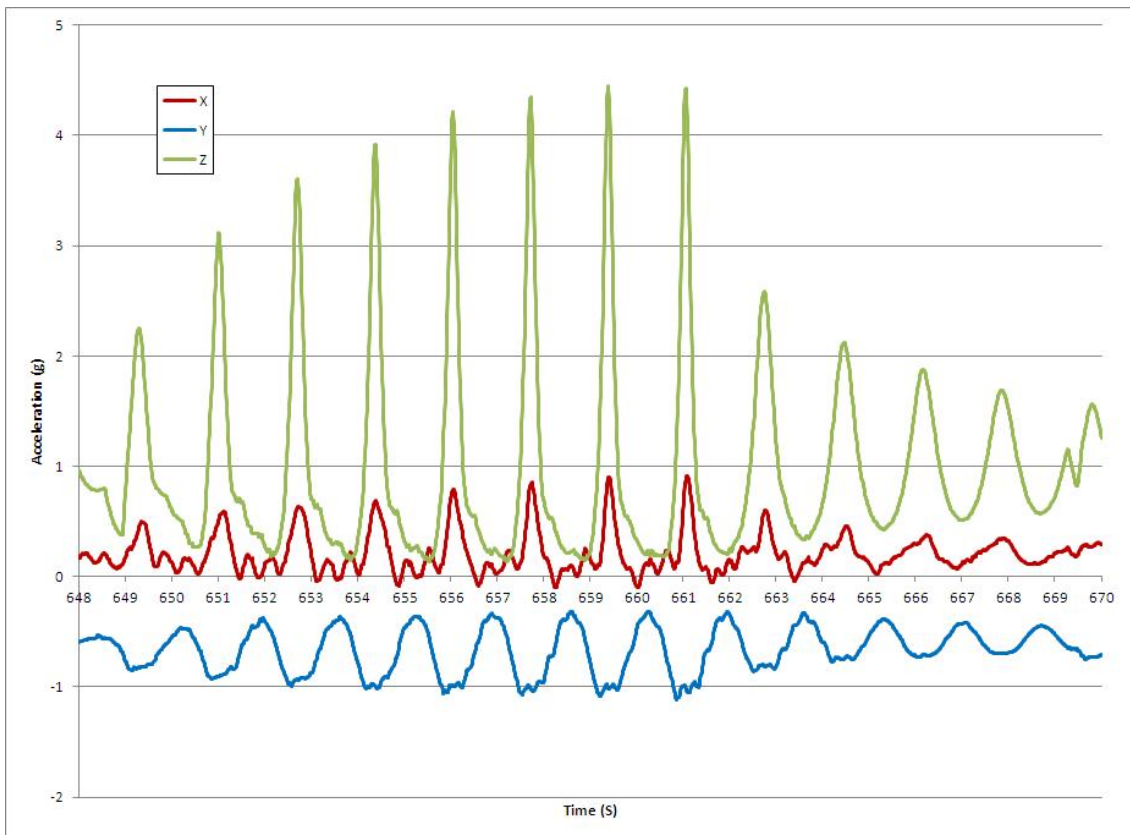


**Figure 100** Test run 11, Program 2, C



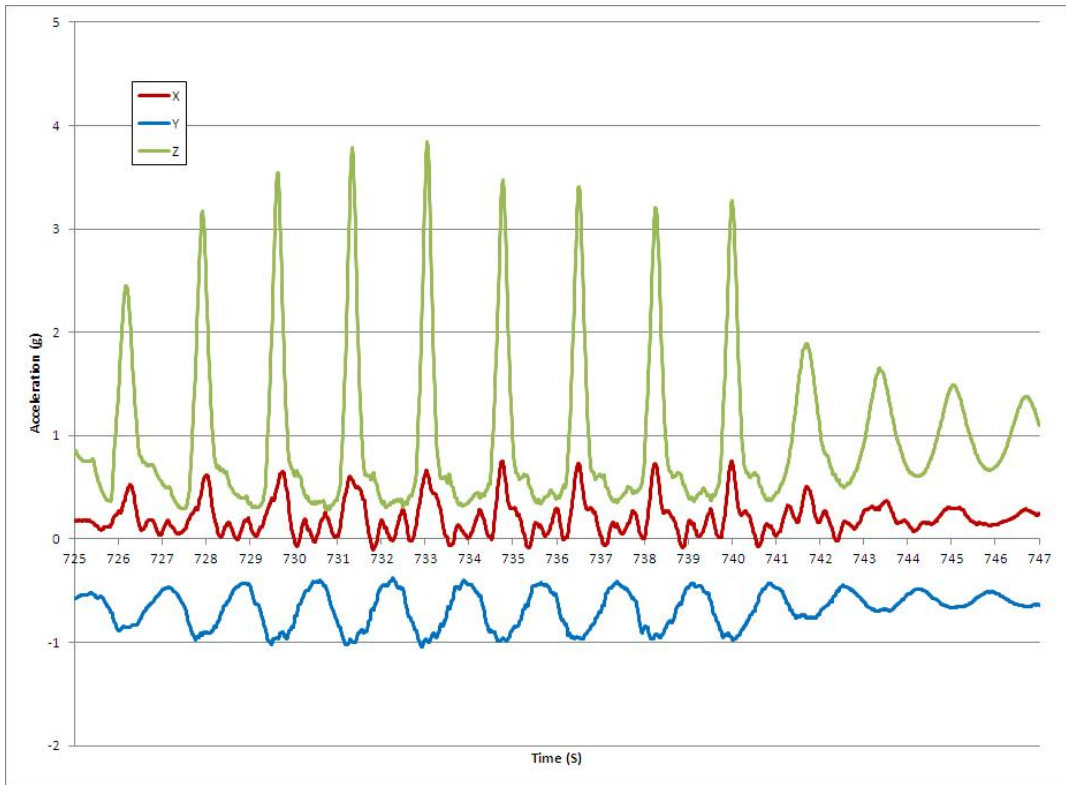


**Figure 101** Test run 11, Program 2, CC

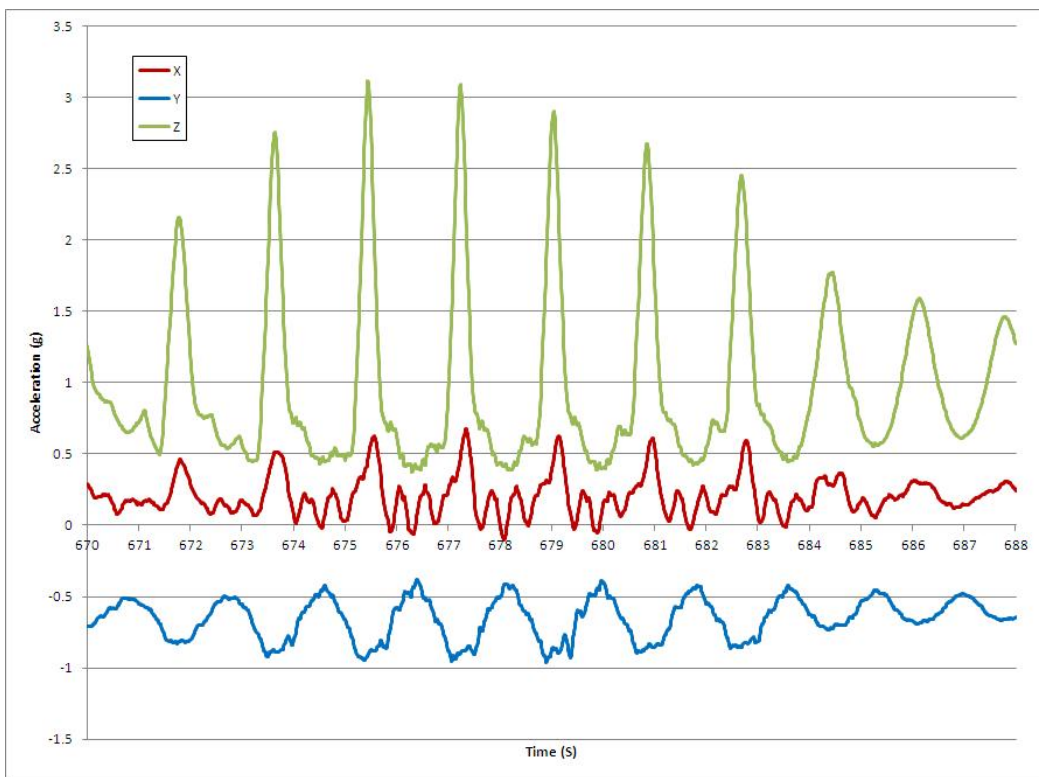


**Figure 102** Test run 11, Program 2, D

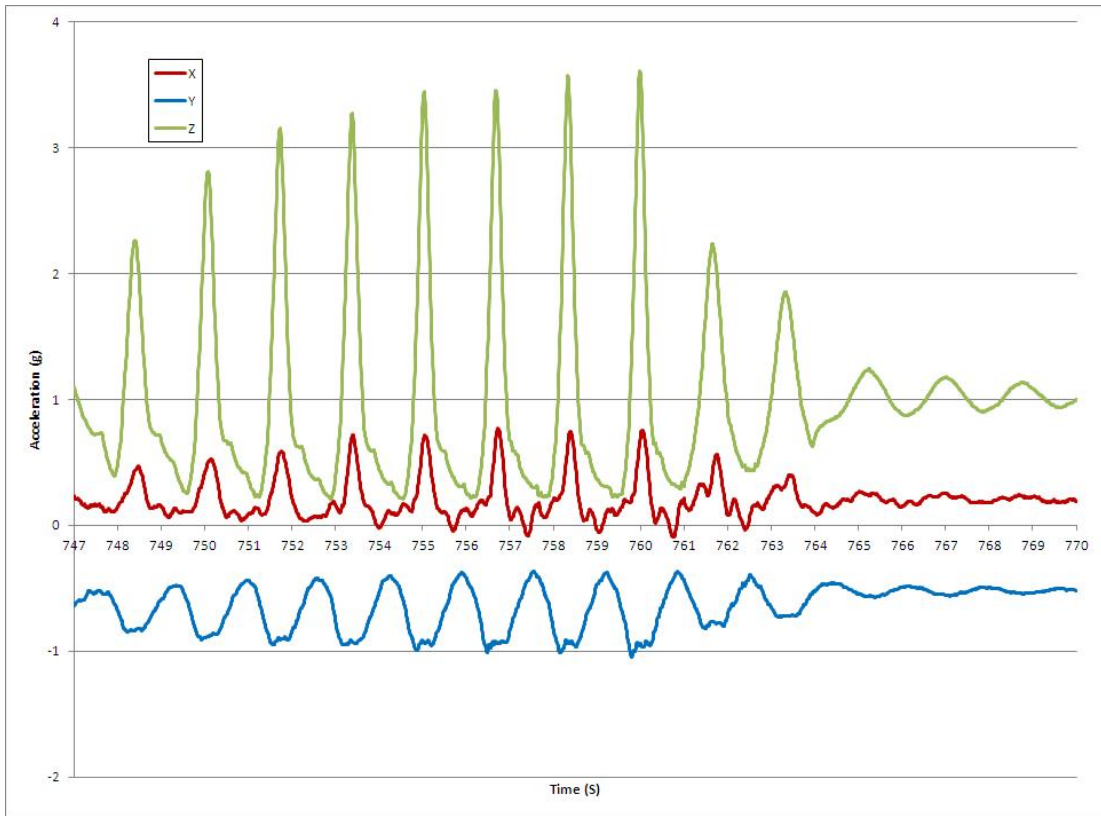


**Figure 103** Test run 11, Program 2, DD

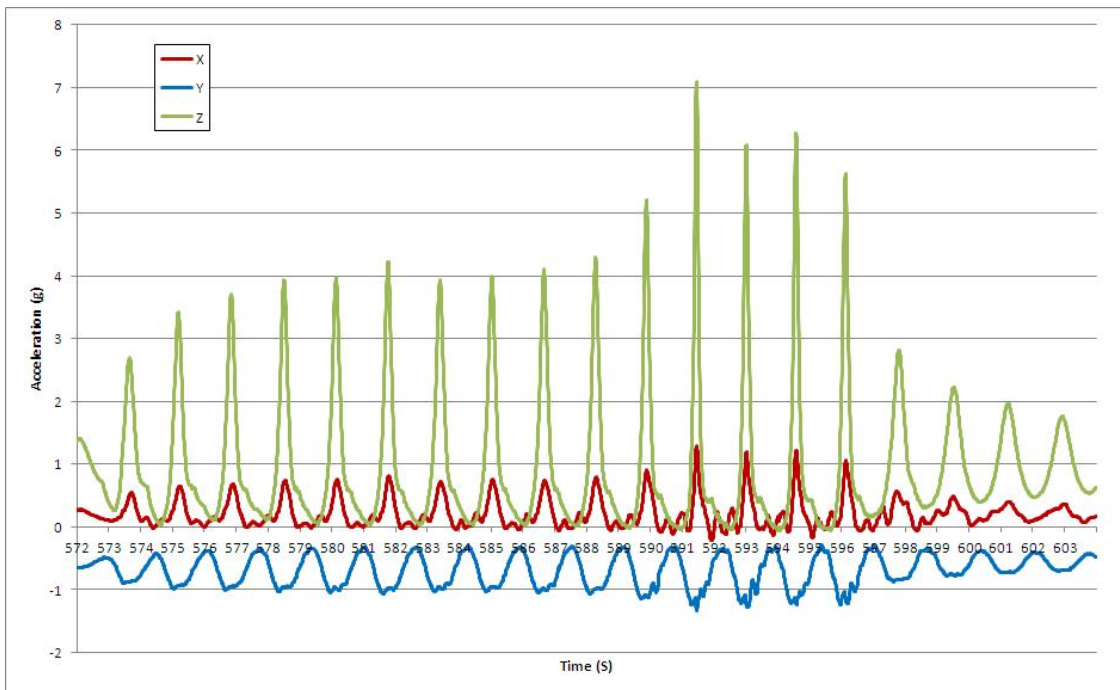


**Figure 104** Test run 11, Program 2, Foot pedal

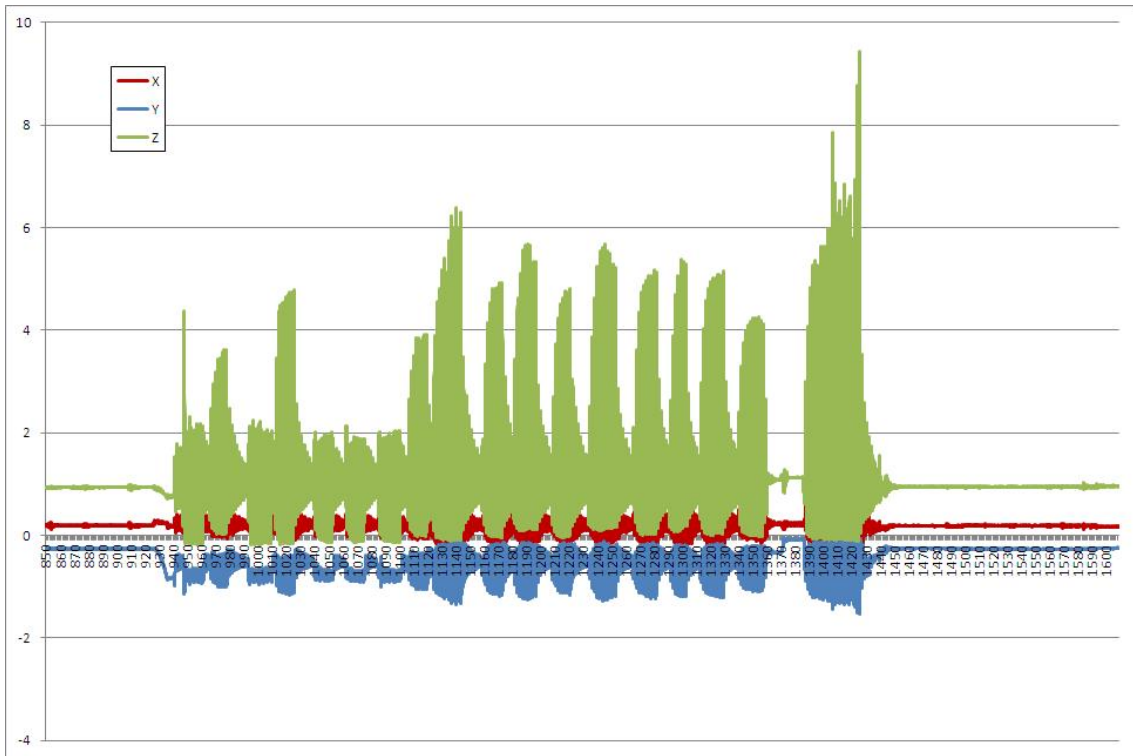


**Figure 105** Test run 12 Full

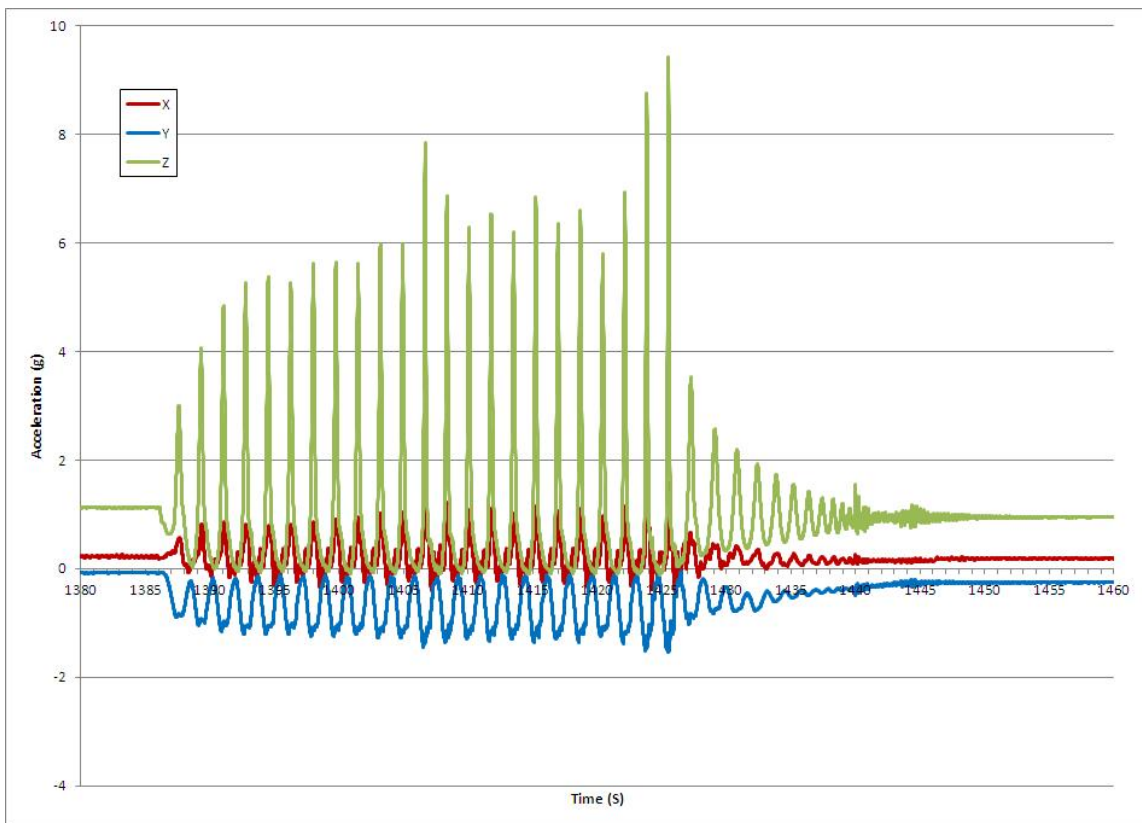


**Figure 106** Test run 12, Program 2, Foot pedal

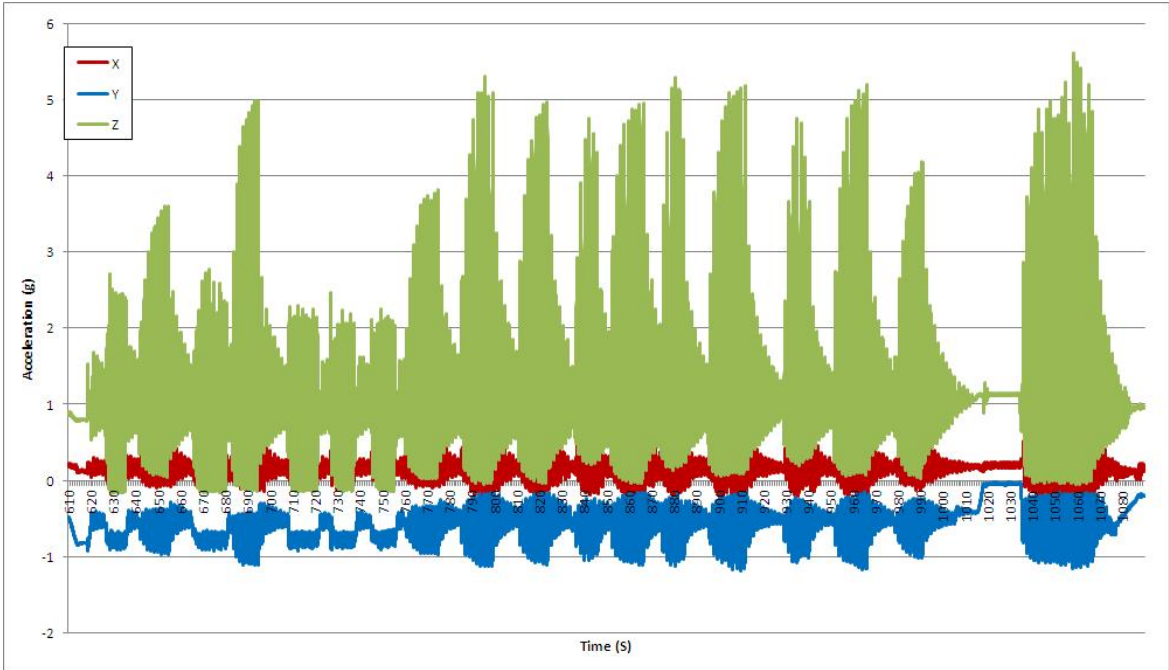


**Figure 107** Test run 16 Full

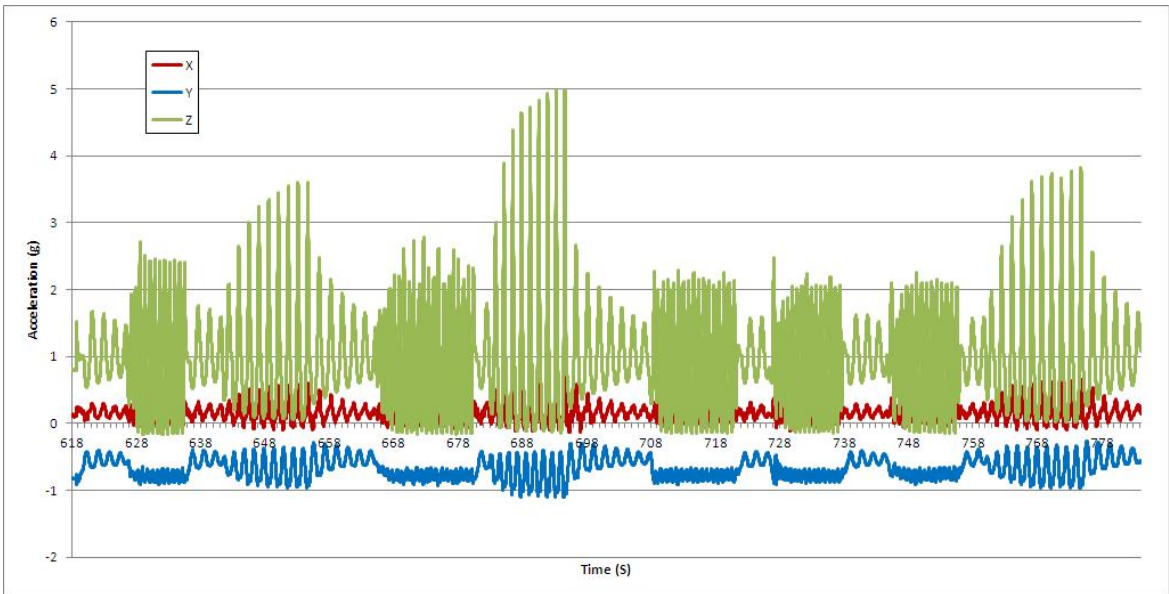


**Figure 108** Test run 16, Program 1

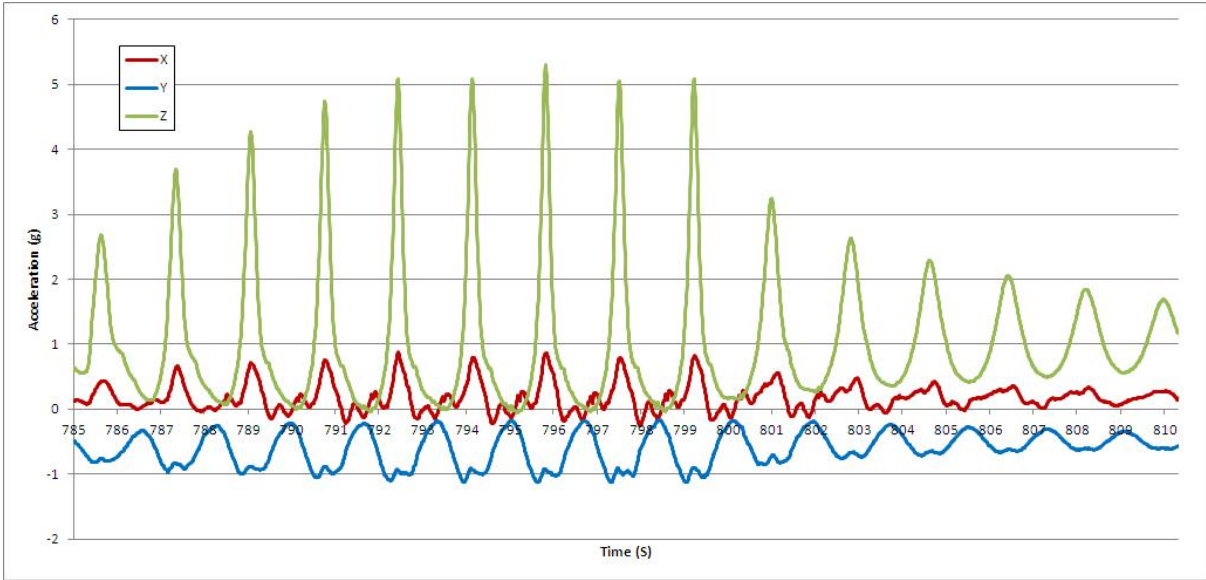


**Figure 109** Test run 16, Program 1, Foot pedal



**Figure 110** Test run 16, Program 2



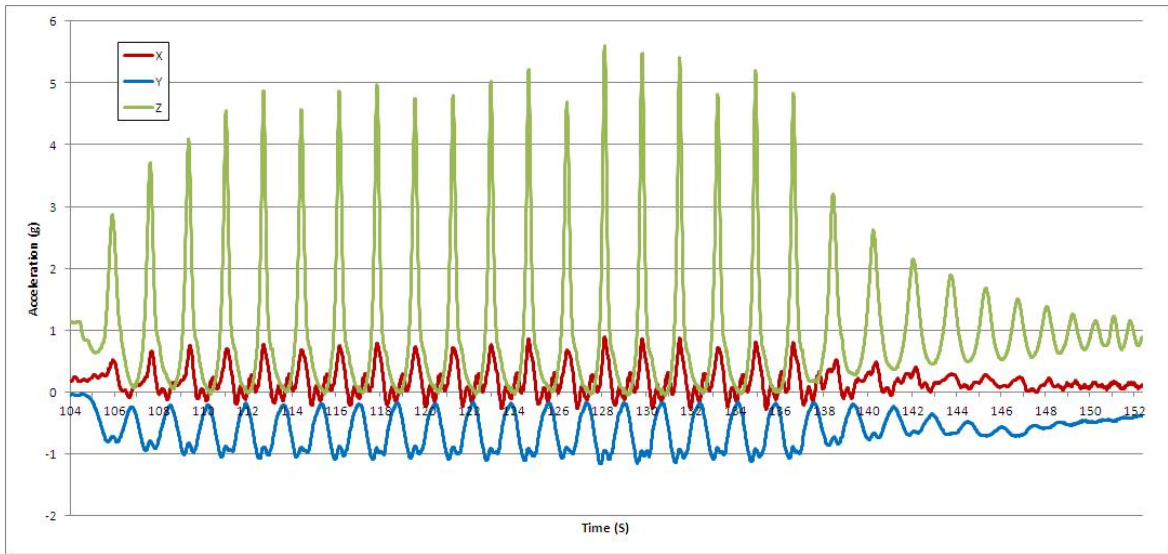


**Figure 111** Test run 16, Program 2, Foot pedal

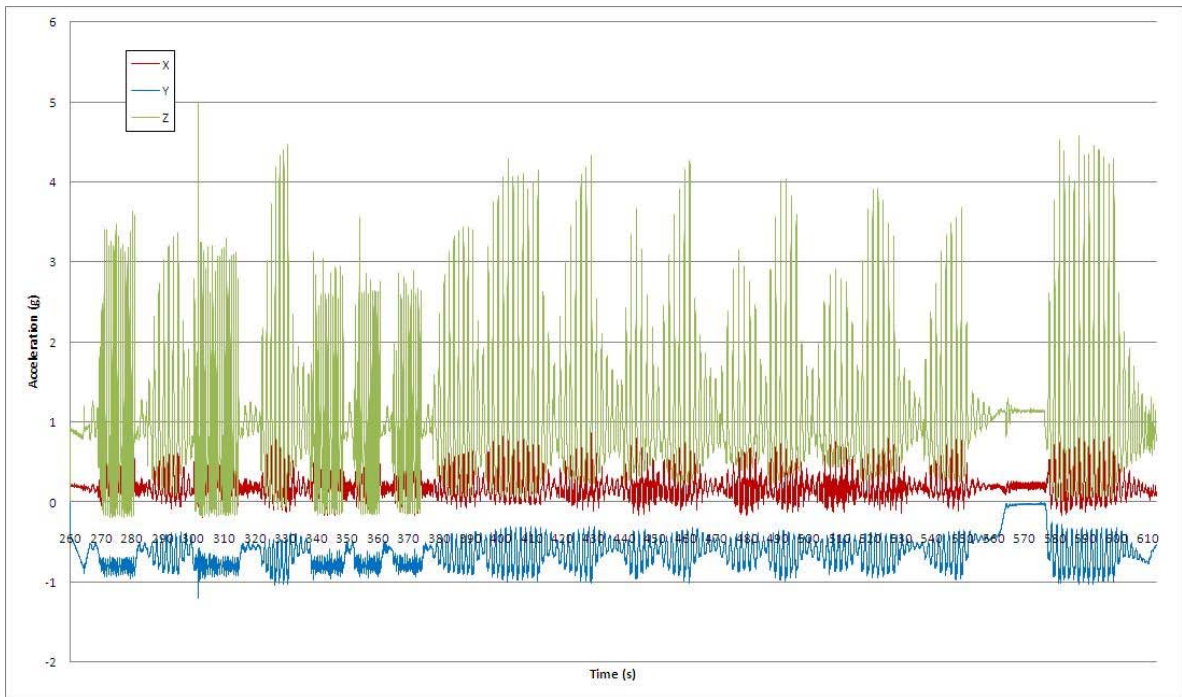


**Figure 112** Test run 19 Full

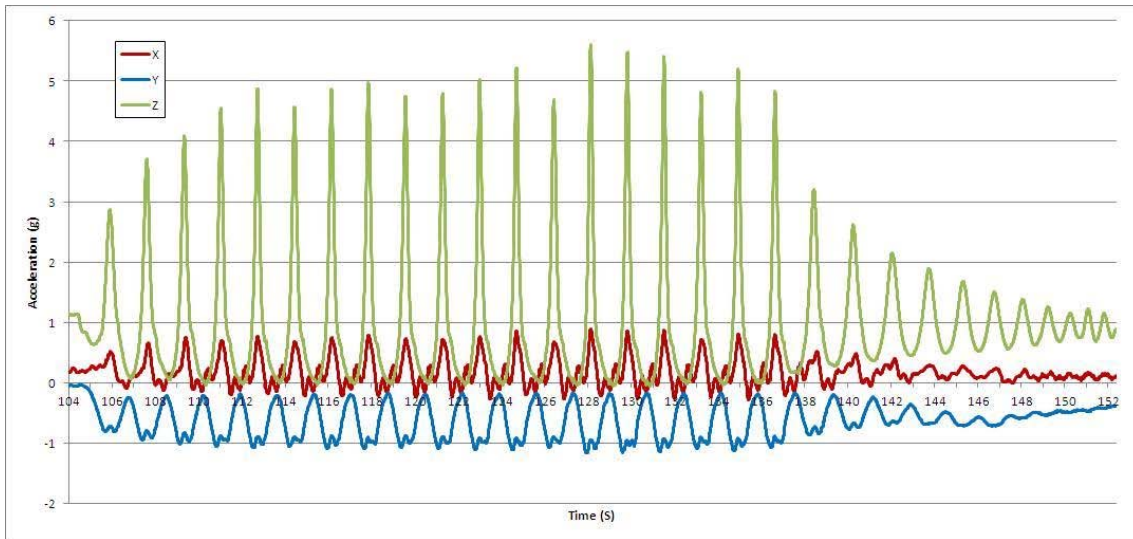


**Figure 113** Test run 19, Program 1

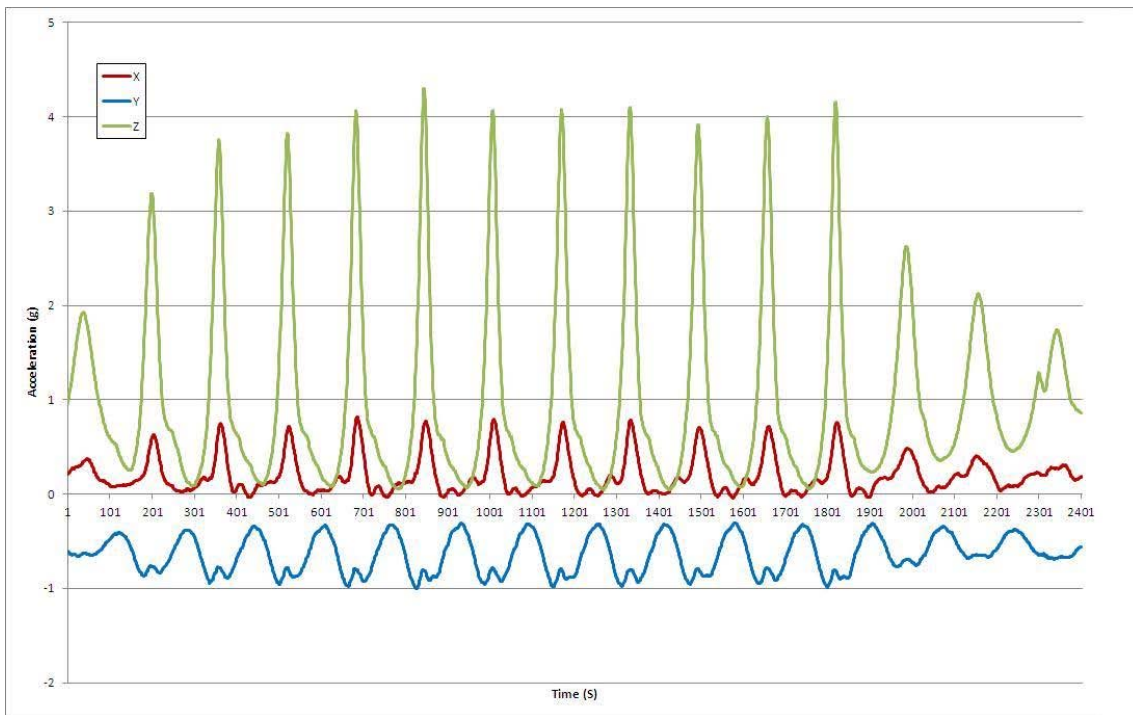


**Figure 114** Test run 19, Program 1, Foot pedal

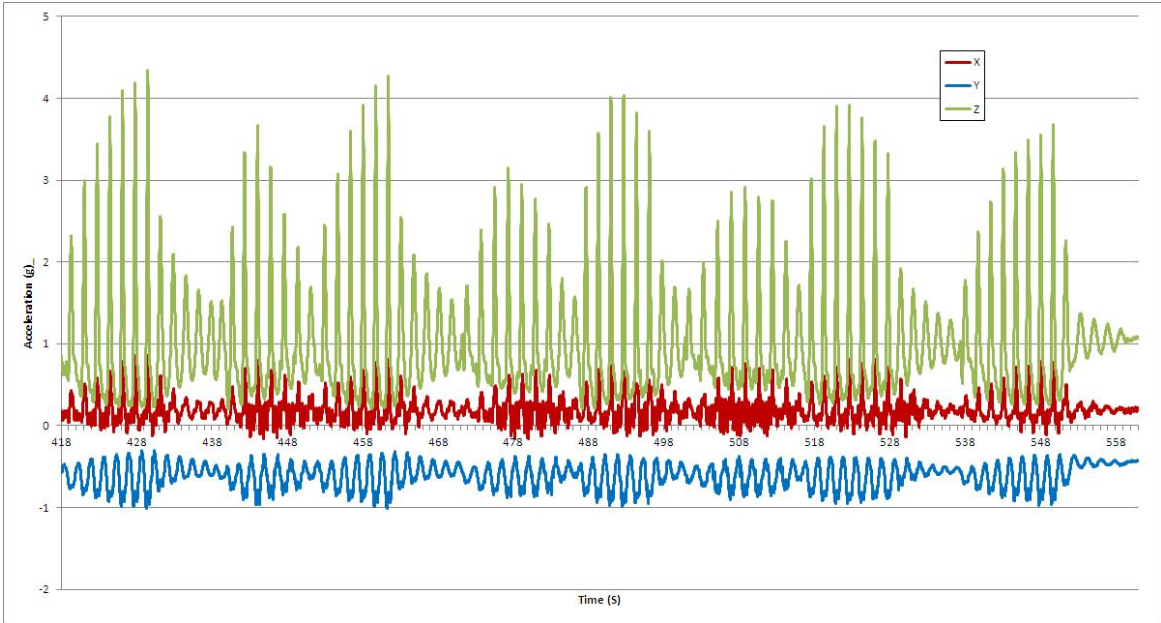


**Figure 115** Test run 19, Program 2

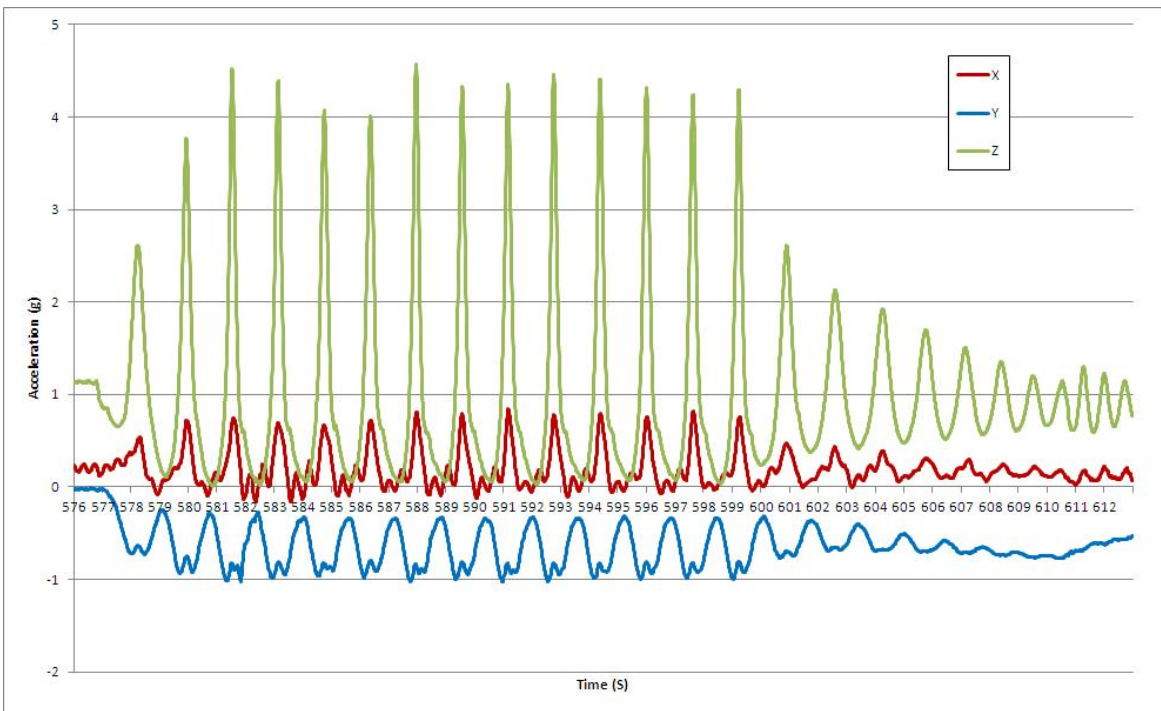


**Figure 116** Test run 19, Program 2, Foot Pedal



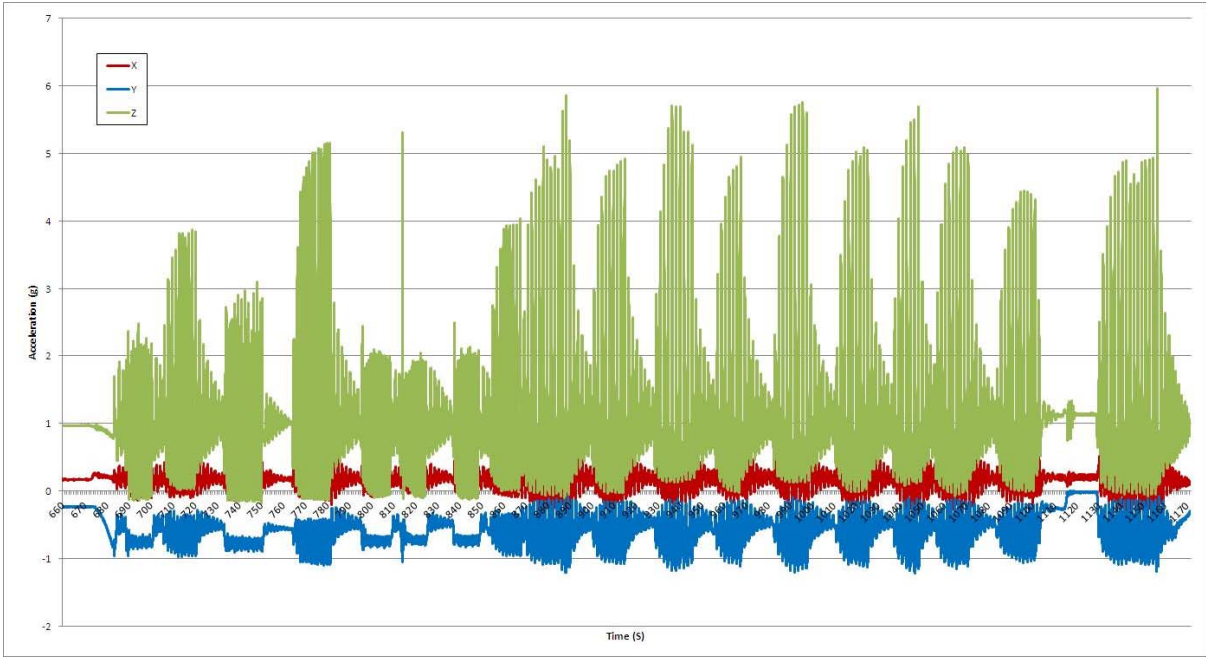


**Figure 117** Test run 20 full

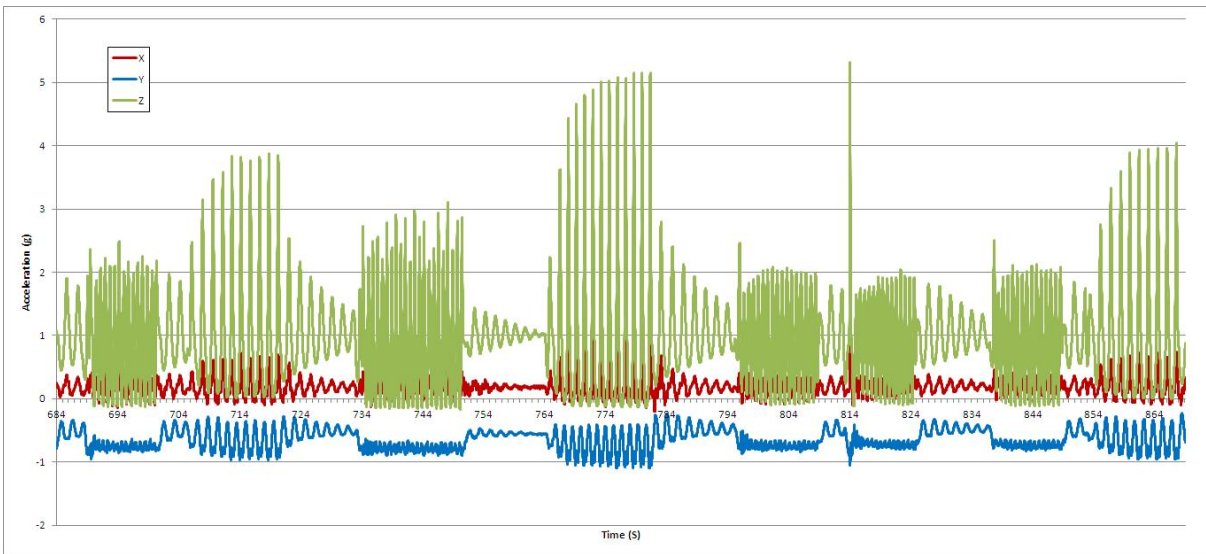


**Figure 118** Test run 20, Program 1

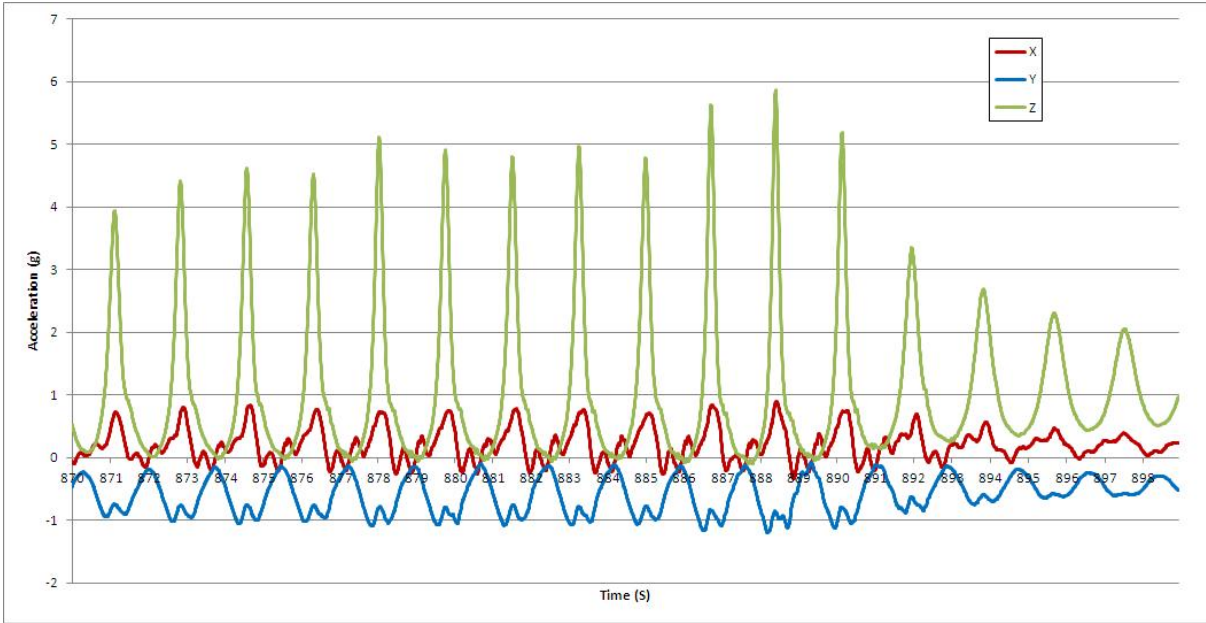


**Figure 119** Test run 20, Program 1, Foot pedal

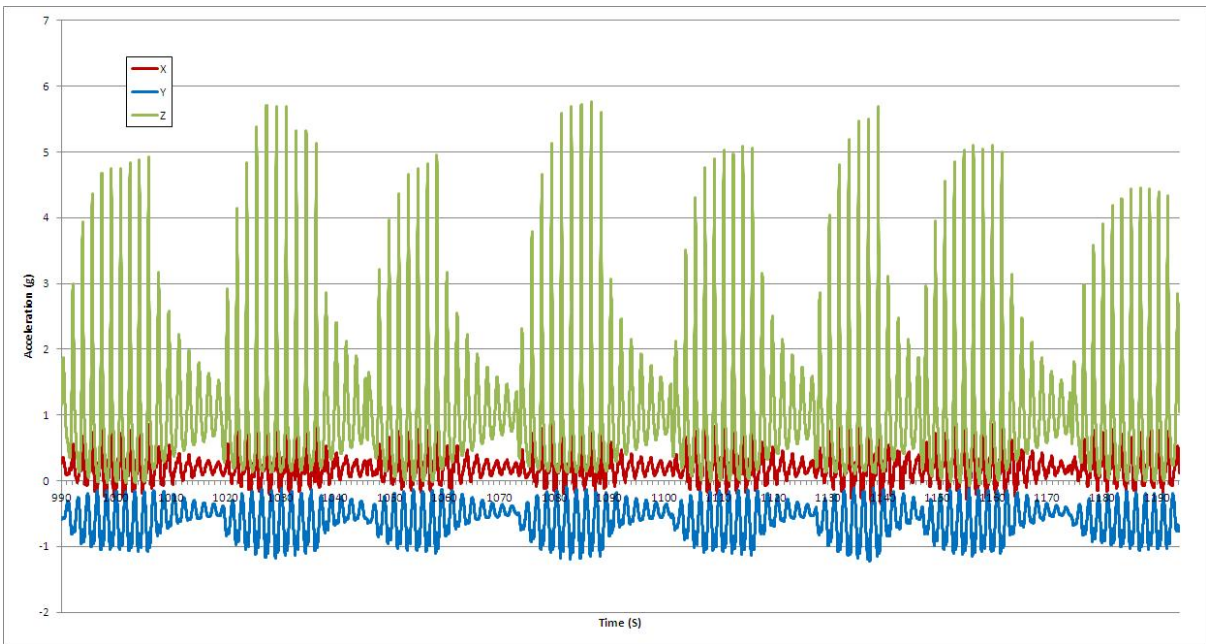


**Figure 120** Test run 20, Program 2

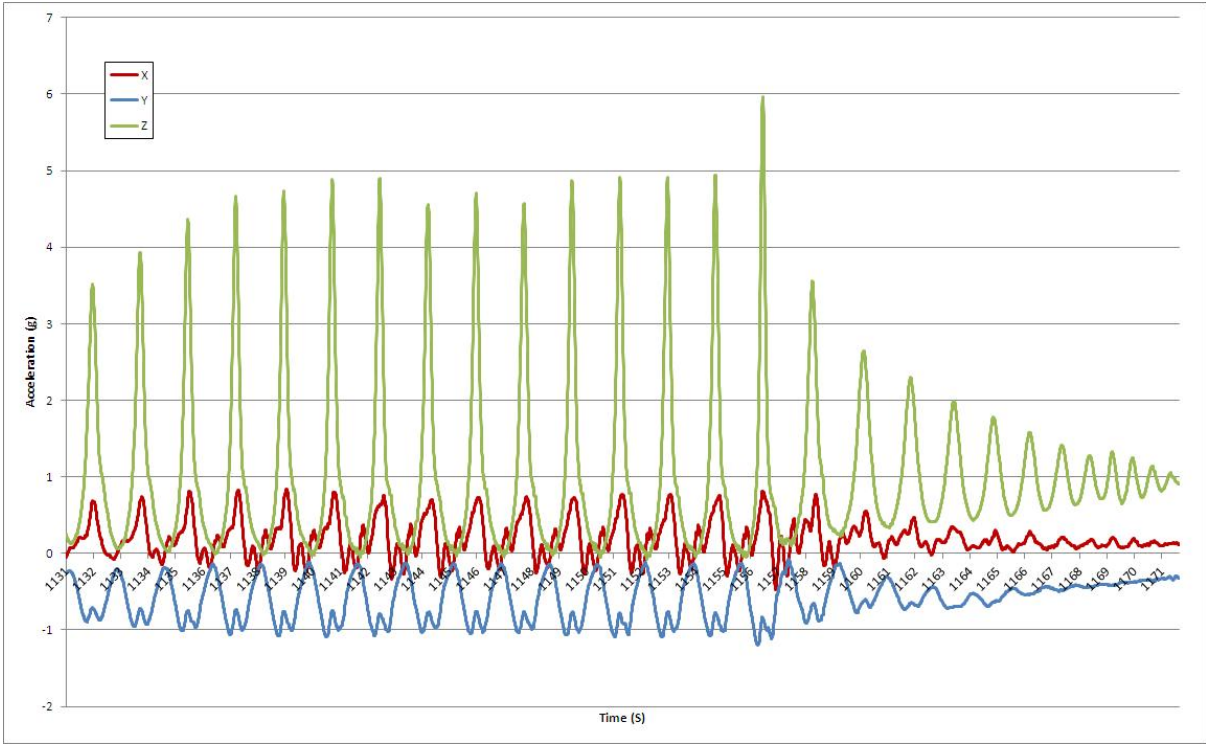


Figure 121 Test run 20, Program 2, Foot pedal

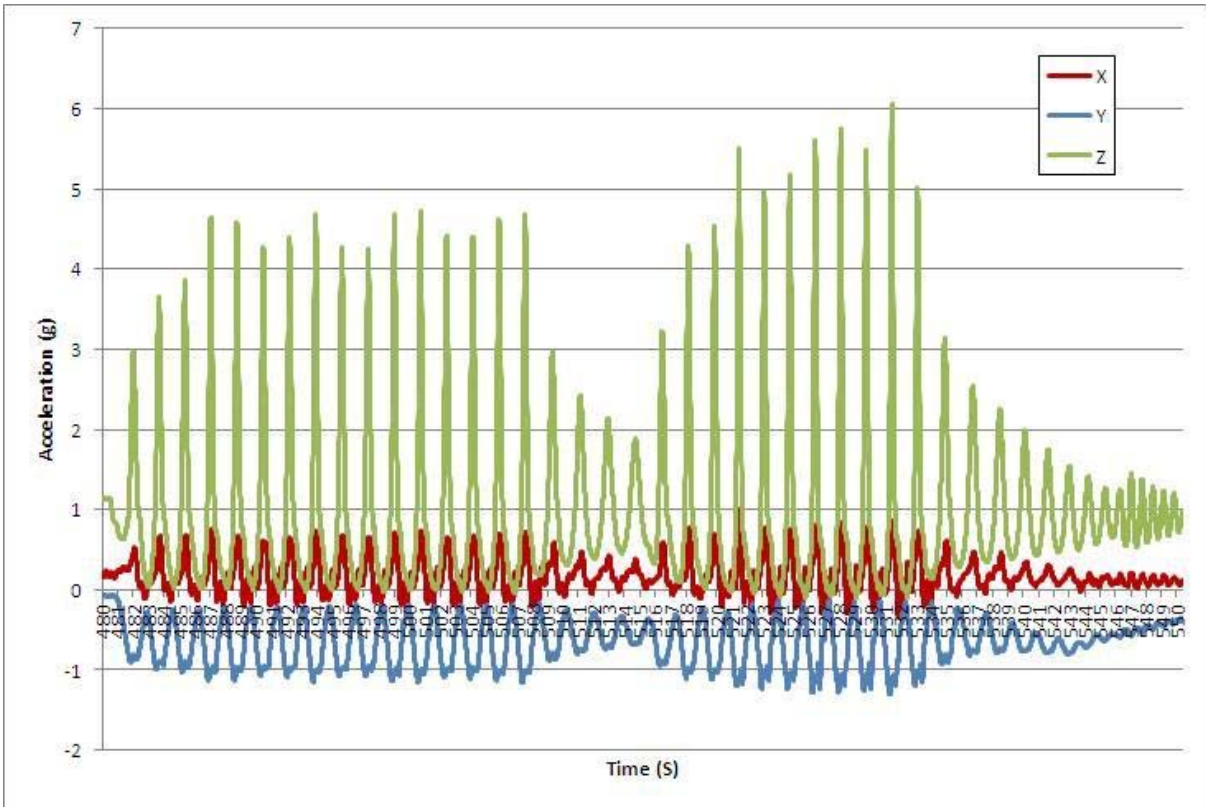
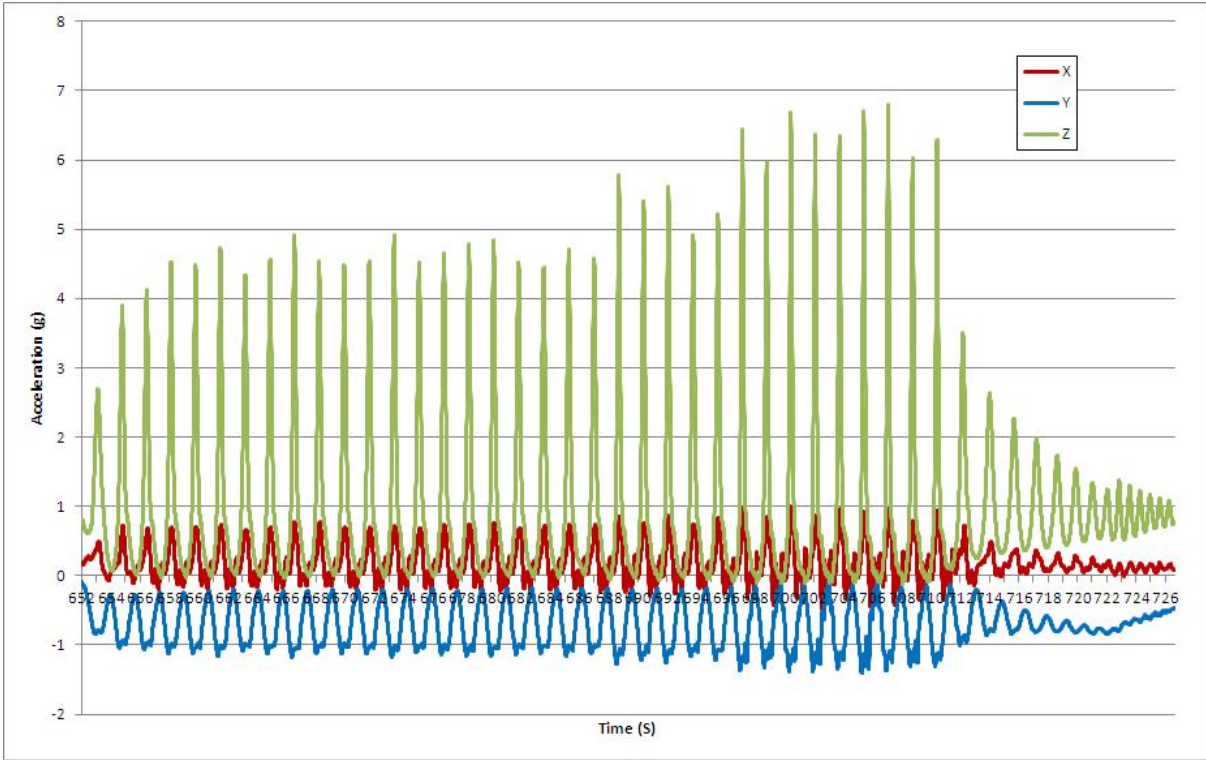
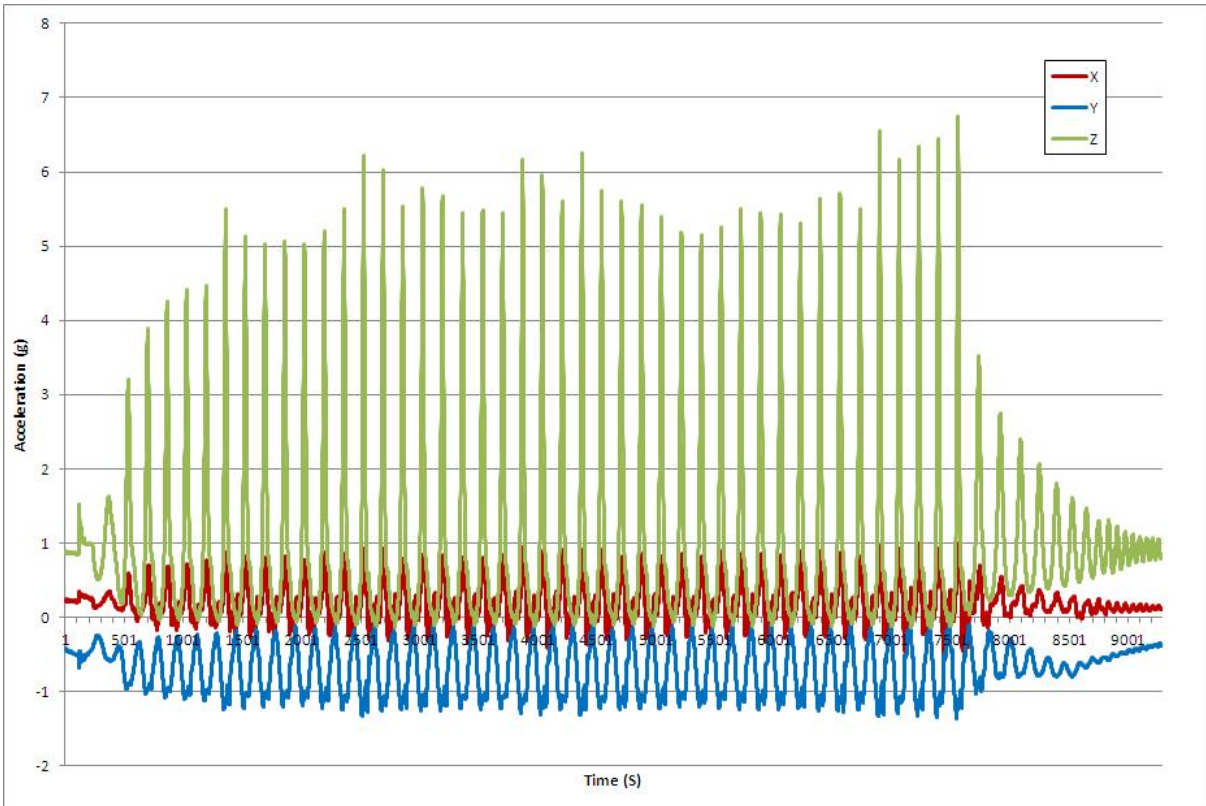


Figure 122 Test run 21 Part 1



**Figure 123 Test run 21 Part 2**



**Figure 124 Test run 21, Part 3**



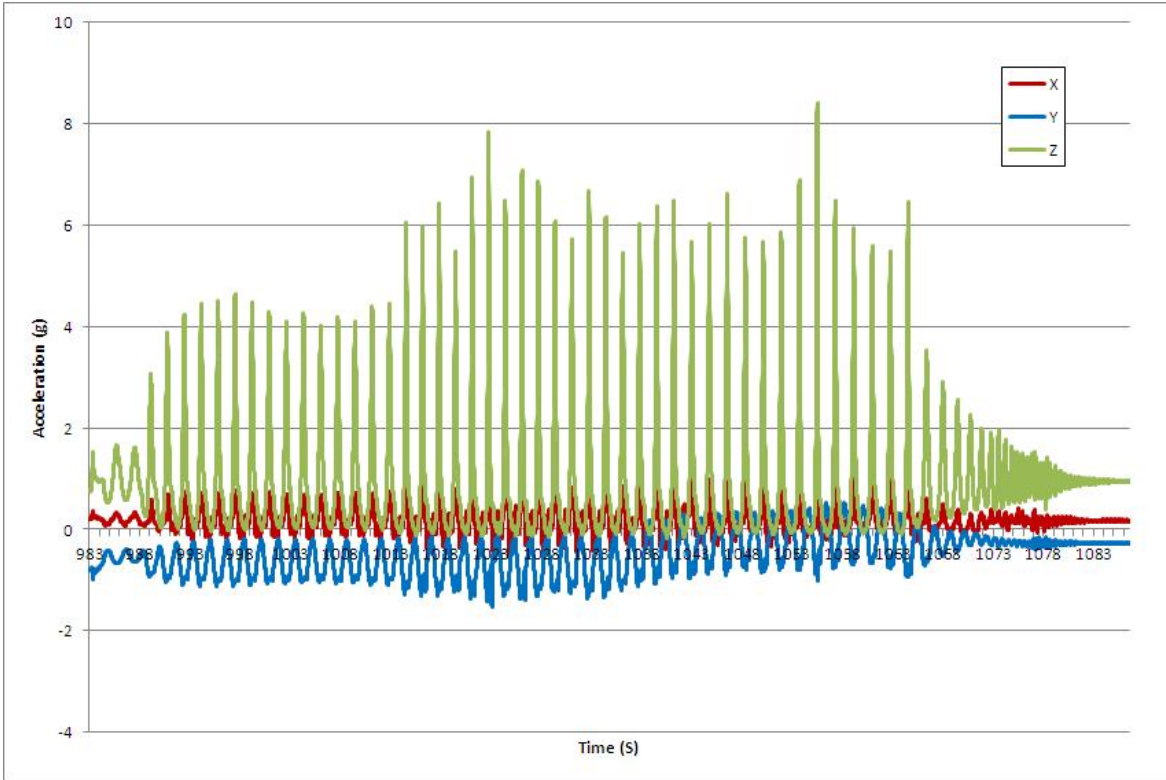


Figure 125 Test run 21, Part 4

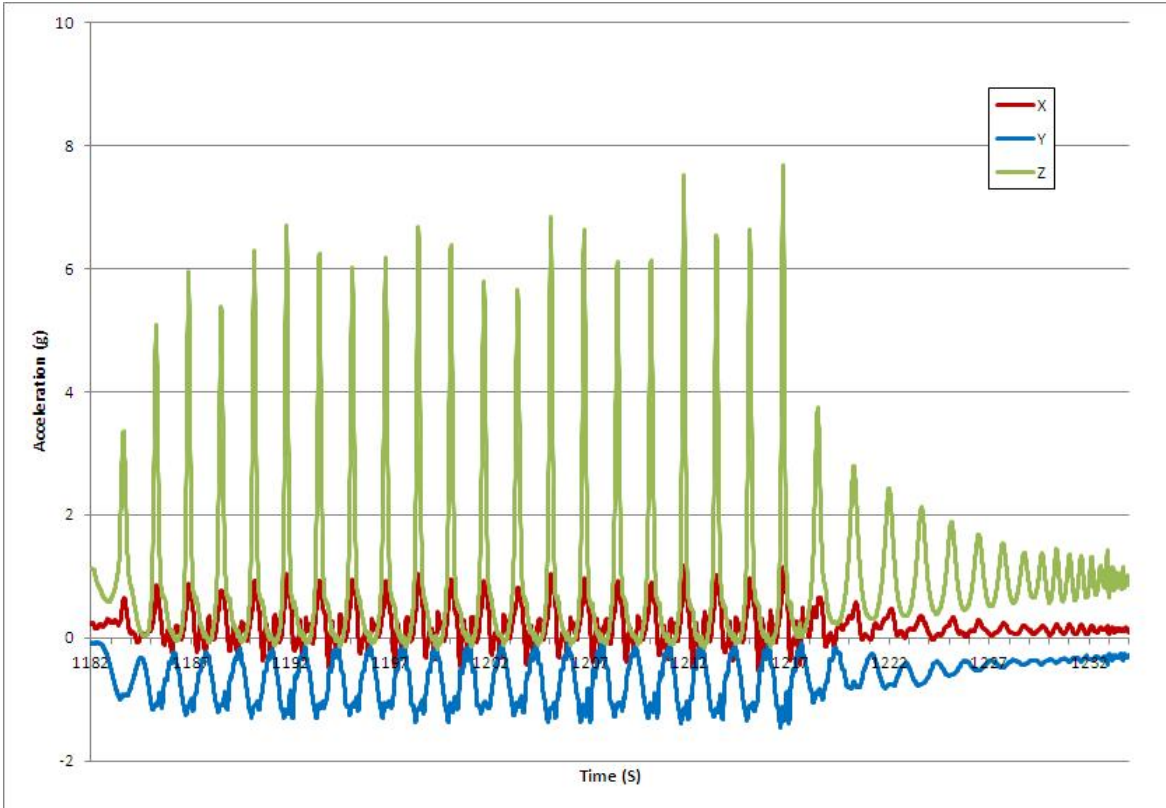


Figure 126 Test run 21, Part 5

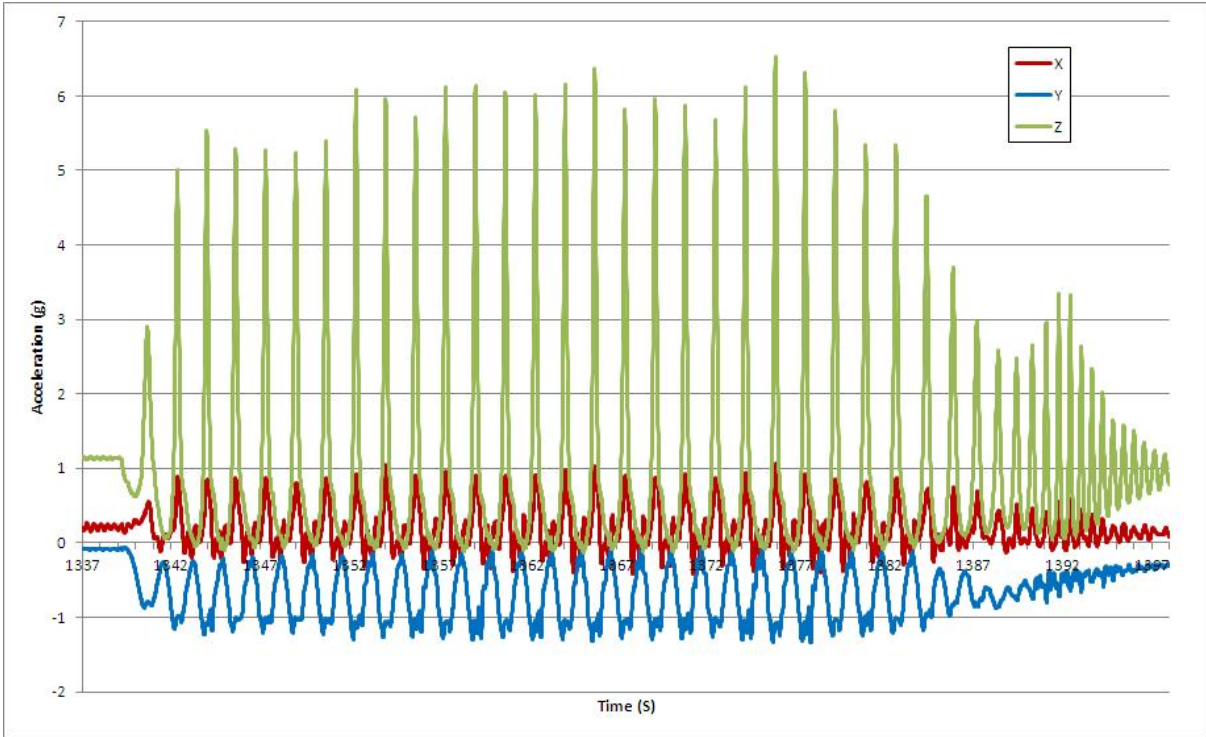


Figure 127 Test run 21, Part 6

## 6.4 ANTHROPOMETRY

Measurement	Age		3 year olds				8 years olds							
	Percentile	Gender	5 <sup>th</sup>		50 <sup>th</sup>		95 <sup>th</sup>		95 <sup>th</sup>					
			Boy	Girl	Boy	Girl	Boy	Girl	Boy	Girl				
Upper thigh depth (standing, US boy/girl, Snyder, 1977)			69		85		99		96	119		141		
Thigh depth (maximum sitting, Belgian, PeopleSize Pro 2008)	69	50 <sup>th</sup>	65	81	77	96	5 <sup>th</sup>	95	93	95	111	109	133	135
Hip breadth (seated, UK, Pheasant, 1986)	175		175	195	195	250		215	200	205	235	245	270	285
Hip breadth (sitting, Belgian, PeopleSize Pro 2008)	173		175	188	190	205		209	210	115	237	145	267	184
Abdominal depth (seated, UK, Pheasant 1986)	135		135	150	150	145		165	135	140	170	180	205	220
Abdominal depth (sitting, Belgian, PeopleSize Pro 2008)	134		136	144	146	157		161	146	150	170	178	201	220
Chest depth (standing, UK, Pheasant 1986)	105		105	125	120	145		140	115	120	150	150	185	180
Popliteal length (UK, PeopleSize Pro 2008)	195		200	230	230	325		260	295	295	325	330	355	365
Buttock – Popliteal length (UK, PeopleSize Pro 2008)	225		215	250	260	330		305	305	310	340	355	375	400

## **6.5 NON-DESTRUCTIVE TESTING SCHEDULE**

This NDT Schedule has been prepared on behalf of the Health and Safety Laboratory by:

P K Raw BSc (Hons) NDT  
ASNT NDT Level III 90629  
PCN Level 3 317085

Date 20<sup>th</sup> March 2013





**Argyll-Ruane Ltd**  
**Learning & Development**

Non-Destructive Testing Schedule for  
the Inspection of Safeco Crazy Frog  
Amusement Device Arms – Fatigue  
Fracture Risk Critical Areas

Improving the world through engineering



Bronze

Registered company number  
1103538

Page 1 of 15

**Argyll-Ruane Ltd**  
**Learning & Development**

Contents	
1.0 Introduction	3
2.0 References	5
Appendix A: Procedure for the Ultrasonic Inspection of Crazy Frog Amusement Device Arms – Fatigue Fracture Risk Critical Areas	7
Appendix B: Procedure for the Magnetic Particle Inspection of Crazy Frog Amusement Device Arms – Fatigue Fracture Risk Critical Areas	13
Table 1: NDT Schedule Crazy Frog Arms – Critical Areas	6
Table 2: Nominal Standoff Distances	10
Figure 1: Crazy Frog Arms	4
Figure 2: Locating Reference Target at Half Skip Distance	9
Figure 3: Locating Reference Target at 1 ½ Skip Distance	9
Figure 4: Fillet welds Roots	10
Figure 5: Inspection using Portable Electromagnet (Yoke)	14

**Argyll-Ruane Ltd**  
**Learning & Development**

NDT Schedule for Safeco Crazy Frog Arm Critical Areas

1.0 Introduction

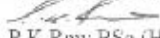
This NDT Schedule has been developed following the failure of one of the arms of a Safeco Crazy Frog amusement device. The subsequent investigation highlighted that the fatigue cracking had initiated from an earlier weld repair from the inside of the arm box section through to the outside in Zone 2 (see Figure 1). Because the cracking had initiated on the inside of the arm box section standard NDT techniques such as visual inspection or magnetic particle testing would not be capable of detecting the cracking at an early stage.

All other arms were inspected using magnetic particle techniques and a serious fatigue crack was located on an arm within Zone 2 running horizontally across the top plate, across the corner and down the horizontal plate.

Further investigation by the Health and Safety Laboratory highlighted higher g-forces than previous assessments with high tensile stresses occurring at the highest point on the arm box section (arm apex) on the inner surface (see Figure 1) and also at the root of the weld attaching the inner stiffening plate to the side walls. The plate runs from about where the ram is attached up to the apex, with the highest stresses near the top. Once again these high tensile stresses could initiate a fatigue crack on the inside surface where standard visual inspection or magnetic particle testing would not be capable of detecting the cracking at an early stage.

**Note the NDT specified in this NDT schedule for supplementary inspection of Crazy Frog Arm critical areas is to be carried out in addition to any NDT specified in earlier NDT schedules for inspection of Crazy Frog amusement devices. Therefore this document does not negate the need to follow other existing NDT procedures for inspection of specified areas of Crazy Frog amusement devices for other arm parts.**

This NDT Schedule has been prepared on behalf of the Health and Safety Laboratory by:

  
P K Raw BSc (Hons) NDT  
ASNT NDT Level III 90629  
PCN Level 3 317085

Date 20<sup>th</sup> March 2013

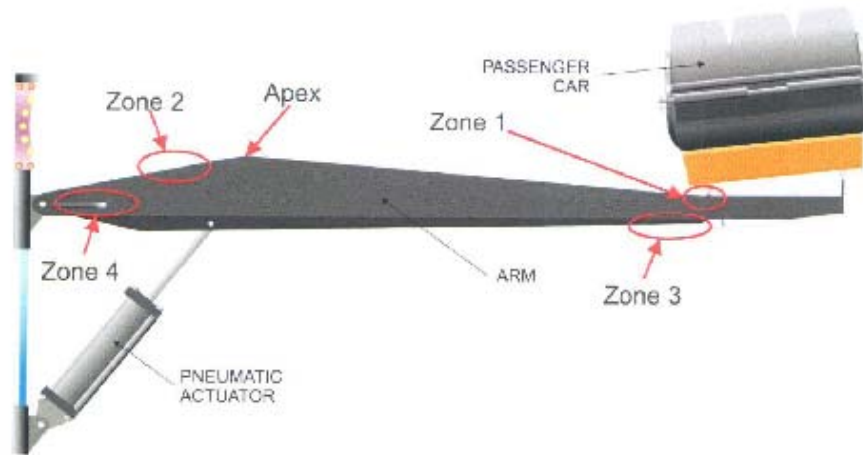


Figure 1 Crazy Frog Arms

**Argyll-Ruane Ltd**  
**Learning & Development**

2.0 References

BS EN ISO 9934-1: 2001 Magnetic Particle Inspection (General)

BS EN ISO 9934-2: 2002 Magnetic Particle Testing (Detection Media)

BS EN ISO 9934-3: 2002 Magnetic Particle Testing (Equipment)

BS 6072: 1981 Magnetic Particle Flaw Detection

BS EN ISO 3059:2012 Magnetic Particle Testing Viewing Conditions

BS EN ISO 9712: 2012 Qualification and Certification of NDT Personnel

BS 667: 2005 Illuminance Meters Requirements and Test Methods

BS EN ISO 17640:2010 Ultrasonic Testing of Welds

BS EN ISO 11666: 2010 Ultrasonic Testing of Welds Acceptance Levels

BS EN 583-1: 1999 Ultrasonic Examination – General Principles

BS EN 12223: 2000 Ultrasonic Examination – Specification for Calibration Block No. 1

Table 1 NDT Schedule Crazy Frog Arms Critical Areas

Item	Location/Description	Test Method	Procedure	Frequency of Test
Arm Apex	Top plate transverse weld	UT	Appendix A	Immediately Then 6 monthly
Arm Apex	Top plate and corner edges down on to horizontal plate	MT	Appendix B	Immediately Then 6 monthly
Arm Zone 2	Top plate and corner edges down on to horizontal plate	MT	Appendix B	Immediately Then 6 monthly
Arm Zone 2	Any weld repairs	UT	Appendix C	Immediately Then 6 monthly
Fillet Welds of Arm Stiffening Inner Plates	Root of fillet welds attaching inner stiffening plate to side walls from where ram is attached up to the arm apex	UT	Appendix C	Immediately Then 6 monthly

Appendix A

Procedure for the Ultrasonic Inspection of Crazy Frog Amusement Device Arms – Fatigue Fracture Risk Critical Areas

1.0 Scope

- 1.1 This procedure specifies techniques for detection of internal fatigue cracks using the manual ultrasonic testing of fusion-welded joints and fusion-weld repairs of Crazy Frog amusement device arms in fatigue fracture risk critical areas with an arm wall thickness of 5 mm. (See note below)

Note: This procedure is generally in accordance with BS EN ISO 17640: 2010 however the standard is written based on metallic materials of thicknesses greater than or equal to 8 mm, as such care should be exercised when using this procedure to locate internal fatigue cracks as the wall thickness of the test area is only 5 mm.

2.0 Qualification and Certification of Personnel

- 2.1 All personnel working to this procedure shall be qualified and certified to Level 2 in accordance with BS EN ISO 9712 in Ultrasonic Testing method weldments sector, for example PCN Level 2 UT weldments 3.1 & 3.7 and shall have a current vision test certificate.

3.0 Equipment

3.1 General

All equipment shall comply with and be calibrated in accordance with BS EN ISO 12668 Parts 1 – 3

3.2 Flaw Detectors

Digital pulse echo A-Scan flaw detectors shall be used.

3.3 Probe Parameters

Probes shall be twin crystal shear waves with refracted angles of 45° and 70°, 5MHz frequency, 6 mm to 12 mm diameter elements.

3.4 Coupling Media

Couplant used shall be compatible with the materials to be examined; the following are suitable to use in accordance with BS EN 583-1: 1999

- Contact paste
- Oil
- Grease
- Cellulose paste containing water



**Argyll-Ruane Ltd**  
**Learning & Development**

The same couplant type shall be used for calibration, sensitivity setting, scanning, and evaluation.  
After examination is completed, the coupling medium shall be removed.

3.5 Calibration Block

Calibration Block No. 1 in accordance with BS EN 12223: 2000 shall be used to calibrate the flaw detector time base. The time base shall be calibrated such that the metal path from either half skip or 1 ½ skip (see figures 2 & 3) can be displayed on the screen.

3.6 Reference Standard

The reference standard shall be manufactured from ferritic steel acoustically similar to the material to be tested, the thickness of the reference standard shall be the same as the wall thickness of the material to be tested: 5.0 mm. The surface of the reference standard shall be prepared to match the surface of the areas under test i.e. if the test areas are painted, the reference standard shall also be painted. The reference reflector shall be a notch milled to a depth of 1.0 mm, width 1.0 mm and length of 20 mm.

4.0 Safety and Environmental Requirements

4.1 National and local accident prevention, electrical safety, handling of dangerous substances and personal and environmental protection regulations shall be observed at all times.

5.0 Surface Preparation

5.1 Remove all external bolt-on paraphernalia such as panels and lighting from the Crazy Frog arms in the region of the test areas: Arm Apex, Zone 2 and Fillet Welds of Arm Stiffening Inner Plates

5.2 Areas to be tested shall be free from dirt scale, loose rust, weld spatter, grease, oil and any other foreign matter that may affect the test sensitivity and or acoustic coupling.

6.0 Setting Scanning Sensitivity

6.1 Note due to the wall thickness of only 5 mm it may not be possible to resolve the reference target at half skip (see figure 2), if this is the case locate the reference target at 1 ½ skip distance (see figure 3)

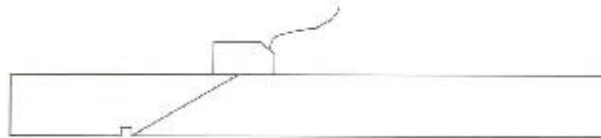


Figure 2 Locating Reference Target at Half Skip Distance

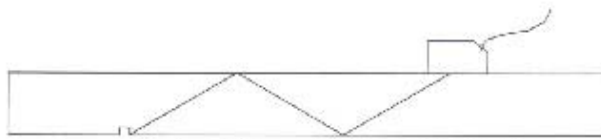


Figure 3 Locating Reference Target at 1 1/2 Skip Distance

- 6.2 Locate and maximise the response from the reference target in accordance with 6.1 and adjust the gain setting to set the amplitude from the reference target to 80% of full screen height. Note the gain setting, this is the reference sensitivity. When scanning the test areas add 6dB, to evaluate indications remove the 6dB added to scan and use the reference sensitivity.
- 6.3 At least every four hours or at the end of the test, check the sensitivity using the reference target. If the amplitude from the reference target has fallen below 80% of full screen height at the reference sensitivity established in 6.2 then the sensitivity shall be re-established and all test areas inspected since the previous acceptable sensitivity check shall be re-tested.

#### 7.0 Testing Techniques

- 7.1 The areas to be tested (see table 1) are welds and weld repairs that are transverse to the length of the Crazy Frog arms, specifically looking for fatigue cracks that have initiated from the weld root. Subsurface planar discontinuities perpendicular to the testing surface are difficult to detect with single angle probe techniques therefore scan the test areas with two probes; 45° and 70° refracted shear waves.
- 7.2 On butt welds; arm apex top plate transverse welds and all weld repairs, establish the test standoff distance on the test surface between the probe emission point to the point above the weld root on both sides of the weld using the following;

**Argyll-Ruane Ltd**  
**Learning & Development**

Standoff = Tan  $\theta$  x plate thickness

Where:

$\theta$  is the probe angle either 45° or 70°

plate thickness is 5 mm for half skip distance or 15 mm for 1 ½ skip distance.

Note the standoff distance will depend on which skip distance is being used; either half skip or 1 ½ skip distance see section 6.1 and table 2 below.

	45° Refracted Angle	70° Refracted Angle
Standoff at Half Skip Distance	5 mm	13.7 mm
Standoff at 1 ½ Skip Distance	15 mm	41.2 mm

Table 2 Nominal Standoff Distances

- 7.3 On the fillet welds of arm stiffening inner plates there are two roots from which to establish standoff test distances, see figure 4 below;

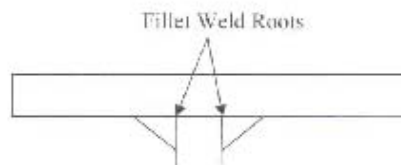


Figure 4  
Fillet Weld  
Roots

- 7.4 At each test area use a suitable marker to mark across the arm parallel to the weld roots on both sides of the weld at the relevant test standoff distances obtained from table 2 for both probe angles on both sides of the weld.

Note 1: it may not be possible to test across the full width of the arm as a longitudinal cable conduit may be tack welded down the length of the arm, if this is the case test as much of the width of the inspection area as possible.

Note 2: check the actual probe angles using Calibration Block No. 1 and the actual plate thickness which can be measured using a normal probe at a point adjacent to the weld and if these parameters are different to nominal adjust the standoff distance accordingly.

- 7.5 At each test area place the 45° probe emission point on the relevant marked standoff line with the beam interrogating the weld root and carefully scan the probe across the arm keeping the emission point on the marked standoff line using the scanning sensitivity established in section 6.2 using a maximum

**Argyll-Ruane Ltd**  
**Learning & Development**

scanning speed of 100 mm per second. During the scan along the standoff line a slight swivelling movement up to an angle of approximately 10° on either side of the nominal beam direction shall be applied to the probe. Repeat the scan of the test area along the standoff line on the other side of the weld with the probe interrogating the weld root.

- 7.6 At each test area place the 70° probe emission point on the relevant marked standoff line with the beam interrogating the weld root and carefully scan the probe across the arm keeping the emission point on the marked standoff line using the scanning sensitivity established in section 6.2 using a maximum scanning speed of 100 mm per second. During the scan along the standoff line a slight swivelling movement up to an angle of approximately 10° on either side of the nominal beam direction shall be applied to the probe. Repeat the scan of the test area along the standoff line on the other side of the weld with the probe interrogating the weld root.

8.0 Characterisation and Acceptance

- 8.1 Any indication interpreted as a crack shall be considered unacceptable.

9.0 Compliance to Procedure

- 9.1 If this procedure cannot be complied with fully do not carry out any testing and inform the Health and Safety Laboratory immediately.

10.0 Test Report

The test report shall include at least the following information:

- Identification of the Crazy Frog amusement device under test
- Identification of the specific arm and weld under test
- Dimensions of test areas
- Surface conditions
- Reference to this procedure
- Place and date of testing
- Identification of test organisation and identification and certification of operator
- Make and type of flaw detector used with serial number
- Make, type, frequency, size, actual refracted angle and serial number of probes
- Identification of reference blocks used
- Couplant type
- Extent of testing
- Time base range

**Argyll-Ruane Ltd**  
**Learning & Development**

- Gain setting for reference levels
- Result of test including sizes of any cracks located

Appendix B

Procedure for the Magnetic Particle Inspection of Crazy Frog Amusement Device Arms –  
Fatigue Fracture Risk Critical Areas

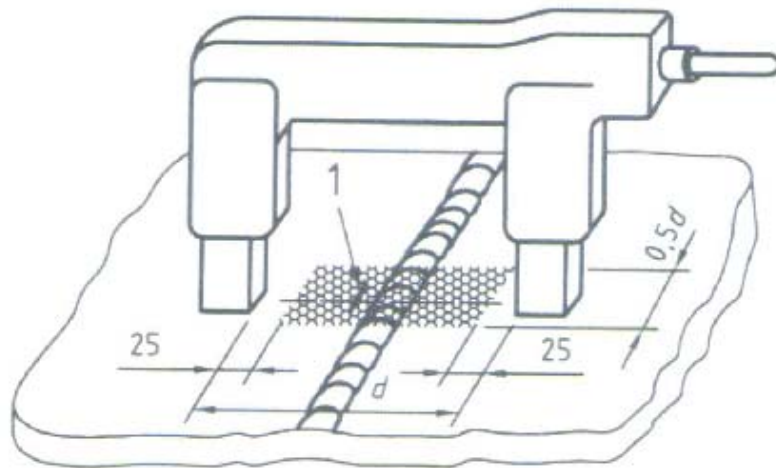
- 1.0 Qualification and Certification of Personnel
  - 1.1 All personnel working to this procedure shall be qualified and certified to Level 2 in accordance with BS EN ISO 9712 in Magnetic Particle Inspection method for example PCN Level 2 and shall have a current vision test certificate.
- 2.0 Safety and Environmental Requirements
  - 2.1 Magnetic particle testing may require the use of toxic, flammable and/or volatile materials. In such cases, working areas shall therefore be adequately ventilated and far from sources of heat or flames. Extended or repeated contact of detecting media and contrast paints with the skin or mucous membranes shall be avoided.
  - 2.2 Testing materials shall be used in accordance with the manufacturer's instructions. National and local accident prevention, electrical safety, handling of dangerous substances and personal and environmental protection regulations shall be observed at all times.
- 7 Surface Preparation
  - 7.1 Remove all external bolt-on paraphernalia such as panels and lighting from the Crazy Frog arms in the region of the test areas - arm apex and Zone 2.
  - 7.2 Areas to be tested shall be free from dirt scale, loose rust, weld spatter, grease, oil and any other foreign matter that may affect the test sensitivity.
  - 7.3 Non-ferromagnetic coatings up to approximately 50µm thick, such as unbroken tightly adherent paint layers, do not normally impair detection sensitivity. Thicker coatings reduce sensitivity. Under these conditions, the sensitivity shall be verified. If suitable sensitivity cannot be achieved strip the paint layer down to bare metal.
  - 7.4 There shall be a sufficient visual contrast between the indications and the test surface. It may be necessary to apply a uniform, thin, adherent layer of approved contrast paint.



**Argyll-Ruane Ltd**  
**Learning & Development**

- 8 Magnetisation Technique
- 8.2 Portable Electromagnet (Yoke) – The poles of an a.c. electromagnet (yoke) are placed in contact with the test area as shown in Figure 5. The test area shall not be greater than that defined by a circle inscribed between the pole pieces and shall exclude the zone immediately adjacent to the poles.
- 8.3 The poles shall be repositioned after each area has been magnetised and inspected such that sufficient overlap between test areas as defined in 4.1 ensures the arm areas of interest are fully inspected.

Dimensions in millimetres



**Key**

- 1 Flaw

Figure 5 Inspection using Portable Electromagnet (Yoke)



**Argyll-Ruane Ltd**  
**Learning & Development**

- 9 Detection Media
  - 9.2 The characterisation of detection media shall be in accordance with BS EN ISO 9934-2
  - 9.3 The detection media shall be a suspension of black ferromagnetic particles in a carrier fluid
- 10 Application of Detecting Media
  - 10.2 Magnetisation shall be accomplished using the continuous method where the detecting media shall be applied immediately prior to and during the magnetisation. The application shall cease before magnetisation is terminated. Sufficient time shall be allowed for indications to develop before moving or examining the component or structure under test.
  - 10.3 During application of a magnetic ink, it shall be allowed to flow onto the surface with very little pressure so that the particles are allowed to form an indication without being washed off.
  - 10.4 After applying ink, the component shall be allowed to drain so as to improve the contrast of any indications.
- 11 Viewing Conditions
  - 11.2 For inspection the illuminance at the test surface shall be 500 lux or greater even illumination with daylight or artificial light, this shall be checked using a photometer calibrated to BS 667.
  - 11.3 The entire surface under test shall be viewed before proceeding to the next stage in the testing procedure. Where viewing is obstructed, the component or equipment shall be moved to permit adequate viewing of all the test area. Care shall be taken to ensure that indications are not disturbed after magnetisation has stopped and before the component has been inspected and indications recorded.
- 12 Overall Performance Test
  - 12.2 The strength of the portable electromagnet (i.e. yokes) shall be assessed by measuring the lifting power or the pull-off force.
  - 12.3 The lifting power shall be equivalent to not less than 4.5 kg for a pole spacing of 300 mm or less, and the pull-off force shall have a value equivalent to not less than 2.25 kg for the same pole spacing.

**Argyll-Ruane Ltd**  
**Learning & Development**

- 12.4 The strength of the portable electromagnet shall be assessed at intervals not to exceed 6 months; results of the performance test shall be documented.

13 Test Areas

- 13.1 Arm Apex; The test area for the arm apex shall be across the full width of the arm apex top plate including the corners down onto the horizontal plates and for 200 mm along the arm in both directions. Position the portable electromagnetic yoke poles such that they are aligned with the direction of the arm, such that transverse cracks can be detected. Note it may not be possible to test across the full width of the arm as a longitudinal cable conduit may be tack welded down the length of the arm, if this is the case test as much of the width of the inspection area as possible.

- 13.2 Zone 2 (See Figure 1); The test area for the arm zone 2 shall be across the full width of the zone 2 arm top plate including the corners down onto the horizontal plates. Position the portable electromagnetic yoke poles such that they are aligned with the direction of the arm, such that transverse cracks can be detected. Note it may not be possible to test across the full width of the arm as a longitudinal cable conduit may be tack welded down the length of the arm, if this is the case test as much of the width of the inspection area as possible.

14 Interpretation and Recording of Indications

- 14.1 Care shall be taken to differentiate between true indications and spurious or false indications, such as scratches, changes of section, boundary between regions of different magnetic properties, or magnetic writing. The NDI inspector shall carry out any necessary testing and observations to identify and, if possible, to eliminate the reason for such false indications.
- 14.2 All indications which cannot be confidently discounted as false shall be classified as linear or rounded, and shall be recorded on the test report.
- 14.3 Linear indications are those indications in which the length is more than three times the width. Rounded indications are indications that are circular or elliptical and where the length is less or equal to three times the width.

15 Acceptance Criteria

- 15.1 No linear indications; for example cracks are permitted.

**Argyll-Ruane Ltd  
Learning & Development**

16. Cleaning

- 16.1 After testing and acceptance all test areas shall be cleaned to remove detecting media.

17. Compliance to Procedure

- 17.1 If this procedure cannot be complied with fully do not carry out any testing and inform the Health and Safety Laboratory immediately.

18. Test Report

Record the following as a minimum:

- Name of the company
- Work location
- Description and identity of the test areas
- Reference to this procedure
- Description of equipment and detection media/contrast paint used
- Magnetisation technique including pole spacing
- Surface preparation
- Viewing conditions
- Indications located
- Date of test
- Name, qualification and signature of the person performing the tests